Geometric Phases and Factorisation in Quantum Physics and Gravity

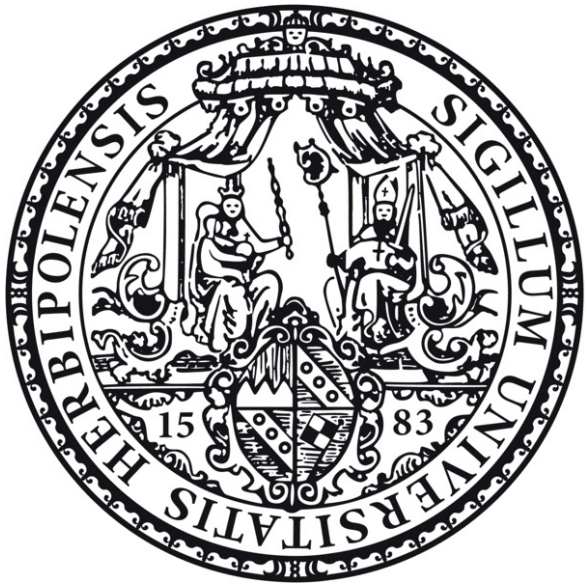

Dissertation zur Erlangung des naturwissenschaftlichen Doktorgrades
an der Fakultät für Physik und Astronomie
der Julius–Maximilians-Universität Würzburg

vorgelegt von

Moritz Dorband
aus Schönbrunn bei Ebelsbach

Würzburg, im November 2023

This document is licensed under the Creative Commons Attribution-NonCommercial-NoDerivatives 4.0 International License (CC BY-NC-ND 4.0):
http://creativecommons.org/licenses/by-nc-nd/4.0 This CC license does not apply to third party material (attributed to another source) in this publication.

Eingereicht bei der Fakultät für Physik und Astronomie am

08.11.2023

Gutachter der Dissertation

1. Gutachter: Prof. Dr. Johanna Erdmenger

2. Gutachter: Prof. Dr. Björn Trauzettel

3. Gutachter: Prof. Dr. Paweł Caputa

Prüfer des öffentlichen Promotionskolloquiums

1. Prüfer: Prof. Dr. Johanna Erdmenger

2. Prüfer: Prof. Dr. Björn Trauzettel

3. Prüfer: Prof. Dr. Matthias Bode

4. Prüfer:

5. Prüfer:

Tag des öffentlichen Promotionskolloquiums

26.07.2024

Doktorurkunde ausgehändigt am

_____

to my family & friends

In a world where you can be anything, be kind

Acknowledgements

This thesis is the result of the many interactions and discussions I had with different people during my time as a PhD student. The following is an attempt to put my gratitude into words.

First of all, I thank my supervisor, Johanna Erdmenger, for her continuous support during all of the time of my PhD, specifically for enabling me to work on many magnificent projects. My work as a physicist has greatly benefited from her guidance and advice on penning publications and arranging talks. This thesis would not have been written without her.

Next, I thank all of my collaborators and discussion partners. First and foremost, this includes Souvik Banerjee and Anna-Lena Weigel. Our countless discussions and us bouncing ideas off each other have led to most of the physics discussed in this thesis, which would be merely a glimpse of its actual version without these two people. I am also particularly grateful to Pablo Basteiro and Giuseppe Di Giulio for always having an open ear and many illuminating interactions and suggestions. Furthermore, I thank Rathindra Nath Das, Daniel Grumiller, René Meyer, who also guided me through my BSc and MSc, Flavio Nogueira, Jeroen van den Brink and Suting Zhao for many helpful discussions and their collaboration in various projects.[1] I also enjoyed insightful discussions with Martin Ammon, Bastian Heß, Haye Hinrichsen, Jani Kastikainen, Christian Northe, Henri Scheppach, Yanick Thurn, Björn Trauzettel and Zhuo-Yu Xian, for which I thank them very much. A special thanks also goes to Tim Schuhmann, not only for the great discussions but also for being a splendid office mate.

I also thank every member of TP 3 (and our neighbours of TP 4) for creating a pleasant work environment, which made getting to the office every day something to look forward to. Particularly noteworthy are our lunch breaks, where we discussed anything but physics. Of course, I have to thank my parents, Utz and Karin, and my sister, Nina, for their everlasting support in every aspect of my life, and my close friends Valentin Seinige and Franziska Wolf. Their questions about what I am actually doing have more than once helped me to obtain a deeper understanding myself. The same goes for Jürgen Dahlke and the whole team of the Disharmonie Schweinfurt, who allowed my colleagues Pablo Basteiro, Manuel Graf, Tobias Kehrer, Yanick Thurn, Anna-Lena Weigel and me to initiate a series of popular science talks on physics. Great support in this direction I have also received from Katharina Leiter and Tobias Kießling. I also have to thank Katharina Leiter

[1] Here and in upcoming lists of names, the order is chosen alphabetically and not to imply any ranking.

and the remaining ‘magnificent seven’, namely Lakshmi Bhaskaran, Kerstin Brankatschk, Alessio Calzona, Maria Herz and Philipp Kagerer, for the great experience in planning the QMA retreat 2021. Furthermore, I thank the ct.qmat Cluster of Excellence for financial support and the opportunity to discuss with many people from different areas in physics during all of the QMA and cluster retreats. Last but certainly not least, I am grateful to Nelly Meyer for helping me traverse the jungle of German bureaucracy.

Finally, I am indebted to Souvik Banerjee, Pablo Basteiro, Giuseppe Di Giulio, Bastian Heß, Jani Kastikainen, Henri Scheppach, Tim Schuhmannn, Valentin Seinige, Yanick Thurn, Anna-Lena Weigel, Franziska Wolf and both of my parents for a lot of proof-reading and helpful comments on this thesis.

Abstract

By the holographic principle, theories of (quantum) gravity have a dual description by a field theory without gravity in one dimension lower. That is, quantities in gravity with a geometric interpretation are dual to objects in quantum information theory. The most prominent realisation of this principle is known as the AdS/CFT correspondence. In particular, this gave rise to the ER=EPR proposal, stating that the gravitational geometry arises from the entanglement structure of the field theory. However, AdS/CFT also gives rise to the factorisation puzzle, which describes the conflicting statements about the Hilbert space structures expected from the bulk and boundary perspectives on the eternal black hole. Resolving this puzzle is one of the main ingredients to obtaining a deeper understanding of the mechanism behind the holographic principle. In light of this puzzle, in this thesis, I investigate relations between entanglement measures and geometry. In particular, I consider geometric phases and their use in light of the factorisation properties of the Hilbert space.

To start, I study geometric phases in a simple quantum system consisting of two interacting qubits. I show that the geometric phase of this system determines the entanglement entropy uniquely. I discuss this result in terms of submanifolds of the projective Hilbert space of this system. This enables me to associate a particular value of the geometric phase to a factorised projective Hilbert space. Building on that construction, I introduce a fine structure of entanglement entropy where the geometric phase is considered a measure distinguishing states with the same entanglement entropy. This enables me to associate wormhole-like physics with simple quantum systems. To connect to theories of gravity and the AdS/CFT correspondence, I examine the geometric phase for the thermofield double state (TFD state). In that, I first derive the thermofield double state for the interacting two-qubit system and, in particular, the entanglement temperature in terms of the geometric phase. This manifests that the (entanglement) temperature can be understood using a notion of geometry in quantum theory, similar to gravity, where temperature naturally arises when restricting the observer to a subregion in spacetime. For the TFD state, the fine structure of entanglement provides a probe for the topology of the parameter space. After discussing this on the quantum mechanical side, I then proceed to work out the topological phase for the thermofield double state by a gravity calculation, in particular within JT gravity. I comment on the possibilities of measuring this fine structure both for the qubit system as well as for the TFD state in actual laboratories.

In the next step, I generalise the previous results by considering geometric phases in the

setting of AdS_3/CFT_2. In particular, I discuss Virasoro Berry phases and modular Berry phases. Considering the eternal black hole in the bulk, computing Virasoro and modular Berry phases shows that they both depend on the properties of the wormhole. Therefore, both Virasoro and modular Berry phases, but also the topological phase of the TFD state, probe features of the bulk wormhole and can be used to diagnose non-factorisation. In particular, these phases are computed in the boundary theory, i.e. they probe the non-factorisation for the boundary Hilbert space. This result highlights how geometric phases are imperative to diagnose non-factorisation in the AdS/CFT correspondence.

Thirdly, I establish a direct bridge between geometric phases as discussed above and the classification of operator algebras. Such algebras belong to the realm of an axiomatic/algebraic approach to quantum field theory. Using state vectors that can be understood as describing a spin chain, I show that the value of the geometric phase of a given state vector determines whether this state vector defines a trace functional on the algebra. In particular, this provides a geometric explanation for the fundamentally different properties of algebras of type II and type III. In an application to the eternal black hole in AdS/CFT, I discuss how the topological phase of the thermofield double state is connected to a non-trivial centre of the corresponding operator algebras. In that, the topological phase is understood as an indicator for the non-factorisation of the operator algebras, or in other words, for a non-trivial centre. Building on that, I establish geometric and topological phases as a more general indicator of information inaccessible to a local observer. I discuss this for various examples, ranging from a single qubit in a magnetic field to Virasoro and modular Berry phases in AdS/CFT.

Last but not least, I propose geometric quantum discord as a second geometric measure for non-factorisation. Geometric quantum discord provides a qualitative measure for the generically hard-to-compute measure of quantum discord. I study this in particular for pure states, where quantum discord reduces to the entanglement entropy. I derive a general formula for geometric quantum discord for pure states. This formula shows non-factorisation in terms of a ratio of modular partition functions. I discuss how this notion of non-factorisation is consistent with the geometric phase criterion discussed earlier. In particular, I analyse the implications of this result for the eternal black hole in AdS/CFT. Finally, I discuss how a straightforward generalisation of geometric quantum discord enables the study of black hole microstates.

The results discussed in this thesis are published in the original works listed in app. A.

Zusammenfassung

Nach dem holographischen Prinzip haben Theorien der (Quanten-)Gravitation eine duale Beschreibung durch eine Feldtheorie ohne Gravitation in einer Dimension darunter. Das heißt, Größen in der Gravitation mit einer geometrischen Interpretation sind dual zu Objekten in der Quanteninformationstheorie. Die prominenteste Realisierung dieses Prinzips ist als AdS/CFT-Korrespondenz bekannt. Dies führte insbesondere zum ER=EPR-Vorschlag, der besagt, dass sich die Raumzeitgeometrie aus der Verschränkungsstruktur der Feldtheorie ergibt. Die AdS/CFT-Korrespondenz führt jedoch auch zu dem Faktorisierungsproblem, das die widersprüchlichen Aussagen über die Hilbertraum Strukturen beschreibt, die aus der Gravitations- und der Feldtheorieperspektive des ewigen Schwarzen Lochs erwartet werden. Die Lösung dieses Problems ist einer der Hauptbestandteile, um ein tieferes Verständnis des Mechanismus hinter dem holographischen Prinzip zu erlangen. Vor dem Hintergrund dieses Problems untersuche ich in dieser Arbeit die Beziehungen zwischen Verschränkungsmaßen und Geometrie. Insbesondere betrachte ich geometrische Phasen und ihre Verwendung im Lichte der Faktorisierungseigenschaften des Hilbertraums.

Zu Beginn untersuche ich geometrische Phasen in einem einfachen Quantensystem, das aus zwei wechselwirkenden Qubits besteht. Ich zeige, dass die geometrische Phase dieses Systems die Verschränkungsentropie eindeutig bestimmt. Dieses Ergebnis diskutiere ich im Rahmen von Untermannigfaltigkeiten des projektiven Hilbertraums dieses Systems. Dadurch zeige ich, dass ein bestimmter Wert der geometrischen Phase mit einem faktorisierten projektiven Hilbertraum assoziiert ist. Aufbauend auf dieser Konstruktion führe ich eine Feinstruktur der Verschränkungsentropie ein, bei der die geometrische Phase als ein Maß betrachtet wird, das Zustände mit gleicher Verschränkungsentropie unterscheidet. Dies ermöglicht es mir, Wurmloch-ähnliche Physik mit einfachen Quantensystemen zu assoziieren. Um eine Verbindung zu Gravitationstheorien und der AdS/CFT-Korrespondenz herzustellen, untersuche ich die geometrische Phase des Thermofeld-Doppelzustands (TFD-Zustand). Zu diesem Zweck leite ich zunächst den TFD-Zustand für das wechselwirkende Zwei-Qubit-System und insbesondere die Verschränkungstemperatur in Abhängigkeit der geometrischen Phase her. Damit wird deutlich, dass die (Verschränkungs-)Temperatur mit Hilfe eines geometrischen Konzepts in der Quantentheorie verstanden werden kann, ähnlich wie in Gravitationstheorien, wo Temperatur dadurch entsteht, dass der Beobachter auf einen Teilbereich der Raumzeit beschränkt ist. Für den TFD-Zustand liefert die Feinstruktur der Verschränkung einen Hinweis auf die Topologie des Parameterraums. Nachdem ich dies auf der quantenmechanischen Seite erörtert habe, fahre ich damit fort, die topol-

ogische Phase für den TFD-Zustand durch eine Gravitationsberechnung, insbesondere im Rahmen der JT-Gravitation, zu ermitteln. Ich kommentiere die Möglichkeiten, diese Feinstruktur sowohl für das Qubit-System als auch für den TFD-Zustand experimentell zu messen.

Im nächsten Schritt verallgemeinere ich die bisherigen Ergebnisse, indem ich geometrische Phasen in AdS_3/CFT_2 betrachte. Insbesondere diskutiere ich Virasoro-Berry-Phasen und modulare Berry-Phasen. Betrachtet man das ewige Schwarze Loch in der Gravitationstheorie, so zeigt die Berechnung der Virasoro- und der modularen Berry-Phasen, dass sie beide von den Eigenschaften des Wurmlochs abhängen. Daher sind sowohl die Virasoro- als auch die modulare Berry-Phase, aber auch die topologische Phase des TFD-Zustands, Indikatoren für die Eigenschaften des Wurmlochs und können zur Diagnose der Nicht-Faktorisierung verwendet werden. Insbesondere werden diese Phasen in der Feldtheorie berechnet, d.h. sie untersuchen die Nicht-Faktorisierung für den Hilbertraum der Feldtheorie. Dieses Ergebnis zeigt, wie geometrische Phasen für die Diagnose der Nicht-Faktorisierung in der AdS/CFT-Korrespondenz unerlässlich sind.

Als dritten Punkt schlage ich eine direkte Brücke zwischen den oben beschriebenen geometrischen Phasen und der Klassifizierung von Operator-Algebren. Solche Algebren gehören in den Bereich eines axiomatischen/algebraischen Ansatzes für die Quantenfeldtheorie. Anhand von Zustandsvektoren, die als Beschreibung einer Spin-Kette verstanden werden können, zeige ich, dass der Wert der geometrischen Phase eines bestimmten Zustandsvektors bestimmt, ob dieser Zustandsvektor ein Spurenfunktional auf der Algebra definiert. Dies liefert insbesondere eine geometrische Erklärung für die grundlegend unterschiedlichen Eigenschaften von Algebren vom Typ II und Typ III. In einer Anwendung auf das ewige Schwarze Loch in AdS/CFT diskutiere ich, wie die topologische Phase des Thermofeld-Doppelzustands mit einem nicht-trivialen Zentrum der entsprechenden Operator-Algebren verbunden ist. Dabei wird die topologische Phase als Indikator für die Nicht-Faktorisierung der Operator-Algebren verstanden, oder anders gesagt, für ein nicht-triviales Zentrum. Darauf aufbauend führe ich geometrische und topologische Phasen als allgemeineren Indikator für Informationen ein, die für einen lokalen Beobachter unzugänglich sind. Ich diskutiere dies an verschiedenen Beispielen, die von einem einzelnen Qubit in einem Magnetfeld bis zu Virasoro- und modularen Berry-Phasen in AdS/CFT reichen.

Zu guter Letzt schlage ich geometrische Quantendiskordanz als ein zweites geometrisches Maß für Nicht-Faktorisierung vor. Geometrische Quantendiskordanz bietet ein qualitatives Maß für das allgemein schwer zu berechnende Maß der Quantendiskordanz. Ich untersuche dies insbesondere für reine Zustände, bei denen sich die Quantendiskordanz auf die Verschränkungsentropie reduziert. Ich leite eine allgemeine Formel für geometrische

Quantendiskordanz für reine Zustände ab. Diese Formel zeigt die Nicht-Faktorisierung in Form eines Verhältnisses von modularen Zustandssummen. Ich erörtere, wie dieser Begriff der Nicht-Faktorisierung mit dem zuvor diskutierten Kriterium mittels geometrischer Phasen vereinbar ist. Insbesondere analysiere ich die Implikationen dieses Ergebnisses für das ewige schwarze Loch in AdS/CFT. Schließlich erörtere ich, wie eine einfache Verallgemeinerung der geometrischen Quantendiskordanz die Untersuchung von Mikrozuständen des schwarzen Lochs ermöglicht.

Die in dieser Arbeit diskutierten Ergebnisse sind in den in App. A gelisteten Originalveröffentlichungen publiziert worden.

Contents

1 Introduction

The beginning of the 20th century saw a surge in studies of physical phenomena at the microscopic level. The theoretical analysis of atoms, combined with complementary experimental results, led to the establishment of the Rutherford–Bohr model, where electrons orbit the nucleus, much like planets orbit a star [1, 2]. Stable orbits about the nucleus were postulated to be quantised, with electrons jumping between the orbits by the emission or absorption of a (correspondingly quantised) amount of energy. While this model was largely consistent with the experimental results of the time, it also had its drawbacks and puzzles. To name one of each, this model assumes that the electrons do not radiate, although they are accelerated to stay in the orbit. Moreover, this model does not account for the quantised orbits. In particular, this quantisation of energy involves the (reduced) Planck constant $\hbar$, which was found by Planck when studying the spectrum of a radiating black body [3]. Resolving these shortcomings was eventually possible by using the back then freshly developed theory of *quantum mechanics* [4, 5], resulting in the current understanding of atoms in terms of orbitals.

The advent of quantum mechanics at the beginning of the last century turned our perception of reality upside down. The Copenhagen interpretation of quantum mechanics, which ascribes an inherently probabilistic character to quantum mechanics, is the most popular interpretation. Still, this interpretation was widely debated in the early days of quantum mechanics, reflected in (seemingly absurd) statements about felines being dead and alive. The objections to an intrinsically probabilistic nature were shared even by Albert Einstein, summarised in his famous remark that "[...] god does not throw dice" [6]. Even harder to justify is the fact that quantum mechanics has many other interpretations, a popular one being the many worlds interpretation [7], which provides a deterministic description of quantum mechanics. Interestingly, as all of these interpretations are consistent with experimental results and in particular do not predict different measurement outcomes for the same process, all interpretations have to be considered equally valid. These difficulties in interpreting quantum mechanics are probably best summarised by Niels Bohr, himself one of the founding fathers of quantum mechanics, stating that "Those who are not shocked when they first come across quantum theory cannot possibly have understood it" [8].

Despite these, also philosophical, issues of quantum mechanics, it proved to be indispensable in describing microscopic physics to astounding precision. Moreover, well-known classical relations such as $p = mv = m\dot{x}$ can be derived from the Schrödinger equation

when replacing the classical quantities p and x by the expectation values of the corresponding operators $\hat{p}$ and $\hat{x}$. This is formalised in the Ehrenfest theorem [9]. In the limit $\hbar \to 0$, where the uncertainty in measuring $\hat{x}$ and $\hat{p}$ goes to zero, Newton's second law follows from the Schrödinger equation by the Ehrenfest theorem. Therefore, the laws of classical physics are contained within quantum mechanics and are valid when $\hbar \to 0$, which correspondingly has the interpretation of the classical limit. Since classical mechanics is a limit of quantum theory, the latter is more fundamental and provides a description closer to nature. More precisely, given a property of a classical particle, this property is also present quantum mechanically. However, the converse is generally not true as there exist properties characteristic to quantum mechanics that are absent in the classical limit. Examples are given by spin [10] and the uncertainty principle [11]. An extensive discussion on this point is provided in the classic work on quantum mechanics by Paul Dirac [12]. However, the most striking distinction between classical and quantum physics is given by *entanglement* [13, 14]. This is based on a thought experiment conducted by Einstein, Podolski and Rosen [15] who famously coined entanglement as a "spooky action at a distance". Given two entangled particles, measuring one of the particles leads to a collapse of the wave function. In turn, this determines the measurement outcome of the second particle, although this has not yet been measured. The peculiarity of this property lies in the fact that, for this effect, the particles do not have to be 'close' to each other. Rather, once the particles are entangled by a local interaction, suppose that one of them is transported to the summit of Kilimanjaro, while the other is sent to the Röntgen lecture hall at Würzburg University. Irrespective of the large spatial separation, the statement about the measurement results remains valid.

Shortly before the time that quantum mechanics blossomed, a further field of physics experienced substantial progress. In contrast to quantum mechanics, this field is mainly concerned with large-scale structures such as planets, galaxies and the universe as a whole, i.e. classical physics. The first important development due to Albert Einstein is *special relativity* [16, 17]. This theory states that the speed of light c is a constant and nothing can move faster than light. Special relativity is particularly important at velocities v close to the speed of light. In the limit $\frac{v}{c} \to 0$, i.e. slow velocities compared to the speed of light, the laws of special relativity reduce to Newton's laws. To formulate gravity in a relativistic way, Albert Einstein extended his theory to *general relativity* [18–20]. The power of this theory was first shown by resolving a difference in the perihelion motion of mercury between the experimental observations and the predictions according to Newton's law of gravity [21]. Moreover, general relativity explained the bending of light in the presence of mass. More generally, the Einstein field equations of general relativity tell how masses and the corresponding gravitational force determine the paths of any matter, and vice versa,

how spacetime emerges as a consequence of a matter distribution. The simplest vacuum solutions to these field equations give rise to black hole spacetimes where the gravitational attraction in a region of spacetime is so strong that not even light can escape [22, 23]. In honour of their discoverer, such regions are defined by their Schwarzschild radius. Finally, cosmological models such as the Big Bang theory and the steady state theory are based on solving the field equations of general relativity with a simplified matter content [24], backed up by experimental observations on the expansion rate of the universe [25].

Unifying special relativity and quantum mechanics led to quantum field theory (QFT), where particles are understood as excitations of the underlying quantum fields [26–28]. This provided a hugely successful framework to study particle physics at high energies, leading to quantum descriptions of the electric force [26, 29, 30], the weak force [31–34] and the strong force [35–37]. These theories together make up the standard model of particle physics. In particular, the quantum theory of electrodynamics (QED) has undergone many measurements confirming the theoretical description. An outstanding example is the theoretical explanation using QED for the deviation of the electron g-factor from 2 [38, 39], which is experimentally known with a relative standard uncertainty of the order of 10^{-13}, see e.g. [40]. In a sense, the standard model is even a little 'too successful'. There is unpleasantly little room for extensions within this model to explain the open questions, such as gravitational effects on the quantum level and the matter/antimatter asymmetry, while keeping consistency with the experimental observations.

Attempting a unification of the principles of quantum mechanics with general relativity, the standard techniques of QFT fail. To be more precise, a QFT-like description of the exchange particle of gravity, dubbed the graviton, is not straightforwardly attainable at high energies. Indeed, at low energies, scattering of so-called 'soft gravitons' can be studied by the established methods of QFT [41] (for detailed explanations, see e.g. [42, 43]). However at high energies, the renormalisation of scattering amplitudes requires infinitely many renormalisation constants. Since such constants have to be fixed by experiment, infinitely many constants can never be fixed (in finite time). This follows from the fact that the coupling constant of gravity, i.e. the Newton constant G_N, has a negative mass dimension. Therefore, gravity described by general relativity is a non-renormalisable theory and can only be valid as an effective field theory up to some high energy scale. Typically, this scale can be understood as the Planck scale, in particular the Planck mass m_P, which can be understood as follows. Collecting an amount of mass of the order of m_P in a region small enough, gravity becomes strong at the quantum level, as this can be interpreted as a tiny black hole with Schwarzschild radius proportional to the Planck length l_P [44, 45].

Due to these problems, new approaches to a unification, i.e. a theory of quantum gravity valid at any energy, have to be studied. Among other ideas, this sparked a geometric ap-

proach to quantum mechanics. The development of classical mechanics, and in particular general relativity, was a powerful demonstration of how the use of geometric notions such as curvature enables to understand physics and the corresponding theoretical description. Motivated by this idea, physicists started to reformulate quantum mechanics in geometric terms, associating a geometric equivalent to every property of quantum systems [46, 47]. An early result showed that the Schrödinger equation can be reformulated in terms of the Hamilton equations of motion [48]. Further examples include reformulating the notion of the Heisenberg uncertainty principle [49] and the collapse of the wave function [50] in terms of a Riemannian metric. Moreover, quantum states were associated with points on a Kähler manifold [49]. This also dispelled the remaining doubts about how fundamental quantum mechanics is, as discussed e.g. in [49]. As mentioned before, classical mechanics follows from quantum mechanics in the limit $\hbar \to 0$, so quantum theory is considered to be more fundamental. Moreover, there exist phenomena in quantum mechanics without classical limits. However, in its usual formulation in terms of linear operators and Hilbert spaces, quantum mechanics is an inherently linear theory without any non-trivial notion of geometry. On the other hand, classical mechanics has a rich geometric description by symplectic geometry, resulting in a non-linear theory. In physics, linear treatments usually arise as approximations to the non-linear theory. Expanding the non-linear equations in small perturbations, the resulting linear equations can typically be solved. This seemed to suggest that classical mechanics is more fundamental, or at the very least, the usual occurrence of linear theories as approximations is different in quantum mechanics. The geometric formulation of quantum mechanics provided a non-linear (and obviously geometric) theory, clearing out these concerns.

In a complementary development, the currently most successful theory of quantum gravity was established by reinterpreting an early approach to a quantum theory of the strong force, where colour flux tubes were described by strings [51–54]. While this approach was discarded as a description of the strong force, the string excitations were shown to include a massless degree of freedom with spin 2, matching the properties of the graviton [55, 56]. This observation led to the development of *string theory*, replacing point particles as the fundamental objects with strings, objects with spatial extension. What we conceive as different particles are different excitations of a string. Every known version of string theory contains the graviton and is therefore a theory of quantum gravity. While quantum gravity is notoriously impossible to be described by QFT, it appears automatically in the formulation of string theory. In particular, the entropy of specific black holes has been computed in string theory [57]. Moreover, all particles of the standard model and their various interactions are expected to be described by string theory. The five versions of string theory obtained in these studies [58–60] were later argued to follow from a single theory, called

M-theory [61]. While the five versions of string theory require ten spacetime dimensions [62], M-theory requires eleven spacetime dimensions where strings are generalised to membranes [63]. Since this theory is expected to include every particle and interaction known to physicists, it provides a candidate for a 'theory of everything'. However, the precise understanding of this theory is not yet complete and is the subject of ongoing research. Nevertheless, the study of string theory has allowed for many insights into the nature of quantum gravity as well as QFT. Moreover, it led to new results in pure mathematics, manifesting the long and fruitful interplay between physics and mathematics. Examples include the Verlinde formula for the volume of state space of Chern—Simons theory [64] as well as the Witten conjecture on intersections in the moduli space of curves [65]. Both were inspired by string theory considerations and rigorously proven later on in [66–68] and [69–71] respectively. With general relativity being heavily based on differential (in particular Riemannian) geometry, string theory as its (potential) generalisation to include quantum mechanics involves many geometric notions as well. In particular, scattering amplitudes in string theory are characterised by the genera of Riemann surfaces. Correspondingly, operator insertions are understood as punctures of the string theory worldsheet. In other words, as summarised by Edward Witten, "String theory at its finest is, or should be, a new branch of geometry" [72].

In a specific setting, M-theory has been given a precise non-perturbative treatment as a matrix theory [73]. However as mentioned before, M-theory and also string theory are not yet fully understood. The most significant development in this area in recent years, leading to a plethora of new insights, was the proposal of the *AdS/CFT correspondence* by Juan Maldacena [74]. Here, AdS is short for Anti-de Sitter, with CFT the acronym for conformal field theory, i.e. a QFT with conformal symmetry. This correspondence states a duality between a string theory on a D-dimensional Anti-de Sitter spacetime background, referred to as the bulk, and a CFT in $D-1$ dimensions, defined on the conformal boundary of the Anti-de Sitter spacetime [75]. In particular, the boundary values of the fields propagating on Anti-de Sitter spacetime are identified with the sources for the operators in the CFT [76]. It is worth highlighting that this duality relates two theories that are well-defined on their own. In seemingly similar dualities such as the bulk-boundary correspondence in solid-state physics (see e.g. [77] for a review) or algebraic holography [78, 79] the boundary description exists only as a limit of the bulk description. While such dualities of course have their use, they do not come as surprising as a duality between a priori completely independent theories. The AdS/CFT correspondence relates fundamentally different theories, while the theories in the bulk-boundary correspondence or algebraic holography are intrinsically linked by definition. In light of the search for a theory of quantum gravity, the correspondence provides a powerful tool. The string theory,

which includes quantum gravity degrees of freedom, is dual to a CFT defined on a fixed (usually flat) background, i.e. a theory without gravity. Therefore, the CFT must include knowledge about quantum gravity without itself having an (obvious) notion of gravity built in. A precise understanding of how the quantum gravity degrees of freedom are encoded within the CFT is paramount to developing a theory of quantum gravity describing our world and an evergreen question in pinpointing why AdS/CFT works. It should be noted that an Anti-de Sitter spacetime has constant negative curvature, while experiments show that we live in a universe with either vanishing or positive curvature [80, 81]. However, while some observed features of quantum gravity are specific to the Anti-de Sitter spacetime, AdS/CFT nevertheless provides a platform for developing an expectation on the general behaviour of theories of quantum gravity. Moreover, there exist generalisations of AdS/CFT to dS/CFT [82–86] and flat space holography [87–92] with a particularly well understood version known as celestial holography [93–95], providing analogous dualities for spacetimes observed in our universe. Last but not least, it is interesting to note that AdS/CFT has been useful as a computational tool to analyse strongly coupled quantum systems in terms of the dual theory of gravity. This led to the fields of AdS/CMT, with CMT short for condensed matter theory, and AdS/QCD, with QCD short for quantum chromodynamics. One of the most famous results of these areas is the holographic computation of the shear viscosity in strongly coupled supersymmetric gauge theory using the AdS/CFT correspondence [96]. In an application to the quark-gluon plasma in QCD, using holography it has been argued that the ratio of the shear viscosity to the entropy density has a universal lower bound [97, 98]. This result has indeed been confirmed by experiment [99]. For more details on AdS/CMT and AdS/QCD, we refer the interested reader to [100–103] and [104–107], respectively, and references therein.

One of the properties expected to be present in any theory of quantum gravity is the *holographic principle*. This principle is based on the Bekenstein bound, which states that the entropy of a region in spacetime must not exceed the boundary area of the region divided by $4G_{\mathrm{N}}$, with G_{N} the Newton constant [108]. Before the entropy can exceed this ratio, a black hole forms and the Bekenstein bound is saturated, matching Stephen Hawking's calculation of the black hole entropy [109, 110]. Proposed by Gerard 't Hooft shortly before AdS/CFT arrived, the holographic principle states that the degrees of freedom in any theory of quantum gravity do not scale with the volume but with the boundary area of the volume that the theory is defined in [111]. The AdS/CFT correspondence provides an explicit (and the first) realisation of the holographic principle, which is why a better understanding of AdS/CFT is expected to also shed more light on the nature of quantum gravity in general. In particular, the AdS/CFT correspondence allows to study black holes by the dual field theory. A remarkable example of this duality was proposed in [112], which

relates the *thermofield double state* (TFD state) to the eternal black hole. The latter can be interpreted as a non-traversable wormhole. More precisely, the eternal black hole as the maximal extension of the Schwarzschild black hole geometry in Anti-de Sitter spacetime has two asymptotic boundaries, on each of which a copy of the same CFT is defined. The dual to this bulk geometry is given by the two CFTs entangled in the TFD state,

$$|\mathrm{TFD}\rangle = \frac{1}{\sqrt{Z(\beta)}} \sum_n e^{-\beta \frac{E_n}{2}} |n_L, n_R^*\rangle \,, \tag{1.1}$$

where $|n_{L/R}\rangle$ are the energy eigenstates and $\beta = \frac{1}{T}$ is the inverse temperature of the black hole. This duality is a first indication that entanglement in the CFT, which is a purely quantum feature, is important when it comes to describing classical spacetime geometry. In fact, by the *Ryu–Takayanagi formula* (RT formula), the entanglement between two subregions of the CFT is holographically dual to the area of a minimal surface in the bulk. This minimal surface connects the endpoints of the CFT subregions through the bulk [113, 114]. Similar to the Bekenstein bound and the black hole entropy, the RT formula provides a characterisation of entanglement in terms of a geometric object, in particular an area. Combining these two insights on the interplay between entanglement and spacetime geometry, it has been suggested that this is a general principle and 'entanglement creates spacetime' [115–117]. In particular, by the RT formula it is clear that the area interfacing two regions of spacetime vanishes if and only if these regions are not entangled. As the surface in this case vanishes, this implies that the spacetime describing two unentangled regions is not connected. These considerations entered the *ER=EPR* proposal [118], which states the equivalence between entanglement as first discussed by Einstein, Podolski and Rosen [15] (the EPR part) and spacetime wormhole solutions as first introduced by Einstein and Rosen [119] (the ER part).

The duality between the eternal black hole and the TFD state however also leads to a puzzle within the AdS/CFT correspondence. From the field theory perspective, the two CFTs do not share any classical interaction and therefore the Hilbert space of the CFT is expected to factorise as $\mathscr{H} = \mathscr{H}^{(L)} \otimes \mathscr{H}^{(R)}$, with $\mathscr{H}^{(L/R)}$ the Hilbert spaces of the CFTs defined on the left and right boundaries. On the contrary, as discussed in the previous paragraph, the bulk spacetime is given by a smooth geometry. In particular, there exist geodesics connecting the left and right boundary, so the bulk Hilbert space is manifestly non-factorised. This difference in the Hilbert space structure has been coined the *factorisation puzzle* [120]. An important part of better understanding the mechanism behind the AdS/CFT correspondence, as an eventual non-perturbative theory of quantum gravity, lies in resolving this puzzle, as we explain in more detail shortly. Significant progress in this direction has been achieved using methods of *axiomatic quantum field*

theory (AQFT), which reformulates QFT using sets of axioms [121–123]. Of central importance to this field is the characterisation of the algebra of observables, usually a von Neumann algebra. Such algebras were developed in the early days of quantum mechanics by John von Neumann and also Francis Murray in a series of papers [124–131]. Applying these methods to the eternal black hole and the dual CFTs, it has been discussed how the black hole interior can be studied [132, 133]. Moreover using von Neumann algebras, the black hole entropy has been computed [134–138] and the quantisation of two-dimensional gravity with matter was analysed [139, 140]. In general, the study of such algebras for specific systems provides a rigorous way to discuss entanglement for quantum systems. Both the ER=EPR proposal as well as the factorisation puzzle are deeply tied to the existence of entanglement between subregions of the CFT on the boundary. Correspondingly, operator algebraic methods are well suited to refine the statements about the ER=EPR proposal but also to pinpoint the origin of the factorisation puzzle.

Resolving the factorisation puzzle is very likely to provide a much more precise understanding of the mechanism behind the holographic principle, and thereby of the mechanism behind the AdS/CFT correspondence. As the holographic duality states the dynamical equivalence between a theory of quantum gravity and a QFT, such a resolution is expected to answer or at the very least address the question of how different quantum mechanics and general relativity actually are. Taking the ER=EPR proposal seriously, these two theories should be fully equivalent, as has also been argued by Leonard Susskind [141]. In fact, the Einstein equations have been derived from entanglement properties in various instances [142–144]. With gravitational effects mapped to entanglement dynamics, this should in principle enable to understand gravitational dynamics through the experimental study of entangled quantum systems. This has led to developing *analogue gravity*, where systems, usually from condensed matter physics, are prepared such that measurements of the systems provide insights about the gravitational theory modelled by the system, as reviewed e.g. in [145]. In particular, significant progress has been made in establishing protocols that realise teleportation of information through analogues of traversable wormholes [146, 147] (see also [148]). More generally speaking, in the 21st century experiments probing the regime of quantum gravity are advancing [149]. Examples include measuring gravitational waves [150], the Unruh effect [151], taking pictures and detailed data collections of the astrophysical black holes Messier 87 [152] and Sagittarius A* [153] [1] and mapping the gravitational wave background [154]. With such measurement results becoming more frequent and gaining in precision, predictions of theories of (quantum) gravity can be tested for

[1] It should be noted that, while these measurements provide immensely strong evidence that these objects are indeed black holes, strictly speaking the measurements do not prove it, as these objects could be other unknown formations of enormous mass. However, there are no candidates for such alternative massive objects, so current wisdom considers these objects to actually be black holes.

their validity in our universe. Especially for analogue systems modelling gravity, in order for such tests to be reliable, it is important to establish criteria discerning to which degree the analogue system captures the properties expected from gravity.

In light of these developments, let us now discuss in more detail the goals pursued in this thesis, and by which methods we approach these goals. In view of the above described exciting advancements, in this thesis we study entanglement properties and non-factorisation both from a quantum mechanical as well as a gravitational point of view. Apart from contributing to an eventual resolution of the factorisation puzzle, this also is an important step towards studying ER=EPR and the factorisation puzzle in the lab. As alluded to in the previous paragraphs, notions of geometry have often been useful in gaining a deeper understanding of physics [155]. In this spirit, we probe non-factorisation by calculating geometric phases both in quantum mechanics and gravity. Geometric phases have many applications in physics. Important examples include the topological invariants explaining the quantisation of the Hall conductance in the quantum Hall effect [156–159], the topological invariants classifying topological insulators [160] and the instanton number in the quantum theory of the strong force classifying the observed vacuum structure of this theory [161, 162]. As discussed by Sir Michael Berry in the seminal paper [163], geometric phases, which are also known as Berry phases, arise when the parameters of a system vary adiabatically to form a closed path in parameter space. Mathematically, geometric phases can be understood as the holonomy of a fibre bundle [164]. More precisely, geometric phases are related to the properties of the symplectic form defined for the bundle. If this symplectic form is non-exact, the geometric phase defined as the integral of the symplectic form is non-trivial. This has an interesting connection to wormhole physics. Given any quantum system with a non-exact symplectic form, it was shown that the corresponding path integral includes contributions from replica wormholes [165].[2] This provides a strong hint that geometric phases become important when discussing wormhole physics and non-factorisation. By the ER=EPR proposal, this non-factorisation and the corresponding wormhole physics should have a counterpart in terms of properties of the entanglement. In this context, an important tool is what we will refer to as the *SZK construction* [166]. This establishes a geometric interpretation of entanglement for bipartite quantum systems in terms of submanifolds of the projective Hilbert space of the system. Analysing the symmetries of a pure state for a fixed value of the entanglement entropy allows for a straightforward derivation of the corresponding submanifold.

One of the main results of this thesis concerning non-factorisation is the calculation

[2] A physical wormhole, such as the eternal black hole in Anti-de Sitter spacetime, is a solution to the Einstein equations and hence has a precise spacetime interpretation, connecting two space-like separated regions. Contrary, replica wormholes represent correlations between several copies of the same theory and do not necessarily have a similar spacetime interpretation.

of geometric phases within the SZK construction. We show explicitly for a model of two interacting qubits how the geometric phase arises and how the submanifolds of the projective Hilbert space are associated to different values of the geometric phase. This in particular allows us to establish the geometric phase as a measure for non-factorisation of the projective Hilbert space. Due to the relation between non-exact symplectic forms and wormhole physics, we interpret our result as a manifestation of entanglement creating space(time). In a setting more akin to AdS/CFT, we apply the same techniques to the TFD state dual to the eternal black hole. Making use of an independent choice of time in the left and right exterior region of the black hole, we define a geometric phase for the TFD state that is sensitive to the non-factorised bulk geometry. We show how the same phase can be obtained from a bulk computation in two-dimensional AdS gravity. We further propose experimental platforms to measure these geometric phases, both for the interacting two-qubit system as well as for the TFD state. We show that analogous results on geometric phases and non-factorisation hold in AdS_3/CFT_2 for Virasoro Berry phases [167] and modular Berry phases [168–170], which arise from conformal transformations and deformations of the subregion in the CFT, respectively. While the geometric phase of the TFD state, the Virasoro Berry phase and the modular Berry phase all probe different aspects of the bulk spacetime, we show that they are all useful in detecting the wormhole, and thereby non-factorisation.

We furthermore use geometric phases to characterise von Neumann algebras. These algebras are one of the fundamental objects in the framework of AQFT. The methods of AQFT allow for rigorous statements about the system under consideration. In particular, the type classification of von Neumann algebras establishes Hilbert space factorisation and entanglement as properties of the algebra. The most familiar algebras, which describe the notions of quantum mechanics we are used to, are type I algebras. For this type, irreducible representations can be defined, and correspondingly a bipartition of the Hilbert space can be defined without technical subtleties. Type I algebras describe finite-dimensional systems or special cases of infinite-dimensional systems. For arbitrary infinite-dimensional systems there exist the types II and III. Both these types lack an irreducible representation and correspondingly, the Hilbert space cannot be factorised rigorously. Closely related is the fact that both these types have a universal divergence of entanglement entropy, which associates the notion of entanglement to the operator algebra rather than to a specific quantum state of the system. When discussing entanglement, a particularly curious property of type III algebras is the absence of a well-defined trace on the algebra. Correspondingly, reduced density operators and the entanglement entropy are not defined. For type II and type I, this issue does not arise. For type I, all the familiar notions of textbook quantum mechanics work out. For type II, entanglement entropy can be understood as a rescaled version of the

type I entanglement entropy. Finally, von Neumann algebras $\mathscr{A}$ can have commutants $\mathscr{A}'$, consisting of all operators that commute with operators of $\mathscr{A}$. The operators common to both $\mathscr{A}$ and $\mathscr{A}'$ form the centre of the algebra. If the centre consists only of operators proportional to the identity, the centre is said to be trivial and the corresponding algebra is referred to as a factor. Non-trivial centres arise e.g. in the presence of global symmetries. In the context of operator algebras, apart from Hilbert space factorisation also exists the notion of algebraic factorisation. That is, two algebras are deemed factorised if their centre is trivial, i.e. if they do not share any non-trivial operators. As quantum mechanics can be entirely phrased using geometry, it is an interesting question how properties of operator algebras are encoded geometrically. Furthermore in a series of recent papers, operator algebraic methods have been applied to the eternal black hole in Anti-de Sitter spacetime. The operator algebras describing QFT on a classical black hole spacetime are of type III [132, 133] and have a non-trivial centre related to the Hamiltonian of the system. Including gravitational corrections, it has been shown that the algebra can be deformed to type II with a trivial centre [134]. Remarkably, this is not entirely specific to Anti-de Sitter spacetime but also holds for black holes in asymptotically flat and asymptotically de Sitter spacetimes [171, 172]. It is worth clarifying that while a Hilbert space factorisation is only achievable for type I algebras, this transition between type III and II addresses the factorisation of the operator algebras. In the type III description, there exists a central element common to both algebras, while the centre is trivial in the type II case.

In this thesis, we show that the classification of von Neumann algebras, in particular between type II and type III, can be understood geometrically using the geometric phase. The trace can be defined using a state vector with a vanishing geometric phase. Using the insights gained on the geometric phases determining the entanglement by the SZK construction, we show that any state vector of a type III algebra has a non-vanishing geometric phase. This provides a geometric explanation for the absence of the trace on type III algebras, related to the geometric properties of the projective Hilbert space. However, for type II we show that there exists a state with a vanishing geometric phase. Correspondingly, the trace is defined, as it should be for type II algebras. We relate this to the aforementioned results on von Neumann algebras for the eternal black hole in Anti-de Sitter spacetime. In particular, we show that the geometric phase for the TFD state defined earlier can be understood as resulting from the non-trivial centre of the type III algebra found in [132, 133]. Correspondingly, this geometric phase is non-trivial for the type III description but vanishes when transitioning to the type II description of [134]. This provides an explicit realisation of our general result on von Neumann algebras for the eternal black hole within AdS/CFT. Moreover, this shows that the geometric phase of the TFD state is a probe for the factorisation of the operator algebras.

Apart from the entanglement entropy, there also exist other measures of entanglement, which in particular are better suited to quantify entanglement in mixed states. As the ER=EPR proposal does not restrict to the entanglement entropy, it is an interesting question how geometry and in particular non-factorisation is detected by other measures of entanglement. One of these measures is given by quantum discord proposed independently in [173, 174] and [175]. This measure captures quantum correlations contained in separable states, as quantum discord can be non-zero when other measures of mixed state entanglement such as the entanglement of formation vanish [174]. Apart from quantum information science, quantum discord has also been studied in cosmological settings, such as de Sitter spacetime [176]. A particularly interesting approach is taken in [177–179], where quantum discord is analysed in relation to fluctuations in the cosmic microwave background. Non-vanishing quantum discord indicates quantum correlations between spatially separated regions. This enables to gain insights into the (entanglement) dynamics of the big bang [176–179]. Unfortunately, computing quantum discord for an arbitrary state is demanding, and it was shown that this is an NP-complete problem [180]. A measure that is easier to compute is given by geometric quantum discord (GQD), proposed by the authors of [181] based on their discussion of a sufficient and necessary condition for non-vanishing quantum discord. GQD is significantly easier to calculate as this measure requires a minimisation only over states, as opposed to the minimisation over measurements necessary for quantum discord. Furthermore, GQD is defined in terms of the Hilbert–Schmidt norm and therefore provides a notion of distance between different states in terms of the correlations within the states.

In this thesis, we propose GQD as an alternative measure of non-factorisation. We show this explicitly for arbitrary pure states. For the interacting two-qubit system analysed previously, we show that the non-factorisation indicated by GQD is consistent with the non-factorisation indicated by the geometric phase and the corresponding submanifold of the projective Hilbert space. We apply these results to the TFD state to show non-factorisation purely from the boundary perspective. This also amounts to deriving the thermomixed double state (TMD state), defined in [182] based on bulk considerations as a decohered mixed state describing the black hole with only classical correlations, in a purely quantum information theoretic way. Based on these considerations, we propose that a non-vanishing quantum discord always leads to non-factorisation.

To properly explain our results, we first review some details on entanglement entropy in sec. 2.1, followed by introducing the AdS/CFT correspondence and the factorisation puzzle for the eternal black hole in sec. 3. The remaining secs. 4, 5, 6 and 7 contain the derivation and discussion of our results. In more detail, the outline of this thesis is as follows:

- In section 2 we review properties and measures of entanglement. We do so in great detail to provide a comprehensive picture and to introduce the notation used in later sections of this thesis. We start in sec. 2.1 by discussing entanglement and its most famous measure, the von Neumann entropy, in quantum mechanics and QFT. We also discuss two alternative measures of entanglement, namely the Rényi entropy and quantum discord. The notion of entanglement as correlations manifestly of a quantum nature will be of central importance in this thesis. In sec. 2.2 we start by briefly reviewing a geometric reformulation of quantum mechanics, in particular the projective Hilbert space and geometric phases defined as holonomies of principal fibre bundles. Subsequently, we review two ways to analyse entanglement using geometry, namely the SZK construction defining submanifolds of the projective Hilbert space for given values of the entanglement entropy as well as geometric quantum discord, each of which are core elements to later sections of this thesis. Finally in sec. 2.3, we review aspects of AQFT relevant to this thesis. In particular, we introduce operator algebras and the type classification of von Neumann algebras. We then discuss entanglement in this setting, which for two of the three types can be understood as a property of the algebra rather than a property of the quantum state.

- In section 3 we review the second pillar of this thesis, namely the AdS/CFT correspondence. We start in sec. 3.1 by revisiting the holographic principle, based on the black hole entropy and the Bekenstein bound. We then introduce the AdS/CFT correspondence as an explicit realisation of the holographic principle. We briefly explain the idea behind the holographic dictionary and focus on a particular entry, namely the relation between entanglement entropy in the CFT and the dual geometric description. Next in sec. 3.2, we discuss the factorisation puzzle arising for black holes in the context of the AdS/CFT correspondence. We start by explaining the duality between the eternal black hole in Anti-de Sitter spacetime and the TFD state using the Hartle–Hawking wave functional. We briefly touch on time-shifted TFD states as a bigger class of states dual to the eternal black hole. We then explain one of the main topics of this thesis, namely the factorisation puzzle, in detail. We also discuss the ER=EPR proposal relating quantum entanglement to classical geometry, which is realised by the eternal black hole and the TFD state.

- In section 4 we discuss the new results obtained in [183] and parts of [184]. First off in sec. 4.1, we discuss a system of two interacting qubits, in particular the entanglement properties of the ground state of this system in using the SZK construction introduced earlier. We derive a way to calculate the geometric phase for this ground state within the SZK construction and show how this geometric phase, capturing the geometry

of the projective Hilbert space, determines the entanglement entropy. Moreover, in light of the SZK construction, we establish how the factorisation of the projective Hilbert space is captured by the value of this geometric phase. We finally discuss a second type of geometric phase that distinguishes between states with the same entanglement entropy, which we dub as a fine structure of the entanglement. Next in sec. 4.2, we turn towards studying geometric phases for the TFD state. As a partially preparatory task, we derive the TFD state and the entanglement temperature for the two-qubit system previously discussed. Our brief analysis of the TFD state within the SZK construction is followed by defining a topological phase for the TFD state, sensitive to the topology of parameter space rather than the geometry of the projective Hilbert space. For the two-qubit system, we show that this topological phase is related to the geometric phase defined earlier. Also for the topological phase of the TFD state, we define the fine structure of entanglement. We conclude this section by discussing how this topological phase can be computed in the dual gravitational picture by an explicit example in two-dimensional AdS gravity, namely Jackiw–Teitelboim (JT) gravity.

- In section 5 we discuss the new results published in [185]. In this work, we generalise the insights before to the higher-dimensional case of AdS_3/CFT_2. In this setting, we discuss two kinds of geometric phases. We start in sec. 5.1 by briefly introducing the Virasoro Berry phase. Next, we discuss the toy model of $U(1)$ Chern–Simons theory on an annulus geometry to illustrate how the holonomy and its canonical conjugate signal non-factorisation between the two boundaries of the annulus geometry. We generalise this to $SL(2,\mathbb{R})$ Chern–Simons theory, which describes gravity on a three-dimensional asymptotic Anti-de Sitter spacetime, and show that again, the holonomy signals non-factorisation. Next in sec. 5.2, we discuss modular Berry phases. We first briefly describe how these are defined. In this setting, we study the modular Berry curvature for various thermal two-dimensional CFTs. For the eternal black hole setting, this again allows us to diagnose non-factorisation using the modular Berry curvature. We finally discuss which bulk features are probed by Virasoro and modular Berry phases, as well as the topological phase of the TFD state, by specifying and comparing the type of bulk diffeomorphisms corresponding to each of these phases.

- In section 6 we discuss the remaining new results derived in of [184]. The first part of this section concerns properties of operator algebras and their explanation using geometric phases. We start in sec. 6.1 by deriving a relation between a tracial state on the operator algebra and the geometric phase of the ground state for the interacting two-qubit system discussed in the earlier sec. 4. While this calculation

is mostly for illustrative purposes, we generalise this to infinite-dimensional settings subsequently. With this generalisation, we derive a relation explaining the absence of a tracial state on von Neumann algebras of type III in terms of the geometry of the projective Hilbert space. Finally, we apply these insights to the von Neumann algebras found in the context of the eternal black hole, which we also briefly review. This in particular relates the topological phase of the TFD state to the existence of a non-trivial centre for the von Neumann algebra, probing whether the algebras are factorised. Next in sec. 6.2, we discuss how geometric phases can be understood as signalling missing information for a local observer. We illustrate this in several examples, each for vanishing and non-vanishing entanglement. In the former case, we consider a single qubit in a magnetic field and Virasoro Berry phases for a single CFT. In the latter case, we consider Virasoro Berry phases for two entangled CFTs, the topological phase of the TFD state and the modular Berry phase with a wormhole geometry in the bulk.

- In section 7 we discuss the new results published in [186]. We first derive an expression for GQD for general pure states in sec. 7.1. We show that the result can be expressed using the second Rényi entropy as well as the modular Hamiltonian. The latter reformulation enables us to propose a non-vanishing GQD as an indicator for non-factorisation. We utilise again the interacting two-qubit system, for which we have already established non-factorisation in terms of the geometric phase, to demonstrate GQD indicating non-factorisation in an explicit example, consistent with the results on non-factorisation obtained using the geometric phase. In sec. 7.2 we first briefly provide details on the TMD state. We then apply our result for GQD to the thermofield double state to show non-factorisation from the boundary perspective. This analysis enables us to associate a new interpretation to the TMD state as the closest classical state to the TFD state. Finally in sec. 7.3 we show how GQD and a straightforward generalisation thereof can be used to analyse the time-shifted TFD states as microstates of the eternal black hole. We finish the section by discussing non-factorisation from the perspective of the path integral using the time-shifted TFD states.

- In section 8 we conclude this thesis by summarising and pointing out possible future directions.

Based on these calculations and considerations, there are four main results obtained in this thesis, which we summarise in the following.

- We establish an explicit relation between entanglement and the geometric phase in

an interacting two-qubit system. The geometric phase determines the factorisation properties of the projective Hilbert space. This can be viewed as a manifestation of entanglement creating space(time) and we interpret this result in terms of wormhole physics. We show that there exists a second type of geometric phase that distinguishes between states with the same entanglement entropy, which we interpret as a fine structure of entanglement. We propose experimental setups to measure this fine structure. Applying the analogous methods to the TFD state, we first show that temperature can be understood as arising from entanglement for the two-qubit system. In particular, we derive the entanglement temperature in terms of the geometric phase for the two-qubit system. We define a phase of topological nature for the TFD state, which has the interpretation of a winding number. This definition is possible since the time coordinates in the left and right exterior of the black hole can be chosen independently. This winding number arises due to the non-trivial topology of the corresponding parameter space. Also for this topological phase, we define a fine structure of entanglement analogously to the two-qubit system. Moreover, we propose an experimental setup to measure this fine structure. Finally, we show how this topological phase arises in the dual gravitational picture using an explicit example in JT gravity. These results are published in [183] and [184].

- We generalise the quantum mechanical results in the previous point to the higher-dimensional setting of AdS_3/CFT_2. By calculating Virasoro Berry phases and modular Berry phases, we show that these types of geometric phases also indicate the presence of a wormhole in the bulk. In particular, we show that the corresponding symplectic forms interpreted as the Berry curvatures are non-exact in the presence of the wormhole. For the Virasoro Berry phase, this is made manifest by a coupling term between the left and right asymptotic boundaries. The coupling is related to the mass of the black hole, which has to be equal when measured from both boundaries. This is the intuitive explanation for the non-factorisation. Moreover, the dual variable to the coupling is interpreted as an open Wilson line connecting both boundaries. For the modular Berry phase, calculating the symplectic form we find contributions from both the left and the right boundary in a non-factorised way. These terms appear whenever the time coordinates are not perfectly aligned, similar to the topological phase defined for the TFD state. Although these three kinds of phases probe slightly different aspects of the bulk spacetime, this shows the importance of geometric phases for diagnosing non-factorisation and wormholes in the dual bulk description. These results are published in [185].

- We characterise von Neumann algebras using the geometric phase in the spirit of

the SZK construction. In particular, we show that a trace on the algebra is defined using a state vector with a vanishing geometric phase. This provides an explanation for the absence of the trace on algebras of type III in terms of the geometry of the projective Hilbert space, as all state vectors appearing for such algebras have non-vanishing geometric phases. On the contrary, among the state vectors of type II algebras there is one state with vanishing geometric phase, which in particular is maximally entangled. This state therefore defines a trace on the von Neumann algebra. In light of recent results on von Neumann algebras in AdS/CFT and the eternal black hole, we apply our result to this setting. We discuss how the topological phase of the TFD state indicates the non-trivial centre of the type III description of the eternal black hole. The topological phase is therefore regarded as a diagnostic tool for the (non)-factorisation of the algebras. This also allows us to explain the transition between type III and type II algebras using this topological phase, as this phase vanishes precisely for one state of the type II description. We also discuss this result in the light of geometric quantisation of the classical phase space in gravity. We finally introduce a new interpretation of geometric phases in general as indicators of missing information for a local observer. We discuss this interpretation both for systems with and without entanglement, in particular a single qubit in a magnetic field, Virasoro Berry phases in a single CFT, Virasoro Berry phases in two entangled CFTs and modular Berry phases. These results are published in [184].

- We establish GQD as a second geometric measure of entanglement signalling non-factorisation from the boundary point of view. We first provide an explicit expression for GQD evaluated for pure states. Relating this result to the (modular) partition function, we find that GQD vanishes if and only if the modular partition function factorises. Using the interacting two-qubit system as an example, we show that this way of diagnosing non-factorisation is consistent with the earlier method using geometric phases. We then apply this result to the TFD state to diagnose non-factorisation from the boundary perspective dual to the eternal black hole. The computation of GQD provides a quantum information theoretic derivation of the TMD state. Moreover, the definition of GQD allows us to interpret the TMD state as the closest classical state to the TFD state. Based on these results, we conjecture that in general, non-vanishing quantum discord is responsible for non-factorisation. We comment on a possible dual bulk computation of GQD. Finally, we discuss GQD and a straightforward generalisation thereof as a probe for black hole microstates, given by the time-shifted TFD states. We discuss how these microstates can be understood as a source for non-factorisation in the path integral. These results are

published in [186].

Conventions and Notation

Unless stated otherwise, throughout this thesis we will use natural units, $c = \hbar = k_B = 1$. Metrics in Lorentzian signature are considered in the mostly plus convention, $\eta = \text{diag}(-1, 1, ..., 1)$. When counting dimensions, the time direction is always included. A theory in D dimensions therefore has $D - 1$ spatial dimensions and one time dimension.

Entanglement in Quantum Mechanics and Quantum Field Theory

2

The discovery of quantum mechanics at the beginning of the previous century has undoubtedly revolutionised the field of physics. One of the key features distinguishing quantum and classical mechanics is entanglement [13–15]. This phenomenon does not have a classical analogue, yet generic quantum states do have non-vanishing entanglement. To be more precise, entanglement describes quantum correlations between (at least) two subsystems of the full quantum system. Without an explicit choice of such subsystems, discussing entanglement is not possible. In the cases usually discussed in physics, this however is often naturally given. As an example, given a system of two particles, it is natural to consider each single particle as one subsystem, such that entanglement between the two particles can be discussed. More generally in QFT, usually one fixes a spatial region A and considers the complement of this region $\bar{A}$. This enables to discuss the entanglement in QFT as the quantum correlations between spatial regions. While entanglement in finite-dimensional quantum systems may be zero or non-zero depending on the particular setting, in QFT entanglement has a universal divergence. To quantify entanglement, the standard object to consider is the *entanglement entropy* or, named after its inventor, *von Neumann entropy*. For quantum systems described by a state vector, this measure is sufficient to capture all possible quantum correlations. For quantum systems without such a description, i.e. quantum systems in a mixed state, the entanglement entropy does not capture all quantum correlations. There exist many generalisations, although at the time of writing this thesis, it is not yet clear which measure (if it exists) captures best the entanglement within a mixed state.

We will mostly focus on studying entanglement for systems described by a state vector in this thesis. Moreover, we will derive methods to discuss entanglement by geometric means. For this reason, it suggests itself to make use of the geometric formulation of quantum mechanics [46, 47]. Within this description, one object of particular focus is the projective Hilbert space $\mathscr{P}(\mathscr{H})$. The Hilbert space $\mathscr{H}$ contains state vectors that differ by a global phase, and in particular treats such vectors as two different elements. However, no measurement is able to distinguish between two such state vectors and they should be considered as physically equivalent. This leads to defining the projective Hilbert space, where states are understood as equivalence classes of state vectors differing only by a phase. The geometric properties of projective Hilbert space allow for a geometric

interpretation of entanglement in terms of particular submanifolds of the projective Hilbert space [166]. This method is of central importance in this thesis as it will allow us to diagnose non-factorisation in quantum mechanics by the properties of the submanifolds of the projective Hilbert space. Finally, in the algebraic formulation of quantum theory involving the algebra of observables and quantum states defined as states on this algebra, entanglement can be understood as a property of the algebra in certain cases and more generally by the Reeh–Schlieder theorem [187]. One major goal of this thesis is to find a bridge between the geometric notion characterising entanglement and the algebraic notion of entanglement.

In the following, in sec. 2.1 we review in detail how the entanglement entropy is understood in quantum mechanics as well as in QFT, ending with a nod to other measures of entanglement. Subsequently, we introduce a geometric formulation of quantum mechanics and entanglement in particular in sec. 2.2. Finally, we explore formulating quantum mechanics and QFT in terms of algebras of observables in sec. 2.3, again with a particular focus on analysing entanglement in this language.

2.1. Spooky Action at a Distance

We start our review of entanglement by discussing properties of the von Neumann entropy in quantum mechanics in sec. 2.1.1. In this section, presenting basics on the mathematical formulation of quantum mechanics allows us to be complete in our presentation as well as to establish much of the notation used in later sections. We then move on to discuss entanglement entropy in QFT in sec. 2.1.2, in particular the presence of entanglement in the vacuum. Finally, we elaborate on other measures of entanglement of importance in this thesis, different to the entanglement entropy, in sec. 2.1.3, namely the Rényi entropies and quantum discord.

2.1.1. Von Neumann Entropy in Quantum Mechanics

Especially in the early days of quantum mechanics, many of the developments of quantum theory originated from thought experiments and (philosophical) discussions. In order to treat these developments more rigorously than just formulating them in words, the field of linear algebra proved immensely useful. Everything that constitutes quantum mechanics can be formulated in terms of states and operations on the space of all states. The relations between these operations, states and concepts of linear algebra are summarised

in four *postulates of quantum mechanics*.[1] The postulates are based on the *Dirac–von Neumann* axioms [12, 189]. In our discussion of these postulates, we restrict ourselves to closed quantum systems. While extensions to open quantum systems can be defined, this would lead too far from the main aspects of this thesis. Comprehensive reviews of the topics of the following discussion can be found in [188, 190–192].

Preliminaries on Hilbert Spaces and States

The first postulate concerns the notions of state space and states:

Postulate 1:

> The state space of an isolated quantum system is given by a Hilbert space $\mathscr{H}$. The state of the system is determined by the density operator ρ, which is a positive semi-definite operator with trace 1 that acts on the Hilbert space.

Let us give a few more details on the terms appearing in this postulate. First, a Hilbert space is understood as a complex vector space with a few conditions on top. Its precise definition is as follows:

Definition 1: A Hilbert space $\mathscr{H}$ is a complex vector space $\mathscr{V}$ that is

i) equipped with an inner product $\langle\cdot,\cdot\rangle : (v_1, v_2) \in \mathscr{V} \times \mathscr{V} \mapsto \langle v_1, v_2\rangle \in \mathbb{C}$

ii) a complete metric space under the distance function induced by the inner product.

A common example of a Hilbert space is $\mathbb{C}^n$. The inner product for any two elements v_1, v_2 of $\mathbb{C}^n$ is denoted by $\langle v_1, v_2\rangle = \langle v_1|v_2\rangle = \sum_i v_{1,i}^* v_{2,i}$, using the common bra-ket notation introduced by Dirac in the intermediate step. This Hilbert space occurs naturally when discussing finite-dimensional quantum systems, e.g. quantum systems with a finite number (e.g. n) of energy levels. In the following discussion, we always assume to be in such a scenario with a Hilbert space $\mathscr{H} = \mathbb{C}^n$.

As a Hilbert space is a refined vector space, we can associate a basis $\tilde{\mathscr{B}} \subset \mathscr{H}$ to the Hilbert space. The elements $|\tilde{i}\rangle \in \tilde{\mathscr{B}}$ span the full Hilbert space. By the Gram–Schmidt process, any basis $\tilde{\mathscr{B}}$ can be converted into an orthonormal basis $\mathscr{B}$ which also spans the full Hilbert space. Any vector $|\psi\rangle$ of the Hilbert space can correspondingly be written as

[1] The number of postulates depends on the particular exposition of quantum mechanics at hand. In other sources, there also appear three or five postulates. What is considered a 'subpostulate' in the former case is promoted to a postulate in its own right in the latter case. In this thesis, we follow the presentation of [188].

a linear combination of the basis elements $|i\rangle \in \mathscr{B}$ as

$$|\psi\rangle = \sum_{i=1}^{n} a_i |i\rangle \,, \tag{2.1}$$

where $a_i \in \mathbb{C}$. Due to the probability interpretation of quantum mechanics, every vector $|\psi\rangle$ has to be normalised to one, $\langle\psi|\psi\rangle = 1$. This will become more clear shortly when discussing the third postulate. For now, we just note that by evaluating $\langle\psi|\psi\rangle$ explicitly for (2.1), we find that the coefficients a_i are constrained as $\sum_{i=1}^{n} a_i^* a_i = 1$.

Vectors as in (2.1), in the language of quantum mechanics, are more commonly referred to as pure states. For any such vector we can also construct the density operator ρ as $\rho = |\psi\rangle\langle\psi|$. On the level of this operator, the constraint on the coefficients a_i is implemented as $\mathrm{tr}\,\rho = 1$. More generally, we can think of a situation where the density operator is given by a linear superposition of different $\rho_i = |\psi_i\rangle\langle\psi_i|$ weighted with coefficients p_i,

$$\rho = \sum_i p_i \rho_i \,. \tag{2.2}$$

Since ρ is a positive semi-definite operator, $p_i \geq 0$. Since $\mathrm{tr}\,\rho = 1$, we have $0 \leq p_i \leq 1$, consistent with the interpretation of p_i as probabilities. The density operator can therefore be interpreted as a mixture of pure states.

As long as at least two of the p_i's are non-zero, a density operator as given in (2.2) is commonly referred to as a mixed state. Given any density operator ρ without knowledge about the particular values of p_i, there is a simple criterion to determine whether ρ is pure or mixed known as purity $\gamma(\rho)$, defined as

$$\gamma(\rho) = \mathrm{tr}\left(\rho^2\right) . \tag{2.3}$$

If ρ is a pure state, then $\rho^2 = \rho$ since $|\psi\rangle$ is normalised. Correspondingly, for a pure state, $\gamma(\rho) = 1$, providing an upper bound for $\gamma(\rho)$.[2] For a mixed state however, evaluating the square leads to interference terms between different ρ_i. Therefore, for a mixed state $\gamma(\rho) < 1$. The lower bound for γ is provided by the maximally mixed state $\rho = \frac{1}{n}\mathbb{1}_n$, for which $\gamma(\rho) = \frac{1}{n}$.

We have now understood how to define the state space of a quantum system as well as which types of states are contained in the state space. However, we have not yet defined how the dynamics of this system are described. This is the purpose of the second postulate:

[2] Note that in general the trace of any power of ρ cannot exceed 1, i.e. $\mathrm{tr}(\rho^n) \leq 1$, since $0 \leq p_i \leq 1$.

Postulate 2:

The time evolution of a closed quantum system is governed by a unitary transformation U. The unitary transformation relating the states $\rho(t_2)$ and $\rho(t_1)$ depends only on the times t_1 and t_2.

In terms of formulas, the states are related as $\rho(t_2) = U\rho(t_1)U^\dagger$. This postulate is equivalent to demanding that the time evolution of pure states is subject to the Schrödinger equation.

At first, this postulate might seem to give rise to a technical problem. Will acting with a unitary transformation on $\mathscr{H}_1$ project us out of the initial Hilbert space? Luckily, this is not the case. It can be shown that the following holds:

Definition 2: Two Hilbert spaces $\mathscr{H}_1$ and $\mathscr{H}_2$ are isomorphic if they are related by a map $U : \mathscr{H}_1 \to \mathscr{H}_2$ that is

i) linear

ii) a bijection

iii) preserving the inner product $\langle \cdot, \cdot \rangle$.

In particular, analysing the third condition for an arbitrary linear bijection B acting as $B : |\psi\rangle \mapsto B|\psi\rangle$ shows that $B^\dagger B = \mathbb{1}$ has to be satisfied, constraining B to be a unitary transformation. Therefore, time evolution (or any other unitary transformation) of $\mathscr{H}_1$ results in a Hilbert space that is isomorphic to $\mathscr{H}_1$.

The final ingredient required to make linear algebra a useful toolset for studying quantum systems is the notion of a measurement, which is addressed by the third postulate:

Postulate 3:

Any physically measurable quantity, i.e. any observable O is described by a Hermitian operator $\mathfrak{O}$ that acts on the Hilbert space. The eigenvectors of $\mathfrak{O}$ form a basis for $\mathscr{H}$. The measurement of any O must result in one of the eigenvalues o_i of $\mathfrak{O}$.

As a formula, the expectation value of $\mathfrak{O}$ in a mixed state ρ is given by $\langle \mathfrak{O} \rangle = \mathrm{tr}(\mathfrak{O}\rho)$. For simplicity, in the following we assume that the spectrum of $\mathfrak{O}$ is discrete and non-degenerate. Then, the probability of obtaining the eigenvalue o_i is given by $p(o_i) = \mathrm{tr}\big(|o_i\rangle\langle o_i|\rho\big)$, where $|o_i\rangle$ is the eigenvector corresponding to o_i.[3]

[3] Note that, for the product $|o_i\rangle\langle o_i|\rho$ to make sense, both objects have to be formulated in the same basis. However, since $|o_i\rangle$ does provide a basis for $\mathscr{H}$, there always exists a transformation to reformulate $|o_i\rangle$ in terms of the basis that ρ was originally formulated in, and vice versa.

The measurement of an observable is understood as a collapse of the wave function onto one of the eigenstates of the observable. Therefore, immediately after the measurement is performed, the state ρ' is no longer given by the original ρ, but by projecting ρ into the sector of the measurement outcome and rescaling by the probability to ensure $\operatorname{tr}\rho' = 1$,

$$\rho' = \frac{|o_i\rangle\langle o_i|\rho|o_i\rangle\langle o_i|}{p(o_i)}\,. \tag{2.4}$$

Given these notions defining measurements, our comments below (2.1) and (2.2) regarding the probability interpretation become much clearer. Given a pure state $|\psi\rangle$, suppose it is written in a basis which is also the eigenbasis to an operator $\mathfrak{O}$. Measuring this operator with outcome o_i results in collapsing $|\psi\rangle$ onto $|o_i\rangle$. The probability $p(o_i)$ is then given by

$$\operatorname{tr}\big(|o_i\rangle\langle o_i|\psi\rangle\langle\psi|\big) = |\langle o_i|\psi\rangle|^2 = a_i^* a_i. \tag{2.5}$$

Therefore, the absolute squares of the coefficients a_i in (2.1) correspond to probabilities. Since it is not possible that the measurement has no outcome but something has to be the result, the probabilities of all different outcomes have to sum up to one, providing the physical interpretation of the constraint $\sum_{i=1}^{n} a_i^* a_i = 1$.

This concludes the discussion of the necessary ingredients to analyse closed quantum systems. We have seen how to define states and state space. Dynamics and measurements are described by unitary transformations and Hermitian operators, respectively. Note that the above postulates do not only give rise to a mathematical description of quantum mechanics but also relativistic formulations of quantum mechanics.

As of yet, we have assumed that we are working with a given closed quantum system. We have however not specified what kind of system this should be. As far as the discussion above goes, the system could be as simple as a single qubit, but it could also be a fairly complicated system of 42 interacting spins. For practical purposes, it would be highly beneficial if we were able to, at least partially, formulate the building blocks of a system with N spins utilising the insights we gain by analysing the much simpler system of $\frac{N}{2}$ spins, or even simpler by analysing a single qubit. This leads us to discuss composite quantum systems and in particular bipartite quantum systems. The case of a bipartite quantum system is one of the main objects considered throughout the rest of this thesis. In this analysis we will also naturally encounter a notion of quantum entanglement.

Bipartite Quantum Systems

We start by stating the fourth and final of the postulates of quantum mechanics which concerns composite quantum systems:

Postulate 4:

The Hilbert space $\mathscr{H}$ of a system of N components is given by the tensor product of all of the Hilbert spaces $\mathscr{H}^{(i)}$ of the individual components. If the individual states are prepared as $\rho^{(i)}$, the state in the composite quantum ρ is given by the tensor product of all of the $\rho^{(i)}$.

In formulas, this says that $\mathscr{H} = \bigotimes_{i=1}^{N} \mathscr{H}^{(i)}$. As a simple example, considering two quantum systems with Hilbert spaces $\mathscr{H}^{(1)} = \mathbb{C}^2 = \mathscr{H}^{(2)}$, the composite Hilbert space is given by $\mathbb{C}^4$. The state in $\mathscr{H}$, as stated above, is given by

$$\rho = \bigotimes_{i=1}^{N} \rho^{(i)}. \tag{2.6}$$

This tensor product structure also allows for independent measurements between the composite systems. Given observables $\mathfrak{O}^{(i)}$ acting only on the i-th Hilbert space, the measurement of all of these operators factorises,

$$\mathrm{tr}\left(\bigotimes_{i=1}^{N} \mathfrak{O}^{(i)} \rho\right) = \prod_{i=1}^{N} \mathrm{tr}\left(\mathfrak{O}^{(i)} \rho^{(i)}\right). \tag{2.7}$$

Related to this result, measurements in one component do not influence the other systems,

$$\mathrm{tr}\left(\mathfrak{O}^{(i)} \rho\right) = \mathrm{tr}_i\left(\mathfrak{O}^{(i)} \rho^{(i)}\right), \tag{2.8}$$

where tr_i is the partial trace, acting only on operators of the i-th component.

However, it is clear that not every state of the composite Hilbert space can be of the simple structure as in (2.6). In particular, we saw earlier that a linear combination of density operators with appropriate coefficients is also a valid density operator. Since the sum of tensor products is generally not equal to the tensor product of sums, i.e.

$$\sum_l p_l \rho_l = \sum_l p_l \left(\bigotimes_{i=1}^{N} \rho^{(i)}\right) \neq \bigotimes_{i=1}^{N} \left(\sum_l \tilde{p}_l \rho_l^{(i)}\right), \tag{2.9}$$

these states are not of the same form as (2.6), but are more general states. However, these states are still not the most general state that can be written down for a composite quantum system. States that can be written as in (2.9) are known as *separable* quantum states. Every state of a composite quantum system that cannot be brought to the above form is called *entangled*.

As a side remark, it is generally considered a hard problem to test whether an arbitrary

mixed state is entangled. In fact, it was shown that for an arbitrary bipartite system, this task is NP-hard [193]. For the special cases of bipartite systems with $\dim(\mathscr{H}^{(1)}) = \dim(\mathscr{H}^{(2)}) = 2$ and $\dim(\mathscr{H}^{(1)}) = 2,\ \dim(\mathscr{H}^{(2)}) = 3$ it was shown that a necessary and sufficient criterion for separability of the full state is given by the positive partial transpose condition [194, 195]. As we are mostly concerned with pure states throughout this thesis, we will not go into detail about this.

The prototypical measure to quantify the entanglement within a given state is the *entanglement entropy* or *von Neumann entropy* $S(\rho)$.[4] For pure states, this measure is sufficient to detect any amount of entanglement. For mixed states unfortunately, this is not completely true. Therefore, there exists a zoo of other measures quantifying entanglement for mixed states. At the time of writing this thesis however, to the best of our knowledge, it has not yet been shown which of these measures is the 'best'. We will explain in more detail why entanglement entropy is not a good measure for mixed states later on in sec. 2.1.3 when we discuss a few of the more general measures. Despite the deficiencies of entanglement entropy, we will use it here as it is sufficient for the following discussion.

The von Neumann entropy of any mixed state ρ is defined as

$$S(\rho) = -\operatorname{tr}(\rho \ln \rho)\,. \tag{2.10}$$

In terms of the eigenvalues λ_i of ρ, this can also be expressed as

$$S(\rho) = -\sum_{i=1}^{n} \lambda_i \ln \lambda_i\,. \tag{2.11}$$

Since the eigenvalues of ρ are real numbers between 0 and 1, it follows that the entanglement entropy is positive semi-definite. There also exists an upper bound for the entanglement entropy, provided by the maximally entangled state $\rho = \frac{1}{n}\mathbb{1}_n$ in an n-dimensional Hilbert space. This state has entanglement entropy $S(\rho) = \ln n$.

Given a product mixed state of a bipartite quantum system $\rho = \rho^{(1)} \otimes \rho^{(2)}$, the entropy of ρ is given by

$$S(\rho) = S(\rho^{(1)}) + S(\rho^{(2)})\,. \tag{2.12}$$

For a general separable mixed state ρ, this turns into an inequality

$$S(\rho) \leq S(\rho^{(1)}) + S(\rho^{(2)})\,. \tag{2.13}$$

[4] Throughout this thesis, we will use both names interchangeably.

This relation is known as the *subadditivity* of entanglement. It is one of the main properties distinguishing quantum mechanics from classical probability theory. The Shannon entropy of a classical composite system can never be lower than the Shannon entropy of any of its components. However, due to (2.13), in quantum mechanics, it can happen that even $S(\rho) = 0$ while the individual entropies do not vanish. Furthermore, (2.13) is one half of the so-called Araki–Lieb inequalities [196],

$$|S(\rho^{(1)}) - S(\rho^{(2)})| \leq S(\rho) \leq S(\rho^{(1)}) + S(\rho^{(2)})\,. \tag{2.14}$$

By the left inequality we see that $S(\rho) = 0$ happens exactly when $S(\rho^{(1)}) = S(\rho^{(2)})$.

In terms of the state ρ, the entanglement entropy $S(\rho)$ vanishes if and only if ρ is a pure state, i.e. $\rho = |\psi\rangle\langle\psi|$. Since this state is a projector $\rho^2 = \rho$, its eigenvalues can only take the values 0 and 1. Therefore by (2.11), the entanglement entropy vanishes. However, by (2.14) the entanglement between the subsystems does not necessarily vanish, even when the full system is in a pure state. Given the pure state ρ, the reduced density operators of the subsystems are obtained by calculating the partial trace [197],

$$\rho^{(1/2)} = \mathrm{tr}_{2/1}\rho\,. \tag{2.15}$$

This can be understood as measuring all of one of the subsystems while leaving the other subsystem untouched. The existence of entanglement between the subsystems therefore depends on whether the reduced density operators are pure or not. Only if the reduced density operators themselves are pure states, there is no entanglement at all.[5] A useful criterion to distinguish between these cases is provided by the purity γ introduced earlier in (2.3), summarised in table 2.1. In short, a pure state of a bipartite system is not entangled if and only if the reduced density operators are also pure states.

From now on we restrict the discussion to pure states. For a bipartite system, to each subsystem a basis $\mathscr{B}_{1/2}$ is associated. As the Hilbert space of the full bipartite system is given by the tensor product of the individual Hilbert spaces, the basis for the full bipartite system is given by all tensor products of elements of $\mathscr{B}_1$ and $\mathscr{B}_2$. Therefore, any pure state can be written as

$$|\psi\rangle = \sum_{i,j=1}^{n} a_{ij}|i_1, j_2\rangle\,, \tag{2.16}$$

where $|i_1, j_2\rangle$ is short hand for $|i_1\rangle \otimes |j_2\rangle$ and $a_{ij} \in \mathbb{C}$ with $\sum_{i=1}^{n} |a_{ii}|^2 = 1$. Note that for

[5] Note that the existence of entanglement depends on the chosen bipartition. A given state may be entangled for one bipartition, but separable for a different bipartition. So discussing entanglement properties makes sense once a bipartition $\mathscr{H} = \mathscr{H}^{(1)} \otimes \mathscr{H}^{(2)}$ of the system is fixed.

separable pure state ρ:	$\gamma(\rho) = 1 \wedge \gamma(\rho^{(i)}) = 1 \quad \Leftrightarrow \quad S(\rho) = S(\rho^{(i)}) = 0$
entangled pure state ρ:	$\gamma(\rho) = 1 \wedge \gamma(\rho^{(i)}) < 1 \quad \Leftrightarrow \quad S(\rho) = 0,\ S(\rho^{(i)}) \neq 0$

Table 2.1: A separable pure state, sometimes also called a pure product state, is characterised by vanishing entanglement entropy both for the full state as well as for the reduced density operators. An entangled pure state also has vanishing entanglement for the full state, but the reduced density operators are mixed states with non-vanishing entanglement.

arbitrary a_{ij}, this state is entangled since generically it cannot be written as $|\psi_1\rangle \otimes |\psi_2\rangle$. This is only possible if the coefficients a_{ij} are products of the coefficients $a_i^{(1/2)}$ of $|\psi_{1/2}\rangle$, i.e. if $a_{ij} = a_i^{(1)} a_j^{(2)}$ for all $i, j = 1, ..., n$. In order to quantify the entanglement in the state (2.16), a particularly useful way to denote it is given by the *Schmidt decomposition*. This can be considered an application of the singular value decomposition to the coefficient matrix a with entries a_{ij}. Essentially it amounts to diagonalisation of a by redefining the basis of (at least) one of the subsystems. Since the Schmidt decomposition will be elementary throughout parts of this thesis, we provide some more details on it in the following.

The Schmidt decomposition is given by the following statement:

Theorem 1: Any vector $|\psi\rangle$ of a bipartite Hilbert space $\mathscr{H} = \mathscr{H}^{(1)} \otimes \mathscr{H}^{(2)}$ can be expressed as

$$|\psi\rangle = \sum_{i=1}^{n} \kappa_i |i_1, i_2\rangle \,, \tag{2.17}$$

where $0 \leq \kappa_i \leq 1$ are the Schmidt coefficients and $|i_1\rangle$ and $|i_2\rangle$ are orthonormal bases of the respective subsystems.

To show this, consider the state (2.16) with coefficient matrix a. By the singular value decomposition, we can write $a = U \Xi V$, where U and V are unitary matrices and Ξ is a positive semi-definite diagonal matrix with entries κ_i. These κ_i are the eigenvalues of a. Defining $|\tilde{i}_1\rangle = U|i_1\rangle$, $|\tilde{i}_2\rangle = V|i_2\rangle$ yields

$$|\psi\rangle = \sum_{i,j=1}^{n} (U \Xi V)_{ij} |i_1, j_2\rangle = \sum_{i,j=1}^{n} \kappa_i \delta_{ij} |\tilde{i}_1, \tilde{j}_2\rangle = \sum_{i=1}^{n} \kappa_i |\tilde{i}_1, \tilde{i}_2\rangle \,. \tag{2.18}$$

Since U and V are unitary, $|\tilde{i}_{1/2}\rangle$ are orthonormal. □

To see that the representation (2.17) is particularly convenient when computing the entanglement, we point out that the reduced density operators of either subsystem are diagonal when computed starting from the state in Schmidt decomposed form. The di-

agonal entries λ_i of the reduced density operators are simply the squares of the Schmidt coefficients, $\lambda_i = \kappa_i^2$. Correspondingly, the spectrum of both $\rho^{(1)}$ and $\rho^{(2)}$ has to be the same. Using (2.11), we see that the entanglement entropy of a pure state $|\psi\rangle$ is uniquely specified by the values of all Schmidt coefficients,

$$S(\rho^{(1)/(2)}) = -\sum_{i=1}^{n} \kappa_i^2 \ln \kappa_i^2 \,. \tag{2.19}$$

This is another way to see that $S(\rho^{(1)}) = S(\rho^{(2)})$ for a pure state ρ.

Below (2.11) we stated that a maximally entangled state is described by a density operator that is proportional to the identity. This statement can be reformulated in terms of the Schmidt coefficients. A state is maximally entangled if and only if all of its Schmidt coefficients are equal.

An important property of the entanglement entropy is that it is invariant under local unitary transformations $U = U_1 \otimes U_2$ [188]. Transforming a pure state ρ by a local unitary transformation to $\rho' = U\rho U^\dagger$, when computing the reduced density operator of the first (the second) subsystem all influence of U_2 (U_1) drops out due to the cyclicity of the trace.[6] The transformed reduced density operator is then related to the old reduced density operator as $\rho'^{(1)/(2)} = U_{1/2}\rho^{(1)/(2)}U_{1/2}^\dagger$. Since unitary transformations do not change the eigenvalues of a given operator, the spectrum of $\rho'^{(1)/(2)}$ is the same as the spectrum of $\rho^{(1)/(2)}$. Accordingly, also the entanglement entropy does not change.

We have now understood how to quantify the entanglement within a generic state ρ and in particular for pure states. An important object in this analysis is the reduced density operator defined in (2.15), describing only one of the subsystems. Remarkably, the relation between the full and the reduced density operator can also be understood in the opposite direction. Given a mixed state ρ acting on $\mathscr{H}^{(1)}$, there exists a pure state $|\psi\rangle$ in an extended Hilbert space $\mathscr{H}^{(1)} \otimes \mathscr{H}^{(2)}$ such that upon partial tracing over $\mathscr{H}^{(2)}$, the mixed state ρ is recovered as the reduced density operator. This is known as *purification* and is formalised in the purification theorem [14, 198–202]. It states that, given a mixed state $\rho = \sum_{i=1}^{n} p_i |\phi_i\rangle\langle\phi_i|$ acting on $\mathscr{H}^{(1)}$, it is always possible to obtain this state as the reduced density operator of a pure state $|\psi\rangle \in \mathscr{H}^{(1)} \otimes \mathscr{H}^{(2)}$, where

$$|\psi\rangle = \sum_{i=1}^{n} \sqrt{p_i} |\phi_i, \phi_i'\rangle \tag{2.20}$$

and $\dim \mathscr{H}^{(1)} \leq \dim \mathscr{H}^{(2)}$. Here $|\phi_i'\rangle$ is a basis for the auxiliary Hilbert space $\mathscr{H}^{(2)}$. As

[6] The partial trace tr_i is not cyclic w.r.t. the full unitary transformation $U = U_1 \otimes U_2$, but only w.r.t. the part of U that is traced out. That means, $\mathrm{tr}_1(U_1 \mathfrak{O} U_1^\dagger) = \mathrm{tr}_1 \mathfrak{O}$, but $\mathrm{tr}_1(U \mathfrak{O} U^\dagger) = \mathrm{tr}_1(U_2 \mathfrak{O} U_2^\dagger) \neq \mathrm{tr}_1 \mathfrak{O}$.

this Hilbert space is auxiliary, the basis $|\phi_i'\rangle$ is not unique. In fact, it has been shown that for a mixed state ρ there exist infinitely many possible purifications [203]. However, given two purifications $|\psi\rangle$ and $|\psi'\rangle$ of the same state ρ, it was also shown that these two pure states are related by a unitary transformation of the basis of the auxiliary Hilbert space [204]. As discussed in the previous paragraph, the entanglement contained in $|\psi\rangle$ and $|\psi'\rangle$ therefore is the same.

Area vs. Volume

The entanglement entropy is named such as it is defined in an analogous way to the thermodynamic entropy introduced by Clausius [205] and given an interpretation in terms of microstates by Gibbs and Boltzmann [206, 207]. As a formula, the thermal entropy is defined as the logarithm of the number of possible configurations of the system. In terms of microstates, this is expressed as $S_{\text{therm}} = -\sum_i p_i \ln p_i$, where p_i is the probability that the system is described by a particular microstate.[7] This probability is of course a purely classical quantity and arises from employing a statistical description of large macroscopic systems, scenarios in which it is hard to determine the precise state that the system is in exactly. However, as quantum mechanics can be interpreted as a theory of probabilities as well, it is natural to generalise the notion of thermodynamic entropy to quantum mechanics. In particular, the expression for S_{therm} has a striking similarity to the entanglement entropy as given in (2.11). This line of thought motivated von Neumann to define the density operator in the first place in order to develop a statistical interpretation of quantum mechanics [208].[8]

Although entanglement and thermodynamic entropy are defined in an analogous way, the two quantities can behave quite differently. One of the main differences is that the thermal entropy usually scales with the volume while the entanglement entropy scales with an area, at least for the ground state in gapped systems. To give a few more details, the thermodynamic entropy can equivalently be expressed as the logarithm of the phase space volume Ω. As an example, considering a gas of N particles, the phase space is $6N$-dimensional and has elements corresponding to the positions and momenta of all N particles. A particular microstate of the system is given by specifying the position and the momentum of every particle. The volume of the phase space is given by all elements that can be reached from a given starting point defined by the boundary conditions. Therefore, the thermodynamic entropy usually satisfies a *volume law* since it can be written as $S_{\text{therm}} = \ln \Omega$. On the contrary, this is not generally true for the entanglement entropy. Rather,

[7] Note that we use natural units where $k_B = 1$.

[8] In a complementary development, Landau independently introduced the density operator as a tool to study quantum systems that do not admit a description by a state vector [209].

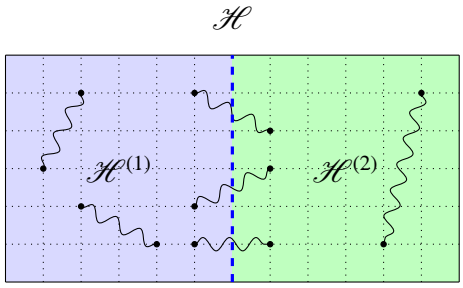

Figure 2.1: Bipartition of a Hilbert space $\mathscr{H}$. The bipartition surface is represented by the dashed blue line. The amount of quantum correlations, i.e. the number of wavy lines, shared between particles on both sides of the bipartition surface quantifies the entanglement between $\mathscr{H}^{(1)}$ and $\mathscr{H}^{(2)}$. Quantum correlations between particles which are not separated by the bipartition surface do not contribute to the entanglement entropy.

for the ground state in gapped systems this quantity scales with the area between the subsystems and therefore satisfies an *area law*. An intuitive reason for this behaviour is that, as discussed previously, entanglement is measured between subsystems which are defined by introducing a bipartition. Associated to the bipartition is the bipartition surface which separates the two subsystems, visualised in fig. 2.1. Entanglement between the subsystems is therefore sensitive only to quantum correlations across the bipartition surface. Quantum correlations purely within one of the subsystems do not lead to any entanglement. The gap ξ is important as spatial correlations between points at a relative distance x are damped by a factor of $e^{-x\xi}$, so only correlations close to the bipartition surface are sufficiently large to contribute to the entanglement and $S \propto A$, where A is the area. If the gap tends to zero and the correlations satisfy a power law, correlations between points farther apart have to be taken into account. This typically leads to a breaking of the area law as then, $S \propto A \ln A$.

This distinction between thermodynamic and entanglement entropy becomes particularly important (as well as interesting) in gravitational settings, especially for black holes. We will discuss this further in sec. 3.1 and in sec. 3.2.1.

Intuitively, the entanglement entropy quantifies how many of the wavy lines in fig. 2.1 representing quantum correlations are cut by the bipartition surface. Wavy lines that are not cut open do not contribute to the entanglement. Mathematically this can be understood as follows. The quantum correlations between two particles within $\mathscr{H}^{(1)}$ can be represented as an entangled state ρ'. Any other two particles sharing quantum correlations are described by $\tilde{\rho}$. According to the fourth postulate discussed above, the full state is then given by $\rho = \rho' \otimes \tilde{\rho}$. Suppose now that the bipartition surface is placed such that it separates the second pair of particles. Since $\mathrm{tr}\,\rho' = 1$ by definition of the density operator, calculating the reduced density operator of the second subsystem receives contributions only from $\tilde{\rho}$

as the partial trace over the first system measures both particles within ρ'. Accordingly, the entanglement entropy is not sensitive to the quantum correlations described by ρ'.

As we have seen previously, thermodynamic and entanglement entropy can be different in their scaling behaviour. However, they also share similarities, which in particular can be seen in terms of entanglement thermodynamics. Here, in analogy to the thermal density operator $\rho_{\text{therm}} = e^{-\beta H}$ of a system at (inverse) temperature β and with Hamiltonian H, the so-called *modular* Hamiltonian K is defined as

$$\rho =: e^{-K} \quad \Leftrightarrow \quad K = -\ln \rho \,, \tag{2.21}$$

where ρ is an arbitrary entangled quantum system. In particular, ρ might be the reduced density operator associated with a subsystem of a larger Hilbert space $\mathscr{H}$. With the above definition, the thermal density operator can be viewed as the special case $K = \beta H$. The modular Hamiltonian defined in this way is one of the main objects in Tomita–Takesaki theory, which is an algebraic approach to quantum mechanics. We will discuss this in more detail in sec. 2.3.2.

The modular Hamiltonian is sometimes also referred to as the entanglement Hamiltonian, as it contains information about the entanglement spectrum of ρ. Moreover, with K as defined on the right-hand side of (2.21), the entanglement entropy (2.10) is written as the expectation value of the modular Hamiltonian,

$$S(\rho) = \operatorname{tr}(\rho K) \,. \tag{2.22}$$

The definition in (2.21) can be used to show that the entanglement entropy satisfies what is called the *first law of entanglement entropy*, again in analogy to the thermodynamic entropy. In the simplest case, the first law of thermodynamics states that the derivative of the energy E with respect to the thermodynamic entropy S_{therm} equals the temperature T, i.e. $\frac{\partial E}{\partial S_{\text{therm}}} = T$. For the entanglement entropy, an analogous relation can be established. Upon a small variation of the reduced density operator $\rho^{(1)} \to \rho^{(1)} + \delta\rho^{(1)}$, to first order the entanglement entropy (2.10) changes as [142, 210]

$$\delta S(\rho^{(1)}) = -\operatorname{tr}\left(\delta\rho^{(1)} \ln \rho^{(1)}\right) - \operatorname{tr}\left(\rho^{(1)} \delta \ln \rho^{(1)}\right) . \tag{2.23}$$

By the chain rule, the variation of the logarithm is given by the inverse density operator multiplying the variation $\delta\rho^{(1)}$. The second term therefore is simply the trace of $\delta\rho^{(1)}$. As the density operator satisfies the normalisation $\operatorname{tr}\rho^{(1)} = 1$, by consistency $\operatorname{tr}\left(\delta\rho^{(1)}\right) = 0$. Furthermore, invoking (2.21) for $\rho^{(1)}$ the logarithm in the first term reduces to $-K^{(1)}$. As $\langle A \rangle = \operatorname{tr}\left(\rho^{(1)} A\right)$, the right-hand side of the above equation equals the variation of the

expectation value of the modular Hamiltonian,

$$\delta S(\rho^{(1)}) = \delta\langle K^{(1)}\rangle\,, \tag{2.24}$$

resembling $\frac{\partial E}{\partial S_{\text{therm}}} = T$ for $T = 1$. This is consistent with the above definition (2.21) when comparing to the thermal density operator $\rho_{\text{therm}} = e^{-\beta H}$. Alternatively, to have an even closer analogy to thermodynamics, we might also redefine the modular Hamiltonian by rescaling $K \to \beta_{\text{ent}} K$, where β_{ent} is the entanglement temperature. In this case, the first law of entanglement entropy reads

$$\delta S(\rho^{(1)}) = \beta_{\text{ent}}\delta\langle K^{(1)}\rangle\,. \tag{2.25}$$

With this formulation, the entanglement entropy can be formally interpreted as a thermal entropy. Remarkably, applied to holographic CFTs the first law of entanglement entropy was shown to put constraints on the dual spacetime in that it has to satisfy the linearised Einstein equations [142].

As an aside, the analogy between entanglement and thermodynamic entropy also has certain limitations, in particular regarding the second law of thermodynamics. The second law concerns the reversibility of processes, characterised by an increase in the thermodynamic entropy for irreversible processes and no change in the entropy for a reversible process. In this classification, the thermodynamic entropy must provide a unique measure. To establish an analogous statement for entanglement, a unique measure of entanglement is required [211–214]. While for pure states the entanglement entropy is sufficient [211, 215], as we commented earlier, generally such a measure is not yet known. Nevertheless, there exist proposals for reversibility of entanglement transformations under certain conditions [213, 216–219]. However, it has been shown that reversibility of such manipulations in general requires generating macroscopic amounts of entanglement, ruling out the existence of a second law of entanglement [220].

This concludes our discussion of the entanglement entropy in quantum mechanics.

2.1.2. Von Neumann Entropy in Quantum Field Theory

In the previous section we have analysed in quite some detail how entanglement entropy is understood and computed in quantum mechanics. In particular, we have focused on finite-dimensional Hilbert spaces. However, in the context of QFTs, usually the Hilbert space is infinite-dimensional as there are infinitely many degrees of freedom.[9] In generalising the

[9] The field operators, whose values fluctuate, are defined at every point in the allowed spacetime, typically $\mathbb{R}^{1,d-1}$ for a QFT in d dimensions. Correspondingly, there are infinitely many degrees of freedom.

statements of sec. 2.1.1 to infinite-dimensional quantum systems, some subtleties arise. We will discuss these subtleties together with the corresponding necessary adjustments in more detail in sec. 2.3. In the following, we discuss general features of entanglement entropy in QFTs, in particular pointing out which characteristics discussed in sec. 2.1.1 are still present and where entanglement entropy in QFT behaves differently than in quantum mechanics.

Entanglement in the Vacuum

First of all, as we have seen before, in quantum mechanics there exist states with non-trivial entanglement, but there also exist separable states without entanglement. This is different in QFT, as here every state contains entanglement. This holds in particular also for the vacuum state $|0\rangle$. The vacuum state in a QFT is understood as a superposition of states corresponding to different field configurations, constrained only by the fact that the full state is the state of the lowest energy. This can also be formulated as having no physical particle excitations in the state.[10] However, the different field configurations corresponding to fluctuations of the quantum fields lead to entanglement between such fluctuations. A simple way to see this is to consider the vacuum expectation value of two operators at different points in spacetime,

$$\langle 0|\phi(x)\phi(y)|0\rangle\,. \tag{2.26}$$

Suppose that we introduce a bipartition surface such that x is contained in a spatial region A while y is contained in the complement of A, denoted as $\bar{A}$.[11] This is visualised in fig. 2.2. Note that compared to the previous section we have switched from labelling subregions by numbers as (i) to directly using the region (and its complement) as a label, as this is more common in the field theory literature.

Without entanglement between A and $\bar{A}$, the vacuum state can be written as the product of the vacuum states in A and $\bar{A}$. If this was the case, the above expectation value (2.26) factorises into the individual expectation values,

$$\langle 0|\phi(x)\phi(y)|0\rangle \overset{|0\rangle=|0_A 0_{\bar{A}}\rangle}{=} \langle 0_A|\phi(x)|0_A\rangle\langle 0_{\bar{A}}|\phi(y)|0_{\bar{A}}\rangle\,. \tag{2.27}$$

However, this is not generally true in QFT. Therefore, the assumption that the vacuum

[10] A physical particle excitation would e.g. be the state of one electron. In the vacuum, no such states are contained. However, states with particle-antiparticle pairs due to quantum fluctuations are allowed since these pairs do not yield physical particles.

[11] In QFT, strictly speaking such a bipartition is not well-defined since it is not clear what happens to the degrees of freedom on the bipartition surface. This is one of the subtleties mentioned earlier. We will address this point in more detail in sec. 2.3.1.

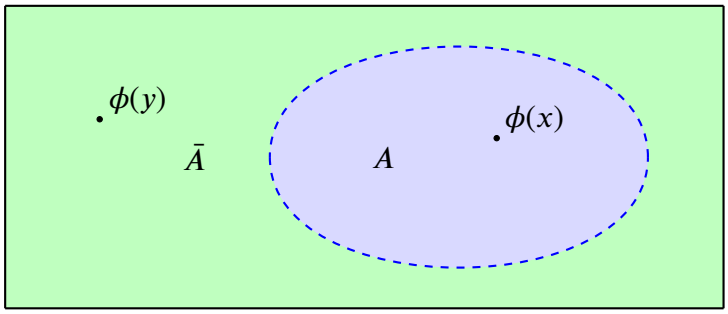

Figure 2.2: Two operators $\phi(x)$ and $\phi(y)$ are placed in regions A and its complement $\bar{A}$ respectively, separated by a bipartition surface represented by the dashed blue line.

$|0\rangle$ is a product state must not be true. In other words, the reduced density operator of regions A and $\bar{A}$ following from $|0\rangle$ is a mixed state.

Explicit computations of entanglement entropy in QFT are sparse as they are technically very involved, both numerically and analytically. However, there do exist special cases where these computations can be performed. This is usually related to the presence of a large amount of symmetry as for two-dimensional CFTs [221] or to the simplicity of the considered system. For the latter case, a setup explaining the entanglement in the vacuum state is the entanglement entropy for Rindler space [222, 223]. Here, empty Minkowski space, denoted as Min in the following, is split into two half spaces $x > 0$ and $x < 0$, denoted $\text{Min}_>$ and $\text{Min}_<$ respectively. Fixing a slice of constant time then defines two initial value surfaces $\text{Min}_{>,t}$ and $\text{Min}_{<,t}$. This is visualised on the left of fig. 2.3. These initial value surfaces are the domains of dependence for the two Rindler wedges $\text{Rin}_>$ and $\text{Rin}_<$ [224]. While this argument can be made for Minkowski space in arbitrary dimensions (for reviews, see e.g. [192, 225]), in the following, we restrict to two dimensions since this already exhibits all of the interesting properties relevant to our discussion. Accordingly, $\text{Min} = \mathbb{R}^{1,1}$, $\text{Min}_> = \mathbb{R} \times \mathbb{R}_+$ and $\text{Min}_< = \mathbb{R} \times \mathbb{R}_-$ with metric

$$\mathrm{d}s^2 = -\mathrm{d}t^2 + \mathrm{d}x^2 \,. \tag{2.28}$$

This metric trivially splits into the metrics on $\text{Min}_<$ and $\text{Min}_>$ when restricting x. As we are in two dimensions, the initial value surfaces $\text{Min}_{>,t}$ and $\text{Min}_{<,t}$ are lines and the bipartition surface is simply the point $t = 0 = x$. In the following we compute the reduced density operator for the vacuum state when treating the initial value surfaces as regions $A = \text{Min}_{>,t}$ and $\bar{A} = \text{Min}_{<,t}$. For simplicity, in this computation we choose the initial value surfaces at $t = 0$, as depicted on the left of fig. 2.3.

To compute the reduced density operator for one of the initial value surfaces, we need an expression for the vacuum state $|0\rangle$ on this surface in terms of degrees of freedom of

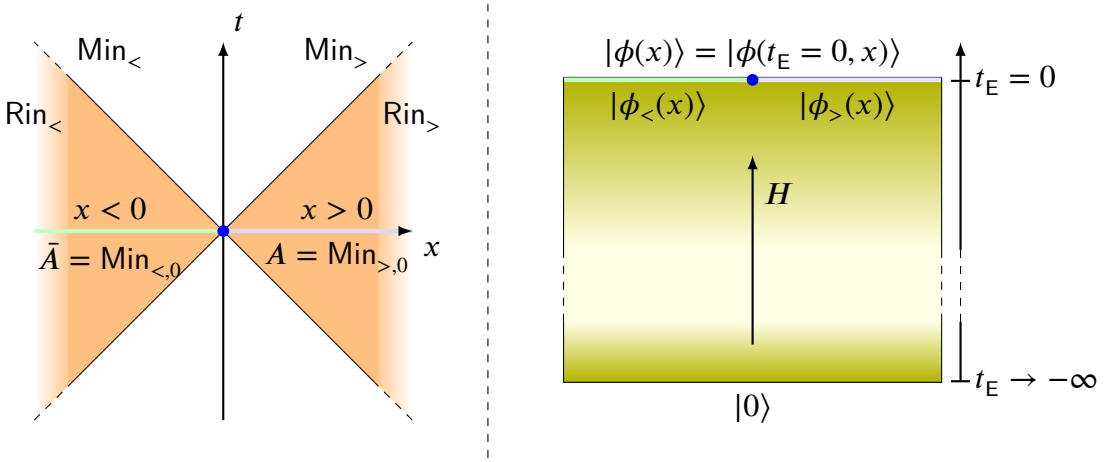

Figure 2.3: On the left, the bipartition of empty Minkowski space into the half spaces $\mathrm{Min}_<$ and $\mathrm{Min}_>$ is depicted. The initial value surfaces $\mathrm{Min}_{<,t}$ and $\mathrm{Min}_{>,t}$ at $t = 0$ are separated by the bipartition surface at $t = 0 = x$, represented by the blue dot. The surfaces coloured in light green and light blue are the domains of dependence for $\mathrm{Rin}_<$ and $\mathrm{Rin}_>$, respectively. On the right, a state $|\phi(x)\rangle$ is prepared from the vacuum $|0\rangle$. The state is obtained by performing the Euclidean path integral over the shaded area with an appropriate boundary condition, which can be understood as an Euclidean time evolution by the Hamiltonian H. Taking into account the bipartition, the field $\phi(x)$ splits into $\phi_<(x)$ and $\phi_>(x)$ for $x < 0$ and $x > 0$, respectively. These fields describe degrees of freedom on the respective initial value surfaces, represented by the green and blue lines at $t_\mathrm{E} = 0$.

the half spaces. To obtain this, we utilise the Euclidean path integral to first express the vacuum by a generic field configuration $\phi(x)$ inserted at Euclidean time $t_\mathrm{E} = 0$, related to the Minkowskian time by a Wick rotation $t = -\mathrm{i}t_\mathrm{E}$. By the completeness relation of the basis $|\phi(x)\rangle$, we write

$$|0\rangle = \int \mathscr{D}\phi(x)\, \langle\phi(x)|0\rangle |\phi(x)\rangle\,, \tag{2.29}$$

where

$$\langle\phi(x)|0\rangle = \int_{\phi(t_\mathrm{E}=-\infty,x)=0}^{\phi(t_\mathrm{E}=0,x)=\phi(x)} \mathscr{D}\phi'(t_\mathrm{E}, x)\, \exp\bigl(-S_\mathrm{E}[\phi']\bigr)\,. \tag{2.30}$$

Here S_E is the Euclidean action. The exponential factor can be interpreted as evolving the vacuum state with the Hamiltonian for an amount of Euclidean time. In this way, a generic state $|\phi(x)\rangle$ at time slice $t_\mathrm{E} = 0$ can be prepared from the vacuum by performing the path integral with the boundary condition $\phi(t_\mathrm{E} = 0, x) = \phi(x)$, visualised on the right of fig. 2.3. This right part of the figure representing half of the Euclidean plane should be thought of as being glued along the initial value surfaces to the left part of the figure, such that the Euclidean plane the $t = 0$ surface. An analogous expression to (2.29) can be

found for $\langle 0|$. Here, the overlap $\langle 0|\phi(x)\rangle$ is required. This overlap is defined analogously to (2.30) by exchanging the upper and lower borders of the integral as well as replacing the infinite past $t_{\mathrm{E}} = -\infty$ by the infinite future $t_{\mathrm{E}} = \infty$.

We now have obtained an expression for the density operator of the vacuum as a double integral over the intermediate fields $\phi(x)$ and $\phi'(x)$. To account for the bipartition, we split both these fields into their components in $\mathrm{Min}_{<,0}$ and $\mathrm{Min}_{>,0}$, i.e. $\phi^{(\prime)} = \phi^{(\prime)}_{<}\phi^{(\prime)}_{>}$ as shown on the right of fig. 2.3. As pointed out before in the footnote below (2.26), we note that this factorisation of the Hilbert space $\mathscr{H} = \mathscr{H}_{<} \otimes \mathscr{H}_{>}$ is strictly speaking not correct, for reasons that we will elaborate on in sec. 2.3.1. The original approach of [222] however did not rely on this path integral approach but made use of analyticity properties of correlation functions. Fortunately, the path integral approach first utilised in [226] yields the same result for the reduced density operator as derived in [222]. Moreover, this approach is important in the context of the discussion in [223], which will also be important for our discussion in sec. 3.2.1.

To compute the reduced density operator we need to trace over one of the half spaces. For concreteness, we choose to trace out $\mathrm{Min}_{<,0}$. For the path integral, that means that we trivially identify $\phi_{<}$ and $\phi'_{<}$ by inserting a Dirac–Delta $\delta(\phi_{<} - \phi'_{<})$. Pictorially speaking, this takes the right side of fig. 2.3 together with its reversed version, i.e. where $|0\rangle$ is placed at $t_{\mathrm{E}} = \infty$, and glues these two surfaces along the edges of $x < 0$, as visualised on the left of fig. 2.4. Performing the integral over $\phi'_{<}$, the reduced density operator is given by

$$\rho_{>} = \mathrm{tr}_{<}\left(|0\rangle\langle 0|\right) = \int \mathscr{D}\phi_{<}\mathscr{D}\phi_{>}\mathscr{D}\phi'_{>}\, \langle \phi_{<}, \phi_{>}|0\rangle\langle 0|\phi_{<}, \phi'_{>}\rangle |\phi_{>}\rangle\langle \phi'_{>}|\,. \tag{2.31}$$

This result can be given a form that invites a simple physical interpretation. To obtain this form, it is helpful to observe that the open surfaces of $\phi_{>}$ and $\phi'_{>}$ on the right of fig. 2.4 are related by a rotation in the $t_{\mathrm{E}} - x$-plane, in particular by a rotation about an angle of 2π. Therefore, we may rewrite the Hamiltonian evolution within the overlaps (2.30) as an angular evolution by a different operator that we denote by $\tilde{K}_{>}$. As this operator generates rotations, we can write it as $\tilde{K}_{>} = -\partial_{\theta}$, where θ is the polar angle and the minus sign tells that the integration path is clockwise. From the point of view of the path integral, this is only a change of coordinates since it simply reparametrises the way that the integral over the same domain is performed. This is visualised on the right of fig. 2.4. However, this allows to obtain a surprisingly simple expression for the reduced density operator,

$$\rho_{>} = \int \mathscr{D}\phi_{>}\mathscr{D}\phi'_{>}\, \langle \phi_{>}|e^{-2\pi\tilde{K}_{>}}|\phi'_{>}\rangle |\phi_{>}\rangle\langle \phi'_{>}| = e^{-2\pi\tilde{K}_{>}}\,. \tag{2.32}$$

By analogous arguments, the reduced density operator $\rho_{<}$ is obtained in the same way with

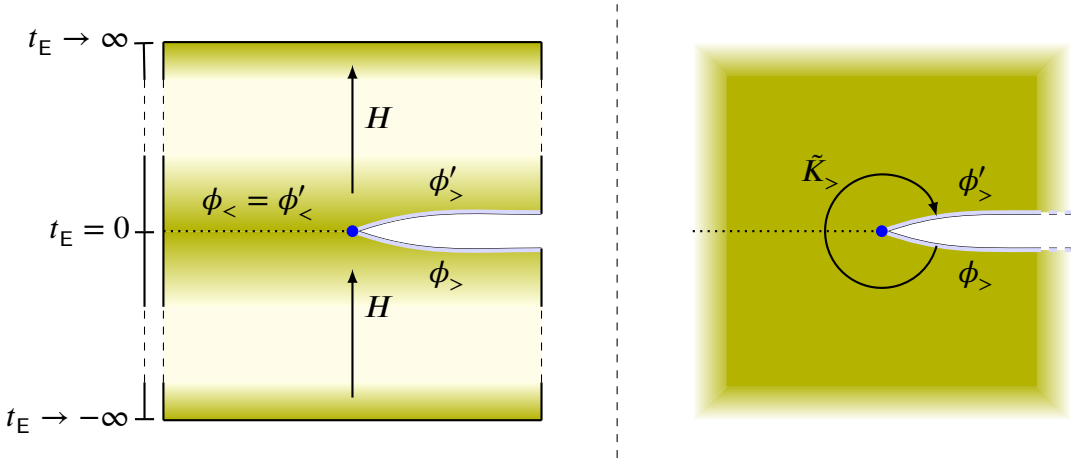

Figure 2.4: On the left, the reduced density operator $\rho_>$ is obtained by gluing two vacuum states obtained on the right of fig. 2.3. The partial trace is performed by setting $\phi_< = \phi'_<$ and integrating over all $\phi_<$. The indices of the reduced density operator correspond to the open surfaces of the states $\phi_>$ and $\phi'_>$, marked in light blue. On the right, the integral of the left part using Hamiltonian evolution is replaced by the evolution using $\tilde{K}_>$.

$\tilde{K}_< = -\partial_\theta$.

The above result (2.32) offers for a few interesting interpretations. First of all, we can give $\tilde{K}_>$ a Lorentzian interpretation by reversing the Wick rotation. We find that $\tilde{K}_>$ is simply the generator of Lorentz boosts [222],

$$\tilde{K}_> = -\partial_\theta = x\partial_{t_E} - t_E\partial_x \quad \overset{t_E = it}{\to} \quad ix\partial_t - it\partial_x \,. \tag{2.33}$$

Note that in this formula we no longer restrict to the initial value surface at $t = 0$, but reinstated the dependence for general t.

The physical interpretation of this result is the following. The time evolution of the Rindler wedge of the half space $x > 0$ is described by $\tilde{K}_>$.[12] The Rindler wedge $\text{Rin}_>$ is understood as the domain of dependence of $A = \text{Min}_{>,0}$. The operator $\tilde{K}_>$ generates orbits of constant acceleration a in Minkowski space, in our particular example for $a = 1$. For $a \neq 1$, the accelerated Rindler observer discerns their world at finite temperature $T = \frac{a}{2\pi}$. Different values of a can be interpreted as moving on trajectories of different constant radii [227]. This temperature arises due to their ignorance about the other pieces of Minkowski space which have been traced out in order to derive $\rho_>$. This is visualised in fig. 2.5, where the two arrows represent two different trajectories. Equivalently, this can be interpreted as resulting from the non-trivial entanglement within the vacuum state to which the Rindler observer does not have access. The Rindler observer of the half space $x > 0$ can never

[12] The coordinate transformation between polar coordinates r and θ of Minkowski space and the natural coordinates R and T of the Rindler wedge $ds^2_{\text{Rindler}} = -R^2 dT^2 + dR^2$ relates $\theta = iT$.

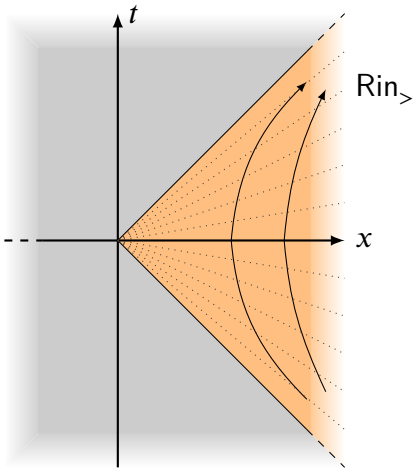

Figure 2.5: The arrows represent orbits of $\tilde{K}_>$ in the Rindler wedge (orange) and correspond to lines of constant Rindler radial coordinate. The dotted lines correspond to constant Rindler time T. The precise orbit for an observer is determined by the value of their acceleration a. notion of temperature from entanglement with the inaccessible regions (grey)

cross the lines $x = |t|$ but only has access to the region $x > |t|$. These lines act as a horizon for this observer. As realised for the first time in [223], this result is akin to the Hawking temperature of a black hole. This close relation was first pointed out in [228] where the analysis of [222] was generalised to black hole spacetimes.

In a Lorentz invariant theory, a Lorentz boost $\tilde{K}_>$ is a symmetry. Accordingly, by Noethers theorem it is accompanied by a conserved charge $K_>$. This conserved charge turns out to be the modular Hamiltonian that we already encountered in a simpler setting in (2.21). It is given by the spatial integral over the Lorentz boost $\tilde{K}_>$,

$$K_> = \int_{x>0} \mathrm{d}x\, \tilde{K}_> \,. \tag{2.34}$$

In this sense, $\tilde{K}_>$ can be interpreted as the modular Hamiltonian density. This expression can be cast into a covariant form utilising the energy-momentum tensor $\hat{T}_{\mu\nu}$,

$$K_> = \int_{x>0} \mathrm{d}x\, n^\mu \hat{T}_{\mu\nu} k^\nu \,, \tag{2.35}$$

where n^μ is a normal vector on the initial value surface and k^ν is the direction of the Lorentz boost. The normal vector can always be given the simple form $n^\mu = (1, 0)$,[13] such that only $\hat{T}_{0\nu}$ contributes. The direction of the boost is specified by the two entries of $k^\nu = (x, t)$,[14]

[13] In higher dimensions, $n^\mu = (1, 0, ..., 0)$.
[14] In higher dimensions a boost in the spatial direction x_i has $k^\nu = (x_i, 0, ..., 0, t, 0, ..., 0)$, such that $k^i = t$.

reproducing (2.34) by noting that $\hat{T}_{00} = H = \mathrm{i}\partial_t$ and $\hat{T}_{01} = p = -\mathrm{i}\partial_x$. However, since Lorentz boosts are a symmetry, without loss of generality we can always choose to work at $t = 0$, resulting in

$$K_> = \int_{x>0} \mathrm{d}x\, x\hat{T}_{00}\,. \tag{2.36}$$

The factor of x in front of $\hat{T}_{00}$ can be understood as a weight function. The formula (2.36) generalises to settings different than a half line in empty Minkowski space by adjusting this weight function to some $f(x)$. As an example, for the modular Hamiltonian of a ball-shaped region of radius R in a d-dimensional CFT this function is given by [229]

$$f(x_i) = \frac{R^2 - x_i x^i}{2R}\,. \tag{2.37}$$

For an arbitrary setting with general function $f(x)$, it is not known how to compute the integral. In two-dimensional CFTs, due to the large amount of symmetry, some of these computations can be performed [230]. Generally however, the modular Hamiltonian is expected to be a highly non-local operator. However, in a holographic context, to leading order the modular Hamiltonian has to account for the gravitational entropy, which is a local term. In sec. 5.2.2 we will make use of this property to compute modular Hamiltonians for various holographic settings in a three-dimensional gravitational theory.

The Area Law in QFT

As in quantum mechanics, the entanglement entropy in QFT satisfies an area law, at least for the ground state. However, obtaining this result is not as straightforward as in quantum mechanics. This is because in QFT we have to deal with infinitely many degrees of freedom, all of which might share some entanglement with other constituents. Indeed, generically the entanglement in any QFT state diverges. Therefore, in order to calculate entanglement entropy, the theory has to be regularised. The most common approaches to do so are either putting a UV cutoff Λ on the momentum $|k|$ or putting the theory on a lattice, where the lattice spacing acts as the UV cutoff ϵ. In the limits $\Lambda \to \infty$, $\epsilon \to 0$, results from both regularisation schemes have to agree. In either approach, by introducing the cutoff we essentially disregard all degrees of freedom above the cutoff which renders the entanglement entropy finite. This is visualised in fig. 2.6 for the case of the lattice regularisation. By analogy to quantum mechanics, intuitively speaking such a regularisation enables counting the quantum correlations across the bipartition surface. This makes clear why in QFT, the entanglement entropy satisfies an area law. This behaviour led to considering this quantity

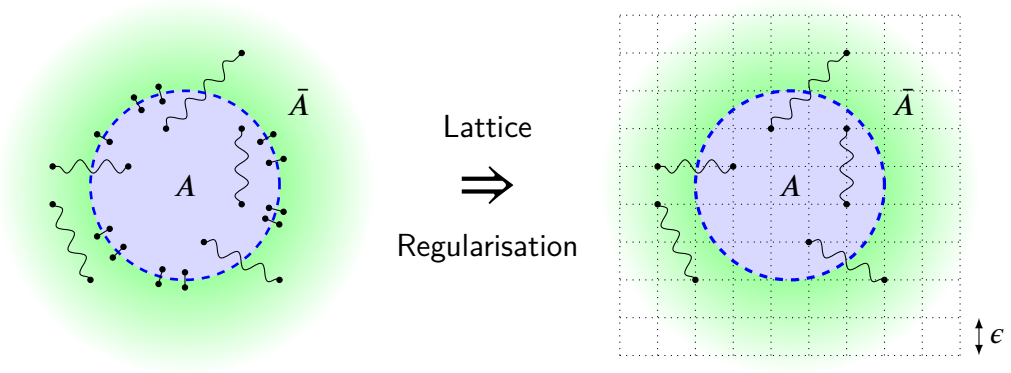

Figure 2.6: On the left, a bipartition surface (dashed blue) between regions A and $\bar{A}$ in a QFT is depicted. The infinite amount of correlations across the surface exemplarily shown, leads to a divergent amount of entanglement. Introducing a lattice regularisation depicted on the right, correlations above the cutoff are discarded. This enables computing the entanglement entropy analogously to quantum mechanics by counting the correlations across the bipartition surface.

in the context of black holes [231]. As we will discuss later on in sec. 3.1, an area law for the entropy arises naturally for theories with gravity.

In QFT we are usually interested in states with finite energy, corresponding to a finite amount of physical particle excitations. By arguments that will be discussed in detail in sec. 2.3.1, any such state looks like the vacuum state at sufficiently high energies. Therefore, the entanglement entropy of any (usually considered) state is expected to satisfy an area law, at least in a perturbative sense. Indeed, to leading order in the cutoff ϵ the entanglement entropy can be written as [231, 232]

$$S(\rho_{(A)}) = c_{d-2}\frac{\text{Area}(\partial A)}{\epsilon^{d-2}} + \mathcal{O}(\epsilon^{d-1}), \tag{2.38}$$

where c_{d-2} is a numerical constant that depends on the theory, ∂A is the bipartition surface, $\rho_{(A)}$ is the reduced density operator of region A and d is the dimension of the QFT. Terms of higher order also depend on geometric quantities associated to the bipartition surface, such as the curvature of ∂A. If we assume that the QFT also has conformal symmetry, by dimensional analysis the expression for the entanglement entropy can be further constrained. Since the only two scales of the theory are the cutoff ϵ and the length L of 'one side' of the region A,[15] In a scale invariant theory only the ratios $\frac{L}{\epsilon}$ can appear.

[15] The nth power of the cutoff ϵ defines small hypercubes as the smallest cells of the theory. By analogy, the region A can be approximated as a hypercube with edge length L.

Accordingly, the entanglement entropy has the general form

$$S(\rho_{(A)}) = c_{d-2}\left[\frac{L}{\epsilon}\right]^{d-2} + c_{d-4}\left[\frac{L}{\epsilon}\right]^{d-4} + \ldots + \begin{cases} (-1)^{\frac{d-1}{2}} c_{\text{finite}} + \mathcal{O}(\epsilon) & \text{for } d \text{ odd} \\ (-1)^{\frac{d-2}{2}} c_{\frac{d}{2}} \ln \frac{L}{\epsilon} + \mathcal{O}(\epsilon^0) & \text{for } d \text{ even.} \end{cases} \tag{2.39}$$

The constants c_{finite} and $c_{\frac{d}{2}}$ are referred to as the central charges of the theory. While generically the other coefficients c_{d-n} depend on the specific scheme used to calculate the entanglement entropy, these two are independent of the choice of scheme and therefore carry information about the theory only, in particular about the conformal anomaly that can arise during quantisation of such theories [233].

In the above form of the entanglement entropy, the case $d = 2$ is special since in this case, the area law fails as only the logarithmic term is present. However, in this instance the bipartition surface consists of disconnected points. The logarithm can then be understood as a limit of a power law divergence [221, 226, 234]. The logarithmic scaling of the entanglement entropy is universal for all two-dimensional CFTs [221].

This concludes our discussion of von Neumann entropy in quantum field theory.

2.1.3. Other Measures of Entanglement

As we have seen above, there exist certain settings where the modular Hamiltonian can be computed explicitly. In general, this is however an extremely difficult task. This in particular is related to the problem of calculating the logarithm of the reduced density operator.[16] For the same reason, having in mind the expression (2.22) for the entanglement entropy, it is generally complicated to compute the entanglement entropy directly in QFT, or even in large systems such as 666 spins, with subsystems of equal size containing 333 spins. The logarithm of an operator is computed by first calculating the eigenvalues of this operator. Computing the logarithm of the reduced density operator therefore requires diagonalising an operator represented by a matrix of dimension $2^{333} \times 2^{333}$, which is challenging at best, even numerically.[17]

[16] As found above, the modular Hamiltonian may also be calculated as an integral of the energy-momentum tensor with an appropriate weight function. However, as we commented below (2.36), in general it is extremely difficult to solve the integral.

[17] The number $2^{333} \sim 10^{100}$ is of the order of seconds it takes for realistic black holes to evaporate in a universe that realises the big freeze scenario.

Rényi Entropy

However, there exists an alternative way to determine the entanglement entropy that does not require computing the logarithm of the reduced density operator, but only powers of this operator. Based on the mathematical identity $\partial_\eta x^\eta = x^\eta \ln x$ and the rule of Bernoulli–de L'Hospital, the entanglement entropy can be written as

$$S(\rho_{(A)}) = \lim_{\eta \to 1} \left[\frac{1}{1-\eta} \ln \mathrm{tr} \left(\rho_{(A)}^\eta \right) \right] . \tag{2.40}$$

This was first discovered in [235] in an attempt to generalise the von Neumann entropy to a general measure of information while preserving the additivity of the information for independent systems. Named after its discoverer, for every η the term in brackets in (2.40) is known as the *η-th Rényi entropy*,

$$S^{(\eta)}(\rho_{(A)}) = \frac{1}{1-\eta} \ln \mathrm{tr} \left(\rho_{(A)}^\eta \right) , \tag{2.41}$$

where $\eta \in \mathbb{R}_+$.

The Rényi entropies contain the information about the entire entanglement spectrum, i.e. all eigenvalues of $\rho_{(A)}$. In more detail, for a reduced density operator ρ represented by an $N \times N$ matrix, knowledge of the first N Rényi entropies is sufficient to deduce all eigenvalues of $\rho_{(A)}$ [236]. In QFT, where intuitively $N \to \infty$, in particular the integer powers of ρ are much simpler to compute than the entanglement entropy itself. Having an expression for $S^{(n)}(\rho_{(A)})$ depending on the integer n, the usual strategy amounts to analytically continuing this expression to a continuous variable η such that the limit $\eta \to 1$ can be taken. Following (2.40), this computes the entanglement entropy. As an aside, we point out that if the reduced density operator corresponds to a pure state, we have seen before that the entanglement entropy vanishes. As in this case, the purity γ equals one, the trace of every integer power of $\rho_{(A)}$ equals one as well. Accordingly, the Rényi entropies evaluated for $\rho_{(A)}$ corresponding to a pure state vanish for every n.

Computing the integer powers of the reduced density operators is performed by using the *replica trick*. This was first introduced in the context of disorder averaging the partition function of a spin glass [237]. For entanglement entropy, this trick was used for specific systems in [234]. Since then, it has become an immensely useful tool also in general QFT (for a review see e.g. [238]). The nth integer power of $\rho_{(A)}$ is interpreted as considering n different copies of the same system. Given a reduced density operator calculated by the Euclidean path integral approach as discussed in sec. 2.1.2, pictorially the reduced density operator can be understood as a sheet $\mathscr{B}$ with an entanglement cut, corresponding to the field configurations ϕ and ϕ'. The nth power is then understood as identifying one of

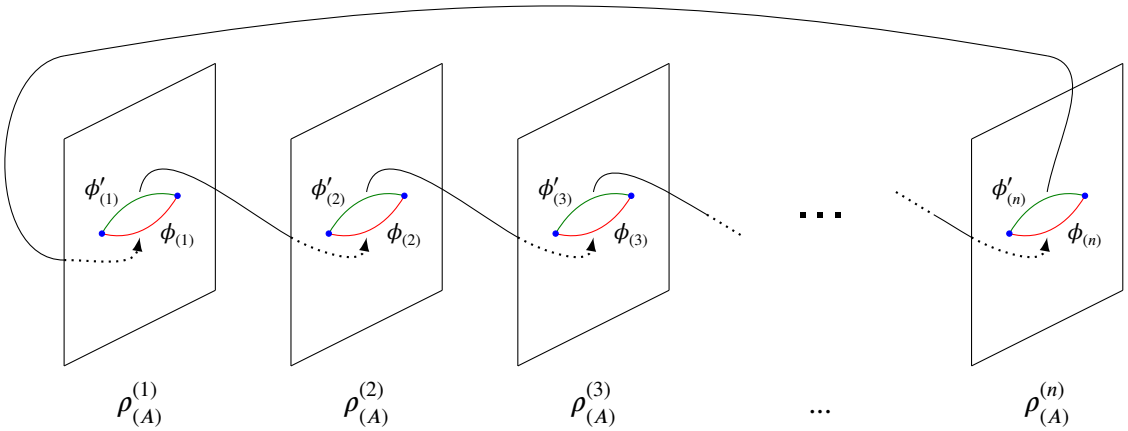

Figure 2.7: This visualises the replica trick. The upper field of the i-th copy $\phi'_{(i)}$ is identified with the lower field of the $i+1$-th copy $\phi_{(i+1)}$, thereby gluing the manifolds to each other. The trace of the power of the density operators identifies the last upper field with the lower field of the first copy.

the field configurations of the i-th reduced density operator, say the primed one, with the unprimed field of the $i+1$th reduced density operator,

$$\phi'_{(i)} = \phi_{(i+1)} \,. \tag{2.42}$$

To account for the trace, the primed field of the nth reduced density operator, $\phi'_{(n)}$, is identified with the unprimed field of the first reduced density operator, $\phi_{(1)}$. This gluing procedure is visualised in fig. 2.7.

The gluing procedure involved in the computation of $\mathrm{tr}\left(\rho^n_{(A)}\right)$ defines a single manifold known as the replica manifold $\mathscr{B}_n$. An example for $n = 3$ is shown in fig. 2.8. The trace of $\rho^n_{(A)}$ can be expressed as a ratio of partition functions Z evaluated on $\mathscr{B}_n$ and the original manifold $\mathscr{B}$ as

$$\mathrm{tr}\left(\rho^n_{(A)}\right) = \frac{Z[\mathscr{B}_n]}{Z[\mathscr{B}]^n} \,. \tag{2.43}$$

Although $\mathscr{B}_n$ looks complicated in general, topologically it is equivalent to a manifold with conical defects but flat otherwise. As an example, the manifold depicted in fig. 2.8 can be given the metric $\mathrm{d}s^2 = \mathrm{d}r^2 + r^2\mathrm{d}\varphi^2$ where $\varphi \sim \varphi + 6\pi$. For general n, the angular coordinate has periodicity $2\pi n$. However, in a general QFT it is still complicated to find this metric explicitly and therefore to compute the Rényi entropies. As in previous cases, again the presence of conformal symmetry significantly simplifies the situation, especially for two-dimensional CFTs. Here, it is known how to give the replica manifold $\mathscr{B}_n$ a flat metric using a conformal transformation. The trace of $\rho^n_{(A)}$ is known analytically and leads

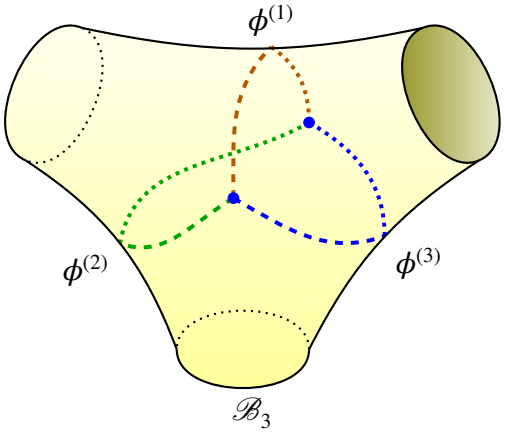

Figure 2.8: The figure shows a replica manifold for the case $n = 3$. The three manifolds are glued along the coloured dashed lines following the prescription of fig. 2.7. The blue dots are the bipartition surfaces.

to the Rényi entropies [221]

$$S^{(n)}(\rho_{(A)}) = \frac{c_1}{2}\left(1 + \frac{1}{n}\right)\ln\frac{L}{\epsilon}\,, \tag{2.44}$$

where c_1 is the constant that also appeared in (2.39), L is the size of the considered region A and ϵ is the UV cutoff. Analytically continuing this expression $n \to \eta$ and taking the limit $\eta \to 1$, the well known result [221]

$$S(\rho_{(A)}) = c_1 \ln\frac{L}{\epsilon} \tag{2.45}$$

is obtained.

Quantum Discord

As we pointed out in the previous section above (2.10), the entanglement entropy has certain limitations in capturing quantum correlations when it comes to mixed states. That is based on the fact that the entanglement entropy is not sensitive to whether the correlations within a given state are of a classical or quantum nature. As an example, calculating the entanglement entropy between two spins prepared in a Bell state results in $S(\rho) = \ln 2$, as the Bell states are defined as the maximally entangled states. This result is purely due to the quantum entanglement between the two spins. However, suppose that in a different situation, we only have one spin and purely due to classical uncertainty cannot decide whether the spin is up or down. The 'entanglement entropy' of the corresponding *classically* mixed state takes the same value, $S(\rho) = \ln 2$. Given access only to one spin, using the entanglement entropy we are unable to decide whether this really is a

classical mixture or the mixed state resulted as a reduced density operator. Therefore, the entanglement entropy fails to be a measure of purely quantum correlations when it comes to mixed states, in that it does not distinguish between classical and quantum correlations within the state.

Since this was observed, there have been a lot of proposals for measures quantifying entanglement within mixed states. Overviews are provided in [239–241] as well as in references within this overview. Examples include quantities such as the entanglement of formation [242, 243], distillable entanglement [244], the relative entanglement entropy [245, 246], the entanglement negativity [247, 248] and its logarithmic cousin [247, 249]. Between these measures there exist relations, such as the logarithmic negativity being an upper bound for the distillable entanglement. Moreover, some measures such as the entanglement of formation reduce to the entanglement entropy for pure states, while other measures such as the (logarithmic) negativity do not. Rather, this particular measure reduces to the $\frac{1}{2}$th Rényi entropy [247, 248]. This is qualitatively visualised on the left of fig. 2.9. While all of these measures are well-suited for certain types of mixed states, they still have shortcomings. As an example, the logarithmic negativity may vanish if the state is entangled but satisfies the positive partial transpose condition [194, 195]. As a second example, relative entropy has the downside that a reference state is required while usually, we are interested in the properties of the state itself, independent of any choice of reference.

None of the measures described above capture all of the quantum correlations within a given mixed state. A more general measure defined for this purpose is known as *quantum discord*, developed independently in [173, 174] and [175]. This measure quantifies quantum correlations even beyond entanglement, as visualised on the left of fig. 2.9. In particular, it can be non-zero for separable mixed states [250]. Moreover, quantum discord is non-zero for states of vanishing entanglement of formation [174, 251] and entanglement negativity [252]. For the former case, this is demonstrated explicitly using Werner states [253]. As we will study a measure very closely related to quantum discord in sec. 7, we give a few more details on quantum discord itself in the following.

The definition of quantum discord is inspired by generalising two classically equivalent ways of writing the mutual information [254] to the quantum setting. Given two random variables A and B, the mutual information $I(A:B)$ between these variables is usually denoted as

$$I(A:B) = H(A) + H(B) - H(A,B)\,, \tag{2.46}$$

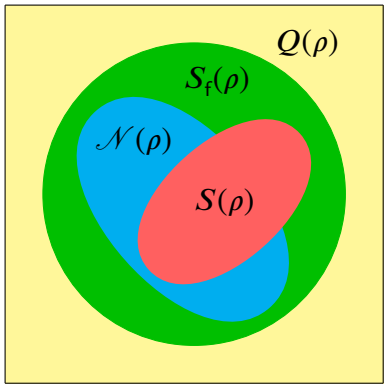

comparison of quantum correlations

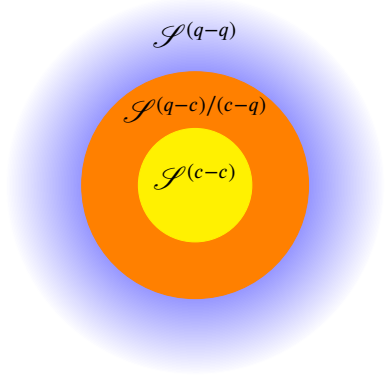

$\mathcal{S}^{(q-q)} \supset \mathcal{S}^{(q-c)/(c-q)} \supset \mathcal{S}^{(c-c)}$

Figure 2.9: On the left, different measures of entanglement are set in (qualitative) comparison, where ρ is an arbitrary bipartite mixed state. Quantum discord $Q(\rho)$ is the most general measure. It is more general than entanglement of formation $S_f(\rho)$ and entanglement negativity $\mathcal{N}(\rho)$. Entanglement entropy $S(\rho)$ is not a good measure for mixed states. For pure states, $\mathcal{N}(\rho)$ does not reduce to $S(\rho)$, while $S_f(\rho)$ and $Q(\rho)$ do. On the right, sets of states are set in comparison w.r.t. the entanglement of the states. An arbitrary state is a q-q state. Bipartite states with one of the subsystems in a classical state are q-c or c-q states. If both subsystems are classical, the state is c-c.

where H is the Shannon entropy.[18] Equivalently, the mutual information can also be written as

$$I(A:B) = H(A) - H(A|B)\,, \tag{2.47}$$

where $H(A|B) = H(B) - H(A,B)$ is the conditional entropy. Adapting to quantum systems, the Shannon entropies are replaced by von Neumann entropies. This goes well except for the conditional entropy $H(A|B)$. In this case, straightforwardly replacing $H \to S$ yields an expression for $I(A:B)$ that is no longer positive definite [255–258]. The classical quantity $H(A|B)$ quantifies the entropy of A, provided that the value of B is known. Generalising to quantum systems, this means that a measurement in subsystem B has been performed. Accordingly, the generalisation of the conditional entropy for quantum systems proposed in [174, 175] involves measurements in one of the subsystems,

$$S(A|B) = \min_{\{\Pi_k^{(B)}\}\in\mathcal{M}^{(B)}} \sum_k q_k S(\rho_{(A)}^{(k)})\,. \tag{2.48}$$

Here, $\{\Pi_k^{(B)}\}$ are projective measurements performed on subsystem B. The outcome of

[18] The Shannon entropy is defined analogously to the von Neumann entropy (2.10) with the density operator replaced by the classical probability distribution $p(X)$ of the variable X.

the measurement is labelled by the index k. The minimisation is performed over all such measurements contained in the set $\mathscr{M}^{(B)}$. The conditioned reduced density operators $\rho^{(k)}_{(A)}$ and the probabilities q_k for an outcome are defined as

$$q_k = \mathrm{tr}\left[\left(\mathbb{1}\otimes\Pi^{(B)}_k\right)\rho\left(\mathbb{1}\otimes\Pi^{(B)\,\dagger}_k\right)\right], \tag{2.49}$$

$$\rho^{(k)}_{(A)} = \frac{1}{q_k}\,\mathrm{tr}_B\left[\left(\mathbb{1}\otimes\Pi^{(B)}_k\right)\rho\left(\mathbb{1}\otimes\Pi^{(B)\,\dagger}_k\right)\right], \tag{2.50}$$

where ρ is the full density operator. The quantum version of (2.47), given by

$$J(A:B) = S(\rho_{(A)}) - S(A|B), \tag{2.51}$$

is known as asymmetric mutual information. The asymmetry results from the second term, which due to the measurements $\{\Pi^{(B)}_k\}$ is not symmetric under $A \leftrightarrow B$. An analogue definition can however be established with the roles of A and B exchanged.

It was argued in [175] that the asymmetric mutual information captures only classical correlation. Correspondingly, as the quantum version of (2.46) captures all types of correlations, their difference captures quantum correlations exclusively. This is consistent with the fact that the classical counterparts are equivalent such that their difference vanishes. This observation motivates the definition of quantum discord $Q(A:B)$ as this difference,

$$Q(A:B) = I(A:B) - J(A:B). \tag{2.52}$$

For pure states, quantum discord reduces back to the entanglement entropy since in this case $S(\rho) = 0 = S(A|B)$. Moreover, quantum discord is always bigger than or equal to zero. If a state has only classical correlations, quantum discord vanishes. Such classical-classical (c-c) states form the set $\mathscr{S}^{(c-c)}$. More generally, quantum discord vanishes if and only if there exists a measurement on B that does not influence the system [174, 181]. This determines a class of states $\mathscr{S}^{(q-c)}$ known as quantum-classical (q-c) states, all of which have vanishing quantum discord.[19] The possible sets of states with distinct properties are shown in fig. 2.9. Unfortunately, evaluating quantum discord for an arbitrary state is demanding, in particular due to the minimisation over projective measurements. In fact, it was shown that this is an NP-complete problem [180].

As (2.52) contains $S(A|B)$, it is also asymmetric in general, i.e. $Q(A:B) \neq Q(B:A)$. However, evaluated on states that are symmetric under the exchange of the two parties, also the two versions of quantum discord coincide [259]. By generalising the measurements

[19] This is true for quantum discord as defined in (2.52). If J is defined with A and B exchanged, i.e. measurements are performed in A instead of B, the zero discord states are called classical-quantum (c-q).

$\{\Pi_k^{(B)}\}$ to also measuring subsystem A, a symmetric version of quantum discord can be defined [260]. An extensive review of quantum discord and closely related quantities can be found in [261]. One of those quantities known as *geometric quantum discord* (GQD) we will discuss in more detail in sec. 2.2.2. This quantity will also be the object of primary focus in sec. 7.

This concludes our discussion of other entanglement measures but also of entanglement in general. Next, we discuss how geometry can be used to study quantum systems and the entanglement within.

2.2. Geometric Interpretation of Entanglement

We have discussed above in detail how entanglement is understood within quantum theory, starting from the very basics of the latter. In this discussion, the use of linear algebra was paramount. Linear algebra arises due to *canonical quantisation*, where the usual Poisson brackets of classical mechanics are promoted to graded commutators. Simultaneously, the variables of classical mechanics are replaced by corresponding operators. However, while this approach is very successful, it also seems to lead to a fundamental difference between these two frameworks. While classical mechanics is treated as a geometric and non-linear theory (see e.g. [262] for an exposition), quantum theory is algebraic and linear. This seeming difference motivated studies discussing geometric methods also in the context of quantum mechanics. This in particular led to defining the *projective Hilbert space* and *geometric quantisation* as an alternative to canonical quantisation which made explicit use of the geometry of classical phase space [263–265]. In the following sec. 2.2.1, we first provide more details on geometric quantum mechanics. Elements of this discussion, such as the projective Hilbert space, will be of central importance in the upcoming secs. 4, 5 and 6. Second, we focus on discussing entanglement entropy within the geometric setting in sec. 2.2.2.

2.2.1. Geometrising Quantum Mechanics

As previously described, classical mechanics have a geometric and non-linear description. In more detail, the classical phase space Γ allows for the definition of a symplectic form Ω, i.e. the classical phase space is a symplectic manifold, $\Gamma = (\mathscr{M}, \Omega)$. By the symplectic form, also a Poisson bracket is defined. Observables are described by real-valued functions f. These functions act on elements $x \in \mathscr{M}$ as $f : \mathscr{M} \to \mathbb{R},\ x \mapsto f(x)$, where x is interpreted as the classical state. In this process, x itself is unaffected by applying f. This is imprinted on the algebra described by the observables as this algebra is abelian and

associative. This means that the outcome of a classical measurement is not influenced by other measurements. Moreover, to every observable a vector field X_f is associated. These vector fields describe a flow on the phase space. In particular, time evolution is described by the vector field X_H, where H is the Hamiltonian. The Hamilton equations of motion can then be written as

$$\mathrm{d}H = \iota_{X_H}\Omega\,, \tag{2.53}$$

where d is the exterior derivative and ι_{X_H} denotes contracting the first index of Ω with the vector field X_H. The flow generated by X_H preserves the symplectic form. Correspondingly, X_H generates symplectomorphisms,[20] which is the mathematical expression for canonical transformations.

Quantum mechanics, as we have seen in the sec. 2.1.1, considers states represented by vectors living in a Hilbert space $\mathscr{H}$. Observables are described by Hermitian operators $\mathfrak{O}$ acting linearly on the Hilbert space. Of course, measuring an observable changes the state in that it collapses to an eigenstate of the observable. Correspondingly, the algebra of observables in quantum mechanics generically is non-abelian. Rather, it has the structure of a Lie algebra, defined by the commutator bracket between observables. Moreover, there is a Jordan product (in other words, the anti-commutator). Due to the presence of the latter, the algebra is not associative. Again, each observable can be used to define a flow on the state space, i.e. the Hilbert space. For an observable $\mathfrak{O}$, the flow is generated by $\exp(\mathrm{i}\mathfrak{O}s)$, where s is a real parameter. Time evolution again is generated by the Hamiltonian, with $s = t$ being the physical time. The equation of motion for the quantum states is known as the Schrödinger equation [5],

$$\mathrm{i}\frac{\mathrm{d}}{\mathrm{d}t}|\psi\rangle = H|\psi\rangle\,. \tag{2.54}$$

The linearity of the standard treatment of quantum mechanics is reflected by this equation in that the superposition of any two solutions $|\psi_{1,2}\rangle$ is again a solution.

An intermediate result addressing the relation between classical and quantum mechanics is given by the method of geometric quantisation [263–265]. As opposed to the priorly known methods of canonical quantisation or Weyl quantisation, geometric quantisation makes explicit use of the geometric features present in classical mechanics. In particular, the symplectic form Ω of the classical phase space $\Gamma = (\mathscr{M}, \Omega)$ is regarded as the curvature of a principal fibre bundle over $\mathscr{M}$. The quantised Hilbert space is then understood as the space of all sections of the fibre bundle. We will provide more details on principal fibre

[20] A symplectomorphism is a diffeomorphism that preserves the symplectic form.

bundles shortly within the present section, albeit in a slightly different context. Employing geometric quantisation also leads to quantum features such as the quantisation of spin. Mathematically, this comes about by the requirement that the symplectic form, in order to provide a curvature for the fibre bundle, has to satisfy the Weyl integrality condition, i.e. the integral of the symplectic form over any closed two-dimensional surface $\Sigma \subset \mathscr{M}$ has to be proportional to an integer,

$$\int_\Sigma \Omega \in 2\pi\mathbb{Z}\,. \tag{2.55}$$

For more technical details on geometric quantisation we refer the interested reader to [266] and references therein.

The Projective Hilbert Space

In the following, we restrict the discussion to state vectors, i.e. pure states. To obtain a geometric formulation of quantum mechanics, it is useful to note that from the perspective of physics, the set of all state vectors within the Hilbert space is too large. This can be understood by the following. Two state vectors $|\psi\rangle$ and $|\psi'\rangle = e^{i\alpha}|\psi\rangle$, which are different vectors from the perspective of the Hilbert space, lead to the same result when measuring any observable. Therefore, physically these two state vectors are equivalent since no (local) measurement can distinguish between them. This led to defining equivalence classes of state vectors

$$[|\psi\rangle] := \{\lambda|\psi\rangle : \lambda \in \mathbb{C} \wedge |\lambda| = 1\}\,. \tag{2.56}$$

In other words, two states $|\psi\rangle$ and $\lambda|\psi\rangle$ satisfy an equivalence relation $\sim_\lambda$. State vectors of different equivalence classes generically lead to different measurement results of the same observable. The notion of a (physically distinguishable) state is then interpreted as the equivalence class $[|\psi\rangle]$. These classes are also referred to as rays [267].

Given this identification of certain state vectors, also the structure of the Hilbert changes when imposing the equivalence relation $\sim_\lambda$. Implementing the equivalence relation on $\mathscr{H}$ defines the *projective Hilbert space* $\mathscr{P}(\mathscr{H})$ as the space of rays [46, 47],

$$\mathscr{P}(\mathscr{H}) := \frac{\mathscr{H} - \{0\}}{\sim_\lambda}\,. \tag{2.57}$$

Here, zero vectors have to be excluded. As discussed in sec. 2.1.1, the natural Hilbert space for an n level quantum system is $\mathscr{H} = \mathbb{C}^n$. The corresponding projective Hilbert

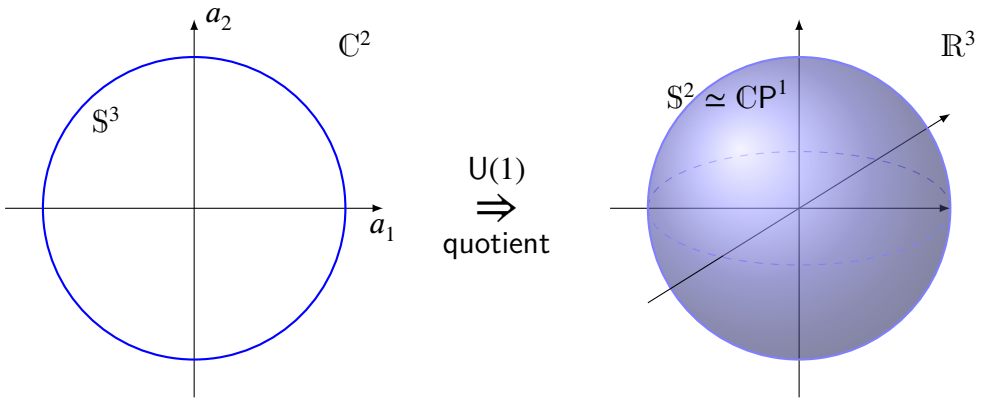

Figure 2.10: On the left, the components a_1, a_2 of a state vector in $\mathscr{H} = \mathbb{C}^2$ are interpreted as coordinates for $\mathscr{C}^2$. The normalisation of quantum states fixes $\mathbb{S}^3$ as submanifold in $\mathscr{H}$. Implementing the equivalence relation, i.e. the quotient by U(1), yields the projective Hilbert space $\mathbb{S}^2$, depicted on the right as a submanifold of $\mathbb{R}^3$.

space is given by

$$\mathscr{P}(\mathbb{C}^n) = \mathbb{C}\mathrm{P}^{n-1} = \frac{\mathbb{S}^{2n-1}}{\mathrm{U}(1)}\,. \tag{2.58}$$

This comes about as follows. Due to the normalisation condition $\langle\psi|\psi\rangle = 1$, the state vectors of the Hilbert space $\mathscr{H} = \mathbb{C}^n$ form the unit sphere $\mathbb{S}^{2n-1}$ as a submanifold of $\mathbb{C}^n = \mathbb{R}^{2n}$. The equivalence relation $\sim_\lambda$ corresponds to quotienting this space by the U(1) action $|\psi\rangle \to \lambda|\psi\rangle$. This is visualised for the first non-trivial example $n = 2$ in fig. 2.10. In this description, since λ is independent of any real world coordinates, U(1) is a gauge group of the first kind. The components of state vectors $|\psi\rangle$ can be used to define coordinates for the projective Hilbert space, see e.g. [190] for a detailed discussion. We will shortly encounter this in a more explicit form when discussing the Riemannian metric in more detail.

With this formulation, also quantum mechanics is given a geometric and non-linear interpretation. To make this manifest, we note that the projective Hilbert space in particular is a Kähler manifold. Such manifolds allow for compatible definitions of a complex structure, a symplectic form and a Riemannian metric. In other words, Kähler manifolds are manifolds that are complex manifolds, symplectic manifolds and Riemannian manifolds simultaneously. The interested reader may find a more elaborate discussion of such manifolds in e.g. [268, 269]. In the following we are mostly interested in the notions of the Riemannian metric as well as the symplectic form. Consistent with the presence of a symplectic form, it was found that the Schrödinger equation (2.54) can be rephrased as Hamilton equations of motion (2.53), where the generalised coordinates of the symplectic manifold are given by the real and the imaginary parts of the state vector components [48]. The Riemannian

metric on the other hand was found to enter the computation of quantum uncertainty relations [49]. In a broader sense, the Riemannian metric is important whenever quantum features without classical analogue are discussed [49], including also the collapse of the state under a measurement [50].

We have now discussed a few general properties of this Riemannian metric, however without giving it an explicit form. This is our goal in the following. As we have seen above, the projective Hilbert space for an n level quantum system is given by the complex projective space $\mathbb{C}\mathrm{P}^{n-1}$ which is a Kähler manifold and therefore admits a Riemannian metric. The metric on $\mathbb{C}\mathrm{P}^{n-1}$ can be defined using the real part of the Hermitian inner product defined for the original Hilbert space $\mathscr{H}$ [270]. This was made explicit in [271], generalising earlier results of [272]. As we discussed in def. 1, a Hilbert space $\mathscr{H}$ is equipped with an inner product $\langle\cdot|\cdot\rangle$ that maps two state vectors $|\psi_1\rangle$ and $|\psi_2\rangle$ to a complex number. As this inner product is anti-linear in the first slot, i.e. $\langle\alpha\psi_1|\psi_2\rangle = \alpha^*\langle\psi_1|\psi_2\rangle$ for any $\alpha \in \mathbb{C}$, it is in particular a Hermitian inner product.[21] The scalar product induces a norm $||\cdot||$ by

$$||\psi||^2 = \langle\psi|\psi\rangle\,. \tag{2.59}$$

This norm is also known as the Hilbert–Schmidt norm. The norm of the difference of two vectors $||\psi_1 - \psi_2||$ defines the distance between the two vectors. This distance can be written in terms of a metric induced by the norm in the following way. First, assume that the state vectors $|\psi_i(s)\rangle$ are parametrised by sets of parameters $s = (s_1, ..., s_k) \in \mathbb{R}^k$. Then computing the (square of the) distance between infinitesimally separated state vectors $|\psi(s)\rangle$ and $|\psi(s + \mathrm{d}s)\rangle$ to second order in $\mathrm{d}s$ yields

$$||\psi(s + \mathrm{d}s) - \psi(s)||^2 = \langle\partial_i\psi|\partial_j\psi\rangle \mathrm{d}s^i \mathrm{d}s^j\,, \tag{2.60}$$

where ∂_i is short for $\frac{\partial}{\partial s^i}$. The inner product between derivatives of the state vector can be split into its real and its imaginary part,

$$\langle\partial_i\psi|\partial_j\psi\rangle = \gamma_{ij} + \mathrm{i}\Omega_{ij}\,. \tag{2.61}$$

Since the inner product is Hermitian, the components of the imaginary part Ω_{ij} have to be anti-symmetric. Therefore, as the product of differentials $\mathrm{d}s^i\mathrm{d}s^j$ is symmetric, the distance between two state vectors can be expressed using only the components γ_{ij}. This quantity may therefore be interpreted as a metric. In particular, under a change of coordinates

[21] In mathematical literature, a Hermitian inner product is defined to be anti-linear in the *second* slot, as opposed to the usual convention in physics. Regarding the Hermitian property, this difference is not important. The defining feature is that one and only one of the slots is anti-linear.

$s \mapsto s'(s)$, γ_{ij} obey the transformation law of the components of a 2-tensor,

$$\gamma_{ij}(s) \mapsto \gamma'_{ij}(s') = \frac{\partial s^k}{\partial s'^i}\frac{\partial s^l}{\partial s'^j}\gamma_{kl}(s)\,. \tag{2.62}$$

However, as we have discussed above in quite some detail, different state vectors do not necessarily lead to different measurement results, which was the reason to introduce the notion of rays in (2.56). Given two state vectors within one ray, they are related by a U(1) transformation, which in particular might depend on the parameters s.[22] Under such a transformation which we may write as $e^{i\alpha(s)}$, the components γ_{ij} are not invariant but receive additional contributions from the derivatives of α. Therefore, the components γ_{ij} do not provide us with a useful notion of a metric tensor on state space as they attribute a non-vanishing distance between physically equivalent state vectors.

Fortunately, there is a somewhat simple cure to this issue by subtracting the unwanted terms. To do so, observe that the quantities

$$A_i = i\langle\psi|\partial_i\psi\rangle \tag{2.63}$$

transform as the components of a local gauge field under the action of U(1),

$$A_i \to A'_i = A_i - \partial_i\alpha\,. \tag{2.64}$$

Note that due to the normalisation $\langle\psi|\psi\rangle = 1$, this local gauge field introduced in (2.63) is real. It can therefore be consistently added to γ_{ij} to define [271]

$$g_{ij} = \gamma_{ij} - A_iA_j\,. \tag{2.65}$$

This quantity still transforms as the components of a 2-tensor under coordinate transformations $s \mapsto s'(s)$ but is also invariant under the action of U(1). Moreover, using the Cauchy–Schwarz inequality

$$|\langle\psi_1|\psi_2\rangle|^2 \leq \langle\psi_1|\psi_1\rangle\langle\psi_2|\psi_2\rangle \tag{2.66}$$

for $|\psi_1\rangle = |\psi\rangle$ and $|\psi_2\rangle = |\partial_i\psi\rangle$ shows that g_{ij} is positive definite.

The components of the imaginary part Ω_{ij} do not enter the definition of the metric on state space, but rather define the symplectic form on this space. We already observed

[22] Above we stated that the U(1) transformation is a gauge group of the first kind, i.e. independent of the coordinates. This statement however refers to the physical coordinates of our world, while s are coordinates in an abstract parameter space. The two statements are therefore not in conflict with each other.

above that Ω_{ij} are anti-symmetric, so they can be used to define a 2-form

$$\Omega = \Omega_{ij} \mathrm{d}s^i \wedge \mathrm{d}s^j \,. \tag{2.67}$$

Moreover, by direct computation it can be shown that the exterior derivative of Ω vanishes, $\mathrm{d}\Omega = 0$, i.e. Ω is a closed 2-form and can be interpreted as a symplectic form [270]. Using $\mathrm{d}^2 = 0$, this property is also obtained trivially by observing that Ω can be written as the exterior derivative of the local gauge field (2.63) introduced earlier,

$$\Omega = \mathrm{d}A \,, \tag{2.68}$$

where we write the local gauge field as a 1-form $A = A_i \mathrm{d}s^i$. Last but not least, while we had to work a bit to obtain a metric tensor invariant under the $\mathrm{U}(1)$ action, due to the anti-symmetry the symplectic form is invariant by definition.

In order to relate these expressions for the metric (2.65) and the symplectic form (2.67) to the previous discussion about the geometry of the projective Hilbert space, it is useful to consider the case where s_i are related to the coefficients of the state vector a_i. To be precise, we consider $s \in \mathbb{R}^{2n}$ and define $a_i = s_i + \mathrm{i}s_{i+n}$ where now $i = 1, ..., n$. As a consistency check, directly evaluating (2.65) and (2.67) results in the natural metric and symplectic form on $\mathbb{C}^n$,

$$g \propto \mathrm{d}a^{*,i} \mathrm{d}a_i, \quad \Omega \propto \mathrm{d}a^{*,i} \wedge \mathrm{d}a_i \,. \tag{2.69}$$

To connect to the above results on projective Hilbert space, as previously mentioned the components a_i can be used to define coordinates on $\mathscr{P}(\mathscr{H})$. First, we note that by implementing the normalisation of $|\psi\rangle$ explicitly, the above metric can be rewritten as the metric on $\mathbb{S}^{2n-1}$. Next, we have to implement the quotient by $\sim_\lambda$. To do so, starting with n coefficients a_i, we may rescale all a_i by any choice of particular $a_{i^*} \neq 0$,

$$a_1, ..., a_{i^*}, ..., a_n \quad \to \quad \frac{a_1}{a_{i^*}}, ..., 1, ..., \frac{a_n}{a_{i^*}} \,. \tag{2.70}$$

The rescaled components $b_j = \frac{a_{j \neq i^*}}{a_{i^*}}$ define affine coordinates on $\mathbb{C}\mathrm{P}^{n-1}$. As indicated, this is possible for every $i^* = 1, ..., n$. For fixed i^*, the affine coordinates are defined in the coordinate chart U_{i^*}. The collection of all charts covers all of $\mathbb{C}\mathrm{P}^{n-1}$. For a thorough review of this topic, both abstract mathematical aspects as well as the relation to quantum

mechanics, we refer to [190]. Using the coordinates b_i the metric for $\mathbb{C}\mathrm{P}^{n-1}$ is written as

$$g = \frac{\left(1 + b^{*,k} b_k\right)^2 \delta_{ij} - b_i b_j^*}{\left(1 + b^{*,k} b_k\right)^2} \mathrm{d}b^{*,i} \mathrm{d}b^j \,. \tag{2.71}$$

This is the Fubini–Study metric, which is the natural Kähler metric on the projective Hilbert space [273, 274]. This manifests that a state vector is geometrically understood as a point in $\mathbb{C}\mathrm{P}^{n-1}$.

To round off the discussion, with the geometric notions discussed above we are now in a position to reformulate the postulates of quantum mechanics in terms of geometric objects [49]. Regarding states and state space, we have

Postulate 1:

> The state space of physically distinct quantum states of an isolated quantum system is given by the projective Hilbert space $\mathscr{P}(\mathscr{H})$, which is a Kähler manifold. Physically distinct quantum states correspond to different points on the manifold.

Note that in this formulation of the postulate, reference is still made to the original Hilbert space, since in our discussion above the projective Hilbert space was introduced as a quotient of the Hilbert space. However, as shown in [49], the projective Hilbert spaces can also be defined in a purely geometric way as Kähler manifolds that possess a maximal amount of symmetry.

As mentioned above and shown in [48], the Schrödinger equation can be written as the set of the Hamilton equations of motion. Accordingly, time evolution can be formulated in terms of a Hamiltonian vector field, resulting in

Postulate 2:

> Time evolution of a closed quantum system is governed by a Hamiltonian vector field X_H (densely) defined on $\mathscr{P}(\mathscr{H})$. The vector field generates a flow on $\mathscr{P}(\mathscr{H})$ where the flow preserves the Kähler structure.

The statement that the flow preserves the Kähler structure on $\mathscr{P}(\mathscr{H})$ is the geometric version of the fact that unitary transformations of Hilbert spaces $\mathscr{H}$ result in Hilbert spaces isomorphic to $\mathscr{H}$.

Apart from the Hamiltonian, all other observables can be described in a geometric fashion as well. In particular, we find

Postulate 3:

Any physically measurable quantity, i.e. any observable O is described by a real valued smooth function f_O defined on $\mathscr{P}(\mathscr{H})$. The smooth functions are associated to vector fields X_{f_O} which generate a flow preserving the Kähler structure.

Furthermore, the collapse of the state vector upon measurement as well as the probabilistic interpretation in terms of geometry are analysed in [49]. In this work, a more thorough discussion of these geometric postulates can be found, as well as in [275]. In the former work a lot of these results were derived for the case of infinite-dimensional quantum systems, complementing other works [48, 50, 276–280]. These works also include generalisations to mixed states.

The fourth postulate addressing composite quantum systems can also be given a geometric version. In postulate four as written originally, we stated that the composite Hilbert space is given by the tensor product over the individual Hilbert spaces. Naively, we might therefore expect that the same is true for the projective Hilbert spaces, i.e. an equation like

$$\mathscr{P}(\mathscr{H}) \stackrel{?}{=} \bigotimes_{i=1}^{N} \mathscr{P}(\mathscr{H}^{(i)}) \tag{2.72}$$

should hold. However, we can easily convince ourselves that this simple expectation cannot be true. Suppose that $\mathscr{H}$ consists of N Hilbert spaces $\mathscr{H}^{(i)}$ of dimension n. Then, the complex dimension of the left-hand side $\mathscr{P}(\mathscr{H}) = \mathbb{C}\mathrm{P}^{n^N-1}$ is n^N-1, whereas the dimension of the right-hand side $\bigotimes_{i=1}^{N} \mathbb{C}\mathrm{P}^{n-1}$ is $N(n-1)$. Except for $N=1$, which is not a composite quantum system, the dimensions cannot match. This is due to the non-linearity of the projective Hilbert space. In other words, implementing the equivalence relation $\sim_\lambda$ does not commute with the tensor product. We summarise this via

Postulate 4:

The projective Hilbert space of a composite quantum system is obtained by implementing the equivalence relation $\sim_\lambda$ on the full tensor product $\mathscr{H} = \bigotimes_{i=1}^{N} \mathscr{H}^{(i)}$. Generic state vectors in the composite projective Hilbert space are given by superpositions of tensor products of the individual state vectors.

This in particular leads to defining a geometric notion of the entanglement entropy. This will be paramount for the discussion in secs. 4 and 6. We will explain this notion in detail shortly in sec. 2.2.2.

A Probe for the Geometry (and Topology) of State Space

We have found that the complex projective space $\mathbb{C}\mathrm{P}^{n-1}$ is of central importance when discussing quantum mechanics. Remembering (2.58), this space can be understood similarly to a sphere. As a special instance, in the simplest non-trivial case $n = 2$ we have $\mathbb{C}\mathrm{P}^1 \simeq \mathbb{S}^2$. Moreover, the components of the Riemann tensor are algebraically determined by the metric components. Also, the metric (2.71) is a solution to the vacuum Einstein equations with positive 'cosmological' constant [190]

$$R_{ij} = \Lambda g_{ij} \quad \text{with} \quad \Lambda = 2n\,, \tag{2.73}$$

attributing $\mathbb{C}\mathrm{P}^{n-1}$ an interesting interpretation both in the realms of quantum mechanics as well as general relativity. Quantities such as the Riemann curvature as well as the Ricci tensor and scalar measure the curvature of the underlying manifold in a local way. However, there are also global aspects to $\mathbb{C}\mathrm{P}^{n-1}$. To analyse those, the notion of fibre bundles is elementary, which in particular makes use of the symplectic form defined on the projective Hilbert space. Throughout this thesis, we will heavily rely on the concept of fibre bundles. We therefore discuss the definition and basic properties of fibre bundles in the following. This will in particular enable us not only to determine the geometry but also the topology of the projective Hilbert space. It will also provide a different and perhaps more intuitive picture of the relation between the Hilbert space and the projective Hilbert space. Among other sources, details on fibre bundles can be found in [269, 281].

Apart from projective Hilbert spaces, fibre bundles are used in physics mostly to analyse global properties, i.e. non-perturbative effects of the underlying physical system. Fibre bundles are useful whenever there is a redundancy in our description of physics. Gauge theories such as Yang–Mills field theories can be formulated using fibre bundles. This construction is therefore particularly useful for analysing non-perturbative aspects of our description of reality as the standard model is based on gauge theories. In general, a fibre bundle consists of five components, namely the *entire space* or *entire manifold* $\mathscr{E}$, a *projection* π, the *base space* or *base manifold* $\mathscr{B}$, the *fibre* $\mathscr{F}$ and a gauge group G. The projection π defines a map from the entire manifold to the base manifold, $\pi : \mathscr{E} \to \mathscr{B}$. Globally, the entire space is different than the Cartesian product of the base space and the fibre, $\mathscr{E} \overset{\text{glob}}{\neq} \mathscr{B} \times \mathscr{F}$. For that reason, the fibre bundle can also be interpreted as a twisted product between $\mathscr{B}$ and $\mathscr{F}$. However locally, the entire space can always be approximated as a product, $\mathscr{E} \overset{\text{loc}}{=} \mathscr{B} \times \mathscr{F}$. Regarding local properties, understanding fibre bundles enables to rigorously define local coordinates for an open region $\mathscr{U} \subset \mathscr{B}$ as well as coordinate transformations U_{ij} between different regions $\mathscr{U}_i, \mathscr{U}_j \subset \mathscr{B}$, which

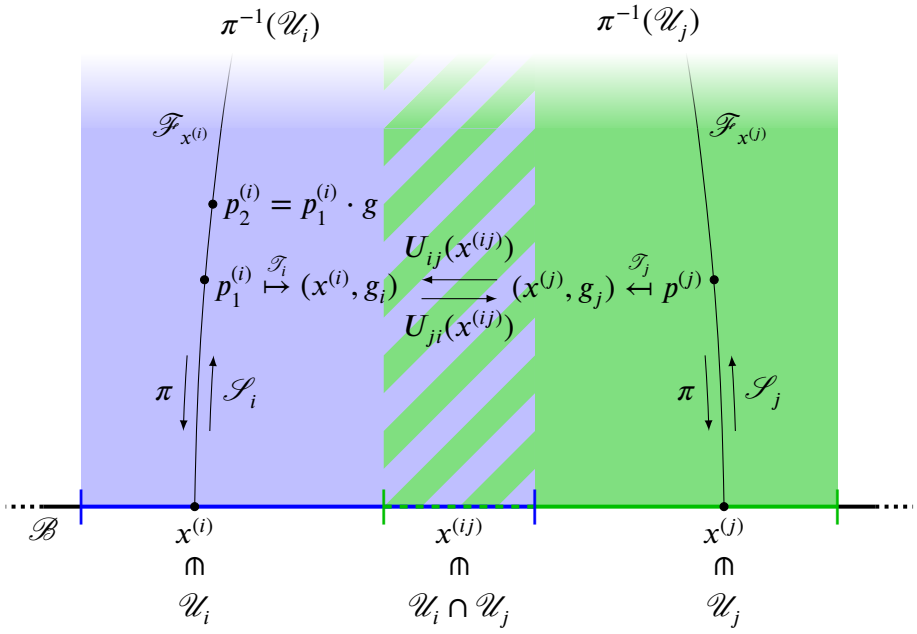

Figure 2.11: The various concepts for fibre bundles introduced in the main text are depicted above. The two regions $\mathscr{U}_1$ and $\mathscr{U}_2$ as well as the part of the fibre bundle defined on top of these regions, marked in blue and green, have a non-trivial overlap. The projection π maps from the fibre to the base manifold and the sections $\mathscr{S}_i, \mathscr{S}_j$ do the opposite. Two points $p_1^{(i)}, p_2^{(i)}$ are related by the right action of G. A trivialisation $\mathscr{T}_i$ locally expresses an arbitrary point $p^{(i)}$ in terms of base manifold points $x^{(i)}$ and group elements g_i. In the overlap region, gauge transformations $U_{ij}(x^{(ij)})$ between the regions are defined.

are also called gauge transformations. A necessary condition for being able to define such coordinate transformations is that the local regions overlap, i.e. $\mathscr{U}_i \cap \mathscr{U}_j \neq \{0\}$. This is visualised in fig. 2.11.

Due to the local product structure, a fibre bundle may locally be visualised as attaching to each point of the base manifold $x \in \mathscr{B}$ a fibre $\mathscr{F}_x$. The projection π then has to satisfy $\pi(p) = x$ for any point in the fibre $p \in \mathscr{F}_x$. For a visualisation see fig. 2.11. In the following, we focus on a subclass of fibre bundles called principal fibre bundles. For this subclass, the fibre is isomorphic to the group, i.e. $\mathscr{F} \simeq G$, such that it is not necessary to distinguish between fibre and gauge group. Principal fibre bundles are often denoted as

$$G \hookrightarrow \mathscr{E} \xrightarrow{\pi} \mathscr{B}\,. \tag{2.74}$$

For principal fibre bundles the relation between two different points in a single fibre $p_1, p_2 \in \mathscr{F}_x$ is particularly simple in that they are related by the right group action, $p_1 = p_2 \cdot g$ for $g \in G \simeq \mathscr{F}_x$. As mentioned above, fibre bundles provide a recipe to define local coordinates. This works as follows. Fixing coordinates or in other words choosing a gauge,

is performed by defining a *local trivialisation* $\mathscr{T}$ of the bundle. To each local region $\mathscr{U}_i$, a local trivialisation $\mathscr{T}_i$ is associated,

$$\mathscr{T}_i : \pi^{-1}(\mathscr{U}_i) \to \mathscr{U}_i \times \boldsymbol{G}, \quad p \mapsto \big(\pi(p) = x, g_i \in \boldsymbol{G}\big) . \tag{2.75}$$

Here $\pi^{-1}(\mathscr{U}_i)$ is understood as the part of the entire fibre bundle that is defined 'on top' of the region $\mathscr{U}_i$ of the base manifold, see again fig. 2.11. The trivialisation essentially disregards the potential twist between the fibre and the base manifold. Different trivialisations $\mathscr{T}_i, \mathscr{T}_j$ correspond to different gauge choices, in that they map p to different elements g_i, g_j of the group. Therefore, for $x^{(ij)} \in \mathscr{U}_i \cap \mathscr{U}_j$ it is possible to switch gauge by

$$\boldsymbol{U}_{ij}(x^{(ij)}) = \mathscr{T}_{i,x^{(ij)}} \circ \mathscr{T}^{-1}_{j,x^{(ij)}} . \tag{2.76}$$

This in particular maps $g_i = \boldsymbol{U}_{ij} \cdot g_j$, i.e. the left action of the group describes gauge transformations.

A physical process describes how different points are related to each other, subject to the dynamics of the underlying theory. Therefore, we may think of curves c on the base manifold. As we also have the fibre above $\mathscr{B}$, the curve can be uplifted into the fibre. This uplift requires the definition of parallel transport and therefore the definition of a connection. To do so, the main idea is to consider the decomposition of the tangent space at an arbitrary point p of the total space $\boldsymbol{T}_p\mathscr{E}$ into its vertical and horizontal components, $\boldsymbol{V}_p$ and $\boldsymbol{H}_p$ respectively. The vertical component is canonically fixed to contain all tangent vectors $v = \mathrm{d}_s\big(p \cdot g(s)\big)|_{s=0}$ pointing along the fibre. Here s parametrises the curve c defined by $g(s)$ a path in $\boldsymbol{G}$ with $g(0) = \mathbb{1}$. The horizontal component $\boldsymbol{H}_p$ is given by a completion of $\boldsymbol{V}_p$ to $\boldsymbol{T}_p\mathscr{E}$. This completion is not unique and the connection distinguishes between different choices for $\boldsymbol{H}_p$. Any connection that we aim to define has to be consistent with two requirements on curves. First, the connection has to be such that given a curve $c(s) \in \mathscr{B}$ its relative in the fibre $\tilde{c}(s)$ satisfies $\pi(\tilde{c}(s)) = c(s)\ \forall s$. Second, if two curves $\hat{c}$ and $\tilde{c}$ in the fibre are related by g at $s = 0$, $\hat{c}(0) = \tilde{c}(0) \cdot g$, the parallel transport defined by the connection has to be such that this relation holds for all values of s, $\hat{c}(s) = \tilde{c}(s) \cdot g$. A visualisation is provided on the left of fig. 2.12. This can be formalised by the following definition of the connection,

Definition 3: The connection ω_p is a Lie algebra valued linear map $\omega_p : \boldsymbol{T}_p\mathscr{E} \to \boldsymbol{T}_{\mathbb{1}}\boldsymbol{G}$, i.e. a one form satisfying

i) $\omega_p(v) = \hat{v} = \dot{g}(0)$ for $v \in \boldsymbol{V}_p$ and $g \in \boldsymbol{G}$

ii) $\ker \omega_p \simeq \boldsymbol{T}_x\mathscr{B}$, ensuring $\pi(\tilde{c}) = c$

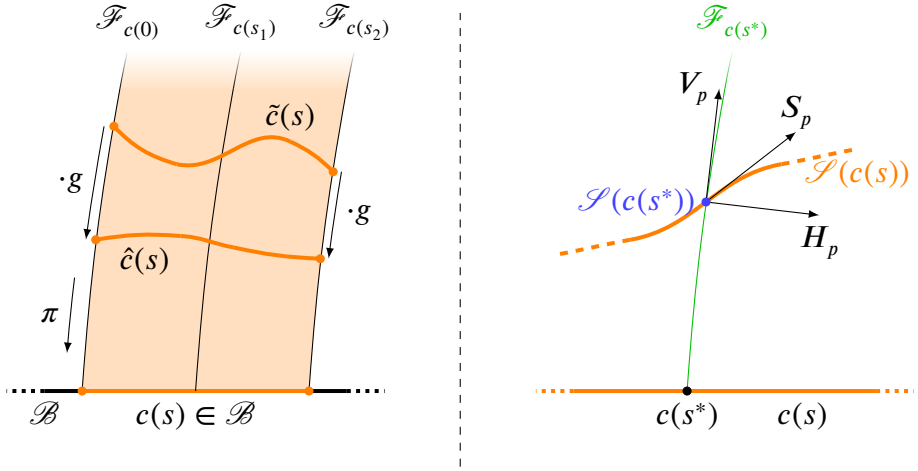

Figure 2.12: On the left, the two conditions on the connection are visualised. Under the projection π, any curve $\tilde{c}$ or $\hat{c}$ has to reduce to c. Moreover, since points within a fibre are related by the right action of G, the same has to be true for every point of curves, i.e. the two curves are also related by the right action of G. On the right, the distinction between H_p, S_p and V_p is depicted. V_p is simply the space of vectors tangential to the fibre. H_p is the horizontal space such that $T_p\mathscr{E} = V_p \oplus H_p$. S_p are vectors tangential to a section of a curve such that $T_p\mathscr{E}$. If $H_p = S_p$, the bundle is trivial and the connection vanishes.

iii) $\omega_{p\cdot g}(v \cdot g) = g^{-1} \cdot \omega_p(v) \cdot g$, ensuring $\hat{c}(s) = \tilde{c}(s) \cdot g$.

Note that the tangent space of G at the identity is the Lie algebra of the Lie group G, $T_{\mathbb{1}}G = \mathfrak{g}$. This definition is closely akin to familiar notions of gauge theory used in physics. Throughout the literature, there exist other definitions which are however equivalent to the definition above [269, 281].

Given the connection ω_p we can also define local gauge fields A_i. The subtle distinction is that the connection is defined as a map from $T_p\mathscr{E}$ while the local gauge fields will be defined as maps from $T_x\mathscr{U}_i$, i.e. from the tangent space of a point x in the base manifold. In order to define this map, we first need to introduce *sections*. A section of a fibre bundle can be visualised as the uplift of a curve c into the fibre direction. To every point x of the base manifold, the section $\mathscr{S}$ associates a point in the fibre. Expressed in formulas, this means

$$\mathscr{S} : \mathscr{U} \to \pi^{-1}(\mathscr{U}), \quad x \mapsto \mathscr{S}(x) = p\,. \tag{2.77}$$

The image of $\mathscr{S}$ as the inverse of π is interpreted as above. In particular, this formula makes clear that a section is the inverse of the projection in that it satisfies

$$\pi\big(\mathscr{S}(x)\big) = x, \quad \pi \circ \mathscr{S} = \mathbb{1}_{\mathscr{U}}\,. \tag{2.78}$$

A section is closely related to the inverse of a local trivialisation. In fact, a section can be understood as the inverse of a local trivialisation where $\mathscr{T}^{-1}$ is applied to a point on the base manifold paired with the identity element of the group, $\mathscr{S}(x) = \mathscr{T}^{-1}(x, \mathbb{1}_G)$. Nevertheless, the purpose of trivialisations and sections is different. A section provides a map from an arbitrary point x in the base manifold to a point p in the fibre. A trivialisation specifies how the point p can be locally expressed as the corresponding x and a group element g, as shown in (2.75).

Using sections, a local gauge field A_i is defined as a map from the tangent space at a point $x \in \mathscr{U}_i$ of a region in the base manifold to the Lie algebra $\mathfrak{g}$,

$$A_i : T_x\mathscr{U}_i \to T_{\mathbb{1}}G, \quad \dot{c}(s) \mapsto A_i = \omega_{\mathscr{S}_i(x)}\big(\mathrm{d}_s\mathscr{S}_i(c(s))\big)\,. \tag{2.79}$$

Here, $\mathrm{d}_s\mathscr{S}_i(c(s))$ defines a vector pointing along the uplift of the curve c into the fibre. The set of all vectors can be defined as a space $S_p = \mathrm{d}_s\mathscr{S}_i(c(s))$ which, together with V_p, spans the full tangent space $T_p\mathscr{E}$. This is visualised on the right of fig. 2.12. Since $\ker\omega_p \simeq T_x\mathscr{B} = H_p$, the gauge field vanishes exactly when $H_p = S_p$. Therefore, as mentioned above, a non-trivial connection and the corresponding non-trivial gauge field measure the mismatch between H_p and S_p. Moreover, given local gauge fields A_i, A_j for two sections $\mathscr{S}_i, \mathscr{S}_j$ corresponding to trivialisations $\mathscr{T}_i, \mathscr{T}_j$, a change of gauge described by U_{ij} relates the two gauge fields as

$$A_i = U_{ij}^{-1}A_jU_{ij} + U_{ij}^{-1}\mathrm{d}U_{ij}\,. \tag{2.80}$$

This is the familiar transformation law of gauge fields within gauge theory, generalising (2.64). In fact, U(1) gauge theory and its generalisation to SU(N) known as Yang–Mills theory can be understood as principal fibre bundles with fibres given by U(1) and SU(N), respectively. For U(1), the gauge field on the fibre bundle is simply the photon field. In Yang–Mills theory, for $N = 2, 3$ the gauge fields are interpreted as the $W^{\pm}$ and Z bosons as well as the gluons, transferring the weak and strong force respectively.

So far we have discussed the connection in a local definition. However, as promised above, the fibre bundle also allows to study non-local, i.e. non-perturbative effects which are sensitive to the twist between the base manifold and the fibre. To see this, we again point out that the connection can be defined once a section is defined. In the simplest case this section is defined everywhere. This is referred to as a *global section*. The existence of such a global section renders the fibre bundle trivial in that there actually is no twist and $\mathscr{E} = \mathscr{B} \times \mathscr{F}$ is true globally. For principal fibre bundles, this is a one-to-one statement: a principal fibre bundle is trivial if and only if there exists a global section. This can

also be phrased as the statement that the connection is nowhere vanishing or that the coordinates introduced by the trivialisation are globally defined. The existence of a global section is however not guaranteed. What can always be defined is a *local section*, relying on a local trivialisation. For each local section, a connection can be established, with the relation between connections of different local sections given in (2.80). The necessity for local sections is indicated by a connection that vanishes at some points when expressed in coordinates, or alternatively by the failure of a coordinate system at a particular point. We will give a simple example of such an instance shortly.

A non-trivial bundle is described by the presence of *holonomies*. These quantify whether the endpoints of a path c that is closed in the base manifold differ once the path is uplifted into the fibre by applying a local section to the path c. Of course, applying the projection π on this path reproduces the closed path on the base manifold. If such paths exist, the difference between the two endpoints measures the holonomy. This is visualised on the left of fig. 2.13. The reason for the endpoints not coinciding is the parallel transport along the path defined by the connection. A prominent instance of this can be found when parallel transporting a vector on a curved manifold. Performing a closed loop, the vector returns to its starting position pointing in a different direction. The change of angle shows by how much the sum of the interior angles of a triangle differs from π. This can be interpreted as a holonomy and is a direct measure for the curvature, and therefore also the geometry, of the underlying manifold. In particular, if the change of angle is positive (negative), the manifold has positive (negative) Ricci curvature. Mathematically, the holonomy can also be understood in terms of the field strength of the connection A. This field strength, obtained as an exterior derivative of A, can also be interpreted as the symplectic form, $\Omega = \mathrm{d}A$. Given that there exists a global section, A is unique and the symplectic form is uniquely computed by this relation. This manifests that Ω in this case is an *exact* two-form such that $\mathrm{d}\Omega = 0$ is trivially satisfied by $\mathrm{d}^2 = 0$. In general, exact n-forms are forms that can be expressed uniquely as the exterior derivative of an $n-1$-form. In close analogy to the above discussion, by the Poincaré lemma such an $n-1$-form can always be defined locally,[23] but not necessarily globally. If there is no global section, we have to use local sections $\mathscr{S}_i$ for each of which a local gauge field A_i is defined. While $\Omega = \mathrm{d}A_i$ holds independently of the index i, the symplectic form is not uniquely determined by a single A_i and is therefore not exact. To test whether a form is exact or not, the integral

$$\int_\Sigma \Omega\,, \tag{2.81}$$

[23] A necessary condition is that the underlying point is contractible, i.e. it can be smoothly deformed to a point.

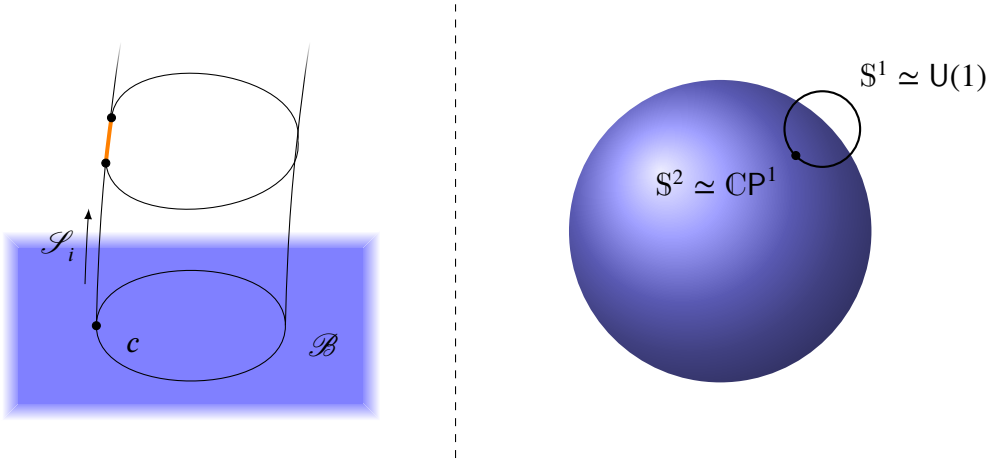

Figure 2.13: On the left, the same path is shown twice, once in the base manifold and once uplifted to the fibre. In the base manifold, the path is closed. When uplifted to the fibre, the same path is no longer necessarily closed due to the non-trivial fibre bundle. The separation marked in orange between the path endpoints, coinciding when projected to the base manifold, is referred to as holonomy. On the right, a visualisation of the local product structure $\mathbb{S}^2 \times \mathbb{S}^1$ is shown. At every point of the sphere, a circle is attached. Globally, this yields a different manifold than $\mathbb{S}^3$.

has to be calculated. This is, up to a proportionality factor, essentially the integral of the first Chern class. Here Σ is any closed two-dimensional surface within the base manifold. By Stokes' theorem, an exact form has to integrate to zero. Therefore, if the integral above is non-vanishing, Ω is not exact and the corresponding fibre bundle has no global section. Moreover, Ω can also be used to determine the topology of the base manifold. By the Chern theorem [282], the symplectic form allows to compute the Euler characteristic χ of $\mathscr{B}$,

$$\chi(\mathscr{B}) = \frac{1}{(2\pi)^n} \int_{\mathscr{B}} \sqrt{\det(\Omega)} = 2 - 2g\,, \tag{2.82}$$

where $\dim(\mathscr{B}) = 2n$ and g is the number of holes of $\mathscr{B}$.

Within physics, holonomies are more commonly referred to as *geometric phase* or *Berry phase*. Originally found by Sir Michael Berry for a system of a single qubit in a magnetic field in the seminal paper [163], it was shortly after pointed out by Barry Simon that the phase factor discussed by Berry is simply the holonomy of a principal fibre bundle with group $G = \mathrm{U}(1)$ [164]. Using the insights gained by the discussion of (2.81), the geometric phase is calculated as

$$\Phi_{\mathrm{G}} = \int_{\Sigma} \Omega\,. \tag{2.83}$$

In fact, this particular geometric phase realises the Hopf fibration in its lowest-dimensional example [283],

$$\mathbb{S}^1 \hookrightarrow \mathbb{S}^3 \xrightarrow{\pi} \mathbb{S}^2 \,. \tag{2.84}$$

Comparing with (2.74), the Hopf fibration describes the total space $\mathscr{E} = \mathbb{S}^3$ as a fibre bundle with base space $\mathscr{B} = \mathbb{S}^2$ and fibre $\mathscr{F} = \mathbb{S}^1$. The physical interpretation is as follows. The system of a single qubit in a magnetic field is a two-dimensional quantum system, i.e. the natural Hilbert space is given by $\mathbb{C}^2$. State vectors single out $\mathbb{S}^3$ by the normalisation condition, providing the total space. The base space is the projective Hilbert space given by $\mathscr{P}(\mathscr{H}) = \mathbb{C}\mathrm{P}^1 \simeq \mathbb{S}^2$, while the fibre accounts for phase factors $e^{\mathrm{i}\alpha} \in \mathrm{U}(1) \simeq \mathbb{S}^1$. The geometric phase described in [163] shows that $\mathbb{S}^3 \neq \mathbb{S}^2 \times \mathbb{S}^1$ in a global sense. The locally valid product structure is visualised on the right of fig. 2.13. Mathematically, this is realised in the non-existence of global coordinates on $\mathbb{S}^2$. Coordinates can only be defined excluding either the north or the south pole of $\mathbb{S}^2$. In each coordinate patch a connection can be defined, which in particular vanishes when naively evaluated on the excluded point. The corresponding symplectic form therefore is not exact and results in the non-trivial phase factor of [163].[24] This is consistent with the hairy ball or hedgehog theorem, stating that any vector field, of which the connection is a special case, defined on $\mathbb{S}^{2n}$ vanishes at some point [284, 285].

In the above example, we saw that the projective Hilbert space appeared as the base manifold of the principal fibre bundle. This is not specific to this simple example but generalises to $\mathscr{P}(\mathscr{H}) = \mathbb{C}\mathrm{P}^{n-1}$ for arbitrary n. As already indicated in (2.58), the projective Hilbert space is obtained as a quotient space of $\mathbb{S}^{2n-1}$ by $\mathrm{U}(1) \simeq \mathbb{S}^1$. Therefore, for any n, the projective Hilbert space may always be understood as the base manifold $\mathscr{B} = \mathbb{C}\mathrm{P}^{n-1} = \mathscr{P}(\mathscr{H})$ of a principal fibre bundle with fibre or gauge group $\mathscr{F} \simeq \boldsymbol{G} = \mathrm{U}(1)$ and the total space given by the Hilbert space $\mathscr{E} = \mathbb{C}^n = \mathscr{H}$. The projection corresponds to implementing the equivalence relation $\sim_\lambda$,

$$\mathbb{S}^1 \hookrightarrow \mathbb{C}^n \xrightarrow{\pi} \mathbb{C}\mathrm{P}^{n-1} \quad \leftrightarrow \quad \mathrm{U}(1) \hookrightarrow \mathscr{H} \xrightarrow{\sim_\lambda} \mathscr{P}(\mathscr{H}) \,. \tag{2.85}$$

The geometric phases or holonomies of such fibre bundles probe the geometry of the projective Hilbert space. Within physics, as we will discuss in broad detail in secs. 4, 5 and 6, geometric phases are vital to understand factorisation properties of the Hilbert space.

[24] In the case $\mathbb{S}^2$, the symplectic form is a top form. It therefore must be proportional to the volume form of $\mathbb{S}^2$. Since the volume of $\mathbb{S}^2$ does not vanish, the volume form must not be exact. The latter statement generalises: the volume form of any compact manifold is non-exact. The symplectic form being proportional to the volume form however is specific to this example.

In particular, they can be used to analyse the entanglement within a quantum system. However, the importance of geometric phases is not specific to high energy physics. Also in condensed matter theory geometric phases appear, the most famous example being the quantum Hall effect. Here, the Hall conductance is quantised in terms of Chern numbers. This was first discussed in [156] and given more theoretical foundation in [157]. The first measurement, awarded with a Nobel prize, was conducted in [158]. A mathematical rigorous treatment of this effect was given in [159]. Therefore, geometric phases also do play an important role in physics. Moreover, it is worth pointing out that the topic of geometric phases and projective Hilbert space sparked interesting discussions about the nature of reality in the area of philosophy of physics [286, 287]. However, we will not go into detail about this.

Finally we point out that geometric phases fall into two classes based on the origin. Holonomies arise whenever the bundle is non-trivial, i.e. whenever coordinates are not defined globally and $\mathscr{E} = \mathscr{B} \times \mathscr{F}$ holds only locally. Above we have discussed in quite some detail phase factors that arise due to the non-trivial curvature of the base manifold, in the above case given by $\mathbb{S}^2$ which has positive curvature. This is accompanied by a non-vanishing field strength given by the symplectic form, which in particular is not exact. However, there is also a different origin for holonomies related directly to the topology of the base manifold. In particular, if the base manifold is not simply connected, coordinates may not be defined globally and the holonomy is non-trivial. In this case, the field strength of the connection vanishes and the connection itself is non-exact. An instance of this is the Möbius strip, which can be regarded as a fibre bundle with base manifold $\mathscr{B} = \mathbb{S}^1$ and fibre given by an interval $\mathscr{F} = [a, b]$. Locally, this is indistinguishable from the cylinder, but globally, these spaces are of course different. This shows via computing the holonomies. Parallel transport of a vector along a closed path on the cylinder does not yield any changes, but returning to the same point on the Möbius strip leads to a sign difference, i.e. a holonomy of π appearing as prefactor $e^{i\pi}$ of the vector. Another example for topological phases is given by closed paths on the punctured plane $\mathbb{R}^2\backslash\{0\}$, where winding numbers can be defined, counting how often the path winds around the puncture. In fact, such topological phases only take discrete values independent of the path, while geometric phases vary smoothly and depend on the path.

This concludes our discussion on aspects of geometry within quantum mechanics important for this thesis. In the next section we discuss two ways in which entanglement can be understood in a geometric fashion.

2.2.2. State Space Geometry and Entanglement

In the last section, we have discussed in detail how quantum mechanics can be phrased in terms of geometry. We in particular focused on elementary objects such as states and state space. Moreover, we explained how these geometric notions are grouped into a fibre bundle. However, we have not yet understood how entanglement, which we reviewed in detail in sec. 2.1, is phrased in terms of geometry. Intuitively, in the spirit of [15], we might ask which geometries are 'spooky', i.e. which geometries represent entanglement. In the following, we discuss two geometric notions of entanglement. We start with the construction of [166] which, based on a detailed analysis of the symmetries of the state vector, gave a prescription to determine such 'spooky' geometries as submanifolds of the projective Hilbert space. We will refer to this method as the *SZK construction*. This method will be indispensable for the discussions in secs. 4, 6 and to a lesser extend also in sec. 5. Next, we will review a quantity known as *geometric quantum discord* [181], abbreviated as GQD in the following. This provides an alternative to the generically hard-to-compute quantum discord. In sec. 7 we will study GQD in the context of factorisation properties of quantum systems.

Manifolds of Equal Entanglement

In standard quantum mechanics, as reviewed extensively in sec. 2.1.1, the entanglement is quantified using the von Neumann entropy (2.10). In particular, given that the full system is described by a pure state, the entanglement entropy provides a unique measure of any quantum correlations between the subsystems separated by a bipartition surface. Moreover, the entanglement entropy is the same when computed for either of the subsystems, $S(\rho^{(1)}) = S(\rho^{(2)})$, where $\rho^{(i)}$ are the reduced density operators defined in (2.15). Moreover, the entanglement entropy is invariant under local unitary transformations $U = U_1 \otimes U_2$ [188], as in particular the Schmidt coefficients of the state vector $|\psi\rangle$ are invariant under such transformations. Within local unitary transformations, there exists a smaller class of transformations which relate state vectors in a reversible way. In particular, such transformations do not mix between sectors of base vectors associated to different Schmidt coefficients. Two state vectors are called *interconvertible* if they are related by such a transformation [288]. For two such state vectors, the invariance of the entanglement entropy is trivial since they are already equal at the level of the state vector. The set of all interconvertible state vectors therefore forms an orbit of the local unitary transformations. Aspects of this were analysed in [289–292] and a complete treatment was given in [166]. Although we focus on pure states based on state vectors in the following, we point out that a similar analysis for mixed states was conducted in [293].

The SZK construction is based on carefully analysing the Schmidt coefficients of the state vector $|\psi\rangle$. The Schmidt decomposition (2.17) exists for any state vector of a bipartite Hilbert space $\mathscr{H} = \mathbb{C}^{n^2} = \mathbb{C}^n \otimes \mathbb{C}^n = \mathscr{H}^{(1)} \otimes \mathscr{H}^{(2)}$ and allows to express $|\psi\rangle$ as

$$|\psi\rangle = \sum_{i=1}^{n} \kappa_i |i_1, i_2\rangle \,, \tag{2.86}$$

where κ_i are the Schmidt coefficients.[25] As we have seen in sec. 2.2.1, the space of physically distinguishable states is formed by rays $[|\psi\rangle]$ defined in (2.56) and is referred to as the projective Hilbert space $\mathscr{P}(\mathscr{H}) = \mathbb{C}\mathrm{P}^{n^2-1}$. The local unitary transformations are given by $U = U_1 \otimes U_2$ where $U_{1/2} \in \mathrm{U}(n)$. To obtain the orbits, we have to determine which states are interconvertible, in particular by what kind of unitary transformations. To do so, it is convenient to choose a basis such that the reduced density operator of (2.86) is expressed as[26]

$$\rho^{(1)} = \mathrm{diag}\big(\underbrace{0, ..., 0}_{m_0}, \underbrace{\kappa_1^2, ..., \kappa_1^2}_{m_1}, ..., \underbrace{\kappa_n^2, ..., \kappa_n^2}_{m_n}\big) = \big(0 \cdot \mathbb{1}_{m_0}\big) \oplus \Big[\bigoplus_{i=1}^{n} \big(\kappa_i^2 \mathbb{1}_{m_i}\big)\Big] \,, \tag{2.87}$$

i.e. $\rho^{(1)}$ is block diagonal with each block corresponding to all Schmidt coefficients of value κ_i^2. Moreover, the basis is chosen such that the blocks are written in ascending order, $0 < \kappa_1^2 < ... < \kappa_n^2$. The values m_i denote the algebraic multiplicities of κ_i^2 and therefore satisfy $\sum_{i=0}^{n} m_i = n$.

This diagonal form of the reduced density operator is particularly convenient since the square root of $\rho^{(1)}$ can be used to write $|\psi\rangle$ in Schmidt decomposed form as[27]

$$|\psi\rangle = \sum_{i,j=1}^{n} \sqrt{\rho^{(1)}}_{ij} |i_1, j_2\rangle \,. \tag{2.88}$$

To determine which transformations define interconvertible states, have to find unitary transformations $U_{\mathrm{int}}, V_{\mathrm{int}} \in \mathrm{U}(n)$, acting on the first and second subsystem respectively,

[25] Note that it is a matter of a taste whether one calls the coefficients of the state or the eigenvalues of the reduced density operator Schmidt coefficients. The authors of [166] chose the latter option, while we work with the former. While this is of course only a matter of convention, we point it out to deflect potential confusion.

[26] For concreteness, we choose to trace over $\mathscr{H}^{(2)}$. The analogous arguments presented in the following however also apply when tracing over $\mathscr{H}^{(1)}$.

[27] The square root of a diagonal matrix A with entries a_i is again diagonal with entries $\sqrt{a_i}$.

such that the above state changes only up to an overall phase,

$$U_{\text{int}} \otimes V_{\text{int}}^T = \sum_{i,j=1}^{n} \left(U_{\text{int}} \sqrt{\rho^{(1)}} V_{\text{int}}\right)_{ij} |i_1, j_2\rangle \stackrel{!}{=} e^{i\alpha} |\psi\rangle \,, \tag{2.89}$$

i.e. the unitary transformations do not mix between blocks of different κ_i. Due to the block diagonal form of $\rho^{(1)}$, it is straightforward to see that such transformations take the form [166]

$$U_{\text{int}} = U_0 \oplus U_1 \oplus \ldots \oplus U_n \quad \text{and} \quad V_{\text{int}} = e^{i\alpha} V_0 \oplus U_1^\dagger \oplus \ldots \oplus U_n^\dagger \,. \tag{2.90}$$

Both U_{int} and V_{int} take the same block diagonal structure as $\rho^{(1)}$. The unitary transformations U_i within U_{int} act on the corresponding blocks in $\rho^{(i)}$ and therefore are part of $\mathrm{U}(m_i)$ with $\dim(U_i) = m_i$. In order to guarantee invariance of the state vector, the entries V_i within V_{int} are constrained by U_i to satisfy $V_i = U_i^\dagger$ in order to cancel each other. Accordingly, also $V_i \in \mathrm{U}(m_i)$ with $\dim(V_i) = m_i$. The case for m_0 is however special. Since both U_0 and V_0 are multiplied by zero, V_0 is not constrained by U_0 but can be an arbitrary unitary transformation.

Given this subclass described by U_{int} and V_{int} of arbitrary local unitary transformations, *manifolds of equal entanglement* or *entanglement orbits* $\mathscr{O}_{|\psi\rangle}$ are defined as a quotient space [166],

$$\mathscr{O}_{|\psi\rangle} = \frac{\mathrm{U}(n) \times \mathrm{U}(n)}{\mathscr{G}(m_i)} \,. \tag{2.91}$$

Here $\mathscr{G}(m_i)$ is a subgroup of the local unitary transformations $\mathrm{U}(n) \times \mathrm{U}(n)$ formed by U_{int} and V_{int} for a specific configuration of m_i. The real dimension of this orbit follows as [166]

$$\dim_{\mathbb{R}} \left(\mathscr{O}_{|\psi\rangle}\right) = 2n^2 - 2m_0^2 - \sum_{i=1}^{n} m_i^2 - 1 \,. \tag{2.92}$$

Since this dimension is always smaller than the real dimension of $\mathbb{C}\mathrm{P}^{n^2-1}$, $\dim_{\mathbb{R}} \left(\mathbb{C}\mathrm{P}^{n^2-1}\right) = 2n^2 - 2$, the entanglement orbits can be understood as submanifolds of the projective Hilbert space. It was also shown that this quotient can be given a simple form in terms of the individual factors of $\mathrm{U}(m_i)$ [293, 294],

$$\mathscr{O}_{|\psi\rangle} = \frac{\mathrm{U}(n)}{\mathrm{U}(m_0) \times \mathrm{U}(m_1) \times \ldots \times \mathrm{U}(m_n)} \times \frac{\mathrm{U}(n)}{\mathrm{U}(1) \times \mathrm{U}(m_0)} \,. \tag{2.93}$$

This structure can be understood in the following way. The first factor in (2.93) arises

by quotienting the local unitary transformations $\mathrm{U}(n)$ acting on the subsystems by the transformations U_{int}. The local unitary transformations $\mathrm{U}(n)$ acting on the other subsystem are quotiented by the remaining groups, which are the second factor of $\mathrm{U}(m_0)$ resulting from the freedom in V_0 as well as a factor of $\mathrm{U}(1)$ due to the freedom of the global phase. This orbit structure can be given an interpretation in terms of fibre bundles. The first factor in (2.93), describing all reduced density operators with the same spectrum, provides the base manifold. For a given class of reduced density operators with the same spectrum, the fibre consists of all state vectors leading to a reduced density operator of that class upon partial tracing. We will make use of this fact later on in sec. 4 to define geometric phases as a probe of the entanglement structure.

With the above expression (2.93), given a particular state vector, it is straightforward to obtain the manifold of equal entanglement by calculating the Schmidt coefficients and determining the multiplicities. As an example consider a state vector with every Schmidt coefficient non-vanishing but with different values of all other Schmidt coefficients. In this case, $m_0 = 0$ and, since all Schmidt coefficients take different values, $m_{i\neq 0} = 1$. This is a fairly generic state vector with some intermediate value for the entanglement entropy, $0 < S(\rho^{(1)}) < \ln n$. The structure of the entanglement orbit follows as

$$\mathscr{O}_{|\psi\rangle_{\text{intermediate}}} = \frac{\mathrm{U}(n)}{\mathrm{U}(1)^n} \times \frac{\mathrm{U}(n)}{\mathrm{U}(1)} = \frac{\mathrm{U}(n)}{\mathrm{U}(1)^n} \times \frac{\mathrm{SU}(n)}{\mathbb{Z}_n}\,, \tag{2.94}$$

The orbit structure for generic states, also including cases where $m_0 \neq 0$, is complicated and, with a growing value of n, the number of different orbits grows drastically, although the structure is straightforward to obtain in principle. A detailed list up to $n = 4$ can be found in [166].

The two special cases of vanishing and maximal entanglement however allow for somewhat simpler geometric interpretations. First, we consider the case of maximal entanglement. In terms of the Schmidt coefficients, that means that $m_0 = 0$ and $m_1 = n$, since for maximal entanglement all Schmidt coefficients are equal. In this case, the orbit structure is given by

$$\mathscr{O}_{|\psi\rangle_{\text{maximal}}} = \frac{\mathrm{U}(n)}{\mathrm{U}(n)} \times \frac{\mathrm{U}(n)}{\mathrm{U}(1)} = \mathbb{1} \times \frac{\mathrm{SU}(n)}{\mathbb{Z}_n}\,. \tag{2.95}$$

This orbit has an interesting geometric interpretation in that it is a *Lagrangian submanifold* of the projective Hilbert space as pointed out in [295]. A Lagrangian submanifold is defined as follows [296],

Definition 4: A Lagrangian submanifold L of a symplectic manifold M with symplectic form Ω is defined such that

i) L is an isotropic submanifold, i.e. $\Omega|_L = 0$

ii) L is maximal, i.e. $\dim(L) = \frac{1}{2}\dim(M)$.

A simple example for a Lagrangian submanifold is given by $\mathbb{R}$ within $\mathbb{R}^2$. As required, $\dim(\mathbb{R}) = \frac{1}{2}\dim(\mathbb{R}^2)$ and $\Omega = \mathrm{d}x \wedge \mathrm{d}y$ vanishes when x or y are held fixed. As a more physical example, the symplectic manifold of classical mechanics spanned by p_i and q_i both position and momentum space are Lagrangian submanifolds by fixing either all p_i or all q_i, respectively. For the orbit (2.95), the condition on the dimension can be easily seen to be satisfied since $\dim_{\mathbb{R}}\left(\mathbb{C}\mathrm{P}^{n^2-1}\right) = 2n^2 - 2$ and $\dim_{\mathbb{R}}\left(\mathscr{O}_{|\psi\rangle_{\text{maximal}}}\right) = n^2 - 1$. The vanishing of the symplectic form can be understood as follows. By the Poincaré lemma and the Darboux theorem [297], the symplectic form of any symplectic manifold can locally be written in the canonical form $\Omega = \mathrm{d}p_i \wedge \mathrm{d}q_i$, i.e. locally every symplectic manifold looks like $\mathbb{R}^{2n}$. As L has half the dimension of M, we have to fix n of the coordinates of M. For all $i = 1, ..., n$, fixing either p_i or q_i shows that the symplectic form vanishes. This is explained in more detail in [295], where the Darboux coordinates for $\mathbb{C}\mathrm{P}^{n^2-1}$ are discussed as well. Note that in this analysis, n is not restricted, i.e. the entanglement orbit of maximally entangled states is a Lagrangian submanifold of $\mathbb{C}\mathrm{P}^{n^2-1}$ for any n.

Finally, we discuss the case of vanishing entanglement. In this case, the state vector is a product state such that the reduced density operator is a projector. Accordingly, only one of the Schmidt coefficients is non-zero and in particular equal to one, while all others vanish. The multiplicities therefore are $m_0 = n - 1$ and $m_1 = 1$. The corresponding orbit structure is given by

$$\mathscr{O}_{|\psi\rangle_{\text{vanishing}}} = \frac{\mathrm{U}(n)}{\mathrm{U}(n-1)\times\mathrm{U}(1)} \times \frac{\mathrm{U}(n)}{\mathrm{U}(n-1)\times\mathrm{U}(1)} = \mathbb{C}\mathrm{P}^{n-1} \times \mathbb{C}\mathrm{P}^{n-1}\,. \tag{2.96}$$

This orbit also has a known geometric interpretation in that it is the *Segre variety* of the projective Hilbert space $\mathbb{C}\mathrm{P}^{n^2-1}$. This can be interpreted as the Cartesian product of the projective Hilbert spaces $\mathbb{C}\mathrm{P}^{n-1}$ of the subsystems. In fact, this result is reminiscent of (2.72) where we discussed the projective Hilbert space for composite systems. The above orbit structure shows that the product of the subsystem projective Hilbert spaces describes precisely the separable state vectors of the composite system. This analogy between state vectors and geometries is quite intuitive. In standard quantum mechanics, separable states are formed as products of base vectors of the subsystems. Entangled states are then obtained by taking linear combinations of separable states. In the geometric version (2.96), separable states are described by a geometry which is simply the product of the individual pure state geometries, i.e. the individual projective Hilbert spaces. In this product, no further structure between the subsystem geometries is included. Entangled

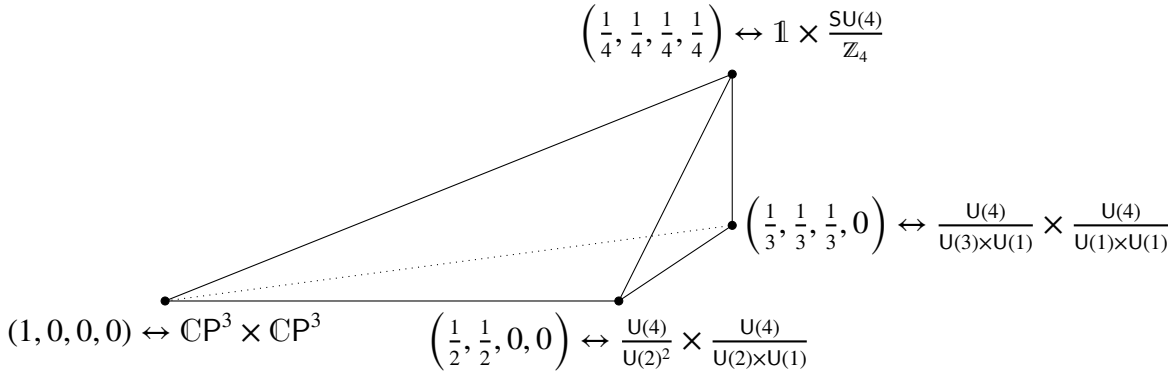

Figure 2.14: Depiction of the Weyl chamber for a bipartite system consisting of two four-level systems. Every point of the Weyl chamber corresponds to a unique configuration of the Schmidt coefficients. The interior corresponds to all Schmidt coefficients differing. On each of the edges, at least two coefficients are equal. The vertex points correspond to particularly symmetric configurations of the Schmidt coefficients, which are given explicitly with the corresponding geometry. Note that the lengths of the edges have no quantitative meaning. The figure is freely adapted from [166].

states, as described by (2.94) or (2.95), are obtained by providing more structure, i.e. by deviating from the simple Cartesian product. For a detailed discussion of the Segre variety and the Segre embedding we refer the interested reader to [190]. See also [298] for a discussion in the context of multipartite entanglement.

The characterisation of entanglement in terms of the Schmidt coefficients can be nicely visualised in the following way. Grouping all Schmidt coefficients into a vector λ, the set of all such vectors spans the $n-1$-dimensional Schmidt simplex. The n corners of this simplex represent all of the separable states, while the maximally entangled states sit at the centre of the simplex. Since the simplex contains duplicates in terms of the entanglement, i.e. both cases $\kappa_1 = \frac{1}{3}, \kappa_2 = \frac{2}{3}$ and $\kappa_1 = \frac{2}{3}, \kappa_2 = \frac{1}{3}$ are shown but have the same entanglement, it suffices to restrict to the so-called Weyl chamber, where every point corresponds to a different value of the entanglement. This Weyl chamber, also known as the asymmetric part of the Schmidt simplex, is visualised in fig. 2.14 for the case $n = 4$. As indicated in the figure, each of the corners, edges, faces and the interior volume of the Weyl chamber is associated to a particular entanglement orbit. As pointed out before, a complete list of entanglement orbits up to $n = 4$ can be found in [166], where the placement of each geometry within the Weyl chamber is also discussed.

Geometric Quantum Discord

The entanglement orbits defined above provide a geometric interpretation for the von Neumann entropy as a measure of entanglement, in particular for pure states with a state vector

description. As we discussed in sec. 2.1.3, there also exist other measures of entanglement. In particular, we discussed quantum discord as the most general measure of quantum correlations, which however has some drawbacks in terms of computability. As mentioned above, computing quantum discord is an NP-complete problem [180]. Fortunately, there exists a way of at least partially circumventing this problem. In [181] a necessary and sufficient condition for non-vanishing quantum discord was defined. Given any state ρ, evaluating this condition allows to claim whether the quantum discord between the subsystems of ρ is trivial or not. Based on this condition, [181] also proposed the measure known as *geometric quantum discord* (GQD). This quantity also provides a qualitative measure for quantum discord [181]. Analogous to quantum discord providing upper bounds to other measures of entanglement, it was shown that GQD is an upper bound for the entanglement negativity for bipartite systems of two n-level subsystems [299]. As we study GQD in sec. 7 concerning its implications on the factorisation properties of the Hilbert space, in the following we provide details on its definition and computation.

GQD is defined in terms of the Hilbert–Schmidt norm defined in (2.59) for state vectors. The Hilbert–Schmidt norm for arbitrary operators is defined as

$$||X|| = \sqrt{\mathrm{tr}\left(X^\dagger X\right)}\,, \tag{2.97}$$

which for the case of Hermitian operators $X = X^\dagger$ relevant to our discussion slightly simplifies as then $X^\dagger X = X^2$. In terms of this norm, GQD denoted by $Q^{(2)}$ is defined as [181]

$$Q^{(2)}(A:\bar{A}) = \min_{\chi\in\mathscr{S}^{(q-c)}} ||\rho-\chi||^2\,. \tag{2.98}$$

Here, ρ is an arbitrary density operator describing the full system, with subsystems labelled as A and $\bar{A}$. Compared to quantum discord, the minimisation over projective measurements is replaced by a more feasible minimisation over states χ. These states are elements of $\mathscr{S}^{(q-c)}$ which is the set of all states of vanishing quantum discord. As we discussed in sec. 2.1.3, such states are given by quantum-classical (q-c) states which can be denoted as

$$\chi = \sum_k q_k \rho_k^{(A)} \otimes |\phi_k^{(\bar{A})}\rangle\langle\phi_k^{(\bar{A})}|\,, \tag{2.99}$$

where $q_k \geq 0$, $\sum_k q_k = 1$ and $\langle\phi_k^{(\bar{A})}|\phi_l^{(\bar{A})}\rangle = \delta_{kl}$. The reduced density operators $\rho_k^{(A)}$ describe the quantum state in subsystem A while subsystem $\bar{A}$ is in a classical state specified by the probabilities q_k.

Due to the definition of GQD in terms of a norm, the GQD can be interpreted as the distance between the two states ρ and χ. Moreover, once the minimisation is performed, the state χ_{min} singled out by the minimisation is the q-c state closest to ρ. In other words, it is the q-c state that best approximates the quantum state ρ. Explicit computation of GQD has been performed in [181] for an arbitrary mixed state of a system consisting of two qubits. This has been generalised in [300] to arbitrary mixed states of $\mathscr{H} = \mathscr{H}^{(A)} \otimes \mathscr{H}^{(\bar{A})}$ with $\dim(\mathscr{H}^{(A)}) = m$ and $\dim(\mathscr{H}^{(\bar{A})}) = n$. As pointed out before, we will study GQD in sec. 7 and its use in the light of Hilbert space factorisation. In this analysis, we will focus on GQD for pure states.

This concludes our review of the relationship between geometry and quantum mechanics in general and geometric notions of entanglement in particular. Next, we consider a more rigorous approach to studying quantum systems based on types of operator algebras and Tomita–Takesaki modular theory.

2.3. The Axiomatic Approach: Entangling Operator Algebras

We have discussed in secs. 2.1 and 2.2 how quantum mechanics and in particular entanglement can be phrased in terms of linear algebra and geometry, respectively. Both approaches, while fully equivalent in principle, have advantages in certain areas. The approach using linear algebra provides a fairly simple toolbox to analyse quantum systems with respect to dynamics as well as computing observables, i.e. measurement results. For this reason, this approach is also most useful in relating abstract concepts to actual measurements in experimental physics. The geometric approach on the other hand, due to its access to geometrical and topological properties, is useful when aiming at general statements, in particular for systems where the local dynamics are either highly complicated or even (partially) unknown. However, even the combination of these two approaches is not satisfactory in general. We will mention three reasons in the following.

The first, which admittedly is motivated more by mathematical idealism than physical necessity, is the wish for generalisation and mathematical rigour. Given that we can access nature only by measurements, the fundamental objects of a theoretical treatment should be observables. To a certain extent, this is already implemented in the Heisenberg picture, where state vectors are only used to compute expectation values, but not to describe the dynamics of the system. In general however, it would be advantageous to be able to define quantum mechanics purely in terms of observables and the relations between them, i.e. their algebra. As an aside, we point out that there also exists an approach of

axiomatising the Schrödinger picture [301, 302]. The two axiomatic versions of the two pictures should be dual to each other, the precise relation is however not yet understood in general and is a field of ongoing research [303–305].

Second, the presence of global symmetries puts a challenge on the definition of an observable. As discussed above, observables are represented by Hermitian operators. On the other hand, a Hermitian operator that is not invariant under the global symmetry must not correspond to an observable. This leads to defining so-called superselection sectors which effectively splits the Hilbert space into a direct sum over Hilbert spaces of fixed charge [306]. Understanding how superselection sectors arise in QFT was one of the main motivations for developing a formulation of quantum theory, and in particular QFT, based on observables (see also [307]).

The third and probably most compelling reason we point out is the failure of the previously discussed formalisms for infinite-dimensional quantum systems. In both descriptions given previously, the Hilbert space was finite-dimensional, i.e. $\mathscr{H} = \mathbb{C}^n$ and $\mathscr{P}(\mathscr{H}) = \mathbb{C}\mathrm{P}^{n-1}$ with $n \in \mathbb{N}$. In fact, by the Stone–von Neumann theorem [308–311] it is guaranteed that the quantisation of any finite-dimensional system with canonical variables (x_i, p_i), $i, j = 1, ..., n$, satisfying $[x_i, p_j] = \mathrm{i}\delta_{ij}$ provides a Hilbert space that is unique up to isomorphisms. An analogous argument can be made for fermionic variables. The existence of such isomorphisms is related to the dimension of the (projective) Hilbert space being *countable* or, in other words, that it is spanned by finitely many base vectors. In the limit of infinite-dimensional systems, the Stone–von Neumann theorem does not apply [312]. Still, there do exist cases where the dimension of the Hilbert space is infinite yet countable. Such Hilbert spaces are also called *separable*. While this yields some technical difficulties, much of our previous discussion still applies or at least appropriate analogues can be defined. However, generically the Hilbert space of an infinite-dimensional system has an *uncountable* dimension. Such Hilbert spaces, also referred as *inseparable*, require uncountably many base vectors. In other words, it is not possible to assign a reasonable basis. Unfortunately, inseparable Hilbert spaces occur within theoretical physics quite naturally, ranging from generic QFTs to systems of infinitely many (even non-interacting) spins.

In order to provide a rigorous treatment of such theories describing our reality, the notions of Hilbert space and states have to be refined. This development led to the field of *axiomatic quantum field theory* (AQFT). Every QFT, be it of direct relevance to our nature such as the standard model of particle physics or more abstract versions, fits into sets of axioms known as the *Gårding–Wightman* axioms [121], the *Osterwalder–Schrader* axioms [122] and the *Haag–Kastler* axioms [123]. The first two sets of axioms focus on properties of correlation functions and how the Hilbert space is recovered from correlation

functions, in Lorentzian and Euclidean QFTs respectively. The third set formulates QFT in terms of the algebra of observables. We will study properties of such algebras, also in relation to AdS/CFT, in secs. 5 and 6. Therefore in sec. 2.3.1, we describe certain elements of this vast field, focussing in particular on the different types of algebras that observables can satisfy and some of the physical consequences thereof. Next in sec. 2.3.2 we turn to discussing entanglement from the perspective of the algebras of observables. For more details, standard references include [313–317]. Moreover, the review articles [192, 318–321] provide useful discussions and examples and we will follow parts of their explanations. In particular, the immediately following discussion is based on [319], while the later part of sec. 2.3.1 and sec. 2.3.2 also follow the expositions of [192, 320].

2.3.1. Essentials on von Neumann Algebras

As mentioned above, the framework of AQFT is based on studying properties of the observables O and the algebra $\mathscr{A}$ formed by these observables. Measuring an observable represents using a measurement device. The result of the measurement, indicated by a number on the scale of the device, is therefore obtained as a map from the algebra to the real numbers. Given two observables, their linear combination gives rise to a third observable. In terms of the measurement device, this can be interpreted as using two different devices and combining their output into a single scale. Moreover, we might apply functions to observables. This is understood as changing the numerical steps on the scale, e.g. from linear to quadratic steps. Mathematically, the algebra of such observables is given by a so-called *unital $*$-algebra*, defined as follows:

Definition 5: A $*$-algebra $\mathscr{A}$ is an algebra over $\mathbb{C}$ that is equipped with an involutive map $*\colon \mathscr{A} \to \mathscr{A},\ \mathfrak{a} \mapsto *(\mathfrak{a})$ satisfying

i) $*(\mathfrak{a}+\mathfrak{b}) = *(\mathfrak{a}) + *(\mathfrak{b})$ and $*(\mathfrak{a}\mathfrak{b}) = *(\mathfrak{b})\,*(\mathfrak{a})$ for all $\mathfrak{a},\mathfrak{b} \in \mathscr{A}$

ii) $*(\alpha\mathfrak{a}) = \alpha^* *(\mathfrak{a})$ for all $\alpha \in \mathbb{C}, \mathfrak{a} \in \mathscr{A}$

iii) $*(*(\mathfrak{a})) = \mathfrak{a}$ for all $\mathfrak{a} \in \mathscr{A}$.

Note that the $*$-operation is different from complex conjugation in general. This is particularly important for property **ii)** in this definition (the $*$ in superscript on α^* is the familiar complex conjugation). Of course, when $\mathscr{A}$ is the algebra of complex numbers, the star operation can be identified with complex conjugation. A $*$-algebra is called unital if it contains an element $\mathbb{1}$ that acts as the identity for multiplications, $\mathbb{1}\mathfrak{a} = \mathfrak{a}$, for every $\mathfrak{a} \in \mathscr{A}$. As an example, the collection of all bounded operators $\mathscr{B}(\mathscr{H})$ acting on a

Hilbert space $\mathscr{H}$ is a unital $*$-algebra with the $*$-operation provided by the adjoint $\dagger$. We will keep using this particular $*$-operation in the following. Each self-adjoint[28] operator $\mathfrak{O} = *(\mathfrak{O}) = \mathfrak{O}^\dagger$ represents an observable O.

We can also define a norm $||\cdot||$ for algebra elements. Algebras with a norm are called *normed* algebras and satisfy $||\mathfrak{a}\mathfrak{b}|| \leq ||\mathfrak{a}|| \cdot ||\mathfrak{b}||$ for all $\mathfrak{a}, \mathfrak{b} \in \mathscr{A}$. A few properties of such algebras are stated in the following. Connecting to the above, normed unital algebras satisfy $||\mathbb{1}|| = 1$. The norm defined for algebra elements also induces a topology. A normed algebra is said to be a *Banach algebra* if the algebra is complete in the induced topology. If a given $*$-algebra satisfies these properties, it is denoted as a B^*-algebra, where B is short for Banach. By specifying the properties of the norm, this motivates the definition of a C^*-*algebra*,

Definition 6: A C^*-algebra is a B^*-algebra whose norm satisfies

$$||\mathfrak{a}^\dagger \mathfrak{a}|| = ||\mathfrak{a}^\dagger|| \cdot ||\mathfrak{a}|| = ||\mathfrak{a}||^2 \quad \text{for all } \mathfrak{a} \in \mathscr{A}. \tag{2.100}$$

This definition was first used in [322]. The term C^*-algebra was introduced in [323], with C short for closed. An example for such an algebra is again given by all bounded operators $\mathscr{B}(\mathscr{H})$ acting on a Hilbert space and the norm given by the operator norm. In the following, unless specified otherwise, operators are always assumed to be bounded operators.

The properties of the algebras of observables allow for very abstract and universal characterisations of quantum systems and the corresponding states of the system. Before discussing that however, we first have to specify what we mean by a state. States are defined as linear functionals on the algebra, in particular as positive and normalised linear functionals $\omega : \mathscr{A} \to \mathbb{R}$. These properties ensure that $\omega(\mathfrak{a}^\dagger \mathfrak{a}) \geq 0$ (positive), $\omega(\mathbb{1}) = 1$ (normalised) and $\omega(\mathfrak{a} + \mathfrak{b}) = \omega(\mathfrak{a}) + \omega(\mathfrak{b})$ (linear) for any $\mathfrak{a}, \mathfrak{b} \in \mathscr{A}$. The state is pure if there is no $\lambda \in]0, 1[$ such that $\omega = \lambda\omega' + (1 - \lambda)\omega''$ for $\omega' \neq \omega''$ and mixed otherwise. For any operator $\mathfrak{O} = \mathfrak{O}^\dagger$, the state $\omega(\mathfrak{O})$ is interpreted as the expectation value of the observable O represented by $\mathfrak{O}$. This interpretation comes about since the states ω can be expressed using normalised state vectors $|\psi\rangle$ of the corresponding Hilbert space. In particular,

$$\omega_{|\psi\rangle}(\cdot) = \langle\psi| \cdot |\psi\rangle \,. \tag{2.101}$$

[28] In physicists' language, the term 'Hermitian' is more common. This is however meaningful only for matrices representing operators in finite dimensions. The discussion in sec. 2.1 referred to this instance which is why we used Hermitian operators. In the present section, where we generalise to infinite dimensions, we will be more careful and use the phrase 'self-adjoint'.

This definition clearly satisfies the aforementioned properties and explains why $\omega(\mathfrak{O})$ has the interpretation of an expectation value. Moreover, by (2.101) we can naturally associate a reduced density operator ρ to the state vector $|\psi\rangle$. For any operator $\mathfrak{a}$ we rewrite (2.101) using the trace as

$$\omega_{|\psi\rangle}(\mathfrak{a}) = \mathrm{tr}\left(|\psi\rangle\langle\psi|\mathfrak{a}\right) = \mathrm{tr}\,\rho\mathfrak{a}\,, \tag{2.102}$$

so the reduced density operator ρ corresponds to the state vector $|\psi\rangle$.

Constructing the Hilbert Space by Observables

The link between the above algebraic notion of states and the more familiar Hilbert space version in usual quantum mechanics is provided by the *GNS construction* due to Gelfand and Naimark [322] and Segal [323]. Here, roughly speaking one associates the identity element of the algebra to a particular state vector $|\psi\rangle$ with certain properties to be specified shortly. Then, any other operator $\mathfrak{a}$ is associated to the state vector $\mathfrak{a}|\psi\rangle$. In this way, a Hilbert space containing state vectors is constructed from the algebra. The more precise version of the GNS construction requires the notion of a *representation* of the algebra on a Hilbert space, defined as follows:

Definition 7: A representation of a C^*-algebra $\mathscr{R}(\mathscr{A})$ requires a Hilbert space $\mathscr{H}$, a dense subspace $\mathscr{D}$ of the former and a map $\mathscr{R}$ from the algebra to operators acting on $\mathscr{H}$ such that

- **i)** for each element of $\mathscr{R}(\mathscr{A})$ the domain $D(\mathscr{R}(\mathscr{A}))$ is equal to $\mathscr{D}$ and the range is contained in $\mathscr{D}$
- **ii)** it preserves the identity, i.e. $\mathscr{R}(\mathbb{1}) = \mathbb{1}_{\mathscr{D}}$
- **iii)** it preserves linearity and products, i.e. $\mathscr{R}(\mathfrak{a}+\alpha\mathfrak{b}+\mathfrak{c}\mathfrak{d}) = \mathscr{R}(\mathfrak{a})+\alpha\mathscr{R}(\mathfrak{b})+\mathscr{R}(\mathfrak{c})\mathscr{R}(\mathfrak{d})$ for all $\alpha \in \mathbb{C}$ and $\mathfrak{a},\mathfrak{b},\mathfrak{c},\mathfrak{d} \in \mathscr{A}$
- **iv)** the adjoint of the representation has $\mathscr{D} \subset D(\mathscr{R}(\mathscr{A})^\dagger)$ and its restriction to $\mathscr{D}$ satisfies $\mathscr{R}(\mathscr{A})^\dagger|_{\mathscr{D}} = \mathscr{R}(\mathscr{A}^\dagger)$.

If the kernel of the map $\mathscr{R}$ is trivial, this representation is called *faithful*. For such representations, $\mathscr{R}(\mathfrak{a}) = 0$ implies that $\mathfrak{a} = 0$. Moreover, a representation is said to be *irreducible* if the Hilbert space does not contain invariant subspaces under the action of $\mathscr{R}(\mathscr{A})$ except for trivial (e.g. empty) or dense subspaces. Much like we stated in def. 2 that Hilbert spaces related by a unitary map U are isomorphic, representations are unitarily

equivalent if $U\mathscr{R}_1(\mathscr{A})U^\dagger = \mathscr{R}_2(\mathscr{A})$. With these notions at hand, the GNS construction is formalised in the GNS representation theorem [322, 323]:

Theorem 2: Given a state ω on a unital $*$-algebra, there exists a representation $\mathscr{R}_\omega$ and a state vector $|\Omega_\omega\rangle \in \mathscr{D}_\omega \subset \mathscr{H}_\omega$ such that $\mathscr{D}_\omega = \mathscr{R}_\omega(\mathscr{A})|\Omega_\omega\rangle$ and $\omega(\mathfrak{a}) = \langle\Omega_\omega|\mathscr{R}_\omega(\mathfrak{a})|\Omega_\omega\rangle$ for all $\mathfrak{a} \in \mathscr{A}$. This representation is unique up to unitary equivalent representations. If $\mathscr{A}$ is a C^*-algebra,

i) $\mathscr{R}_\omega(\mathfrak{a})$ is a bounded operator on $\mathscr{H}_\omega$ for all $\mathfrak{a} \in \mathscr{A}$

ii) ω is a pure state if and only if $\mathscr{R}_\omega$ is irreducible

iii) the norms on the Hilbert space and the algebra coincide, i.e. $||\mathscr{R}_\omega(\mathfrak{a})|| = ||\mathfrak{a}||$ for $\mathscr{R}_\omega$ faithful.

For a discussion on how to prove this see e.g. [319]. We will only make two comments on this theorem.

First, since $\mathscr{R}_\omega(\mathscr{A})|\Omega_\omega\rangle$ is dense in $\mathscr{H}_\omega$, the state vector $|\Omega_\omega\rangle$ is referred to as a *cyclic* vector.[29] This is precisely the state vector associated to the identity element of the algebra. In most cases, the cyclic vector is also separating which means that $\mathfrak{a}|\Omega_\omega\rangle = 0$ implies $\mathfrak{a} = 0$. Since $||\mathfrak{a}|\Omega_\omega\rangle|| = \omega(\mathfrak{a}^\dagger\mathfrak{a}) \geq 0$, this is the case when ω is a faithful state, i.e. $\omega(\mathfrak{a}^\dagger\mathfrak{a}) = 0$ implies $\mathfrak{a}$. Relating to usual quantum mechanics, a state vector is cyclic if all of its Schmidt coefficients are non-zero. Therefore, given a quantum system, there are many possible choices for cyclic vectors. Moreover, since $\mathscr{R}_\omega(\mathscr{A})|\Omega_\omega\rangle$ is dense in $\mathscr{H}_\omega$ we do not need knowledge of any state vector of the Hilbert state, but the set of state vectors generated from $|\Omega_\omega\rangle$ by the action of $\mathscr{R}_\omega(\mathscr{A})$ is sufficient to study the corresponding system. This explains how the algebraic approach to study quantum systems allows to analyse infinite-dimensional systems. Given a Hilbert space that is not separable, i.e. with uncountable dimension, we are free to restrict to a countably infinite-dimensional, yet dense, subspace by choosing a set of operators that we are interested in. These operators correspond to the observables of the system that we aim to measure. Moreover, we may specify the cyclic state vector as a state vector with particular physical properties that we want to have in our system. The countably infinite-dimensional Hilbert space then consists of all state vectors obtained by the action of the (representation of the) chosen operators on the cyclic state vector. We note that the state vectors obtained in this way are still elements of the uncountable Hilbert space as well. Intuitively, this reduction of dimension might be understood such that we only care about the parts of the state vectors which are affected by our chosen operators and fix all other parts to something convenient.

[29] Note that the cyclic property of a vector is specific to a representation. Two different representations may give rise to the same state vector, but this state vector is not necessarily cyclic for both representations.

Second, the relation between purity of ω and irreducibility of $\mathscr{R}_\omega$ deserves some explanation, which we provide following [192]. Given two linearly independent state vectors $|\psi\rangle, |\phi\rangle \in \mathscr{H}$, we define a state

$$\omega_{|\chi\rangle} = \lambda\omega_{|\psi\rangle} + (1-\lambda)\omega_{|\phi\rangle} \tag{2.103}$$

for any $\lambda \in]0,1[$. The corresponding reduced density operator follows from a state vector $|\chi\rangle$ that is contained in a Hilbert space with a direct sum structure $\mathscr{H} \oplus \mathscr{H}$,

$$|\chi\rangle = \sqrt{\lambda}\,|\psi\rangle \oplus \sqrt{1-\lambda}\,|\phi\rangle\,. \tag{2.104}$$

Given that the algebra acting on $\mathscr{H}$ is given by $\mathscr{A}$, the algebra acting on $\mathscr{H} \oplus \mathscr{H}$ is given by $\mathscr{A} \oplus \mathscr{A}$. The action of this direct sum algebra is reducible by definition, so although we obtain $\omega_{|\chi\rangle}$ from a state vector, it cannot be a pure state. In relation to our earlier statement on mixed and pure states above (2.101), we note that (2.103) leads to a reducible representation as both $\omega_{|\psi\rangle}$ and $\omega_{|\phi\rangle}$ are states themselves such that $\omega_{|\chi\rangle}$ is a mixed state.

In order to describe QFT using the above language of C^*-algebras, the Haag–Kastler axioms [123] come into play. These axioms, which we will not discuss in detail, encapsulate how, among others, dynamics and causality are formulated in algebraic terms. Moreover they state how local algebras are assigned in a consistent way to local regions of the full spacetime. In particular, to each causally complete subregion $\mathscr{U}$ of Minkowski spacetime, an algebra $\mathscr{A}_\mathscr{U} \subset \mathscr{B}(\mathscr{H})$ is associated. These relations provide what is also called a *net of local algebras*. The full C^*-algebra is recovered in terms of the union $\bigcup_\mathscr{U} \mathscr{A}_\mathscr{U}$ and causality is encoded by the fact that the algebras of two spatially separated regions $\mathscr{U}$ and $\mathscr{V}$ commute, $[\mathscr{A}_\mathscr{U}, \mathscr{A}_\mathscr{V}] = 0$. For a detailed discussion of these axioms see e.g. [314, 319, 324] and references therein.

Von Neumann Algebras

So far we have discussed everything in terms of C^*-algebras. In many physical applications however, a slightly refined version of such algebras appears. These refined versions are known as *von Neumann algebras*, named after the person who introduced these algebras in [124]. The underlying theory was developed shortly afterwards in a series of papers by von Neumann and also Murray [125–131]. Von Neumann algebras are defined as follows:

Definition 8: A von Neumann algebra $\mathscr{A}$ is

i) a unital C^*-algebra that is closed under the weak operator topology

or equivalently

ii) a unital $*$-algebra that is equal to its own double commutant.

The equivalence between the two conditions is shown and formalised by the double commutant theorem [124] (see e.g. [318] for explanations). The commutant of an algebra $\mathscr{A}$, usually denoted by $\mathscr{A}'$, is defined to consist of all operators that commute with all operators in $\mathscr{A}$,

$$\mathscr{A}' = \{\mathfrak{a}' : [\mathfrak{a}, \mathfrak{a}'] = 0 \ \forall \mathfrak{a} \in \mathscr{A}\}\,. \tag{2.105}$$

An example for a von Neumann algebra is again given by the algebra of all bounded operators $\mathscr{B}(\mathscr{H})$. Here in particular, the commutant of this algebra only contains the identity operator and multiples of this operator by any complex number. The set of all bounded operators that commute with (scalar multiples of) the identity is simply $\mathscr{B}(\mathscr{H})$ itself, so $\mathscr{B}(\mathscr{H})'' = \mathscr{B}(\mathscr{H})$ is a von Neumann algebra. We will encounter less trivial examples shortly.

Given a von Neumann algebra $\mathscr{A}$, its commutant $\mathscr{A}'$ is also a von Neumann algebra. Moreover, also the intersection of these two algebras is a von Neumann algebra. The intersection $\mathscr{A} \cap \mathscr{A}'$ is called the *centre* of $\mathscr{A}$, denoted by $\mathscr{Z}(\mathscr{A})$. By analysing $\mathscr{Z}(\mathscr{A})$, the notion of a von Neumann algebra *factor* arises. A von Neumann algebra is a factor if $\mathscr{Z}(\mathscr{A})$ consists only of scalar multiples of the identity.[30] Otherwise, it is not a factor. This case arises in the discussion of superselection sectors mentioned briefly before. Given a global symmetry, the corresponding charge operator commutes with every observable, so the charge operator is an element of the centre. It was shown in [125] that factors can be classified into three different types. Moreover, in [131] is was proven that every von Neumann algebra can be written as a direct integral of factors. This shows the importance of factors as by this result, studying properties of arbitrary von Neumann algebras boils down to studying properties of factors. In the mathematical literature, different types of von Neumann algebras $\mathscr{A}$ are distinguished by analysing the existence of projection operators within $\mathscr{A}$, see e.g. [314, 318, 321]. The different types of factors have particular properties distinguishing them. These are vital when discussing the significance of a particular factor for physics, as we explain in the following.

Type I: von Neumann algebras of type I are the simplest versions. Such algebras are those typically encountered in quantum mechanics. Correspondingly, algebras of type I

[30] An equivalent condition for $\mathscr{A}$ to be a factor is that $\mathscr{A} \vee \mathscr{A}' = \mathscr{B}(\mathscr{H})$, i.e. that there are no bounded operators which are not contained in either $\mathscr{A}$ or $\mathscr{A}'$.

always have an irreducible representation on the separable Hilbert space. Equivalently, pure states can be defined on the algebra. Moreover, there always exists a trace on the algebra. Algebras of type I fall into two subclasses. If the underlying system is finite-dimensional with Hilbert space $\mathscr{H} = \mathbb{C}^n$, the algebra is of type I_n. Examples include n-level systems such as qunits[31] or composite systems of $N < \infty$ qubits with dimension $n = 2^N$. Such algebras can be represented as matrix algebra and the trace is given by the familiar trace of matrices, e.g. for a qunit the algebra is simply $\mathfrak{su}(n)$ with the familiar notion of the trace for $n \times n$ matrices. In the limit of $n \to \infty$, the algebra is of type I_∞. An example is given by a collection of infinitely many spins, which naively has an uncountable dimension. As discussed above, restricting to the states and observables one is interested in, the dimension reduces to countably infinite and the algebra can be defined. For type I_∞, the trace is not defined for every element of the algebra. Operators which have a finite trace are referred to as *trace-class*, but e.g. the trace of the identity in infinite dimensions is infinite, so the identity operator is not trace-class.

Type I algebras are the only algebras that appear for finite-dimensional systems. They may also appear for particular infinite-dimensional systems. The other types, to be discussed in the following, can only appear for infinite dimensions. As in infinite dimensions we are no longer dealing with matrix algebras, we require a different notion of a trace. In this case, a trace is defined by a *tracial state* ω_{tr} on the algebra, defined as follows:

Definition 9: A tracial state ω_{tr} on an algebra $\mathscr{A}$ is a positive linear functional, i.e. a state ω, that is cyclic in its argument,

$$\omega_{\mathrm{tr}}(\mathfrak{a}\mathfrak{b}) = \omega_{\mathrm{tr}}(\mathfrak{b}\mathfrak{a}) \quad \forall \mathfrak{a}, \mathfrak{b} \in \mathscr{A} \,. \tag{2.106}$$

If such a state exists, it satisfies all properties of a trace and so the underlying algebra possesses a trace. In finite dimensions, the tracial state is a rescaled version of the familiar trace as $\omega_{\mathrm{tr}}(\mathbb{1}) = 1$ while $\mathrm{tr}\,\mathbb{1} = n$. In the following discussion, when stating the existence of a trace, we mean the existence of a tracial state as defined here.

In the above, we found that a system of infinitely many spins is an example of an algebra of type I_∞. This works since the spin system can be tuned such that the partition function of the system is finite, $Z < \infty$. However, this is not necessarily true as e.g. infinite-dimensional systems such as continuum field theories at finite temperature may have $Z \to \infty$. This is indicated by the observation that both the expectation value and the variance of the Hamiltonian in such systems diverge. The underlying Hilbert space is not well-defined in

[31] In the literature, these are more commonly referred to as qudits. For consistency, as in this thesis we use n instead of d for the dimension of quantum systems, we refer to the same object as qunits.

the sense that an approximate description using a finite-dimensional system of size n does not have a well-defined limit $n \to \infty$. In this case, to obtain a trustworthy description of the physics of this system, the *thermofield double state* (TFD state) has to be used [324]. For finite systems, the TFD state is given by

$$|\mathrm{TFD}\rangle = \sqrt{\frac{1}{Z_n}} \sum_{l=1}^{n} e^{-\beta \frac{E_l}{2}} |l_1, l_2\rangle \,, \tag{2.107}$$

where E_l is the energy, Z_n the partition function, β the inverse temperature and $|l_1, l_2\rangle = |l_1\rangle \otimes |l_2\rangle$ the combined energy eigenbasis of the two copies of the system. Essentially, a second copy[32] of the original system is introduced such that before the limit of infinite dimension is taken, the Hilbert space is a tensor product $\mathscr{H} = \mathscr{H}^{(1)} \otimes \mathscr{H}^{(2)}$. The TFD state is then interpreted as a state vector within the tensor product Hilbert space and in particular as the cyclic and separating vector. In the limit of infinite dimension, by the GNS construction the separable Hilbert space $\mathscr{H}_{\mathrm{TFD}}$ is obtained. This Hilbert space however is no longer given by a tensor product of the individual Hilbert spaces. If this was the case, it would not have been necessary to introduce a second copy and the TFD state in the first place, as the individual Hilbert spaces would have been defined in the limit of infinite dimensions. Since we have two copies of the system, we also have two algebras $\mathscr{A}^{(1)}$ and $\mathscr{A}^{(2)}$ both acting on $\mathscr{H}_{\mathrm{TFD}}$ in the limit of infinite dimension. In fact, these two algebras are each others' commutants, commonly denoted as $[\mathscr{A}^{(1)}, \mathscr{A}^{(2)}] = 0$. Notably, the action of either of the two algebras is sufficient to generate $\mathscr{H}_{\mathrm{TFD}}$. This scenario naturally leads to defining algebras of type II and type III.

The classification of von Neumann algebras of type II and III in general is quite complicated. However, in applications to physics we usually think of infinite systems as limits of finite systems [320]. In the same spirit, so-called *hyperfinite* von Neumann algebra factors of type II and III can be defined [127, 325, 326]. The classification of these factors is significantly simpler and well understood, yielding an order 1 number of subclasses.

Type II: von Neumann algebras of type II are less familiar. In particular, they never have an irreducible representation. However, algebras of type II allow the definition of a trace. Moreover, as indicated above, an algebra $\mathscr{A}^{(1)}$ of type II always has a commutant $\mathscr{A}^{(2)}$ which is of the same type. This explains the absence of an irreducible representation as either of the algebras $\mathscr{A}^{(1)}, \mathscr{A}^{(2)}$ can be used to generate all states, so both algebras contain the same information. The cyclic vector $|\psi\rangle$ of $\mathscr{A}^{(1)}$ is the separating vector for

[32] Technically it is more convenient to define the second system as the complex conjugate of the original system. The two systems are then related by time reversal. However, since in many discussions (as in this thesis) the systems are time-reversal symmetric, this technical aspect is often dropped.

$\mathscr{A}^{(2)}$ and vice versa. This is often abbreviated by saying that $|\psi\rangle$ is the cyclic separating vector. Again, there are two subclasses with properties similar to the two subclasses of type I algebras. For an algebra of type II_1, the trace is defined for every operator of the algebra, in particular also for the identity operator. This comes about as the tracial state is a rescaled version of the usual trace, for which the rescaling factor is essentially the inverse of the dimension. For the other subclass, called type II_∞, the trace is defined only for trace-class operators. This can be understood by the fact that a type II_∞ algebra can be thought of as a tensor product of II_1 and I_∞.

Algebras of type II, in particular type II_1, can be constructed as limits of two collections of qubits [125] (for reviews see e.g. [192, 320]). In particular, the qubits have to be maximally entangled. To see this, suppose that two qubits are in a maximally entangled state, i.e. a Bell state[33]

$$|\mathrm{Bell}\rangle = \sqrt{\frac{1}{2}}\left(|00\rangle + |11\rangle\right). \tag{2.108}$$

Combining infinitely many of such states in a tensor product $|\psi\rangle = \lim_{N\to\infty} \bigotimes_{l=1}^{N} |\mathrm{Bell}_l\rangle$ provides a cyclic separating vector necessary to construct the separable Hilbert space. Alluding to the earlier comments on states at finite temperature, the state vector $|\psi\rangle$ can be understood as the TFD state (2.107) of the two copies of infinitely many spins with a Hamiltonian $H = 0$, i.e. the energy of every qubit pair vanishes,[34]

$$|\mathrm{TFD}\rangle = \lim_{N\to\infty} \sqrt{\frac{1}{2^N}} \bigotimes_{l=1}^{N} \left(|00\rangle_l + |11\rangle_l\right). \tag{2.109}$$

Defining $\omega_{|\mathrm{TFD}\rangle}$ using (2.109), this state satisfies $\omega_{|\mathrm{TFD}\rangle}(\mathfrak{a}\mathfrak{b}) = \omega_{|\mathrm{TFD}\rangle}(\mathfrak{b}\mathfrak{a})$, so it is a tracial state and the algebra acting on this system has a trace. Moreover, this trace is defined for every element, in particular also the identity operator. However, we are in infinite dimensions and in particular the partition function $Z_N = 2^N$ in (2.109) diverges for $N \to \infty$. Therefore, the algebra $\mathscr{A}^{(1)}$ acting on the spins of the first copy has to be type II_1. Its commutant $\mathscr{A}^{(2)}$ acting on the spins of the second copy is also of type II_1. Moreover, $\mathscr{A}^{(1)} \cap \mathscr{A}^{(2)} = \{\alpha\mathbb{1} : \alpha \in \mathbb{C}\}$, so both $\mathscr{A}^{(1)}$ and $\mathscr{A}^{(2)}$ are factors.

The operators of $\mathscr{A}^{(1)}$ (or of $\mathscr{A}^{(2)}$) acting on (2.109) change only finitely many entries of the vector. Therefore asymptotically, i.e. when 'zooming out' and looking at the system from far away, every state of the separable Hilbert space looks like $|\psi\rangle$. In this sense, the

[33] The analogous arguments can be made using any of the other Bell states as well.

[34] To be precise, this state is the infinite tensor product of the TFD states of each individual qubit pair for $H = 0$. The TFD state of the full system is given by the tensor product of all of the individual TFD states.

small deviations within a state different from $|\psi\rangle$ are washed out. By the *Reeh–Schlieder theorem*, which we will discuss in more detail in sec. 2.3.2, in QFT cyclic separating states appear as vacuum states of local regions [187]. This explains our earlier statement in sec. 2.1.2 that in QFT, every state looks like the vacuum state. However, in QFT algebras are usually of type III rather than type II, although they share some similarities. Algebras of type III are characterised as follows.

Type III: von Neumann algebras of type III behave in the least familiar way. As for type II, they never allow for an irreducible representation and always have a commutant of the same type. Also, the properties of the cyclic separating vector are analogous to type II. However, algebras of type III do not allow for defining a trace. This in particular also implies that the notion of a reduced density operator does not exist. Moreover, also quantities defined using either the trace or the reduced density operator (or both) cannot be defined for an algebra of type III. This in particular includes the entanglement entropy (2.10). For type III there exist three subclasses [128, 325, 326]. These are characterised by the spectrum of the *modular operator* Δ. We will first give explicit examples for these classes and explain the relation to Δ afterwards.

As for algebras of type II, algebras of type III can be constructed as limits of two collections of qubits [128, 325, 326] (again, for reviews see e.g. [192, 320]). This time however, the qubit pairs are supposed to not be maximally entangled. On the other hand, all of them, or at least infinitely many, have to have non-vanishing entanglement. To be specific, each qubit pair is assumed to be in a state

$$|\lambda_l\rangle = \sqrt{\frac{1}{1+\lambda_l}}\left(|00\rangle + \sqrt{\lambda_l}\,|11\rangle\right), \tag{2.110}$$

where $0 < \lambda_l < 1$, quantifying the entanglement of each qubit pair. Again, infinitely many of such states are combined in a tensor product $|\psi\rangle = \lim_{N\to\infty} \bigotimes_{l=1}^{N} |\lambda_l\rangle$. This will be the cyclic separating vector which may also be interpreted as the TFD state of the system by writing $\lambda_l = e^{-\beta E_l}$,

$$|\mathrm{TFD}\rangle = \lim_{N\to\infty} \sqrt{\frac{1}{\prod_{l=1}^{N}(1+e^{-\beta E_l})}} \bigotimes_{l=1}^{N} \left(|00\rangle_l + e^{-\beta\frac{E_l}{2}}|11\rangle_l\right), \tag{2.111}$$

i.e. every qubit pair has a different energy E_l. Defining a state $\omega_{|\mathrm{TFD}\rangle}$ using (2.111), this state is not cyclic in its argument. In particular, $\omega_{|\mathrm{TFD}\rangle}(\mathfrak{a}\mathfrak{b}) = \omega_{|\mathrm{TFD}\rangle}(\mathfrak{b}\mathfrak{a}) + \sum_l \#_l(1-e^{-\beta E_l})$, where $\#_l$ depend on the operators $\mathfrak{a}, \mathfrak{b}$. Since the action of the algebra may change only finitely many of the λ_l, there does not exist a tracial state for this algebra. Moreover,

the partition function $Z_N = \prod_{l=1}^{N}(1 + e^{-\beta E_l})$ diverges in the limit $N \to \infty$ for generic E_l. Therefore, this algebra is of type III. Interpreting E_l as a sequence, it depends on the convergence properties of this sequence which subclass of type III is constructed. If the sequence converges to some value $0 < \lambda^* < 0$, the algebra is said to have type III_{λ^*}, first constructed in [325]. If the sequence converges to zero, there are two options. If the convergence is 'fast', the algebra is actually of type I_∞. Intuitively, a convergence is fast if $\lambda_l = 0$ for infinitely many λ_l such that infinitely many of the qubits are not entangled. If the convergence is slow, i.e. such that still infinitely many qubits are entangled, the algebra has type III_0. If the sequence does not converge but there are at least two accumulation points $0 < \lambda_1^* \neq \lambda_2^* < 1$,[35] the algebra has type III_1 [326].

This concludes our discussion on the essentials of von Neumann algebras. In the next section, we illuminate how such algebras are useful for analysing entanglement.

2.3.2. Entanglement and the Reeh–Schlieder Theorem

In the above, we have discussed a rigorous version of analysing quantum systems which in particular is also valid for infinite-dimensional systems such as QFT. As before, for the purpose of this thesis, we are particularly interested in understanding entanglement in this language. We start with the simplest version of type I algebras which should mostly reproduce what we already know from standard quantum mechanics discussed in sec. 2.1.1. Indeed, for algebras of type I_n, all of our earlier discussion applies. The von Neumann entropy is defined as in (2.10) by the reduced density operator. It is always positive or vanishes in the case of a product state, i.e. when the reduced density operator corresponds to a pure state. It also admits an upper bound provided by the maximally entangled state. If a bipartite quantum system has two copies of type I_n acting on the subsystems, the upper bound is given by $\ln n$. In the limit $n \to \infty$, i.e. for type I_∞, the entanglement entropy therefore may diverge. To summarise, the entanglement entropy for type I takes positive values only and states may contain finite or infinite amounts of entanglement.

The situation is somewhat different for type II. In the construction of type II algebras, infinite collections of qubits are used to define a state where qubits are pairwise maximally entangled [125]. As we take infinitely many of such qubit pairs, the entanglement naively diverges as $N \ln 2$ for $N \to \infty$. This is an important distinction to type I. For states of type II algebras, the (naive) entanglement always diverges, as opposed to type I where entanglement can be finite. Therefore, entanglement for type II is not a property of the state but of the algebra itself. However, as type II admits a tracial state, the formula

[35] If the two values satisfy $\lambda_1^* = \tilde{\lambda}^n, \lambda_2^* = \tilde{\lambda}^m$ for $n, m \in \mathbb{Z}$, the algebra is of type $\mathrm{III}_{\tilde{\lambda}}$.

for von Neumann entropy (2.10) can still be used. This allows for a refined version of entanglement entropy which in particular is not just infinity [327, 328]. To see this, recall that in the GNS construction, each state vector is formally associated to an operator of the algebra. In particular, the cyclic separating vector is associated to the identity operator, which in turn can be understood as the reduced density operator of the cyclic separating vector. This can also be seen using the tracial state, as

$$\operatorname{tr} \mathfrak{a} = \omega_{\text{tr}}(\mathfrak{a}) = \langle \psi | \mathfrak{a} | \psi \rangle = \operatorname{tr} \rho \mathfrak{a} \tag{2.112}$$

implies that $\rho = \mathbb{1}$, where we used (2.102) in the third equality. This result might seem unusual from the perspective of standard quantum mechanics. However, as we pointed out below def. 9, the trace defined by tracial states is a rescaled version of the familiar trace. To ensure $\operatorname{tr} \rho = 1$, the density operators are rescaled with the inverse factor. Since $\ln \mathbb{1} = 0$, the von entanglement entropy of this reduced density operator vanishes, so the entanglement entropy of the cyclic separating vector of a type II_1 algebra vanishes. Matching the two observations of vanishing and maximal entanglement is possible by interpreting entanglement for type II_1 as the naive entropy, which generically diverges, with the entanglement of the cyclic separating vector $N \ln 2$ subtracted. This explains why the cyclic separating vector itself has vanishing entanglement entropy in the refined definition. Moreover, any other state vector obtained by applying some operator $\mathfrak{a}$ on $|\psi\rangle$ has less (naive) entanglement than $|\psi\rangle$ itself as will alter the entries in $|\psi\rangle$ such that some qubit pairs are no longer maximally entangled. Consequently, the refined definition of entanglement entropy yields a negative value for the entanglement of any other state. See also [320] for an analogous discussion. So for algebras of type II_1, the naive entanglement entropy has a universal divergence. The refined entanglement entropy is always negative or vanishes, the latter providing an upper bound.

The situation is different for algebras of type II_∞. This is tied to the fact that $\text{II}_\infty = \text{II}_1 \otimes \text{I}_\infty$ as stated earlier. Both components admit a trace, so entanglement entropy is defined. However, since the tensor product can be formed in many equivalent ways, the trace for type II_∞ has no canonical normalisation. To see this, consider writing an algebra of type II_∞ as a tensor product of type II_1, type I_∞ and type I_n. The trace on this tensor product algebra is given by the product of the individual traces. A particular operator in this tensor product is given by $\mathfrak{a} = \mathbb{1} \otimes \Pi \otimes \mathbb{1}_n$, consisting of the unity operators of II_1 and I_n and a projector Π of I_∞ that (for simplicity) projects into a one-dimensional subspace of the Hilbert space of I_∞. Suppose that we group II_1 and I_n into a new II_1' to have $\text{II}_1' \otimes \text{I}_\infty = \text{II}_\infty$. Correspondingly, the trace of $\mathbb{1} \otimes \mathbb{1}_n$ is canonically normalised to 1, following our discussion of the tracial state for type II above. Moreover, Π projects

into a one-dimensional subspace, so the trace of Π is also canonically normalised to 1. So we find $\mathfrak{a} = 1$. Equivalently, we could also decide to group I_n and I_∞ into I'_∞ to write $\mathrm{II}_1 \otimes \mathrm{I}'_\infty = \mathrm{II}_\infty$. The trace of $\mathbb{1}$ on II_1 is normalised to 1 as before. However, the trace on I'_∞ is canonically equal to n due to the type I_n part. Therefore with this choice, $\mathrm{tr}\,\mathfrak{a} = n$. The trace of II_∞ therefore has no canonical normalisation. This can also be understood by the presence of an outer automorphism group for II_∞ that rescales the trace. For more details see e.g. [134]. Changing the normalisation of the trace by rescaling with a constant Ξ changes the entanglement entropy by $\ln \Xi$. This constant is in particular independent of the state. Due to this arbitrariness, entanglement entropy for II_∞ may take values from $-\infty$ to $+\infty$. While entanglement entropy is defined with an arbitrary yet state-independent constant, entropy differences are defined without this ambiguity since the constant cancels out.

For algebras of type III, the von Neumann entropy is not defined since there is no trace and hence also no reduced density operator. However, a few more statements can still be made. As for type II, algebras of type III can be constructed by considering infinitely many pairwise entangled qubit pairs. Since there are infinitely many qubit pairs with non-vanishing entanglement, a naive counting of the entanglement leads again to a universal divergence. As for type II, this is a property of type III algebras rather than the corresponding states. As a side remark, type III algebras still have well-defined measures of entanglement, just the von Neumann entropy loses its meaning. In particular, the *relative entropy* can be defined for type III using the *relative modular operator* [329, 330]. We will however not go into detail about this.

Relation to Quantum Field Theory

How does this analysis help us in analysing entanglement in QFT? To address this question we first have to clarify which algebra type is relevant for QFT. Generically, a local region of a QFT is associated to an algebra of type III, in particular type III_1 [331, 332]. An intuitive argument can be given as follows [192]. Above we used the convergence properties of the sequence of λ_l to determine the subclass of type III. This is in one-to-one correspondence with discussing the spectrum of the *modular operator* Δ. The modular operator is one of the central elements of *Tomita–Takesaki* theory [333, 334] which studies modular automorphisms of von Neumann algebras. In particular, the main statement of Tomita–Takesaki theory is that Δ generates a modular automorphism of an algebra $\mathscr{A}$ and its commutant $\mathscr{A}'$,

$$\Delta^{is}\mathscr{A}\Delta^{-is} = \mathscr{A} \quad \text{and} \quad \Delta^{is}\mathscr{A}'\Delta^{-is} = \mathscr{A}', \tag{2.113}$$

for every choice of the parameter $s \in \mathbb{R}$. Modular automorphisms are therefore understood as unitary transformations using the modular operator. Correspondingly, it has been suggested that s is an 'emergent' time such that Δ^{is} can be interpreted as a generalised time evolution operator [335]. In fact, Δ is expressed by differences of the modular Hamiltonians $\hat{K}$ as $\Delta = e^{-\hat{K}}$, so s might also be called 'modular' time. This relation can be motivated using a type I description. For type I, the modular operator is given by a tensor product of the reduced density operators as $\Delta = \rho_{(A)} \otimes \rho_{(\bar{A})}^{-1}$, where both reduced density operators can be written in terms of the modular Hamiltonians $K_{(A/\bar{A})}$ following (2.21). Therefore, $\Delta = e^{-K_{(A)}+K_{(\bar{A})}} = e^{-\hat{K}}$. While the intermediate step of the calculation using density operators is questionable for type III, both the left and right hand of this equation are well-defined for type III. In fact, the modular operator is interpreted as the well-defined analogue of the reduced density operator for type III algebras.

For the type III algebras constructed above using qubit collections, the spectrum of the modular operator consists of all integer powers of the accumulation points of the sequence λ_l. As an example, for an algebra of type III_λ where λ_l converges to λ^*, the spectrum of Δ consists of all integer powers of λ^*. For type III_1, as there are at least two accumulation points of the sequence, the spectrum consists of all products of arbitrary integer powers of λ_1^* and λ_2^*. By properly adjusting the integer powers, such products can approximate any positive real number for arbitrary values of λ_1^* and λ_2^*.[36] Therefore the spectrum of Δ consists of all positive real numbers. For QFT, as we have discussed in sec. 2.1.2 analysing the Minkowski vacuum, we found that the modular Hamiltonian is expressed using the Lorentz boost operator. As discussed in the previous paragraph, the modular operator is related to the modular Hamiltonian by the exponential map. Since the spectrum of the Lorentz boost operator consists of all real numbers, the spectrum of the corresponding modular operator is given by all positive real numbers. This provides an intuitive explanation for the type III_1 nature of algebras in QFT. More rigorous versions however also do exist. In particular, it was shown that QFTs satisfying the axioms of AQFT, any representation of an operator algebra is a type III_1 factor [336]. In a complementary development it was shown that, up to isomorphism, there is a unique hyperfinite type III_1 factor [337]. These two results were unified by showing that any local algebra in QFT has to be hyperfinite [338]. This means that all operator algebras associated to local regions in any QFT satisfying the axioms of AQFT are related by isomorphisms.

The type III nature of algebras in QFT also nicely explains the usually divergent entanglement entropy in QFT as we encountered e.g. in (2.38). The particular quantitative behaviour of the divergence depends on the QFT considered in the sense that it depends on

[36] There is again the exception for the case $\lambda_1^* = \tilde{\lambda}^n, \lambda_2^* = \tilde{\lambda}^m$ for $n, m \in \mathbb{Z}$ where the algebra is of type $\mathrm{III}_{\tilde{\lambda}}$.

a theory-dependent constant and the area of the chosen region. Moreover, the possibility to compute entanglement entropies in QFT comes at the price of introducing a UV cutoff ϵ, which also shows up in the final result (2.38). This cutoff effectively reduces the number of degrees of freedom to a finite number such that techniques of type I algebras can be used. Without the cutoff, the computation is not possible. Consistent with this, sending this cutoff to zero leads to a diverging result as expected for a type III algebra.

An Elephant on the Moon

The divergent amount of entanglement present in any typical state in QFT has far-reaching consequences as we describe in the following. Within the GNS construction, we already encountered the statement that by the action of all operators of an algebra $\mathscr{A}$ on a cyclic separating vector $|\omega_\omega\rangle$, a dense subspace of the Hilbert space $\mathscr{H}$ is generated. However, in this theorem, it is not specified to which region the algebra $\mathscr{A}$ is associated. In classical physics, solutions to the differential equations representing the dynamics of the theory are specified uniquely by the initial values. The quantum analogue of this statement is given by the so-called *time slice axiom* of AQFT [314] (see also [339]). Given a complete spacelike hypersurface Σ, this surface can be used to impose initial conditions. Knowledge of the field configurations in an arbitrarily small open neighbourhood $\mathscr{U}$ of Σ then suffices to calculate fields in arbitrary regions. The typical example is to fix the field configurations on the hypersurface $t = 0$ and consider an open neighbourhood $\mathscr{U}$ such that $|t| > \epsilon > 0$. This initial data can then be used to generate every other state, i.e. the Hilbert space. The *Reeh–Schlieder theorem* however provides a much stronger version of this assertion [187]. This theorem makes use of the fact that in QFT we usually refer to nets of local algebras, where the local algebras $\mathscr{A}_\mathscr{U}$ are associated to causally complete subregions $\mathscr{U}$ of the full spacetime:

Theorem 3: For any causally complete subregion $\mathscr{U}$ with local algebra $\mathscr{A}_\mathscr{U}$ and vacuum state vector $|\Omega_\omega\rangle$,

i) the vectors $\mathfrak{a}|\Omega_\omega\rangle$ for $\mathfrak{a} \in \mathscr{A}_\mathscr{U}$ are dense in $\mathscr{H}$

ii) $\mathfrak{a}|\Omega_\omega\rangle = 0$ for $\mathfrak{a} \in \mathscr{A}_\mathscr{U}$ implies $\mathfrak{a} = 0$.

For discussions on proofing this theorem see e.g. [192, 318, 319]. The theorem states that the vacuum state vector is a cyclic separating vector for any local algebra. Conversely, acting with $\mathscr{A}_\mathscr{U}$ of arbitrary $\mathscr{U}$ allows to generate a dense subspace of $\mathscr{H}$. This means that any state of $\mathscr{H}$ can be approximated with arbitrary precision by acting with the local algebra $\mathscr{A}_\mathscr{U}$ on the vacuum state vector. Figuratively speaking, the operators associated to the region that the readers laptop is placed on can be combined into an operator $\mathfrak{a}^\dagger_{\text{Eleph}}$

(a fairly complicated one) that 'creates' an elephant on the moon, or more precisely, acting with $\mathfrak{a}^\dagger_{\text{Eleph}}$ provides a state that approximates the state including an elephant on the moon to arbitrary precision. We could even come up with an even more complicated operator that 'creates' the moon itself. This statement shows how powerful the infinite amount of entanglement included in the vacuum state (or in fact, any other typical state) of QFT is.

Although these examples are true in principle, there do exist some limitations. First of all, the underlying theory has to allow for the state we aim to approximate. That is, if our theory were only to describe our laboratory on the earth, we could never hope to create something on the moon as this is not part of our theory. In other words, this will never work if the vacuum state is not (infinitely) entangled with the moon. If we however allow for a QFT defined throughout the whole universe, the above examples are possible in principle. As already mentioned, the necessary operators such as $\mathfrak{a}^\dagger_{\text{Eleph}}$ are highly complicated. Therefore, while they can be written down on paper, an experimental realisation of such operators is out of the question since this would require immense amounts of energy. Moreover, these 'creation' operators must not be unitary. To see this, consider the spacelike separated regions $\mathscr{U}$ and $\mathscr{V}$ with algebras $\mathscr{A}_\mathscr{U}$ and $\mathscr{A}_\mathscr{V}$. Then, $\mathscr{A}_\mathscr{V}$ contains an operator $\mathfrak{a}_\mathscr{V}$ which we aim to approximate. The vacuum state vector, cyclic separating for $\mathscr{U}$, does not contain this object and hence $\langle\Omega|\mathfrak{a}_\mathscr{V}|\Omega\rangle = 0$. Now suppose that $\mathfrak{a}_\mathscr{U} \in \mathscr{A}_\mathscr{U}$ approximates the state containing $\mathfrak{a}_\mathscr{V}$ to arbitrary precision. We then know that $\langle\mathfrak{a}_\mathscr{U}\Omega|\mathfrak{a}_\mathscr{V}|\mathfrak{a}_\mathscr{U}\Omega\rangle = 1$. Since $\mathscr{U}$ and $\mathscr{V}$ are spacelike separated regions, the operators of these regions commute and $\langle\Omega|\mathfrak{a}_\mathscr{V}\mathfrak{a}^\dagger_\mathscr{U}\mathfrak{a}_\mathscr{U}|\Omega\rangle = 1$. In order to avoid a contradiction with $\langle\Omega|\mathfrak{a}_\mathscr{V}|\Omega\rangle = 0$, the operator $\mathfrak{a}_\mathscr{U}$ must not be unitary. So while the Reeh–Schlieder theorem guarantees that the operator $\mathfrak{a}_\mathscr{U}$ can be constructed, it does not state that this operator is unitary. Therefore, the Reeh–Schlieder theorem cannot be understood as a dynamical statement of creating an elephant on the moon by switching on some complicated interaction Hamiltonian and evolving the state. For all of these reasons, pachyderm phobics do not have to worry about the implications of this theorem and may even successfully work in experimental quantum physics without their phobia affecting their performance.

So far our discussion of AQFT was based on QFT in Minkowski spacetime. This can however be generalised to curved backgrounds as well. We will not discuss this here but point the interested reader to [340–347] and references therein. Also, the Reeh–Schlieder theorem was shown to hold under appropriate circumstances for curved spacetimes [340, 348, 349] (see also [350, 351]). In the context of gravity, the Reeh–Schlieder theorem in particular, but also the use of operator algebras and AQFT methods in general enabled for fairly rigorous analyses of black holes. A special aspect where this is useful is the study of the black hole interior and the question about Hilbert space factorisation in the presence of gravity. The most common arena for these investigations is provided by the *AdS/CFT*

correspondence [74–76]. As this background is elementary to the discussions in the later sections in secs. 4, 5, 6 and 7, in the next section we review the setting of AdS/CFT and black holes within AdS/CFT.

3 The AdS/CFT Correspondence

Dualities between physical theories show that the same underlying physics can have different descriptions. In particular, the dynamics of a system can be described by (in most cases two) sets of different degrees of freedom. An accurate understanding of the nature behind a duality amounts to grasping a fundamental piece of physics. Early examples include the electric-magnetic or Montonen–Olive duality [352] and its supersymmetric extension known as Seiberg duality [353], which are dualities between theories at strong and weak coupling, and the duality between the sine-Gordon model and the massive Thirring model [354], where the fermions of the latter are mapped to the bosons of the former by bosonisation [355]. Moreover, the five different types of string theories in ten dimensions are related by S-dualities [356–360] and T-dualities [361, 362]. While the aforementioned dualities all relate different theories of the same kind and dimension to each other, the *AdS/CFT correspondence* or *holographic duality* stands out as this duality states the dynamical equivalence between a theory of gravity in D dimensions to a CFT in $D-1$ dimensions [74–76]. This duality therefore provides an explicit realisation of the holographic principle [111, 363, 364]. This principle is considered to be a fundamental property of any theory of quantum gravity. It states that the number of degrees of freedom in any theory of quantum gravity scales with the area rather than the volume of the spacetime region where the theory is defined, contrary to what happens in ordinary QFT. Therefore, and since the originally proposed version of AdS/CFT made use of string theory, which at the time of writing is the most promising candidate for a theory of quantum gravity, the AdS/CFT correspondence has received much of its attention because it can be used to study aspects of quantum gravity. In this thesis, we are particularly interested in black holes within the AdS/CFT correspondence. The eternal black hole is conjectured to be dual to two copies of the same CFT entangled in the TFD state [112]. This relation led to considering spacetime as an emergent phenomenon due to the presence of entanglement [115–117] which shortly after entered the ER=EPR proposal [118]. However, the duality between the eternal black hole and the TFD state also led to a contradicting statement. On the one hand, the CFT Hilbert space is expected to factorise due to the lack of classical interactions between the two copies of the CFT, while on the other hand, the Hilbert space of gravity is manifestly non-factorised due to the presence of the smooth and connected black hole geometry [120]. The explanation and eventual resolution of this *factorisation puzzle* is one of the main checkpoints on the road to a theory of quantum gravity. The

factorisation puzzle in the AdS/CFT correspondence is one of the central aspects studied in this thesis.

To provide sufficient context, we briefly review the holographic principle as well as the original proposal for AdS/CFT in sec. 3.1. With this background, we are then in a position to discuss the factorisation puzzle in more detail in sec. 3.2. We start this by explaining the duality between the eternal black hole and the TFD state, followed by an account of the ER=EPR proposal and its consequences in light of the factorisation puzzle.

3.1. A Duality Between Quantum Field Theory and Gravity

Even before the seminal paper proposing AdS/CFT [74], hints that such a duality exists had been found. One of the earliest and most noteworthy hints concerns the particular case of AdS_3/CFT_2. It was shown that the asymptotic symmetries of AdS_3 give rise to two copies of the Virasoro group, which is precisely the symmetry of a CFT_2 [365]. Moreover, the central charge counting the degrees of freedom of this CFT was shown to be determined by the curvature radius L_{AdS} of AdS_3 and the Newton constant as [365]

$$\frac{c}{3} = \frac{L_{AdS}}{2G_N^{(3)}} . \tag{3.1}$$

Although the case of AdS_3/CFT_2 was also considered in [74], the original proposal was phrased for AdS_5/CFT_4. In the following, we first provide details on the holographic principle in sec. 3.1.1. Subsequently we discuss the original argument for AdS_5/CFT_4 in sec. 3.1.2 by considering the physics of D3-branes from two perspectives. Much of this discussion will follow parts of the excellent reviews [366–368], and in particular [369]. Last but not least, we briefly sketch how the holographic dictionary is established by an equality of partition functions in sec. 3.1.3. To conclude this section we explain how entanglement between subregions of the CFT can be calculated using AdS/CFT.

3.1.1. Black Holes and Holography

Deducing a quantum theory from the corresponding classical description is a hard task for several reasons. First of all, there is no unique recipe to do so. Each approach to quantisation has advantages and disadvantages in certain situations. This relates to the second point, i.e. the fact that since quantum theory is (believed to be) more fundamental than classical mechanics, not every principle underlying the quantum theory has an analogue

in the classical description. In the special case of gravity, another reason is that the usual renormalisation techniques of QFT are not applicable. Within our current description of gravity, black holes provide the most interesting objects. In particular, the singularity of the black hole, where our current mathematical description of gravity breaks down, is generally expected to be smoothed out in a theory of quantum gravity. This promotes black holes to an ideal object of study when aiming to learn about quantum aspects of gravity. Such studies led to uncovering what is known as the *holographic principle*, which we explain in the following paragraphs. For a review of this topic, which we partly follow, see [370].

The Generalised Second Law

The holographic principle is based on an observation of Bekenstein in combining black holes with the laws of thermodynamics. In particular, considering the second law concerning the growth of thermodynamical entropy, the following thought experiment was conducted. Given any object in our universe, it can be associated to a certain amount of thermodynamical entropy S_{obj}. If the object is thrown into a black hole, it is lost to the observable universe (i.e. the black hole exterior) as nothing is able to leave a black hole. However, this would imply that the entropy of the observable universe diminishes since $\delta S_{\text{obs}} = -S_{\text{obj}} < 0$. In order for black holes to be consistent with the laws of thermodynamics, Bekenstein proposed that black holes themselves have to have an entropy S_{BH}. With this assumption, the second law is not violated as long as the change of entropy of the black hole balances the loss of entropy for the observable universe, i.e. $\delta S_{\text{BH}} \geq \delta S_{\text{obj}}$. In other words, for any process only the change of the sum of S_{BH} and S_{obj} has to be positive, but not the individual changes on their own. This is known as the *generalised second law* [371–373]. For any process not involving black holes, this reduces back to the usual second law. Bekenstein further conjectured that the entropy of a black hole is proportional to the area of its event horizon, with the proportionality factor given by an order 1 number. This was based on an earlier result by Stephen Hawking called the *area theorem*, stating that the horizon area of a black hole always grows with time [374]. In that regard, the area of a black hole behaves analogous to thermodynamic entropy. If the black hole entropy really is to be interpreted in a thermodynamic sense, there should also be a temperature associated to this entropy. A first indication that this exists was derived in [375] by showing that the Einstein equations for a black hole imply a differential relation

$$\mathrm{d}M = \frac{\kappa}{8\pi G_{\text{N}}}\mathrm{d}A_{\text{S}}\,, \tag{3.2}$$

where G_{N} is Newtons constant, κ is the surface gravity, $\mathrm{d}M$ is an infinitesimal change in the black hole mass, i.e. the energy, and $\mathrm{d}A$ an infinitesimal change in the surface area

of the horizon, i.e. the entropy.[1] Interpreting this as the first law of thermodynamics, the prefactor in this relation has to be related to the temperature. A famous semiclassical computation showed that black holes do emit particles, dubbed *Hawking radiation*, when taking into account quantum field theory effects on the classical black hole spacetime [109, 110]. This radiation is emitted as a thermal spectrum at temperature $T_{\mathrm{BH}} = \frac{\kappa}{2\pi}$. Therefore, taking into account (3.2), the entropy is given by

$$S_{\mathrm{BH}} = \frac{A_{\mathrm{S}}}{4G_{\mathrm{N}}}\,, \tag{3.3}$$

fixing the proportionality factor introduced by Bekenstein.[2] This formula also provides an interesting interpretation of the quantisation of information for black holes. In D spacetime dimensions, the area A has dimension length^{D-2}. Therefore, also G_{N} has to have this dimension as the entropy is dimensionless. By dimensional analysis, the Newton constant can be related to the Planck length l_{P} as $G_{\mathrm{N}} = l_{\mathrm{P}}^{D-2}$ and may therefore be interpreted as a Planck area $A_{\mathrm{P}} = l_{\mathrm{P}}^{D-2}$. The black hole entropy (3.3) therefore is interpreted as the information on the horizon being quantised in terms of Planck areas.

The black hole entropy does not only have a valid thermodynamical interpretation but also provides an upper bound on the entropy of any given object [108]. The bound is obtained by demanding that for any process the generalised second law holds, i.e. the change of the black hole entropy is sufficiently large to compensate for the loss of entropy in the observable universe. This is elucidated by the following thought experiment where for simplicity we assume that $D = 4$. Suppose that there exists an object of mass m and entropy S. This object is to be thrown into a black hole of mass $M \gg m$ and entropy $S_{\mathrm{BH}} = 4\pi G_{\mathrm{N}} M^2$.[3] The mass of the black hole increases as $M \to M + m$. In this process, $\delta S_{\mathrm{obs}} = -S$ and $\delta S_{\mathrm{BH}} = 8\pi G_{\mathrm{N}} M m$, neglecting a term $\propto m^2$ in the latter equality. Demanding that the generalised second law holds, i.e. $\delta S_{\mathrm{obs}} + \delta S_{\mathrm{BH}} \geq 0$, provides the upper bound $S \leq 8\pi G_{\mathrm{N}} M m$ for the entropy of the object. Expressed in terms of the area,[4] this bound can be reformulated as [363]

$$S \leq \frac{A_{\mathrm{S}}}{4G_{\mathrm{N}}}\,. \tag{3.4}$$

If the object itself is a black hole, the bound is saturated.

[1] Note that A_{S} is the surface area and not a subregion of a QFT, which we also denoted by A in earlier sections. The index S is meant to avoid confusion in this unfortunate, but widely adopted abuse of notation.

[2] Note that we work in natural units.

[3] In $D = 4$, the horizon area is given by $A = \pi r_{\mathrm{S}}^2$, with the Schwarzschild radius given by $r_{\mathrm{S}} = 2G_{\mathrm{N}}M$.

[4] This reformulation relates the Bekenstein bound to the spherical entropy bound of [363].

The above discussion is, in spirit on the original work of Bekenstein [108], based on this thought experiment. However, more rigorous treatments of the Bekenstein bound have appeared later on. In [376] the *Bousso bound* was established as a covariant formulation of (3.4). Within QFT, the Bekenstein bound was proven using the relative entropy in [377]. Moreover, the *quantum focussing conjecture* [378] implies the Bousso bound and can therefore be viewed as a more general statement.

The Holographic Principle

As already pointed out below (3.3), this formula suggests that information for black holes is *a)* stored on the horizon area and *b)* is quantised in terms of Planck areas. These observations led Gerard 't Hooft to propose the *holographic principle* as a fundamental law of any theory of gravity [111]. The bound (3.4) on the entropy by the area of the considered region is present due to the effects of gravity. The holographic principle then states that, for any volume containing a theory of quantum gravity, the information about the theory is stored on the boundary of the region, i.e. the area. Put differently, this means that any theory of quantum gravity in D dimensions can equivalently be described by an ordinary QFT without gravity in $D-1$ dimensions, i.e. with one less spatial dimension. The boundary of the volume can therefore be interpreted as a holographic screen on which the physics of the interior of the volume is projected without loss of information. This is also the reason why the principle is dubbed 'holographic'. The information about the volume is stored on a surface, much like in optical experiments when generating holograms. This remarkable property was given a precise formulation in string theory by Leonard Susskind [363], who unified the discussion of [111] with earlier ideas on lower dimensional descriptions of string theory [379]. Moreover, the principle was analysed in the context of gravity in an Anti-de Sitter spacetime [364].

As a side remark, the holographic principle, which is conjectured to hold for any theory of quantum gravity, was also analysed in *loop quantum gravity* (LQG). Although the black hole entropy was also found in LQG [380], whether LQG realises the principle seems to be an open question at the time of writing this thesis. For studies supporting or refusing this claim see e.g. [381, 382] or [383], respectively.

The theory of quantum gravity within the volume and the QFT in one less dimension defined on the boundary of the volume are equivalent descriptions of the same underlying physics. This rather general statement can also be formulated in terms of the actual field content of the two theories, which makes the power of the holographic principle more precise. In particular, it implies that each process or measurement must have a description in both formulations, and every operator in one of the theories must have a dual formulation

in the other theory. The same is true for parameters such as coupling constants and length scales in both theories. Finally, since the thermodynamic entropies in both descriptions have to match, also the number of degrees of freedom has to be the same.

We can use the constraint on the number of degrees of both descriptions to obtain some insights on which kinds of theories are likely to be involved in an explicit realisation of the holographic principle. By the Bekenstein bound (3.4) we know that the entropy, which counts the degrees of freedom, is expressed as a ratio of the area A and the Newton constant $G_{\mathrm{N}}^{(D)}$ in D dimensions. Up to a prefactor, we can express the area in terms of a length scale L as $A \sim L^{D-2}$. So the general expectation on the number of degrees of freedom is that

$$\#\text{ degrees of freedom} \sim \frac{L^{D-2}}{G_{\mathrm{N}}^{(D)}}\,. \tag{3.5}$$

A D-dimensional theory of gravity and a $D-1$-dimensional QFT satisfying the above relation have a chance of providing a realisation of the holographic principle. The typical QFTs considered in physics are gauge theories, i.e. field theories with an (S)U(N) gauge symmetry. Such theories contain $N^2(-1)$ degrees of freedom at every point in spacetime,[5] where the -1 can be neglected for sufficiently large N as we are only interested in the scaling behaviour. Therefore, for such gauge theories, the general expectation is that

$$N^2 \sim \frac{L^{D-2}}{G_{\mathrm{N}}^{(D)}}\,. \tag{3.6}$$

To provide an example of two such theories, consider a gauge theory with U(N) gauge symmetry in $D-1=4$ dimensions. Apart from the factor N^2, the thermodynamic entropy in QFT scales as usual with the volume of a spatial slice Σ. Introducing a discretisation of space into small boxes with edge length ϵ, the entropy is then expressed in a regularised form as

$$N^2 \mathrm{Vol}(\Sigma) \sim N^2 \frac{\mathrm{Vol}(\mathbb{R}^3)}{\epsilon^3}\,. \tag{3.7}$$

A gravitational counterpart to the gauge theory is provided by considering gravity on a $D=5$-dimensional Anti-de Sitter spacetime. We will provide more details on this spacetime shortly in sec. 3.1.2. For now, we just note that this spacetime has a boundary. This boundary can be reached by light rays in finite time, see e.g. [385]. These two properties

[5] Note that there are also instances where scalings such as $N^{\frac{3}{2}}$ appear [384], the reason being that not all degrees of freedom are dynamical in these cases. The gravitational duals in such scenarios are more complicated than what we discuss in the following.

make Anti-de Sitter spacetime particularly interesting in the context of the holographic principle. By calculating the area A_S of a time slice of Anti-de Sitter spacetime as an integral over the volume element of the induced metric γ, the scaling

$$A_S \sim \int d^3x\sqrt{-\gamma} = \frac{\mathrm{Vol}(\mathbb{R}^3)}{\epsilon^3} L^3_{\mathrm{AdS}} \tag{3.8}$$

is obtained, where ϵ is a cutoff as before and L_{AdS} is the curvature radius of Anti-de Sitter spacetime. Combining the results (3.7) and (3.8) using that $S \sim \frac{A_S}{G_N^{(D)}}$, the volume of $\mathbb{R}^3$ as well as the cutoff ϵ cancel and we obtain

$$N^2 \sim \frac{L^3_{\mathrm{AdS}}}{G_N^{(5)}}, \tag{3.9}$$

precisely realising the expected relation (3.6) for $D = 5$ with the length scale L given by the curvature radius L_{AdS}. This provides a hint that (S)U(N) gauge theories in four dimensions may be holographically dual to gravitational theories on Anti-de Sitter spacetime in five dimensions.

Of course, the fact that two theories lead to the relation (3.6) is not a sufficient but only a necessary condition that these two theories are genuinely holographically dual to each other. Moreover, matching the number of degrees of freedoms does not explain how correlation functions and processes are realised in the two theories. Establishing such relations explicitly is a difficult task and not generally clear. That is to say, it is not (yet) known how the relations between observables in arbitrary (S)U(N) gauge theories and gravitational theories on Anti-de Sitter spacetime look like, if they can be established in such generality at all. However, there are specific examples where the relations can be derived explicitly. We will discuss one such instance in the next section.

3.1.2. A Realisation of the Holographic Principle

The first explicit realisation of the holographic principle was found by Juan Maldacena [74]. Essential aspects of this realisation were clarified and derived shortly after by Steven Gubser, Igor Klebanov and Alexander Polyakov [76] as well as Edward Witten [75]. In this approach, the theory of gravity is a special version of string theory while the QFT is a supersymmetric U(N) gauge theory. This realisation is named the *AdS/CFT correspondence* and is one of the main settings to be studied within this thesis.[6] This duality enabled for a plethora of developments in different areas of physics, ranging from new insights into string theory to

[6] Throughout the literature, the terms 'AdS/CFT correspondence', 'holography' and '(gauge/gravity) duality' are often used interchangeably. We will do so as well in this thesis.

using the duality as a computational tool in solid state physics. In the following discussion we briefly introduce this realisation of the holographic principle. We start by motivating this realisation through a property of string theory known as the *open-closed string duality*. We then review how Maldacena established the AdS/CFT correspondence by considering the physics of D-branes in two particular limits. We finish the section by comparing the symmetries on both sides of the duality.

Why String Theory?

Studying string theory enables to obtain explicit realisations of the holographic principle. This is due to the open-closed string duality which implies a relation between gravity and gauge theory. We discuss this property in the following paragaphs. The central idea of string theory is to describe all particles, such as contained in the standard model but also beyond, by excitations of an extended object. The notion of a particle, an object without spatial extension, is replaced by a string as the fundamental degree of freedom, an object with a length l_S and therefore on spatial dimension. Each string excitation is associated to a particular type of particle, much like different notes are obtained by varying the length of the same guitar string. String theory therefore also provides a way of unifying the different forces of nature, as all known particles are described by the same fundamental object. Excellent and extensive reviews are provided in [386–394].

As strings are extended one-dimensional objects, the propagation of strings in spacetime defines a two-dimensional area called the worldsheet. The worldsheet is described by two coordinates τ and σ. In spacetime, this surface is described by functions $X^\mu(\tau, \sigma)$ which may be regarded as maps from the worldsheet to spacetime. The area can be expressed as an integral of X^μ. As this integral depends on derivatives of X^μ, it may be regarded as an action, also known as the Nambu–Goto action. In calculating the equations of motion for this action, which determine the mode expansion for X^μ, boundary conditions have to be put on X^μ in order for the variational principle to be well-defined. A possible choice are periodic boundary conditions, leading to the mode expansion for closed strings. Closed strings therefore do not end anywhere and are topologically a circle. Notably, within the spectrum of closed strings, at the massless level there is an excitation of spin 2 that is described by a symmetric and traceless polarisation tensor. This excitation is identified with fluctuations of the spacetime metric, i.e. the graviton. String theory therefore is a theory of quantum gravity. If the boundary conditions are not chosen periodic, the endpoints of the string have to satisfy either Dirichlet or von Neumann boundary conditions, leading to open strings. For each spacetime direction μ and each of the two endpoints, either of these choices can be made. Dirichlet boundary conditions imply that the string is fixed in this

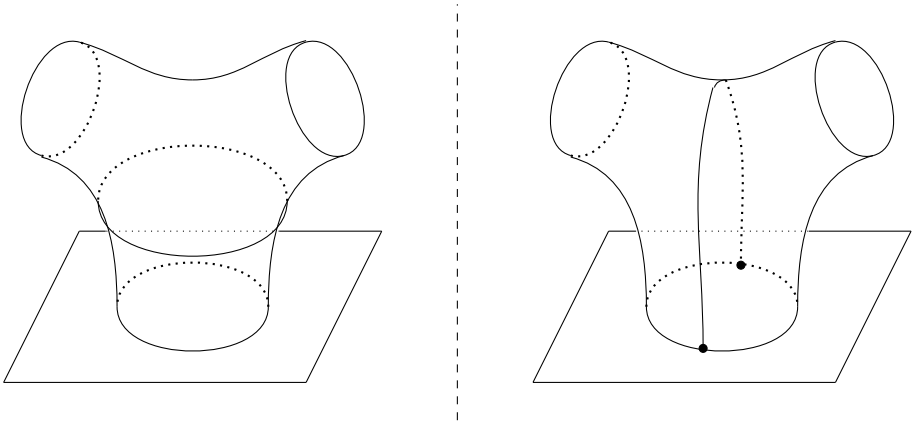

Figure 3.1: Visualisation of the open-closed string duality using the interaction of a closed string with a brane. On the left, the interaction is described by a closed string emitted by the brane. On the right, the incoming closed string converts into an open string upon touching the brane, with the intermediate open string eventually converting back into a closed string. As this represents the same process, the two descriptions have to be equivalent. The figure is inspired by fig. 2 in [396].

direction, while von Neumann boundary conditions allow the endpoint to move. Imposing Dirichlet boundary conditions in p directions singles out a p-dimensional hypersurface in spacetime. Such hypersurfaces are referred to as Dp-branes. All open strings have to end on these branes [395]. A rigid hypersurface in spacetime would not be consistent with the principles of general relativity. Therefore, branes are promoted to dynamical objects as well. In the spectrum of open strings, at the massless level there exist gauge fields with spin 1 as well as scalar fields. The gauge fields correspond to degrees of freedom longitudinal to the brane, while the scalar fields represent the transverse ones.

At first glance, this seems to imply that there exist two kinds of strings, open and closed ones. However, the same physical process can be described using both open and closed strings. A first indication that this is the case can be seen by the fact that via the interaction of two open strings, closed strings can be formed. To understand this better, we note that since branes are dynamical objects, they also may have a mass and interact with closed strings. Then, the open-closed string duality may be understood as follows. Consider a process with an incoming closed string that interacts with a brane. The outgoing string is also closed. We may describe this process in two ways. On one hand, the interaction may be understood by closed strings only in the sense that the brane emits a closed string that interacts with the incoming closed string. By the interaction, a different closed string is produced. This process is visualised on the left of fig. 3.1. On the other hand, we may say that the incoming closed string, upon touching the brane, is converted into an open string. The endpoints of the open string move on the brane and eventually meet again such that the outgoing state is again a closed string. This is visualised on the right of fig. 3.1. As

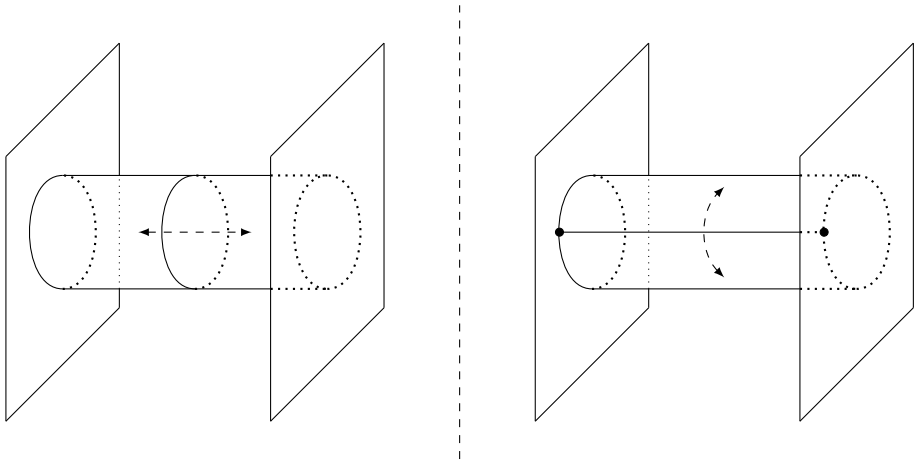

Figure 3.2: Another visualisation of the open-closed string duality. The process can be interpreted either as the exchange of a closed string between the two branes (gravitational attraction) or as an open-string one-loop diagram in a $U(1) \times U(1)$ gauge theory. The figure is inspired by fig. 4 in [396].

the physical process, i.e. the interaction of a closed string with a brane, is the same, the closed string and open string way of describing this process have to be equivalent.

As we mentioned above, at the massless level, closed strings contain graviton excitations, while open strings include gauge field degrees of freedom. The open-closed string duality therefore provides a strong hint that the holographic principle, as a duality between a theory of gravity and an ordinary QFT without gravity, may have a realisation in string theory. This can be given even more strength by noting that the action describing a D-brane, known as the Dirac–Born–Infeld (DBI) action, assembles the gauge field degrees of freedom of the open string sector into the familiar action of a $U(1)$ gauge theory in a certain limit. We will discuss this in more detail shortly when reviewing Maldacenas original proposal for the AdS/CFT correspondence. To show the relation between the open-closed string duality and the holographic principle, we again describe a particular scattering process both using open and closed strings. The process is to describe the interaction between two branes. First we describe this using closed strings. That means, one brane emits a closed string which is then absorbed by the other brane. Second using open strings, the interaction is described by an open string stretching between the two branes. The endpoints form closed paths on each of the two branes such that the open string forms a closed loop. These two descriptions are visualised on the left and right of fig. 3.2. Since closed strings include the graviton mode, the first description may be understood as gravitational attraction between the two branes. On the other hand, open strings describe (in this case, $U(1)$) gauge fields, so the second description may be interpreted as a one-loop exchange diagram in gauge theory. However, while the open-closed string duality provides strong hints for realising

the holographic principle within string theory, a precise version also has to account for the different dimensions of the two theories appearing in the holographic principle.

Maldacenas Argument for AdS_5/CFT_4

The proposal of [74] realises the holographic principle within a specific setting in string theory. We already discussed above that $U(N)$ gauge theories on the one hand and gravity on Anti-de Sitter spacetime on the other hand satisfy the relation between the number of degrees of freedom, cf. (3.6). Indeed, the AdS/CFT correspondence in its strongest form as conjectured in [74] states a holographic duality between

> type IIB superstring theory on $AdS_5 \times \mathbb{S}^5$ with arbitrary string coupling g_S, N units of five form flux through $\mathbb{S}^5$ and arbitrary ratio of Anti-de Sitter radius to string length $\left(\frac{L_{AdS}}{l_S}\right)^2 = \sqrt{4\pi N g_S}$

on the gravity side and

> four-dimensional $\mathcal{N} = 4$ supersymmetric Yang–Mills theory with gauge group $SU(N)$ and coupling constant g_{YM}

on the field theory side. The duality is supplemented by two relations between the parameters of these theories,

$$2\pi g_S = g_{YM}^2 \quad \text{and} \quad 2N g_{YM}^2 = \left(\frac{L_{AdS}}{l_S}\right)^4 . \tag{3.10}$$

On the gravity side, superstring theory accounts for the string theory being supersymmetric as a natural way of introducing fermionic degrees of freedom to the theory. Anti-de Sitter is a maximally symmetric spacetime and has constant negative Ricci scalar $R = -\frac{D(D-1)}{L_{AdS}^2}$. The sphere $\mathbb{S}^D$ has constant positive Ricci scalar, determined by its curvature radius $L_{\mathbb{S}^D}$ analogous to the previous formula as $R = \frac{D(D-1)}{L_{\mathbb{S}^D}^2}$. Type IIB refers to a particular type of string theory in which Dp-brane solutions with p odd are stabilised by the existence of Ramond–Ramond fields $C_{(p+1)}$ with field strengths $F_{(p+2)} = \mathrm{d}C_{(p+1)}$ [397]. The N units of five form flux refer to fluxes of the field strength $F_{(5)}$ through the sphere $\mathbb{S}^5$. On the field theory side, $\mathcal{N} = 4$ refers to the highest amount of supersymmetry there can be in four spacetime dimensions without including gravitational degrees of freedom. We will discuss these properties as well as the relations (3.10) in more detail shortly.

The above version of AdS/CFT is the strongest form of the duality. However, at the

time of writing this thesis it remains a conjecture since it is not known how string theory on $\mathrm{AdS}_5 \times \mathbb{S}^5$ is quantised consistently.[7] Correspondingly, it is not very useful for explicit computations to apply or even test the duality. To make the theory on the gravity side more tractable, the limit of small string coupling $g_\mathrm{S} \ll 1$ is taken which renders the theory classical. The perturbative expansion in g_S is easier to handle as only tree-level scattering processes contribute. As the string coupling is small, to keep the ratio between the Anti-de Sitter radius and string length arbitrary, the number of five form fluxes N has to become large. On the gravity side, the theory is then given by

> classical type IIB superstring theory on $\mathrm{AdS}_5 \times \mathbb{S}^5$ with $g_\mathrm{S} < 1$, $N > 1$ units of five form flux through $\mathbb{S}^5$ and arbitrary ratio of Anti-de Sitter radius to string length $\left(\frac{L_\mathrm{AdS}}{l_\mathrm{S}}\right)^2 = \sqrt{4\pi N g_\mathrm{S}}$.

Using the relations (3.10) between the parameters of the two theories, we can ascertain how the limits affect the field theory. First, since the string coupling is small, also the coupling constant of the Yang–Mills theory has to be small. However, since the ratio of the Anti-de Sitter radius to the string length is kept arbitrary, the degree of the gauge group N has to be large. The dual field theory is then given by

> four-dimensional $\mathcal{N} = 4$ supersymmetric Yang–Mills theory with gauge group $\mathrm{SU}(N)$ with $N > 1$ and small coupling constant $g_\mathrm{YM} < 1$.

This version is also known as the strong[8] or intermediate form of AdS/CFT. On the field theory side, the limit of large N is also referred to as the planar limit of Yang–Mills theory. For large N, interference terms of different Feynman diagrams describing the same incoming and outcoming particles are suppressed by $\frac{1}{N}$. This is best understood using the 't Hooft double line notation [398, 399]. As interference terms are suppressed, the theory becomes more classical with larger N.

This version of AdS/CFT is still quite involved. Moreover, at the time of writing this thesis strings have not been observed experimentally. Therefore, both for simplifying the computations as well as to use AdS/CFT to predict currently observable physics, it is reasonable to take another limit which allows to treat strings effectively as point particles. Naively, this implies $l_\mathrm{S} \to 0$. More precisely, it is sufficient to demand that $\frac{L_\mathrm{AdS}}{l_\mathrm{S}} \gg 1$. The strings are very small compared to the radius of curvature such that they can be treated

[7] Nevertheless, this background is an exact perturbative background for type IIB superstring theory. Moreover, this background is invariant under the maximal amount of supercharges. For details see e.g. [394].

[8] Note that the earlier version was titled the 'strongest' while this is now only called the 'strong' form.

as point particles on a weakly curved background. Since the ratio specifies is proportional to N and g_S, where g_S has to be small, the large ratio also implies that N has to be even larger, i.e. $N \gg 1$. On the gravity side, the theory reduces to

> type IIB supergravity on weakly curved $AdS_5 \times \mathbb{S}^5$ with $g_S < 1$, $N \gg 1$ units of five form flux through $\mathbb{S}^5$ and large ratio of Anti-de Sitter radius to string length $1 < \left(\frac{L_{AdS}}{l_S}\right)^2 = \sqrt{4\pi N g_S}$.

Again, using the relations (3.10), the limits performed on the gravity side also affect the field theory. The limit of $N \gg 1$ implies that the planar limit becomes more precise. Moreover, since $g_S \sim g_{YM} < 1$, the large ratio $\frac{L_{AdS}}{l_S}$ implies that the product $N g_{YM}^2$ becomes large as well. In the discussion of the planar limit of Yang–Mills theory, it was shown that it is this product that determines the actual coupling strength of the theory [398]. This is known as the 't Hooft coupling $\lambda = N g_{YM}^2$. Therefore, since $N \gg 1$ also $\lambda > 1$. The corresponding field theory is given as

> four-dimensional $\mathcal{N} = 4$ supersymmetric Yang–Mills theory with gauge group $SU(N)$ with $N \gg 1$ and large 't Hooft coupling $\lambda = N g_{YM}^2 > 1$.

This is known as the weak form of the AdS/CFT correspondence. It is fairly obvious how the AdS part of the name appears, as the gravity side is defined on a background involving five-dimensional Anti-de Sitter spacetime. The CFT part comes about since the β function of the coupling of $\mathcal{N} = 4$ supersymmetric Yang–Mills theory vanishes [400, 401]. This property indicates that this particular theory is a field theory with conformal symmetry, i.e. a CFT. For particular operators called $\frac{1}{2}$BPS operators, it was shown that the three point function is independent of the coupling strength [402]. This makes AdS_5/CFT_4 highly valuable to perform tests of the duality. Specific calculations can be performed on both sides independently to check whether the result is the same. In [403] it was shown that the three point function of such operators computed on both sides match. More details on tests of the AdS/CFT correspondence, including also a computation of the Weyl anomaly using both sides of the duality [404, 405], can be found in [366, 369].

The weak form of AdS/CFT has the particularly nice feature that a weakly coupled theory of gravity is dual to a strongly coupled gauge theory. While the latter ones are notoriously hard to analyse, as perturbative methods cannot be applied successfully, the weak form of the AdS/CFT correspondence allows to obtain results in strongly coupled gauge theory by calculations in weakly curved classical gravity. These calculations can be performed using familiar perturbative methods. Notably, also the other direction is

interesting. The AdS/CFT correspondence implies that calculations in weakly coupled gauge theory describe a strongly coupled string theory, i.e. a theory of quantum gravity deep in the quantum regime. This however involves the strongest form of AdS/CFT which is, as mentioned above, a conjecture.

The $\mathrm{AdS}_5/\mathrm{CFT}_4$ correspondence in its weak form can be motivated by analysing the physics of a stack of N D3-branes in type IIB superstring theory on Minkowski spacetime. The duality arises by the equivalence of the open and closed string perspectives on this setup, as we briefly discuss in the following paragraphs (see e.g. [369] for a detailed review).

Open String Perspective In the open string picture, D3-branes are objects on which open strings can end. This description is valid when $g_\mathrm{S} N < 1$. Open strings are understood as excitations of the stack of D3-branes, while closed strings describe excitations of the flat background spacetime. The effective action for the massless fields in type IIB superstring theory splits into three parts,

$$S_\mathrm{IIB} = S_\mathrm{closed} + S_\mathrm{open} + S_\mathrm{int}\,. \tag{3.11}$$

In the following, we restrict the discussion to the bosonic parts of these actions as they are sufficient for the argument. The part of the closed string action involving the spacetime metric g as well as the dilaton field Φ is then given by[9]

$$S_\mathrm{closed} = \frac{1}{(2\pi)^7 l_\mathrm{S}^8 g_\mathrm{S}^2} \int \mathrm{d}^{10}X\, \sqrt{-g}\, e^{-\Phi} \left[R[g] + 4(\partial\Phi)^2\right], \tag{3.12}$$

where $(2\pi)^7 l_\mathrm{S}^8 g_\mathrm{S}^2 = 16\pi G_\mathrm{N}^{(10)}$ is related to the Newton constant in 10 dimensions. The asymptotic value of the dilaton field Φ_0 is related to the string coupling constant, $g_\mathrm{S} = e^{\Phi_0}$. In the above action, this has been extracted and Φ denotes only the fluctuations of the dilaton. For details see e.g. [391]. Expanding this action in small fluctuations of the metric about a flat background $g = \eta + \kappa h$, where $\kappa^2 = 8\pi G_\mathrm{N}^{(10)}$, results in the canonically normalised action

$$S_\mathrm{closed} = \frac{1}{2} \int \mathrm{d}^{10}X\, (\partial h)^2 + \mathcal{O}(l_\mathrm{S}^4)\,. \tag{3.13}$$

This action describes the dynamics of the graviton on a flat background, i.e. on $\mathbb{R}^{1,9}$. As mentioned before, the presence of Dp-branes in type IIB superstring theory is due to the existence of corresponding Ramond–Ramond fields $C_{(p+1)}$ with p odd. The field content

[9] Apart from the metric and the dilaton, the massless sector of closed strings also includes the Kalb–Ramond field B. For simplicity, we set it to zero in this discussion.

of type IIB superstring theory includes three Ramond–Ramond fields $C_{(0)}$, $C_{(2)}$ and $C_{(4)}$, which introduce charges stabilising D(-1)-branes, D1-branes and D3-branes. Due to the Poincaré duality

$$\mathrm{d}C_{(p+1)} = F_{(p+2)} = \star F_{(8-p)} = \star \mathrm{d}C_{(7-p)}\,, \tag{3.14}$$

where $\star$ denotes the Hodge dual, $C_{(0)}$ and $C_{(2)}$ have dual forms $C_{(8)}$ and $C_{(6)}$ associated to D7-branes and D5-branes. For $C_{(4)}$, this enforces that the corresponding field strength $F_{(5)}$ is self dual. Moreover, by T-duality there also exists a D9-brane which fills all of spacetime, although there is no $C_{(10}$. For more details on this see e.g. [390]. The field strengths $F_{(1)}$, $F_{(3)}$ and the self dual $F_{(5)}$ are also part of the bosonic closed string action. Expanding the corresponding terms and taking the limit $l_\mathrm{S} \to 0$, combining with (3.13) yields the bosonic part of the supergravity action on Minkowski spacetime.

The other two parts S_open and S_int are obtained from the DBI action. For a single Dp-branes, this action is given by

$$S_\mathrm{DBI} = -\frac{1}{(2\pi)^p l_\mathrm{S}^{p+1} g_\mathrm{S}} \int \mathrm{d}^{p+1}x\, e^{-\Phi} \sqrt{-\det\left(\mathscr{P}[g] + 2\pi l_\mathrm{S} F\right)}\,, \tag{3.15}$$

where we have again set the Kalb–Ramond field to zero and Φ are the fluctuations of the dilaton field. Furthermore, given that x^a are coordinates on the brane, $\mathscr{P}[g]_{ab} = \frac{\partial X^\mu}{\partial x^a}\frac{\partial X^\nu}{\partial x^b} g_{\mu\nu}$ denotes the pullback of the spacetime metric g onto the brane and F is the field strength corresponding to the U(1) gauge field defined on the brane. To obtain the low-energy limit $l_\mathrm{S} \to 0$, we consider the fields X^μ in the configuration

$$X^\mu = \begin{cases} x^a & \text{for} \quad a = 0, \ldots, p \\ 2\pi l_\mathrm{S}^2 \phi^i(\alpha) & \text{for} \quad \alpha = p+1, \ldots, 9 \end{cases} \tag{3.16}$$

together with the approximately flat background $g = \eta + \kappa h$ as for the closed string action. The fields ϕ^α are scalar fields describing fluctuations in the transversal directions of the brane. Expanding the square root to lowest non-trivial order in l_S using

$$\sqrt{\det(\mathbb{1} + \epsilon M)} = 1 - \frac{\epsilon^2}{4}\,\mathrm{tr}\left(M^2\right) + \mathcal{O}(\epsilon^3) \tag{3.17}$$

for M anti-symmetric, neglecting a constant term corresponding to the volume the DBI

action simplifies to

$$S_{\text{DBI}} = -\frac{1}{(2\pi)^{p-2} l_{\text{S}}^{p-3} g_{\text{S}}} \int \mathrm{d}^{p+1}x \left[\frac{1}{4}F^2 + \frac{1}{2}(\partial\phi^\alpha)^2 + \mathcal{O}(l_{\text{S}}^4)\right]. \tag{3.18}$$

The two terms correspond to S_{open}. All possible interaction terms are of higher order in l_{S} and do not contribute in the limit $l_{\text{S}} \to 0$. Therefore, open and closed strings decouple. The above action describes six free scalar fields as well as a U(1) Yang–Mills theory, provided that the Yang–Mills coupling is identified as

$$g_{\text{YM}}^2 = (2\pi)^{p-2} l_{\text{S}}^{p-3} g_{\text{S}}\,. \tag{3.19}$$

Note that for $p = 3$, the case of interest for $\text{AdS}_5/\text{CFT}_4$, the above equation for the Yang–Mills coupling reduces to the first relation in (3.10), $g_{\text{YM}}^2 = 2\pi g_{\text{S}}$. The above action (3.18) describes a single Dp-brane. However, to explain the weak form of the AdS/CFT correspondence we consider a stack of N such branes. If these branes were placed at different locations in spacetime, each brane would correspond to a U(1) Yang–Mills action as above. However, if the branes coincide, the situation changes. Open strings may end on a different brane than they started on. Associating labels t_{ij} to strings starting on brane i and ending on brane j for N coincident D-branes, the gauge theory becomes non-abelian with gauge group U(N). The generators t^k of U(N) contain the labels t_{ij}^k as entries when representing t^k by Hermitian matrices. The labels t_{ij} are also called Chan–Paton factors due to their discoverers [406]. As a side remark, extracting one of the N coincident branes from the stack breaks the symmetry as $\text{U}(N) \to \text{U}(1) \times \text{U}(N-1)$. The symmetry breaking induces a mass for the scalar fields ϕ^α depending on the separation of the branes. This can be understood as a stringy Higgs mechanism. The generalisation of (3.18) to the case of N coincident Dp-branes works as follows. Due to the non-abelian gauge symmetry, partial derivatives have to be replaced by the gauge-covariant derivatives $D_a = \partial_a + \mathrm{i}[A_a, \cdot]$. The scalar fields as well as the gauge fields are valued under the gauge group as $A^a = A^{a,k} t^k$, implying also $F^{ab} = F^{ab,k} t^k$, and $\phi^\alpha = \phi^{\alpha,k} t^k$. The non-abelian gauge symmetry induces self-interaction terms both for the gauge field and for the scalar fields. For the gauge fields, this is automatically included in F^2. For the scalar fields, the non-abelian symmetry gives rise to an additional potential term $\propto [\phi^a, \phi^b]^2$. The action (3.18) is then given by

$$S_{\text{open}} = -\frac{1}{g_{\text{YM}}^2} \int \mathrm{d}^{p+1}x \left[\frac{1}{4}F^2 + \frac{1}{2}(D\phi^\alpha)^2 - \sum_{\alpha\beta} \text{tr}\left([\phi^\alpha, \phi^\beta]^2\right) + \mathcal{O}(l_{\text{S}}^4)\right]. \tag{3.20}$$

This is the bosonic part of the action for $\mathcal{N} = 4$ supersymmetric Yang–Mills theory

with gauge group SU(N).[10] The fermionic part of this action follows from analysing the fermionic part of the DBI action (3.15). To summarise, the low-energy limit $l_S \to 0$ of a stack of N D3-branes in the open string perspective yields supergravity on $\mathbb{R}^{1,9}$ and $\mathcal{N} = 4$ supersymmetric Yang–Mills theory with gauge group SU(N) in four dimensions.

Closed String Perspective In the closed string perspective, D3-branes are solitonic solutions to the supergravity equations of motion that curve the surrounding spacetime. This description is valid for $g_S N > 1$.[11] The low-energy effective action containing everything necessary for this discussion is

$$S = \frac{1}{(2\pi)^7 l_S^8 g_S^2} \int \mathrm{d}^{10}X \sqrt{-g} \left[e^{-\Phi} \left[R[g] + 4(\partial\Phi)^2 \right] - \frac{2}{(8-p)!} F_{(p+2)}^2 \right] . \tag{3.21}$$

Note that we set the Kalb–Ramond field to zero again. To obtain a solution to the equations of motion of this action, we consider the symmetries to write down a convenient ansatz. Empty Minkowski space $\mathbb{R}^{1,9}$ has Lorentz symmetry SO$(1,9)$. Inserting a Dp-brane breaks this symmetry to SO$(1,p) \times$ SO$(9-p)$. This motivates the ansatz

$$\mathrm{d}s^2 = \frac{1}{\sqrt{H_p(r)}} \eta_{\mu\nu} \mathrm{d}x^\mu \mathrm{d}x^\nu + \sqrt{H_p(r)} \delta_{ij} \mathrm{d}y^i \mathrm{d}y^j , \tag{3.22}$$

$$e^\Phi = g_S H_p(r)^{\frac{3-p}{4}} , \tag{3.23}$$

$$C_{(p+1)} = \left(H_p(r)^{-1} - 1 \right) \mathrm{d}x^0 \wedge \ldots \wedge \mathrm{d}x^p . \tag{3.24}$$

Here r is a radial coordinate defined using the transverse directions of the Dp-brane, $r^2 = y_i y^i$. Here indices i, j refer to the transverse directions, while Greek indices refer to the coordinates on the brane. The open function $H_p(r)$ is determined by the equations of motion as

$$H_p(r) = 1 + \left(\frac{L_p}{r} \right)^{7-p} , \tag{3.25}$$

where L_p is a constant. This constant is determined by the units N of flux of $F_{(p+2)}$ through an $8-p$-dimensional sphere,

$$N = \frac{1}{(2\pi l_S)^{7-p}} \int_{\mathbb{S}^{8-p}} \star F_{(p+2)} . \tag{3.26}$$

[10] The N coincident branes constitute a symmetry U(N). However, the U(1) part of U(N) $\simeq$ U(1)×SU(N) decouples from all other degrees of freedom and corresponds to a field confined to the boundary, i.e. the U(1) degree of freedom does not propagate.

[11] Note that the string coupling is still small. Therefore, N has to be sufficiently large such that the surrounding spacetime is significantly curved.

Evaluating this integral using the ansatz (3.24) in $F_{(p+2)} = \mathrm{d}C_{(p+1)}$ yields the relation

$$L_p^{7-p} = N(4\pi)^{\frac{5-p}{2}}\Gamma\Big(\frac{7-p}{2}\Big)l_\mathrm{S}^{7-p}g_\mathrm{S}\,. \tag{3.27}$$

For $p = 3$, this reduces to the second equation in (3.10) with the curvature radius of Anti-de Sitter space given by L_3. The mass M of the stack of branes is given by

$$M = \frac{N\cdot \mathrm{Vol}(\mathbb{R}^{1,p})}{(2\pi)^p l_\mathrm{S}^{p+1} g_\mathrm{S}}\,. \tag{3.28}$$

With this, the ansatz for the metric (3.22) is fully determined. As the horizon is not compact this metric describes a black brane solution [407, 408]. Setting $p = 3$ from now on, this metric has two interesting limits. First, in the limit of large r the function (3.25) goes to 1. The metric then reduces to the Minkowski metric on $\mathbb{R}^{1,9}$. This means that in the region $r \to \infty$ the physics are described by supergravity on $\mathbb{R}^{1,9}$. In the other extreme of $r \to 0$, the additive 1 in (3.25) is negligible and the metric becomes

$$\mathrm{d}s^2 = \frac{r^2}{L_3^2}\eta_{\mu\nu}\mathrm{d}x^\mu \mathrm{d}x^\nu + \frac{L_3^2}{r^2}\big(\mathrm{d}r^2 + \mathrm{d}\Omega^2_{\mathbb{S}^5}\big)\,, \tag{3.29}$$

where compared to (3.22) we rewrote the coordinates y^i in terms of the radial coordinate r and angular coordinates forming the volume element of $\mathbb{S}^5$. The radial coordinate together with the coordinates x^μ form the metric on five-dimensional Anti-de Sitter spacetime. So in the near horizon region $r \to 0$, the metric is that of $\mathrm{AdS}_5 \times \mathbb{S}^5$ where both spaces have curvature radius L_3.

The two kinds of closed string excitations, propagating in the asymptotic region and the near horizon region, decouple from each other such that they can be treated independently. Even if closed string excitations in the near horizon region may have high energies E_r with $l_\mathrm{S}E_r > 1$, due to the non-trivial factor $H_3(r)$ in the metric there is a redshift factor $\sqrt{-g_{00}}$ that renders this energy small for an observe in the asymptotic region,

$$l_\mathrm{S}E_{r\to\infty} = \sqrt[4]{H_3(r)}^{-1} l_\mathrm{S}E_r\,. \tag{3.30}$$

Since in the near horizon region $H_3(r) \approx \frac{L_3^4}{r^4}$, this simplifies to

$$l_\mathrm{S}E_{r\to\infty} \approx \frac{r}{L_3} l_\mathrm{S}E_r\,. \tag{3.31}$$

For $l_\mathrm{S}E_r$ large but fixed, since $L_3 \gg r$ in the near horizon region the energy $l_\mathrm{S}E_{r\to\infty}$ measured in the asymptotic region is small. That is, an observer in the asymptotic region

observes the full spectrum of type IIB superstring theory on $AdS_5 \times \mathbb{S}^5$ in the near horizon region. These modes are separated by a potential barrier from the modes in the asymptotic region. Since both types of modes are considered as low-energy modes, they cannot pass the escape the potential well and therefore decouple. To summarise, the low-energy limit $l_S \to 0$ of a stack of N D3-branes in the closed string perspective yields supergravity on $\mathbb{R}^{1,9}$ and supergravity on $AdS_5 \times \mathbb{S}^5$.

We have discussed the physics of a stack of N D3-branes in Minkowski spacetime in the open and closed string picture. Since these are equivalent descriptions, the physics we have found on both sides also have to be equivalent. In both cases, there is supergravity on $\mathbb{R}^{1,9}$. However, in the open string picture, we found four-dimensional $\mathcal{N} = 4$ supersymmetric Yang–Mills theory with gauge group $SU(N)$, while the open string picture led to (in particular, type IIB) supergravity on $AdS_5 \times \mathbb{S}^5$. Therefore, these two theories have to be dynamically equivalent, which is precisely the statement of the weak form of the AdS/CFT correspondence. Another motivation for the duality is given by the large amount of matching symmetries on both sides of the duality. On the gravity side, these symmetries are the isometries of the spacetime. These are found by defining both AdS_5 as well as $\mathbb{S}^5$ as hypersurfaces in flat six-dimensional spacetimes with coordinates $\mathscr{X}^\mu$ and appropriate signature,

$$AdS_5 : \quad -L_3^2 = -(\mathscr{X}^0)^2 + \sum_{i=1}^{4} (\mathscr{X}^i)^2 - (\mathscr{X}^5)^2 , \tag{3.32}$$

$$\mathbb{S}^5 : \quad L_3^2 = \sum_{i=1}^{6} (\mathscr{X}^i)^2 . \tag{3.33}$$

The isometries are given by $SO(2,4)$ and $SO(6)$ respectively. On the field theory side, there is conformal symmetry and supersymmetry. The conformal symmetry in four dimensions is described by $SO(2,4)$, matching the isometry of AdS_5. The supersymmetry $\mathcal{N} = 4$ gives to the the R-symmetry $SU(4)_R$. Since locally $SU(4) \simeq SO(6)$, the supersymmetry matches the isometry of $\mathbb{S}^5$. Analogous statements can be made for the fermionic pieces on both sides. This results in the statement that both theories are invariant under the superconformal group $PSU(2,2|4)$ [409, 410]. Further developments and details on this topic can be found in [369, 411–414] and references therein.

Finally, we point out that AdS_5/CFT_4 is not the only version of the AdS/CFT correspondence obtained from string theory. Already in [74] it was pointed out that other brane configurations in superstring theory allow for different background spacetimes involving Anti-de Sitter spacetime. Within type IIB superstring theory a setup of D1 and D5-branes leads to the AdS_3/CFT_2 correspondence. This particular version of the du-

ality will become important in sec. 5. In this case, both sides of the theory are quite well understood. This is because, on the one hand, gravity in three dimensions has no propagating degrees of freedom and is exactly solvable [415]. On the other hand, CFT in two dimensions has infinitely many conserved charges, i.e. it is integrable, since the conformal Killing equations in two dimensions reduce to the Cauchy–Riemann differential equations and every (anti)-holomorphic function is a valid conformal transformation. This led to remarkable developments and tests of the duality, see e.g. [416–420]. A review of AdS_3/CFT_2 can be found e.g. in [421]. A more general platform towards proofing AdS/CFT known as Gopakumar–Vafa duality has been discussed in [422, 423]. Furthermore, in eleven-dimensional M-theory similar configurations to the brane constructions above can be made using either M2 or M5-branes. These led to realisations of AdS_4/CFT_3 [74, 424] and AdS_7/CFT_6 [74, 75, 425], respectively. For details on these constructions see [366]. Last but not least, there is also AdS_2/CFT_1. On the gravity side, the theory is Jackiw–Teitelboim (JT) gravity [426, 427] which is a theory of gravity in two dimensions supplemented by a dilaton field. The dual theory is related to the Sachdev–Ye–Kitaev (SYK) model [428, 429]. For a review of this model itself see e.g. [430]. It has also been proposed that the dual theory is given by a version of conformal quantum mechanics [431].

This concludes our review of the AdS/CFT correspondence. In the next section, we discuss how the correspondence can be used to calculate correlation functions and how entanglement is geometrically realised in AdS/CFT.

3.1.3. An Entry in the Dictionary: Entanglement in AdS/CFT

As mentioned before, the AdS/CFT correspondence allows to compute expectation values of observables in one theory and map the result to the other theory. This is particularly useful if one of the theories is hard to analyse, such as the strongly coupled field theories appearing in the weak form of the duality. To translate the results to the other theory, the so-called *holographic dictionary* for the duality has to be established. This corresponds to a one-to-one map between fields of the gravity theory and operators of the gauge theory. In particular, scalar operators $\mathcal{O}$ of the gauge theory are mapped to scalar fields ϕ_0 of type IIB supergravity. Moreover, currents J of the field theory correspond to gauge field fluctuations A in gravity and the energy-momentum tensor $\hat{T}$ of the field theory is connected to the fluctuations h of the bulk metric. As examples for the weak form of AdS_5/CFT_4 as discussed above, the dilaton of type IIB supergravity is related to the Lagrangian of $\mathcal{N} = 4$ supersymmetric Yang–Mills theory. These mappings are supplemented by relations between the conformal dimension Δ of the operators of the field theory and the mass m of the corresponding supergravity field. E.g., for a scalar operator $\mathcal{O}_\Delta$, the mass of the

corresponding scalar field in gravity is determined by $m^2 L^2_{\text{AdS}} = \Delta(\Delta - d)$, where d is the dimension of the field theory. A detailed discussion of these relations can be found in [369].

Brushing through the Dictionary

In practice, these mappings mean that terms as $S_{\text{source}} = \int \mathrm{d}^d x\, \mathcal{O}(x)\phi_0(x)$ and the appropriate generalisations for fields with higher spin can be added to the action to act as source terms. The usual perturbative approach of QFT then allows to compute correlation functions of $\mathcal{O}$ by taking functional derivatives of the generating functional $W = -\mathrm{i} \ln Z$ defined by the partition function Z,[12]

$$\langle \mathcal{O}_1(x_1) \ldots \mathcal{O}_n(x_n) \rangle = (-\mathrm{i})^{n-1} \frac{\delta^n W}{\delta\phi_0^{(1)}(x_1) \ldots \delta\phi_0^{(n)}(x_n)}\bigg|_{\phi_i=0} . \tag{3.34}$$

As pointed out before, this is a perturbative approach, i.e. it fails if the theory is strongly coupled. At this point, the AdS/CFT correspondence shows its power. Since the strongly coupled field theory is dynamically equivalent to a weakly coupled theory of gravity, we may equivalently use the generating functional W of the gravity theory in the computation. In its strongest form, the AdS/CFT correspondence states that the partition function of the conformal field theory is equal to the partition function of the dual string theory [75],

$$Z_{\text{CFT}} = Z_{\text{String}} . \tag{3.35}$$

To make this equality precise boundary conditions on the fields are required, which we will discuss shortly. In principle, when calculating correlation functions either of these partition functions may be used. However, since the partition function Z_{String} is not known explicitly, in practice this relation does not directly help in computations. In the weak form however, when the field theory becomes strongly coupled, the partition function of string theory can be approximated by its saddle point, given by the on-shell action of supergravity. In equations [75, 76],

$$W_{\text{CFT}}[\phi_0(x)] = S_{\text{Sugra}}[\bar{\phi}(r,x)]\Big|_{\lim_{r\to\infty} \bar{\phi}(r,x)=\phi_0(x)} , \tag{3.36}$$

where $\bar{\phi}(r,x)$ is a solution to the equations of motion of supergravity and x is shorthand for the time coordinate as well as all spatial coordinates other than r, i.e. the coordinates of the boundary. As indicated, the boundary condition on this field is that the asymptotic value of the bulk field $\lim_{r\to\infty} \bar{\phi}(r,x)$ is identified with the source $\phi_0(x)$ for the operator $\mathcal{O}(x)$. Using

[12] Using W only yields correlation functions associated to connected Feynman diagrams. If one is interested in the disconnected diagrams, one has to compute functional derivatives of Z.

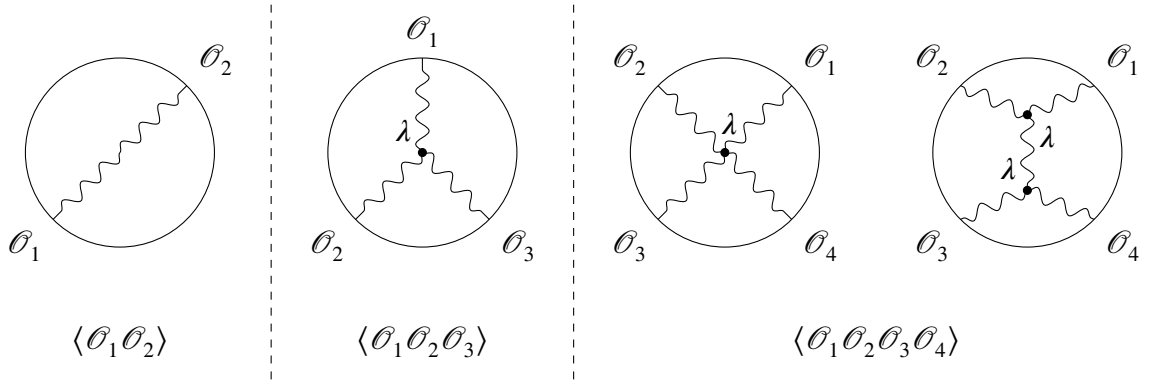

Figure 3.3: tree-level diagrams known as Witten diagrams used to represent the calculation of correlation functions of boundary operators $\mathcal{O}_i$ using the AdS/CFT correspondence. The circle represents the boundary where field theory is defined. The interior of the circle corresponds to the bulk where the gravity theory is defined. Each dot is an interaction vertex with associated vertex factor λ. The wavy lines represent bulk-to-boundary propagators and, in the fourth diagram, bulk-to-bulk propagators. In these simple examples, all vertices have the same factor, but these can be different in general.

(3.36) and this identification, the generating functional of the strongly coupled field theory in (3.34) may be replaced by the on-shell action of weakly coupled supergravity. Since the gravity theory is classical, the boundary correlation functions are computed by tree-level diagrams in the bulk. Remarkably, these so-called *Witten diagrams* can be treated in close analogy to Feynman diagrams in that there exists a simple set of rules to obtain expressions for computing the diagrams. The field theory lives on the boundary of the spacetime that the gravity theory is defined on. The gravity theory is therefore commonly referred to as the theory in the bulk. Correspondingly, there is a bulk-to-boundary propagator which relates operator insertions in the field theory to interaction vertices in the bulk. Moreover, there is a bulk-to-bulk propagator that connects different interaction vertices in the bulk. To each bulk interaction vertex, a vertex factor λ determined by the interaction terms in the supergravity action is associated. This is visualised in fig. 3.3 in a few examples. A detailed discussion of this technique as well as explicit examples can be found in [369].

Making use of (3.36) allows to compute observables in strongly coupled field theory. However, in field theory the naive computation usually leads to divergent quantities and the present case is no exception [402]. In AdS/CFT, many of the divergences can be traced back to the infinite spacetime volume. To remedy these issues, the procedure dubbed *holographic renormalisation* was developed [404, 432–435]. Schematically, this procedure works as follows. First, a cutoff ϵ on the radial coordinate is introduced. The cutoff may be understood as a small but finite distance between the asymptotic boundary and a shell at a large but finite radial coordinate. With this regulator present, the computations yield finite results as the spacetime volume is now finite. By expanding the result as a

power series in the cutoff, the divergent pieces are extracted. For each of the divergent terms, a counterterm S_{ct} is added to the action removing the corresponding divergence. The full action $S_{\text{sugra}} + S_{\text{ct}}$ then yields finite results for correlation functions of boundary operators. For a detailed discussion of this procedure for scalar operators $\mathcal{O}(x)$ and the boundary energy-momentum tensor $\hat{T}$ see [369]. General reviews on this topic are provided in [436, 437].

Entanglement in AdS/CFT

In sec. 2.1.2, we have discussed a few important properties of entanglement entropy in QFT. In particular, it satisfies an area law and has a precise structure if conformal symmetry is assumed as well, cf. (2.38) and (2.39). The AdS/CFT correspondence states that every quantity of the field theory has a dual description in the gravity theory. Therefore there must exist a way to derive the field theory entanglement entropy by a calculation on the gravity side. To motivate the dual description, suppose that the goal is to calculate the entanglement entropy between a subregion A of a CFT_{D-1} and its complement $\bar{A}$. These two regions are then separated by the bipartition surface ∂A. As the CFT_{D-1} is defined on the boundary of the AdS_D spacetime, it is natural to extend the bipartition surface into the bulk spacetime such that it encloses a region $\hat{A}$ in the bulk. This extension should happen in a smooth way, i.e. the bulk bipartition surface $\partial\hat{A}$ should not have any holes if the subregion has none. To make the extension of the bipartition surface into the bulk unique, we might demand that this surface be extremal. A visualisation is provided in fig. 3.4 for $D = 3$. Indeed, it was found that the entanglement entropy in CFT can be calculated using the above prescription, resulting in the *Ryu–Takayanagi formula* (RT formula) [113, 114],

$$S(\rho_{(A)}) = \frac{\text{Area}(\partial\hat{A})}{4G_{\text{N}}^{(D)}}\,. \tag{3.37}$$

This formula manifests that entanglement entropy has a geometric explanation within the AdS/CFT correspondence. The above requirements on the surface in the bulk are formalised as A and $\hat{A}$ sharing the same boundary and being homologous to each other. Moreover, $\hat{A}$ has to be an extremum of the area functional and, if there is more than one extremal surface, the proper choice is the $\hat{A}$ with the smallest area, see e.g. [236] for further discussion. Evaluating (3.37) e.g. for an empty three-dimensional Anti-de Sitter spacetime in Poincaré patch coordinates yields [113]

$$S(\rho_{(A)}) = \frac{c}{3}\ln\frac{L}{\epsilon}\,, \tag{3.38}$$

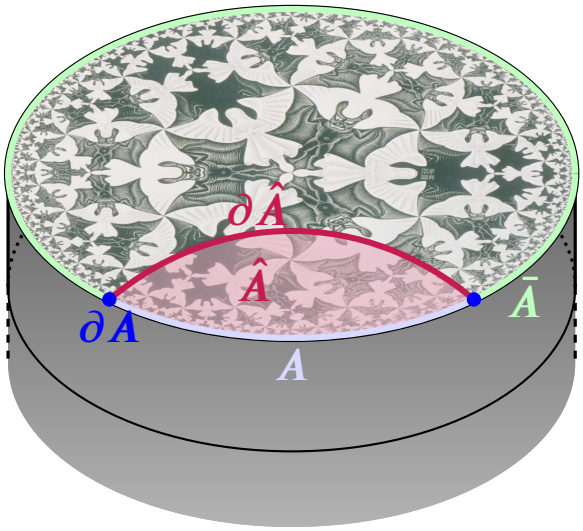

Figure 3.4: Visualisation of the RT construction for $D = 3$. Three-dimensional Anti-de Sitter is represented by the cylinder segment. Eschers Circle Limit IV, adapted from [438], represents a constant time slice of AdS_3. The CFT defined on the boundary circle is separated by the bipartition surface ∂A into two subregions A and $\bar{A}$. On the gravity side, the bulk bipartition surface is obtained by extending the boundary bipartition surface into the bulk. The subregion $\hat{A}$ attached to A is defined by the area bounded by the bulk bipartition surface $\partial\hat{A}$. The minimal area of $\partial\hat{A}$, in this case simply the length of the corresponding geodesic, determines the entanglement entropy $S(\rho_{(A)})$.

which agrees with the well known result given in (2.39) with $c_1 = \frac{c}{3}$ obtained in standard CFT_2 [221]. Here, L is the length of the subregion in the CFT and ϵ is the UV cutoff. In this calculation, the relation (3.1) between the central charge c and the Newton constant $G_N^{(3)}$ as well as the Anti-de Sitter radius L_{AdS} was used. For details on calculating the RT formula in more complicated settings, i.e. black holes in Anti-de Sitter spacetime or generalisations to higher dimensions, see e.g. the reviews [114, 191, 236, 238, 439].

In the original papers [113, 114], the RT formula (3.37) was tested mostly for $D = 3$, where the minimal surface is simply a geodesic between two points in the boundary. Moreover, only static geometries were considered. A covariant version of (3.37) applicable for arbitrary geometries was derived in [440]. Moreover, the RT formula was shown to be true in arbitrary dimension D for static geometries in [441] (see also [229]). The extension of this to include time dependence was discussed in [442]. A semiclassical version of (3.37) including $\frac{1}{N}$ corrections, i.e. quantum corrections, was derived in [443]. Due to the similarity of the Bekenstein bound (3.4) and the RT formula (3.37), it became an interesting question whether the thermal entropy of black holes might actually be interpreted as an entanglement entropy. For discussions in this direction see e.g. [444–446]. Finally, the RT formula can be regarded as an explicit realisation of 'entanglement creating spacetime' as

envisioned in [115–117]. We will provide more details on the last point in sec. 3.2.2.

This concludes our discussion of the general properties of the AdS/CFT correspondence as well as holographic entanglement entropy. In the next section, we will focus on the properties of black holes in AdS/CFT.

3.2. The Factorisation Puzzle

As discussed in the previous sections, the AdS/CFT correspondence establishes a duality between a theory of (quantum) gravity and a QFT without gravity in one spatial dimension less. The holographic dictionary associates objects in the theory of gravity with objects in the field theory. A particular interesting instance, which will be the core theme for most of the remaining sections, is the duality between the eternal black hole in Anti-de Sitter spacetime and the thermofield double (TFD) state [112]. More precisely, the eternal black hole has two asymptotic regions, i.e. two asymptotic boundaries with CFTs defined on each of them. Each of the CFTs is thermal at a temperature equal to the Hawking temperature of the black hole, i.e. each of the CFTs are dual to a one-sided black hole. The TFD state is an entangled state comprised of energy eigenstates of both these CFTs and is dual to the two-sided black hole. This associates a wormhole interpretation to the eternal black hole, where the two CFTs are connected by a wormhole across the black hole interior. This idea was first put forward in [115, 116] and provided the basis for the ER=EPR proposal [118]. However, this duality also gives rise to a puzzle, which can be understood as follows. On the one hand, the two CFTs are spacelike separated and in particular do not share any classical interaction. Therefore, from the boundary perspective, the full Hilbert space is expected to factorise, $\mathscr{H} = \mathscr{H}^{(L)} \otimes \mathscr{H}^{(R)}$. On the other hand, however, the dual picture is a smooth classical geometry. From the dual bulk perspective, there is no reason to expect a factorised Hilbert space. This difference in the Hilbert space structure is an apparent conflict within the AdS/CFT correspondence that has been coined the *factorisation puzzle* [120]. Assuming that the AdS/CFT correspondence is true, either in the gravity or the field theory description (or maybe even in both) something has been overseen, which by incorporating resolves these seemingly conflicting statements. In the following sections, we elaborate on this, starting with a discussion in sec. 3.2.1 how the TFD state arises as the state dual to the eternal black hole using the Hartle–Hawking wave functional [447]. Subsequently, we give an account of the ER=EPR proposal and the factorisation puzzle in sec. 3.2.2.

3.2.1. The Eternal Black Hole and the Thermofield Double State

The TFD state has been used to describe quantum systems at finite temperature using state vectors instead of density operators. Correspondingly, the TFD state is understood as a purification of the thermal density operator. As alluded to in sec. 2.3.1, this state provides a cyclic and separating vector when discussing operator algebras of type II and type III [324]. Moreover, it is an essential part of developing thermofield dynamics, which is a field theory version of quantum statistics [448]. Based on this latter role of the TFD state, it was discussed in [449] how the TFD state arises for generic static spacetimes with a Killing horizon, including in particular black hole spacetimes. This shows the close relation between the temperature experienced by the Rindler observer discussed in sec. 2.1.2 and the temperature of black holes [110, 223]. Due to this close similarity, it should not come as a surprise that the TFD state dual to the eternal black hole can be derived using analogous methods as in sec. 2.1.2 upon replacing the empty Minkowski spacetime with the black hole spacetime. In fact, the thermal density operator associated to the Rindler observer (2.32) can be purified into a state vector schematically given by

$$|\mathrm{TFD}\rangle_{\mathrm{Rin}} \propto \sum_n e^{-\pi E_n} |n_<, n_>^*\rangle \,, \tag{3.39}$$

where E_n and $|n_{</>}\rangle$ are the eigenvalues and eigenstates of $\tilde{K}_{</>}$. The meaning of the asterisk will be explained shortly. The expression in (3.39) resembles the TFD state (2.107) for $\beta = 2\pi$. This can be understood as follows. In sec. 2.1.2 we have discussed how the reduced density operator can be computed using the path integral. By the analogous methods, we may also obtain the above state by changing the integration discussed in and before (2.32). In particular, while for the reduced density operator $\rho_>$ all degrees of freedom $\phi_<$ have to be integrated over, to obtain a state vector we have to keep those. Pictorially speaking, the evolution by $\tilde{K}_>$ depicted in fig. 2.4 has to be halved, i.e. the range of integration corresponds to a rotation by π instead of 2π, which is the factor in the exponential in (3.39). Moreover, this integration requires more care about the relation between the eigenstates in $\mathrm{Rin}_>$ and $\mathrm{Rin}_<$, explaining the asterisk in $|n_>^*\rangle$. This comes about as follows. In the original preparation of the state on the time slice $t_\mathrm{E} = 0$ discussed in sec. 2.1.2, both $\phi_>$ and $\phi_<$ are interpreted as final states, i.e. boundary conditions on the path integral at the end of any path. This makes intuitive sense in the Hamiltonian time evolution depicted in fig. 2.3. However, using the angular evolution defined by $\tilde{K}_>$ this interpretation changes. For a clockwise integration path starting at the time slice $t_\mathrm{E} = 0$ in $\mathrm{Rin}_>$, while $\phi_<$ is still a final state, $\phi_>$ is the boundary condition at the beginning of any path, so it is an initial state. To properly incorporate this, we use an anti-unitary

operator Θ and define the time-reversed state $|\phi_>^*\rangle = \Theta|\phi_>\rangle$.[13] As we briefly review in the following, an analogous computation yields the TFD state as the state vector dual to the eternal black hole in Anti-de Sitter spacetime. For details, see e.g. [450] and the excellent review [225]. Our treatment will follow the latter reference.

The above discussion shows how to obtain the TFD state for the flat Rindler spacetime, while we are actually interested in obtaining this state for the eternal black hole in Anti-de Sitter spacetime. The method to obtain this state relied on the Rindler decomposition of Minkowski spacetime, where in particular the (inverse) temperature $\beta = 2\pi$ can be understood as the periodicity of the 'time' coordinate θ in

$$\mathrm{d}s^2_{\text{Rindler}} = R^2\mathrm{d}\theta^2 + \mathrm{d}R^2\,. \tag{3.40}$$

The temperature therefore arises by demanding that there is no conical singularity and that R and θ are simply polar coordinates. For a Rindler observer with acceleration $a \neq 1$, the prefactor of $\mathrm{d}\theta^2$ in the metric changes to $(aR)^2$, such that the periodicity has to be adjusted to $\frac{2\pi}{a}$ in order to avoid a conical singularity. Accordingly, the inverse temperature is given by $T = \frac{a}{2\pi}$, as stated in sec. 2.1.2. Fortunately, we may obtain the TFD state for the eternal black hole in an analogous way by noting that also this spacetime admits a Rindler decomposition close to the horizon. As an explicit example, for a black hole in four-dimensional Minkowski spacetime, the Euclidean metric is given by

$$\mathrm{d}s^2 = f(r)\mathrm{d}t_\mathrm{E}^2 + \frac{\mathrm{d}r^2}{f(r)} + r^2\mathrm{d}\Omega_2^2 \quad \text{with} \quad f(r) = 1 - \frac{r_\mathrm{S}}{r}\,, \tag{3.41}$$

where $r_\mathrm{S} = 2G_\mathrm{N}M$ is the Schwarzschild radius. This metric has the well-known coordinate and physical singularities at $r = r_\mathrm{S}$ and $r = 0$, respectively. To obtain the Rindler version of this metric, we introduce a new coordinate R that absorbs the non-trivial prefactor of $\mathrm{d}r^2$,

$$\mathrm{d}R = \sqrt{\frac{r}{r - r_\mathrm{S}}}\,\mathrm{d}r\,. \tag{3.42}$$

This new coordinate starts at the horizon and points outward. Close to the horizon, to lowest order in $r - r_\mathrm{S}$ we may approximate

$$\sqrt{\frac{r}{r - r_\mathrm{S}}} = \sqrt{\frac{r_\mathrm{S}}{r - r_\mathrm{S}}} + \mathcal{O}\left(\sqrt{r - r_\mathrm{S}}\right), \tag{3.43}$$

[13] Any anti-unitary operator can be written as a unitary operator V times complex conjugation $\mathscr{K}$. The complex conjugation operator in turn is related to the time-reversal operator $\mathscr{T}$. Therefore, Θ always includes time reversal, converting initial and final states into each other.

such that integrating both sides of (3.42) results in

$$R \approx 2\sqrt{r_S(r-r_S)} \quad \Leftrightarrow \quad r \approx r_S + \frac{R^2}{4r_S}\,. \tag{3.44}$$

Inserting this into the metric (3.41), close to the horizon we obtain the Rindler metric

$$\mathrm{d}s^2 = \frac{R^2}{4r_S^2}\mathrm{d}t_E^2 + \mathrm{d}R^2 + r_S^2\mathrm{d}\Omega_2^2\,, \tag{3.45}$$

where we approximated $r \approx r_S$ in the angular part in the near horizon limit $R \to 0$. This metric is regular everywhere except at $R = 0$. To avoid the conical singularity at this point we have to demand that t_E has periodicity $4\pi r_S$. Therefore, the corresponding TFD state has the temperature $\beta = 4\pi r_S = 8\pi G_N M$, which is the familiar Hawking temperature of a black hole of mass M in four spacetime dimensions [109, 110]. For spacetimes in different dimensions or with different curvature properties, the same calculations can be performed, starting with a metric different from (3.41). For example, the eternal black hole in D-dimensional Anti-de Sitter spacetime is described by replacing $f(r)$ in (3.41) with

$$f(r) = 1 - \frac{16\pi G_N M}{(D-2)\mathrm{Vol}(\mathbb{S}^{D-2})r^{D-3}} + \frac{r^2}{L_{AdS}^2}\,, \tag{3.46}$$

resulting in the temperature

$$\beta = \frac{4\pi L_{AdS}^2 r_h}{(D-1)r_h^2 + (D-3)L_{AdS}^2}\,, \tag{3.47}$$

where r_h is the event horizon defined as the larger solution to $f(r_h) = 0$. For details on deriving these quantities see e.g. [369, 451].

Deriving the TFD state as the dual description of the eternal black hole is then straightforward. We start analogously as in sec. 2.1.2 by defining the Hartle–Hawking wave functional $\Psi_{HH}[\phi]$ as [447]

$$\Psi_{HH}[\phi] = \langle\phi(x)|0\rangle = \int_{\phi(t_E=-\infty)=0}^{\phi(t_E=0,x)=\phi(x)} \mathscr{D}\phi'(t_E,x)\,\exp\left(-S_{E,g}[\phi']\right), \tag{3.48}$$

where $S_{E,g}$ is the Euclidean action of a real scalar field propagating on the Euclidean eternal black hole spacetime g given by (3.41) with $f(r)$ given by (3.46). In the near horizon region, we approximate this metric by the corresponding Rindler metric as in (3.45). To evaluate the path integral, we switch to evolution by an operator analogous to

$\tilde{K}_<$ performing a rotation. The duration of this evolution covers, as discussed before for Minkowski spacetime, a half circle. This half circle has length $\frac{\beta}{2}$ with β given by (3.47), so between $|\phi_>\rangle$ and $|\phi_<\rangle$ we evolve by $e^{-\frac{\beta}{2}\tilde{K}_<}$. To account for the aforementioned subtlety of initial and final states, we define the time-reversed state $\langle\phi_>| = \Theta^\dagger|\phi_>\rangle$ and write

$$\Psi_{\text{HH}}[\phi] = \langle\phi_<, \phi_>|0\rangle = \langle\phi_<|e^{-\frac{\beta}{2}\tilde{K}_<}\Theta^\dagger|\phi_>\rangle\,. \tag{3.49}$$

Note that compared to sec. 2.1.2 we have suppressed the explicit path integral to reduce clutter in the expression. Next, we insert the identity operator in terms of a complete set of eigenstates $|n_<\rangle$ to $\tilde{K}_<$,

$$\begin{aligned}\Psi_{\text{HH}}[\phi] &= \sum_n \langle\phi_<|n_<\rangle\langle n_<|e^{-\frac{\beta}{2}\tilde{K}_>}\Theta^\dagger|\phi_>\rangle = \sum_n e^{-\beta\frac{E_n}{2}}\langle\phi_<|n_<\rangle\langle n_<|\Theta^\dagger|\phi_>\rangle \\ &= \sum_n e^{-\beta\frac{E_n}{2}}\langle\phi_<|n_<\rangle\langle\phi_>|n_>^*\rangle\,,\end{aligned} \tag{3.50}$$

where in going to the second line we used the anti-linearity of Θ and defined $|n_>^*\rangle = \Theta|n_<\rangle$.[14] Comparing this expression with (3.49) allows to identify the (unnormalised) TFD state as the vacuum state $|0\rangle$,

$$|\text{TFD}\rangle \propto |0\rangle = \sum_n e^{-\beta\frac{E_n}{2}}|n_<, n_>^*\rangle\,. \tag{3.51}$$

Including the normalisation $\langle 0|0\rangle = Z(\beta)$ and switching to a notation more common in holography, we arrive at the TFD state dual to the eternal black hole [112],

$$|\text{TFD}\rangle = \frac{1}{\sqrt{Z(\beta)}}\sum_n e^{-\beta\frac{E_n}{2}}|n_L, n_R^*\rangle\,. \tag{3.52}$$

This duality is visualised in fig. 3.5. As pointed out earlier, the TFD state (3.52) is an entangled state. The reduced density operators describing the CFTs on the left and right boundaries, $\rho^{(L)}$ and $\rho^{(R)}$, are mixed states with a thermal spectrum. Therefore, to describe thermal physics in the CFT, by the AdS/CFT correspondence this amounts to considering a black hole in the bulk spacetime, with the mass of the black hole determining the temperature. To conclude this section, we point out that the eternal black hole in Anti-de Sitter spacetime has the interpretation of a wormhole in spacetime. However, this wormhole is not traversable as there is no time- or light-like geodesic that connects the left and right asymptotic boundaries. Traversable wormholes, which can be constructed at least theoretically, require shocks of negative energy that push back the horizon. This can

[14] For an anti-linear operator Υ, $\langle\psi_1|\Upsilon^\dagger|\psi_2\rangle = \langle\psi_2|\Upsilon|\psi_1\rangle$.

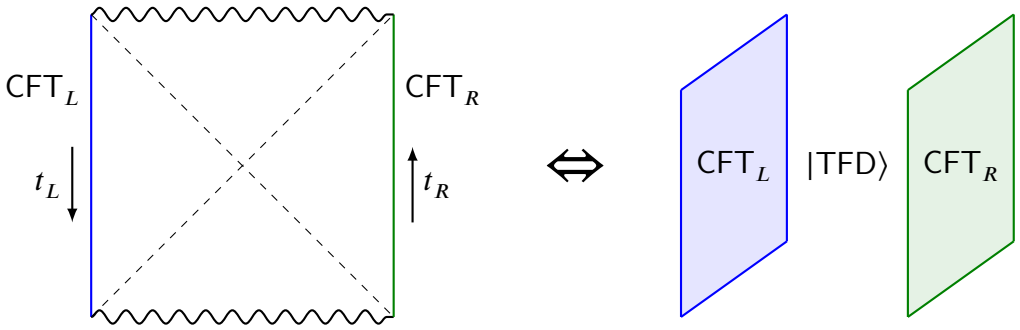

Figure 3.5: Visualisation of the duality between the eternal black hole in Anti-de Sitter spacetime and the two boundary CFTs entangled in the TFD state [112]. On the left-hand side, the eternal black hole in an Anti-de Sitter spacetime is shown in global coordinates. The dashed lines represent the black hole horizon. At the left and right boundaries of the AdS spacetime, marked in blue and green respectively, the left and right boundary CFTs are defined, with time running in opposite directions. The dual description of the eternal black hole is depicted on the right-hand side. The two CFTs, defined on the blue and green planes that represent the left and right asymptotic boundaries, are entangled in the TFD state.

be achieved by including a non-trivial interaction between the fields of left and right CFTs [452, 453]. In the remaining thesis, we will however not go into detail about this and focus on non-traversable wormholes.

The TFD state (3.52) is a single state vector providing a dual description of the eternal black hole. However, the black hole entropy (3.3) counts the number of microstates of the black hole. Therefore, the TFD state must not be the unique state dual to the black hole. Rather, since the black hole entropy is a large number determined by the mass of the black hole, there should be a correspondingly large number of microstates. An approach towards addressing this problem was discussed in [454, 455]. These works utilised the absence of a natural origin of time in gravity to argue for a larger class of states analogous to (3.52) as holographic dual to the eternal black hole. The states constructed in this way are understood as time-shifted TFD states, where the time-shift variable specifies how the boundary is glued to the bulk geometry. This variable arises as follows. Due to the horizon, the time-like Killing vector defined for the static black hole metric is not defined globally (see e.g. [182] for a detailed discussion). In particular, this vector switches sign at the horizon. Therefore, when identifying the Schwarzschild time t with the time on the right boundary, i.e. $t_R = t$, the time on the left boundary t_L has to have a relative sign compared to the Schwarzschild time, i.e. $t_L = -t$. The opposite directions of time on each boundary are visualised in fig. 3.5. Since there is no preferred origin of time, we are free to include a shift in the identifications, say $t_R \to t_R + \delta$ and $t_L \to t_L - \delta$. This corresponds to shifting the Schwarzschild time as $t \to t + \delta$, which is an isometry of the black hole spacetime. In

the boundary, this isometry is represented by the fact that the difference of the boundary Hamiltonians $H_- = H_L - H_R$ annihilates the TFD state (3.52), or equivalently [454]

$$e^{\mathrm{i}H_-\delta}|\mathrm{TFD}\rangle = |\mathrm{TFD}\rangle\,. \tag{3.53}$$

Following [182], this shift variable δ also appears when relating the left and right boundary times. We can naturally identify them at the boundary as $t_L = t_R$, however at the black hole horizon, we may allow again for a shift, $t_L = 2\delta - t_R$. Inserting these relations into each other implies that $t_L = \delta = t_R$, so δ can be used as a time variable on both boundaries. This shift however is locally invisible, as we also have identified $t_L = 2\delta - t_R$ at the boundary and $t_L = t_R$ at the horizon, utilising the isometry to redefine $t_L \to 2\delta - t_L$ in the previous identifications. The new relations as well imply that $t_L = \delta = t_R$. To a local low-energy observer, this shift variable δ is invisible, as no correlation function is sensitive to it [455]. A non-local observer however would be able to measure δ, e.g. by considering two local observers that, after synchronising their clocks in the boundary, jump into the wormhole from different sides and compare the clocks again [182].

As stated in (3.53), evolution with H_- is a symmetry of the TFD state, describing the isometry of the bulk spacetime. However, evolution by the sum of the Hamiltonians $H_+ = H_L + H_R$ acts non-trivially on $|\mathrm{TFD}\rangle$. As discussed above, we may parametrise this evolution by δ. The class of states dual to the eternal black hole is defined by such an evolution, resulting in the time-shifted TFD states [454, 455]

$$|\mathrm{TFD}\rangle_\alpha = e^{\mathrm{i}H_+\delta}|\mathrm{TFD}\rangle = \frac{1}{\sqrt{Z(\beta)}}\sum_n e^{\mathrm{i}\alpha_n} e^{-\beta\frac{E_n}{2}}|n_L, n_R^*\rangle\,, \tag{3.54}$$

where $\alpha_n = 2E_n\delta$. Clearly, the special choice $\delta = 0$ reduces the time-shifted TFD state (3.54) back to the TFD state (3.52) originally considered in [112]. As pointed out in [182, 454, 455], note that since the spectrum E_n for CFTs is chaotic [456], by adjusting δ any value for α_n can be approximated. These arbitrary phase factors however do not influence the entanglement entropy, since the reduced density operators both of (3.52) and (3.54) are simply the thermal density operators. Moreover, above we stated that correlation functions are not sensitive to the particular gluing of the bulk to the boundary specified by δ. The more precise version of this statement is that correlation functions of operators $\mathcal{O}_i(t=0)$ in the time-shifted TFD state (3.54) are equal to correlation functions of operators $\mathcal{O}_i(t=\delta)$ in the original TFD state (3.52). A local low-energy observer cannot distinguish whether the δ-dependence of a correlation function stems from the time evolution of the inserted operators or a non-trivial gluing between the bulk and the boundary.

3.2.2. Einstein–Rosen vs. Einstein–Podolski–Rosen

As discussed in the previous section, the eternal black hole in Anti-de Sitter spacetime has a wormhole interpretation. Wormholes, as solutions to the Einstein equations, have been discussed for the first time in [119]. Due to the authors of this paper, wormholes are also referred to as *Einstein–Rosen bridges* (ER bridges). The same authors in collaboration with Podolski developed the notion of entanglement in [15]. Bipartite entangled states in general settings contain what has been dubbed *Einstein–Podolski–Rosen pairs* (EPR pairs) as a source of the entanglement, inspired by the original discussion of two-particle entanglement in [15]. The TFD state (3.52) and its generalisation (3.54) can be interpreted as containing EPR pairs between the left and right CFTs. As pointed out in [115, 116], the holographic duality between the eternal black hole and the TFD state can be regarded as a hint that in fact, gravitational wormholes arise due to entanglement, which is a quantum mechanical feature. In the opposite direction, one can also say that entanglement is responsible for 'creating' a wormhole. To develop an intuition behind this proposal it is worthwhile to consider the entanglement properties of the TFD state in more detail. Since (3.52) is a state vector, its density operator $\rho_{\text{TFD}} = |\text{TFD}\rangle\langle\text{TFD}|$ has vanishing entanglement entropy $S(\rho_{\text{TFD}}) = 0$. The reduced density operators for the left and right CFTs, $\rho^{(L)}$ and $\rho^{(R)}$, are given by thermal and thereby mixed states. Correspondingly, the entanglement entropy (2.10) for both systems is non-vanishing, $S(\rho^{(L/R)}) \neq 0$. In particular, the mutual information (2.46) is given by $I(L:R) = 2S(\rho^{(L/R)})$. Let us compare this with the setting of thermal Anti-de Sitter spacetime. Here as well, each CFT is described by a thermal density operator, however the state describing the two thermal CFTs is given simply by $\rho_{\text{th}} = \rho^{(L)} \otimes \rho^{(R)}$. Clearly, the reduced density operators are the same as for the TFD state, and correspondingly we again have $S(\rho^{(L/R)}) \neq 0$. However, ρ_{th} is a mixed state, so we also have $S(\rho_{\text{th}}) \neq 0$. In particular, since ρ_{th} is a tensor product, according to (2.12) we have $S(\rho_{\text{th}}) = 2S(\rho^{(L/R)})$, so the mutual information between the left and right CFT in the thermal state vanishes. This shows that in the thermal state ρ_{th}, there are no quantum correlations. To understand how this observation alludes to creating a wormhole, it is useful to consider the dual spacetime descriptions of both the TFD state and the thermal state. We have already established the Penrose diagram of the eternal black hole in fig. 3.5 as a dual description of the TFD state. The thermal state $\rho^{(L)}$ on the other hand can be understood as a single Rindler wedge of the spacetime, i.e. the left exterior region. Likewise, $\rho^{(R)}$ corresponds to the right exterior region. However, since the overall state ρ_{th} is simply a tensor product, these two wedges do not share any connection. In other words, observers of the left and right CFTs in the state ρ_{th} have no way of meeting since there are no geodesics connecting the left and right CFTs. This is contrary to the spacetime dual

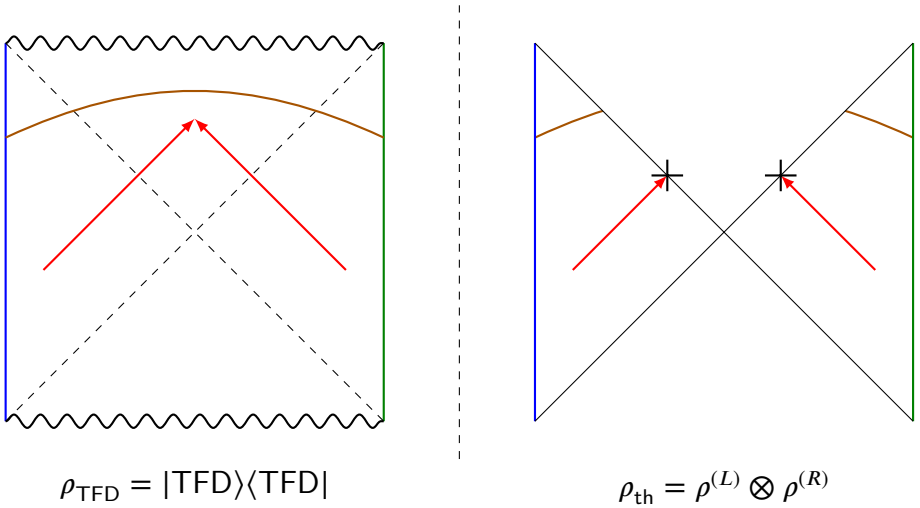

Figure 3.6: On the left, it is visualised how observers, represented by the red arrows, in the eternal black hole geometry can meet behind the horizon. Moreover, spacelike geodesics such as the orange line between the left and right boundaries can be defined. On the right, the geometry corresponding to the thermal state ρ_{th} is shown. Observers cannot meet as there is no region behind the horizon, and correspondingly geodesics between the left and right boundaries cannot be defined.

of the TFD state, where observers can meet behind the horizon, i.e. in the interior region of the black hole. Correspondingly, there exist spacelike geodesics connecting the left and right boundaries. A visualisation of this is provided in fig. 3.6.

This example shows how the entanglement contained in the TFD state is responsible for creating the interior region of the eternal black hole. In terms of the geodesics stretching between the left and right boundaries, we can also phrase this as entanglement being responsible for the connectedness of spacetime. Moreover, the eternal black hole is not the only instance where entanglement creates spacetime. As pointed out in [115, 116] based on the black hole example, an analogous statement is true for more general spacetimes. This comes about by involving the RT formula (3.37), which states that the entanglement between subregions of the CFT is computed holographically by calculating the area of a minimal surface in the bulk spacetime. Given a subregion A of a CFT and its complement $\bar{A}$, the bulk subregion $\hat{A}$ attached to A and its complement $\bar{\hat{A}}$ are separated by the RT surface $\partial\hat{A}$. Reducing the area of this surface reduces the entanglement between the two subregions. In the limit where the entanglement vanishes, the two subregions become disconnected, as the area of the surface separating the subregions vanishes. So also for more general bulk geometries, a non-vanishing entanglement entropy can be interpreted as a geometric connectedness of spacetime between the subregions, as visualised in fig. 3.7. The idea of entanglement creating spacetime was given a solid mathematical analysis in

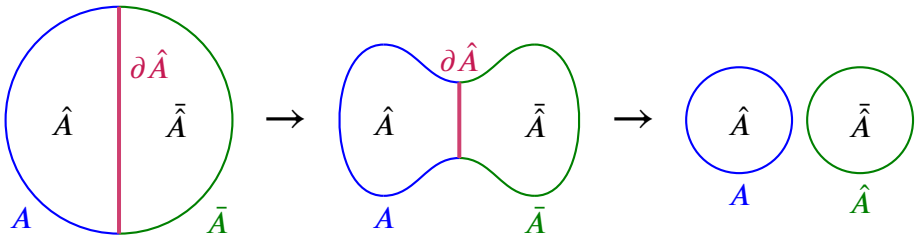

Figure 3.7: Visualisation of the relation between entanglement and the connectedness of spacetime. From left to right, the area of the bipartition surface $\partial\hat{A}$ decreases. On the left and in the middle, two instances of non-vanishing entanglement between A and $\bar{A}$ are shown. In this case, the corresponding bulk subregions $\hat{A}$ and $\bar{\hat{A}}$ are connected. On the right, where the area of $\partial\hat{A}$ and correspondingly the entanglement between A and $\bar{A}$ vanishes, the spacetime is no longer connected.

[118], where it was shown that the creation of a pair of (one-sided[15]) black holes in a constant magnetic field background results in an entangled state describing the two black holes. With this explicit version of the relation between entanglement and spacetime geometry at hand, the same authors proposed that in general, any entanglement leads to some kind of connected geometry and coined this relation *ER=EPR*, stating the equivalence between entanglement described by EPR pairs [15] and wormholes in the sense of ER bridges [119]. This relation has developed into one of the main ingredients of studying aspects of quantum gravity [457], with recent developments on ER=EPR in string theory and dS/CFT in [458] and [86], respectively.

As discussed in the previous paragraphs, ER=EPR provides a relation between entanglement, which is a quantum phenomenon, and spacetime geometry which, as a solution to the Einstein equations, is classical. This is in perfect accordance with the weak form of AdS/CFT, where a classical theory of gravity is dual to a strongly coupled quantum theory. However, the ER=EPR relation was proposed to be more fundamental, in that even the small amount of entanglement between quantum systems as small as two spins amounts to opening a wormhole, i.e. an ER bridge, between the spins [118]. In spirit, this is closer to the strongest form of AdS/CFT and the holographic principle, relating quantum systems with arbitrary coupling to theories of quantum gravity. Correspondingly, the hypothetical ER bridge between two spins is a highly quantum geometry. At the time of writing, such geometries are not generally well understood, yet are considered to be elementary for the ultimate goal of a theory of quantum gravity [459]. A partial aim of this thesis is to provide further insights into this area, as we will discuss in secs. 4 and 6. The ER=EPR proposal also led to the idea that spacetime is an emergent phenomenon. That means, spacetime is not fundamental, but arises only in certain situations as an 'effective' description, e.g. in

[15] Two one-sided black holes can be understood as a single two-sided black hole.

the classical limit where we expect Einstein's theory of general relativity to take over. According to this idea of an emergent spacetime, gravity should be understood as being governed by dynamics of entanglement. In fact, it has been shown in a few ways that the Einstein equations can be derived from properties of entanglement [142–144]. As a final remark, it has been discussed recently that not 'every' entanglement creates the 'same kind' of spacetime. This direction makes use of operator algebraic methods as reviewed in sec. 2.3 to ascertain the properties of wormholes created by entanglement as contained in von Neumann algebras of type I, II and III [460, 461].

Having explained the ER=EPR proposal, we are now in a position to discuss the factorisation puzzle. As alluded to in the introductory paragraph to sec. 3.2, the factorisation puzzle arises due to the absence of classical interactions between the left and right CFTs. This absence suggests that the CFT Hilbert space factorises as $\mathscr{H} = \mathscr{H}^{(L)} \otimes \mathscr{H}^{(R)}$. However, by the ER=EPR proposal [118] and the corresponding theme of entanglement creating spacetime [115–117], the quantum correlations in the form of entanglement between the CFTs on the boundaries lead to the existence of a wormhole connecting the two spacelike separated boundary theories. The wormhole is a solution to the Einstein equations and therefore a classical geometry. Due to the connected smooth bulk geometry, the Hilbert space of the bulk theory does not appear to be factorised. A particularly illuminating example of this apparent contradiction was discussed in [462] by considering a U(1) gauge theory defined on the two-sided black hole background spacetime. To give more details on the factorisation puzzle, we present this example in the following. The U(1)-gauge-invariant operators in the bulk are either local uncharged operators or closed Wilson lines as well as Wilson lines ending on charged operators or the boundary. The reconstruction of such bulk operators in the boundary is, in particular for an empty Anti-de Sitter spacetime, well understood [463–465]. They correspond to gauge-invariant operators in the boundary. Since any boundary operator is invariant under bulk transformations, the gauge-invariant operators are simply all operators of a single CFT. For a black hole background, essentially the same logic applies to bulk operators contained entirely in either the left or the right exterior region of the black hole. However, there also can be Wilson lines that extend all the way from the left to the right boundary, and in that pierce the two-sided black hole. Such Wilson lines are well-defined gauge-invariant operators of the bulk theory. Reconstructing these operators in the boundary however is difficult, since cutting open the Wilson line produces two bulk operators that are not gauge-invariant on their own. On the contrary, due to the factorisation of the boundary Hilbert space, it is expected that every operator acting on both CFTs can be written as a sum over tensor products of operators acting on states of a single CFT. Since such single CFT operators are manifestly gauge-invariant, also the operator acting on both CFTs is gauge-invariant. This

is in conflict with the existence of the non-gauge-invariant operators obtained by cutting open the Wilson line connecting both sides of the wormhole. The existence of such Wilson lines can therefore be understood as an indicator of a connected geometry in the bulk. This poses the factorisation puzzle in a concrete example by making the puzzle manifest in terms of the operator content of both sides of the duality [462]. We will encounter such Wilson lines again in sec. 5 for the specific case of AdS_3/CFT_2, where we discuss non-factorisation in terms of geometric phases related to such Wilson lines.

Geometric Phases and Entanglement in Quantum Mechanics

4

The AdS/CFT correspondence states that every object of the bulk description has a holographically dual description by an object defined in the boundary theory. A particularly interesting example is given by the eternal black hole and its dual description in terms of the TFD state [112]. This is a powerful demonstration of the relation between entanglement and a connected classical spacetime, i.e. the ER=EPR proposal [118] and 'entanglement creating spacetime' [115–117]. However, as we have reviewed in sec. 3.2, this duality also poses a puzzle, as the Hilbert space structure of the boundary appears factorised between the boundaries, while the bulk Hilbert space is manifestly non-factorised [120]. Resolving this puzzle is one of the main research directions to improve our comprehension of the holographic duality, to which also this thesis aims to contribute. By ER=EPR, non-factorisation as a consequence of gravitational wormholes should have an explanation in terms of the properties of the entanglement. It is therefore pertinent to first understand in detail the properties of entanglement in generic quantum systems and by which notions these properties are indicated and/or quantified. The approach we take is to use geometric phases as introduced in sec. 2.2.1 to characterise entanglement as well as the factorisation properties of the projective Hilbert space. Such phases have the advantage of being independent of potentially complicated local dynamics since they are sensitive to the global properties of the system. In more detail, we first investigate factorisation in bipartite quantum systems making use of the SZK construction [166] reviewed in sec. 2.2.2. This provides a precise method to associate states to particular submanifolds of the projective Hilbert space based on the entanglement contained in the state. Analysing this construction for a model of two interacting qubits, we show how the factorisation properties of the projective Hilbert space are captured by the value of the geometric phase. In particular, for a specific value of the geometric phase, the submanifold singled out by the SZK construction is given by the product of the projective Hilbert spaces of the individual qubits, with all other values of the geometric phase corresponding to a non-factorised submanifold. Using the same line of thought, we discuss the TFD state in light of the SZK construction. We also define a phase of topological nature for the TFD state that reflects the non-trivial topology of the gravitational phase space of wormhole geometries. We show this in detail for the wormhole solution in JT gravity analysed in [466]. Here, the path of integration computing this topological phase can be understood as a Wilson line piercing the wormhole.

We start our discussion by analysing factorisation properties of the projective Hilbert space in a bipartite quantum system in sec. 4.1. In particular, we use the SZK construction [166] and calculate geometric phases to characterise the factorisation properties. Further, we define a fine structure of entanglement, where a second type of geometric phase distinguishes states with the same entanglement properties. In all of these discussions, we use a system of two coupled qubits as an explicit example. In sec. 4.2 we apply the techniques developed in the previous section to the TFD state as the holographic dual to the eternal black hole. We define a topological phase for the TFD state that probes non-factorisation. Using the TFD state of the two-qubit system we compute this phase explicitly as an illustrative example. We finish the section by showing how the same topological phase arises from the gravity perspective in an explicit example using JT gravity. The new results discussed in this section appeared in [183] and parts of [184] and we mainly follow the presentation therein.

4.1. Entanglement and Factorisation of the Projective Hilbert Space

As discussed in sec. 2.3, the operator algebras of finite-dimensional systems are always of type I. Correspondingly, there exists an irreducible representation of the algebra and the Hilbert space $\mathscr{H}$ containing the state vectors admits a factorisation into Hilbert spaces corresponding to a subsystem A and its complement $\bar{A}$, $\mathscr{H} = \mathscr{H}^{(A)} \otimes \mathscr{H}^{(\bar{A})}$. However, the physically distinguishable states are contained in the projective Hilbert space $\mathscr{P}(\mathscr{H})$. Even in finite dimensions, this space does not necessarily factorise into the projective Hilbert spaces of the subregions, cf. the discussion following (2.72). As we discussed in sec. 2.2.1, the projective Hilbert space may be understood as the base space of a fibre bundle with fibre $\mathrm{U}(1)$. The geometric phases indicating the non-trivial nature of this bundle can be used to characterise whether the projective Hilbert space factorises. This link is provided by invoking the SZK construction [166] reviewed in sec. 2.2.2. In the following sec. 4.1.1, we discuss the entanglement properties for the ground state of a simple two-qubit model in light of the SZK construction. We then show how geometric phases are used to characterise the entanglement and factorisation properties for the two qubits in sec. 4.1.2. This analysis is followed by introducing the notion of a *fine structure of entanglement* in sec. 4.1.3, which goes beyond the entanglement orbits defined by the SZK construction.

4.1.1. Entanglement for Two Interacting Qubits

We start our analysis by discussing the entanglement properties of two interacting qubits. Each of the qubits is represented using the Pauli matrices as $\vec{S}_i = \frac{1}{2}\vec{\sigma}_i$, where $i = 1,2$ labels the qubits and $\vec{\sigma}$ is interpreted as a vector in $\mathbb{R}^3$ containing the Pauli matrices as its entries.[1] The prefactor $\frac{1}{2}$ indicates the the qubits have spin $j = \frac{1}{2}$. The dynamics of the two-qubit system are described by the Hamiltonian [183]

$$H = J\vec{S}_1 \cdot \vec{S}_2 - 2\mu_B B S_{1,z}\,, \tag{4.1}$$

where J is the coupling strength between the qubits and $\mu_B B$ is the interaction strength of a magnetic field of absolute value B and Bohr magneton μ_B with the first qubit. This Hamiltonian can be understood as describing a hydrogen atom under the influence of a magnetic field. The two qubits $\vec{S}_1$ and $\vec{S}_2$ describe the electron and proton spins, respectively, with hyperfine coupling J. The interaction between the proton spin and the magnetic field can be neglected to first approximation, with only the Zeeman term $\propto \mu_B B S_{1,z}$ of the electron spin and the magnetic field remaining.

We are interested in studying the entanglement properties of this system primarily for the ground state of the Hamiltonian (4.1). Assuming that $J > 0$, the ground state is given by

$$|\psi\rangle = \frac{\cos\frac{\alpha}{2} - \sin\frac{\alpha}{2}}{\sqrt{2}}|\uparrow_1\downarrow_2\rangle + \frac{\cos\frac{\alpha}{2} + \sin\frac{\alpha}{2}}{\sqrt{2}}|\downarrow_1\uparrow_2\rangle\,, \tag{4.2}$$

where we defined $\tan\alpha = 2\mu_B\frac{B}{J}$ and the entries in $|i_1 j_2\rangle$ with $i,j = \uparrow,\downarrow$ refer to the first and second qubit. In light of (2.11), the entanglement entropy of (4.2) is uniquely determined by the Schmidt coefficients of this state. In this simple example, the Schmidt decomposition is particularly easy to obtain. We are looking for a transformation that expresses (4.2) in the form $|\psi\rangle = \sum_i \kappa_i |i_1 i_2\rangle$, so the transformation of the second spin $|\uparrow_2\rangle \to |\downarrow_2\rangle$ and $|\downarrow_2\rangle \to |\uparrow_2\rangle$ suggests itself. The Schmidt coefficients are then simply the prefactors of the base vectors in (4.2). Indeed, this result is obtained also by straightforward calculation, with Schmidt coefficients

$$\kappa_\uparrow = \frac{\cos\frac{\alpha}{2} - \sin\frac{\alpha}{2}}{\sqrt{2}} = \sqrt{\frac{1-\sin\alpha}{2}} \quad \text{and} \quad \kappa_\downarrow = \frac{\cos\frac{\alpha}{2} + \sin\frac{\alpha}{2}}{\sqrt{2}} = \sqrt{\frac{1+\sin\alpha}{2}}\,. \tag{4.3}$$

[1] This is a formal definition. More precisely, $\vec{\sigma}$ should be regarded as a 'vector operator' in that it provides a map between $\mathbb{R}^3$ and the space of traceless 2×2 matrices. In one direction, contracting vector indices $\vec{x}\cdot\vec{\sigma}$ provides a 2×2 matrix with matrix entries related to the vector components x_i. In the other direction, contracting matrix indices $\langle\psi|\vec{\sigma}|\psi\rangle$ results in a three-dimensional vector with entries related to the components of $|\psi\rangle$.

Correspondingly, tracing the pure state $\rho = |\psi\rangle\langle\psi|$ with $|\psi\rangle$ in Schmidt decomposition over the second qubit the reduced density operator for the first qubit is given by

$$\rho^{(1)} = \kappa_{\uparrow}^2 |\uparrow_1\rangle\langle\uparrow_1| + \kappa_{\downarrow}^2 |\downarrow_1\rangle\langle\downarrow_1| \,. \tag{4.4}$$

The entanglement entropy then follows using either (2.10) or equivalently (2.11) as

$$S(\rho^{(1)}) = \sin\alpha \ln \frac{1-\sin\alpha}{\cos\alpha} - \ln\frac{\cos\alpha}{2} \,. \tag{4.5}$$

The angle α measuring the ratio of B and J determines the entanglement entropy. Depending on which term dominates in (4.1), the entanglement differs. In particular, the limit $B \gg J$ implies that the influence of the coupling between the qubits is minimal. Correspondingly, $\alpha = \arctan\left(2\mu_B \frac{B}{J}\right) \to \frac{\pi}{2}$ and the entanglement between the qubits vanishes,

$$\lim_{\alpha\to\frac{\pi}{2}} S(\rho^{(1)}) = 0 \,. \tag{4.6}$$

On the other hand, the first term dominates for $B \ll J$, so the interaction with the magnetic field can be neglected. In this case, $\alpha = \arctan\left(2\mu_B \frac{B}{J}\right) \to 0$ and (4.5) reduces to the maximal value for two qubits,

$$\lim_{\alpha\to 0} S(\rho^{(1)}) = \ln 2 \,. \tag{4.7}$$

In the light of the SZK construction [166] reviewed in sec. 2.2.2, this two-qubit system, i.e. $n = 2$ in the section just mentioned, provides the smallest non-trivial example. We discuss this in detail in the following. The Hilbert space of this system is given by $\mathscr{H} = \mathbb{C}^4$, with projective Hilbert space $\mathscr{P}(\mathscr{H}) = \mathbb{C}\mathrm{P}^3$. To obtain the entanglement orbits, we have to evaluate (2.93). The Schmidt coefficients given in (4.3) are parametrised by a single variable α which determines their value. For generic values $0 < \alpha < \frac{\pi}{2}$, the Schmidt coefficients have different but non-vanishing values, so the multiplicities m_i of the Schmidt coefficients are given by $m_0 = 0$ and $m_1 = m_2 = 1$. The entanglement entropy (4.5) takes a generic non-vanishing and non-maximal value, so the state belongs to the intermediate orbit (2.94). For this particularly simple system, this is the only intermediate orbit. Explicitly, the orbit is given by

$$\mathscr{O}_{|\psi\rangle_\alpha} = \frac{\mathrm{U}(2)}{\mathrm{U}(1)^2} \times \frac{\mathrm{SU}(2)}{\mathbb{Z}_2} = \mathbb{C}\mathrm{P}^1_\alpha \times \mathbb{R}\mathrm{P}^3 \,, \tag{4.8}$$

noting that $\mathbb{C}\mathrm{P}^1 = \frac{\mathrm{SU}(2)}{\mathrm{U}(1)}$. All state vectors related to $|\psi\rangle_\alpha$ at fixed α by local unitary transformations are contained in this orbit. Two comments on this result are in order. First,

the index α on $\mathbb{C}\mathrm{P}^1$ indicates that for every α this part of the submanifold is topologically equivalent to $\mathbb{C}\mathrm{P}^1$, however the volume is different from the standard result for $\mathbb{C}\mathrm{P}^1$ but depends on α. We will provide further explanation of this point when calculating the geometric phases for this system in sec. 4.1.2. Second, the factor $\mathbb{R}\mathrm{P}^3$ appearing in the orbit is a special case for the current two-qubit system that does not generalise to arbitrary n. It makes use of the fact that $\mathrm{SU}(2) \simeq \mathrm{SO}(3)$ and $\frac{\mathrm{SO}(3)}{\mathbb{Z}_2} = \mathbb{R}\mathrm{P}^3$. For general n, relations between $\mathrm{SU}(n)$ and some $\mathrm{SO}(n')$ with $n < n'$ cannot always be established, but only exist for special values of n. Moreover, the real projective space $\mathbb{R}\mathrm{P}^n$ always requires a quotient by $\mathbb{Z}_2$, while for arbitrary n the quotient is given by $\mathbb{Z}_n$.

As discussed above, the entanglement between the qubits is maximal for $\alpha = 0$. In particular, in this case the Schmidt coefficients (4.3) coincide and the multiplicities are given by $m_0 = 0$ and $m_1 = 2$. The orbit for maximal entanglement (2.95) in this particular example then evaluates to

$$\mathscr{O}_{|\psi\rangle_{\alpha=0}} = \mathbb{1} \times \frac{\mathrm{SU}(2)}{\mathbb{Z}_2} = \mathbb{1} \times \mathbb{R}\mathrm{P}^3 \,. \tag{4.9}$$

The states in this orbit are given by the familiar Bell states. In particular, in the limit $\alpha \to 0$ the ground state (4.2) reduces to

$$\lim_{\alpha\to 0} |\psi\rangle = \sqrt{\frac{1}{2}} \left(|\uparrow_1\downarrow_2\rangle + |\downarrow_1\uparrow_2\rangle \right) = |\mathrm{Bell}\rangle \,. \tag{4.10}$$

Finally for $\alpha = \frac{\pi}{2}$ the entanglement vanishes. In this case, the Schmidt coefficients evaluate to $\kappa_\uparrow = 0$ and $\kappa_\downarrow = 1$, so the multiplicities are found as $m_0 = 1$ and $m_1 = 1$. The orbit of vanishing entanglement (2.96) then follows as

$$\mathscr{O}_{|\psi\rangle_{\alpha=\frac{\pi}{2}}} = \frac{\mathrm{U}(2)}{\mathrm{U}(1)^2} \times \frac{\mathrm{U}(2)}{\mathrm{U}(1)^2} = \mathbb{C}\mathrm{P}^1 \times \mathbb{C}\mathrm{P}^1 \,. \tag{4.11}$$

The states in this orbit are simple product states. To be specific, in the limit $\alpha \to \frac{\pi}{2}$ the ground state (4.2) is given by

$$\lim_{\alpha\to\frac{\pi}{2}} |\psi\rangle = |\downarrow_1\uparrow_2\rangle \,. \tag{4.12}$$

The orbit (4.11) is composed of the projective Hilbert spaces $\mathbb{C}\mathrm{P}^1$ of the individual spins. Therefore, states with vanishing entanglement are part of a factorised projective Hilbert space, while for all other states contained in either (4.8) or (4.9), the submanifold of the projective Hilbert space assumes a more complicated form.

In this discussion we considered α only in the interval between 0 and $\frac{\pi}{2}$. However, with

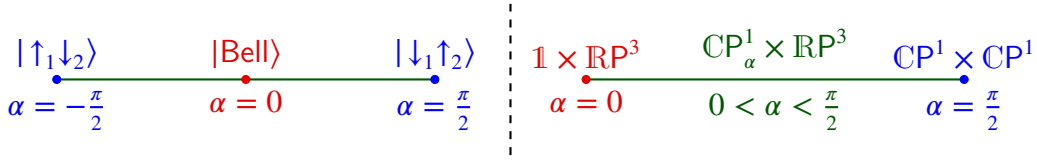

Figure 4.1: On the left, the Schmidt simplex for the coupled two-qubit system is represented by the line. The two endpoints of the line correspond to vanishing entanglement with the corresponding product states, while the centre of the line corresponds to the maximally entangled state. On the right, the Weyl chamber of the Schmidt simplex is shown. All possible values of the entanglement entropy are contained in the Weyl chamber and correspondingly the entanglement orbits (4.8), (4.9) and (4.11) are associated to parts of the Weyl chamber as indicated by the colour coding.

the Schmidt coefficients (4.3) depending on $\sin\alpha$, under the transformation $\alpha \to -\alpha$ the Schmidt coefficients are transformed into each other. Therefore, the region $-\frac{\pi}{2} \leq \alpha \leq 0$ has to have an analogous interpretation in terms of the previous analysis of the entanglement orbits. In fact, this region can be interpreted as the case $J < 0$.[2] In particular, $B \gg |J|$ yields $\alpha = \arctan\left(2\mu_B \frac{B}{J}\right) \to -\frac{\pi}{2}$, for which the entanglement entropy (4.5) again vanishes. Moreover, in this limit the ground state reduces to the other base vector compared to (4.12),

$$\lim_{\alpha \to -\frac{\pi}{2}} |\psi\rangle = |\uparrow_1\downarrow_2\rangle\,. \tag{4.13}$$

In terms of the SZK construction, while $0 \leq \alpha \leq \frac{\pi}{2}$ corresponds to one Weyl chamber, the region $-\frac{\pi}{2} \leq \alpha \leq 0$ corresponds to the other Weyl chamber. Together, these two regions form the full Schmidt simplex. In the current example, this is simply a line, with particular points on the line specified by fixing α to particular values. A visualisation for this is provided in fig. 4.1.

Let us now discuss the above results on the entanglement as well as the submanifolds of the projective Hilbert space in light of the ER=EPR proposal as reviewed in sec. 3.2.2. Taking ER=EPR in its most general form, the entanglement as given in (4.5) is responsible for creating a wormhole between the two qubits. In our discussion on the entanglement orbits, vanishing entanglement corresponds to the factorised structure $\mathbb{C}\text{P}^1 \times \mathbb{C}\text{P}^1$. We may therefore intuitively visualise the wormhole as stretching between the two qubits, in particular between the two individual projective Hilbert spaces, as in fig. 4.2. Of course, this wormhole connecting the two qubits is far from a classical geometry as the quantum system is far from being strongly coupled in the usual sense of AdS/CFT. However, taking

[2] Note that in this case, (4.2) is no longer necessarily the ground state. This does however not affect the discussion of the SZK construction.

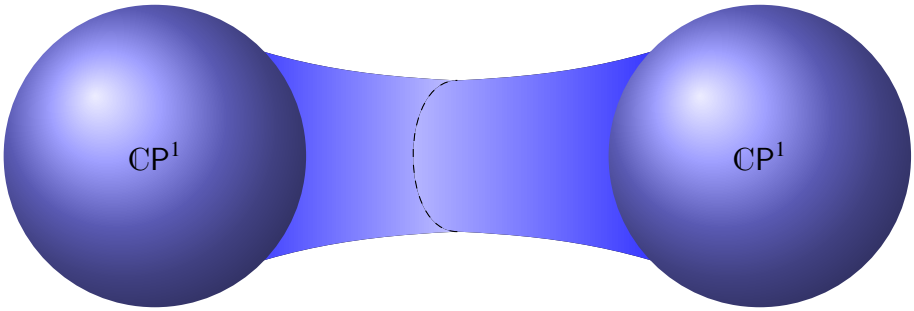

Figure 4.2: Visual representation of the ER=EPR proposal for the interacting two-qubit system. The individual projective Hilbert spaces $\mathbb{C}P^1$ of each qubit are connected by a tiny wormhole.

ER=EPR seriously, geometric connections between entangled particles have to exist, and in particular contribute to the path integral. Indeed, this was investigated in [165]. It was shown that the partition function of an arbitrary quantum system shows wormhole(-like) behaviour if the symplectic form of the system in question is non-exact. Such non-exact symplectic forms lead to the presence of holonomies, as discussed in sec. 2.2.1. In the following section, we analyse this in more detail. In particular, we show how the entanglement, as well as factorisation properties, can be understood in terms of the geometric phase of the state (4.2).

4.1.2. Geometric Phase in the SZK Construction

We have now set the stage to calculate geometric phases as measures of the entanglement and thereby also of the factorisation properties of the projective Hilbert space. As we pointed out in secs. 2.2.1 and 2.2.2, the projective Hilbert space can be regarded as a principle fibre bundle, cf. (2.85). Also in the SZK construction fibre bundles arise naturally due to the structure of the entanglement orbits, as discussed below (2.93). In particular, the base space is given by the first factor in the entanglement orbits (2.93). In the following, we show how the geometric phases measuring the entanglement are calculated for the two-qubit example. This will also enable us to characterise the factorisation properties of the projective Hilbert space by the geometric phase.

To calculate the geometric phase, we need to define a local gauge field A and a corresponding field strength which provides the symplectic form $\Omega = \mathrm{d}A$ for the orbit. The geometric phase is then given by the integral of the symplectic form as discussed around (2.83). To define the local gauge field, we follow the method developed in [292]. The general idea of this method is to choose an arbitrary point p of the orbit and then use unitary transformations to transport p to an arbitrary point q of the orbit. This transport can be used to define the local gauge field independent of the initial choice for p.

A point in the orbit, and in particular on $\mathbb{C}\mathrm{P}^1_\alpha$, is represented by the coefficient matrix of the state vector $|\psi\rangle$ for a fixed value of the entanglement entropy. As the orbits are derived by studying the Schmidt coefficients, this suggests that a natural choice for p, and indeed a particularly convenient one, is the diagonal coefficient matrix with Schmidt coefficients as diagonal entries. For the two-qubit system, that is

$$p = \begin{bmatrix} \sqrt{\frac{1-\sin\alpha}{2}} & 0 \\ 0 & \sqrt{\frac{1+\sin\alpha}{2}} \end{bmatrix}. \tag{4.14}$$

As discussed in sec. 2.1.1, the Schmidt coefficients are invariant under unitary transformations. Therefore, by applying an arbitrary SU(2) local transformation U to p an arbitrary point q in the same orbit is obtained. If p corresponds to the state vector $|\psi\rangle$ written in Schmidt decomposition, the point q corresponds to the state vector $U \otimes \mathbb{1}_2|\psi\rangle$ not written in Schmidt decomposition,[3] but with the same entanglement properties as $|\psi\rangle$. Note that U is a local unitary transformation that acts only on the first spin, as indicated by the identity acting on the second spin. Since the Pauli matrices provide a basis for the Lie algebra $\mathfrak{su}(2)$ of the group SU(2), an arbitrary transformation $U \in \mathrm{SU}(2)$ can be written using exponentials of Pauli matrices. We choose to work with the Euler parametrisation

$$U = e^{-\mathrm{i}\frac{\phi}{2}\sigma_z} e^{-\mathrm{i}\frac{\theta}{2}\sigma_y} e^{-\mathrm{i}\frac{\phi}{2}\sigma_z}, \tag{4.15}$$

where ϕ and θ parametrise $\mathbb{S}^2 \simeq \mathbb{C}\mathrm{P}^1$. The point q is then defined as

$$q = Up\,. \tag{4.16}$$

Since $p^\dagger p = p^2 = \rho^{(1)}$ given in (4.4), the trace of p^2 equals one. The same is true for $q^\dagger q$ since $q^\dagger q = p^2$. Since p does not depend on ϕ or θ, it follows that differentiating $\mathrm{tr}\left(q^\dagger q\right)$ w.r.t. the parameters ϕ and θ vanishes due to $\mathrm{d}(q^\dagger q) = \mathrm{d}p^2 = 0$. In particular, by pulling the derivative inside the trace we find that

$$\mathfrak{Re}\left[\mathrm{tr}\left(q^\dagger \mathrm{d}q\right)\right] \propto \mathrm{tr}\left(q^\dagger \mathrm{d}q\right) + \mathrm{tr}\left(\mathrm{d}q^\dagger q\right) = \mathrm{tr}\left(\mathrm{d}(q^\dagger q)\right) = 0\,. \tag{4.17}$$

So $\mathrm{d}\,\mathrm{tr}\left(\rho^{(1)}\right) = 0$ is realised by the vanishing of the real part of $\mathrm{tr}\left(q^\dagger \mathrm{d}q\right)$. The imaginary

[3] Note that as discussed around (2.17), obtaining the Schmidt decomposition for an arbitrary $|\psi\rangle$ can be understood as a unitary transformation of the basis that $|\psi\rangle$ is written in. Applying a unitary transformation U on a vector in Schmidt decomposition therefore changes the basis away from the Schmidt decomposed form of $|\psi\rangle$. Essentially, U may be understood as the inverse of the transformation that achieves the Schmidt decomposition.

part of this however does not vanish,

$$\mathfrak{Im}\left[\operatorname{tr}\left(q^\dagger \mathrm{d}q\right)\right] \propto \operatorname{tr}\left(q^\dagger \mathrm{d}q\right) - \operatorname{tr}\left(\mathrm{d}q^\dagger q\right) = 2\operatorname{tr}\left(q^\dagger \mathrm{d}q\right), \tag{4.18}$$

where we used $\mathrm{d}q^\dagger q = -q^\dagger \mathrm{d}q$. This allows for defining the local gauge field A as

$$A = \mathrm{i}\operatorname{tr}\left(q^\dagger \mathrm{d}q\right). \tag{4.19}$$

We point out that this definition is nothing but the more familiar definition explicitly using the state vectors as in (2.63) in disguise. Since p is independent of ϕ or θ, we may write (4.19) as

$$A = \mathrm{i}\operatorname{tr}\left(p^2 U^\dagger \mathrm{d}U\right) = \mathrm{i}\operatorname{tr}\left(\rho^{(1)} A_{\mathrm{MC}}\right) = \mathrm{i}\langle\psi|A_{\mathrm{MC}}|\psi\rangle = \mathrm{i}\langle\psi'|\mathrm{d}\psi'\rangle, \tag{4.20}$$

where $|\psi\rangle$ is the state vector in Schmidt decomposition, $|\psi'\rangle$ is the transformed vector $U \otimes \mathbb{1}_2|\psi\rangle$ and $A_{\mathrm{MC}} = U^\dagger \mathrm{d}U$ is the (left-invariant) Maurer–Cartan form. This form is the natural connection on a group manifold defined for any group element U, which in the present case is an element of SU(2) (for details on this form see e.g. [269]).

With the definition of the local gauge field established, evaluating (4.19) explicitly for our choice of p we obtain

$$A_{\mathrm{N}} = -\frac{\sin\alpha}{2}(1+\cos\theta)\mathrm{d}\phi. \tag{4.21}$$

We find that this expression vanishes nowhere except at $\theta = \pi$. This gauge field is therefore well-defined on the coordinate patch of $\mathbb{S}^2$ including the north pole. To obtain a gauge field for the other coordinate patch including the south pole, we have to change the group element U given in (4.15) to

$$U = e^{-\mathrm{i}\frac{\phi}{2}\sigma_z} e^{-\mathrm{i}\frac{\theta}{2}\sigma_y} e^{\mathrm{i}\frac{\phi}{2}\sigma_z}. \tag{4.22}$$

Evaluating (4.19) using this group element, we find

$$A_{\mathrm{S}} = \frac{\sin\alpha}{2}(1-\cos\theta)\mathrm{d}\phi, \tag{4.23}$$

which is nowhere vanishing except at the north pole $\theta = 0$. Since the coordinate patches have a non-trivial overlap, the two gauge fields (4.21) and (4.23) can be transformed into each other as in (2.64) or (2.80) by a U(1) transformation, $A_{\mathrm{S}} = A_{\mathrm{N}} - \mathrm{i}U^\dagger \mathrm{d}U$ with $U = e^{\mathrm{i}\sin(\alpha)\phi}$.

As there is no nowhere vanishing gauge field, by the discussion of sec. 2.2.1 on principal

fibre bundles we already know that the fibre bundle must be non-trivial. To make this manifest in terms of the geometric phase we first compute the field strength of the local gauge fields A_N and A_S,

$$\Omega = \mathrm{d}A_N = \mathrm{d}A_S = \frac{\sin\alpha}{2}\sin\theta\,\mathrm{d}\theta\wedge\mathrm{d}\phi\,. \tag{4.24}$$

The prefactor $\frac{\sin\alpha}{2}$ indicates that the symplectic form (4.24) is defined for the orbit with entanglement entropy given by (4.5) at a fixed value for α. The coordinate dependent term $\sin\theta\,\mathrm{d}\theta\wedge\mathrm{d}\phi$ results from the geometry of the base space $\mathbb{S}^2\simeq\mathbb{C}\mathrm{P}^1$ in that this term is simply the volume form of $\mathbb{S}^2$. By (2.83), the geometric phase Φ_G follows by integrating the symplectic form. The closed two-dimensional surface Σ within the base manifold left arbitrary in (2.83) in the present case has to be equal to the base manifold itself, resulting in

$$\Phi_G = \int_{\mathbb{S}^2}\Omega = 2\pi\sin\alpha\,. \tag{4.25}$$

The geometric phase is uniquely determined by the value of α, as is the entanglement entropy (4.5). Therefore, the entanglement entropy can be expressed as a function of Φ_G. In other words, the geometric properties of the fibre bundle determine the entanglement between the two qubits. In particular, the factorisation properties of the projective Hilbert space are determined by the geometric phase. If $\Phi_G = 2\pi$, the projective Hilbert space factorises into the projective Hilbert spaces of the individual qubits, $\mathbb{C}\mathrm{P}^3\to\mathbb{C}\mathrm{P}^1\times\mathbb{C}\mathrm{P}^1$. This associates a precise value for the geometric value to a factorised submanifold of the full projective Hilbert space. Indeed if $0<\Phi_G<2\pi$, the entanglement orbit determines a more complicated, i.e. non-factorised, submanifold of the projective Hilbert space, $\mathbb{C}\mathrm{P}^3\to\mathbb{C}\mathrm{P}^1_\alpha\times\mathbb{R}\mathrm{P}^3$. Finally if $\Phi_G=0$, the entanglement orbit is the Lagrangian submanifold $\mathbb{R}\mathrm{P}^3$ of the projective Hilbert space $\mathbb{C}\mathrm{P}^3$. As discussed in sec. 2.2.2, Lagrangian submanifolds are isotropic submanifolds, i.e. the symplectic form Ω of the full symplectic manifold vanishes when restricted to the Lagrangian submanifold. Indeed, the symplectic form (4.24) vanishes on the orbit of maximal entanglement as $\sin\alpha|_{\alpha=0}=0$. Consistent with this, the geometric phase (4.25) of the maximally entangled orbit vanishes.

The vanishing of the geometric phase for maximally entangled states can also be given an alternative interpretation in terms of the volume of the base space. As the symplectic form (4.24) is proportional to the volume form of $\mathbb{S}^2\simeq\mathbb{C}\mathrm{P}^1$, the geometric phase (4.25) can also be interpreted as the volume of the corresponding entanglement orbit. The elements of the orbits are states with the same entanglement properties, so the volume of the orbit can be understood as a characterisation of the number of states within the orbit. Therefore, given

the result (4.25), the orbits with less entanglement contain 'more' states.[4] This can be understood as follows. Our method above to define the local gauge field used a point p as a starting point which is then transported to an arbitrary point q in the same orbit. In terms of state vectors, these points correspond to $|\psi\rangle$ written in Schmidt decomposition and $|\psi'\rangle = U \otimes \mathbb{1}_2|\psi\rangle$, with U given by (4.15). The entanglement properties of these states are the same. However, they lead to different measurement results for certain observables. Consider e.g. the operator $\mathfrak{s}_z = \sigma_z \otimes \mathbb{1}_2$ measuring the magnetisation of the first spin. Then, evaluating in $|\psi\rangle$ and $|\psi'\rangle$ yields

$$\langle\psi|\mathfrak{s}_z|\psi\rangle = -\sin\alpha \quad \text{and} \quad \langle\psi'|\mathfrak{s}_z|\psi'\rangle = -\cos\theta\,\sin\alpha\,. \tag{4.26}$$

For fixed θ, these measurement results become parametrically more distinct for $\alpha \to \frac{\pi}{2}$, i.e. when $|\psi\rangle$ and $|\psi'\rangle$ become product states. In this sense, orbits with less entanglement have larger volume (4.25) as they contain more states leading to different measurement results. In the other limit of maximal entanglement $\alpha \to 0$, the two measurement results coincide. Correspondingly, the orbit of maximal entanglement contains the least 'number' of states. In terms of reduced density operators, the same considerations can be made. In fact, the reduced density operators associated to a particular orbit are elements of SU(2) consistent with the structure of $\mathbb{C}\mathrm{P}^1_\alpha$. In the limit of maximal entanglement, $\mathbb{C}\mathrm{P}^1_\alpha$ reduces to a point. Correspondingly, this orbit contains only one state, i.e. the reduced density operator given by $\rho^{(1)} \propto \mathbb{1}$ as the first factor in (4.9). This observation also provides a simple and intuitive explanation for the vanishing of the geometric phase for maximal entanglement. If the base space is a single point, there is no room for defining several coordinate patches covering the base space with non-trivial overlaps. Correspondingly, there cannot be any non-trivial holonomy or geometric phase.

The relation between a larger volume, i.e. more states, and less entanglement might seem counter-intuitive at first. Usually, more available states lead to more entanglement between those states. However, this is precisely where the subtlety lies, as this interpretation of entanglement is not the same as the one we discussed above. The volume of an entanglement orbit characterises the number of states with the same entanglement properties, i.e. with the same amount of entanglement *contained in* the state. In particular, the volume does not measure any potential entanglement *between* states in the same orbit.

[4] Note that Φ_G for $\alpha = \frac{\pi}{2}$ equals 2π, which is half of the volume of $\mathbb{S}^2$, $\mathrm{Vol}(\mathbb{S}^2) = 4\pi$. This is since we consider qubits with spin $\frac{1}{2}$. Had we considered an arbitrary spin j, the geometric phase would read $\Phi_G = 4\pi j \sin\alpha$.

4.1.3. Fine Structure of Entanglement

In the previous section we have shown how geometric phases associated to the first factor in the entanglement orbits (4.8), (4.9) and (4.11) can be used to characterise the entanglement properties as well as the factorisation of the projective Hilbert space. In the following, we will study how a different notion of geometric phase can be used to distinguish between states with the same entanglement.

For this analysis, we reconsider the two-qubit system described by the Hamiltonian (4.1). In terms of this Hamiltonian, the transformation $U \otimes \mathbb{1}$ discussed in the previous section, with U given by either (4.15) or (4.22), can be understood as a rotation to adjust the axis of the first qubit $\vec{S}_1$ and the, for now arbitrary, axis of the magnetic field $\vec{B}$. In particular, writing $\vec{B}$ as an arbitrary vector $\vec{B} = B\,(\sin\theta\,\cos\phi, \sin\theta\,\sin\phi, \cos\theta)^T$ with $B = |\vec{B}|$, the rotations are such that they align the magnetic field with the z-direction of $\vec{S}_1$,

$$U^\dagger \vec{B}\cdot\vec{S}_1 U = B S_{1,z}\,, \tag{4.27}$$

provided that the angles ϕ and θ of U given by (4.15) or (4.22) are the same angles as those of $\vec{B}$. Of course, a converse relation also holds, $U B S_{1,z} U^\dagger = \vec{B}\cdot\vec{S}_1$. Therefore, while the Hamiltonian H given in (4.1) describes the interaction between the first qubit and the magnetic field for a specific alignment between $\vec{B}$ and $\vec{S}_1$, the Hamiltonian $UHU^\dagger$ amounts to the same type of interaction but with an arbitrary alignment. The ground state $|\psi\rangle$ given in (4.2) is an eigenstate to H. Therefore, the transformed ground state $U|\psi\rangle$ is an eigenstate to the transformed Hamiltonian $UHU^\dagger$. We may therefore interpret the geometric phase (4.25) derived in the previous section as follows. Suppose that the system is prepared such that the first qubit and the magnetic field are aligned as $BS_{1,z}$ with ground state $|\psi\rangle$. Letting the system evolve in time, this fine-tuned alignment will eventually be lost and turn into the more generic alignment described by $UHU^\dagger$ with ground state $U|\psi\rangle$. The geometric phase (4.25) is the phase picked up by the state $|\psi\rangle$ when the qubit $\vec{S}_1$ and the magnetic field $\vec{B}$ become unaligned.

In this analysis, the transformation U (denoted as U_1 in the following) acting on the first qubit $\vec{S}_1$ is fixed by the requirement that it transforms between $BS_{1,z}$ and $\vec{B}\cdot\vec{S}_1$. However, there is no constraint on a potential transformation U_2 acting on the second spin. In sec. 4.1.2, we used a trivial transformation $U_2 = \mathbb{1}$. In the context of the above considerations with U_1 a rotation between $\vec{B}$ and $\vec{S}_1$, it is intuitive to make this choice since the second spin does not interact with the magnetic field and correspondingly does not require a realignment. However, the first term of the Hamiltonian (4.1) describing the interaction between the two qubits $\propto \vec{S}_1\cdot\vec{S}_2$ is not invariant under the transformation $U_1 \otimes \mathbb{1}$, which amounts to a highly complicated form for the Hamiltonian $U_1 H U_1^\dagger$. There

is however a simple fix to this by considering a non-trivial transformation U_2. In particular, setting $U_2 = U_1$, the interaction term $\vec{S}_1 \cdot \vec{S}_2$ is invariant. Moreover, the interaction between the first qubit and the magnetic field is not affected by this. Since $BS_{1,z}$ is to be read as $\frac{B}{2}\sigma_z \otimes \mathbb{1}$, any non-trivial unitary U_2 cancels out. So the transformation $U = U_1 \otimes U_2$ with U_1 and U_2 given by (4.15) or (4.22) is equally reasonable to consider in relation to physical properties. Moreover, this choice is convenient in the sense that the Hamiltonian $UHU^\dagger$ does not become as complicated as when using $U_2 = \mathbb{1}$.

To summarise, as far as the alignment between $\vec{S}_1$ and $\vec{B}$ is concerned, both $U_2 = U_1$ and $U_2 = \mathbb{1}$ are reasonable choices. Moreover, both choices do not affect the entanglement properties of the ground state (4.2). Since in both cases, $U = U_1 \otimes U_2$ is a local unitary transformation, the Schmidt coefficients of $|\psi\rangle$ are unaltered, i.e. they are still given by (4.3). However, as we show in the following, the two choices for U_2 amount to different geometric phases picked up by $|\psi\rangle$ in the course of the evolution by U. Within the computations, we denote $U^{(\lambda)} = U_1 \otimes U_2$ where U_1 is given as before by either (4.15) or (4.22) and U_2 is given by the same expression as U_1, however with the angles ϕ and θ replaced by $\lambda\phi$ and $\lambda\theta$, respectively. The parameter $\lambda \in [0, 1]$ is introduced to present the computations in a unified form, where $\lambda = 0$ corresponds to $U_2 = \mathbb{1}$ and $\lambda = 1$ to $U_2 = U_1$. With this parametrisation of the full transformation $U^{(\lambda)}$ we calculate the local gauge fields using (4.20). Using either (4.15) or (4.22) for the transformation U_1 and (the form of) U_2, we find

$$A_{\mathrm{N}} = -\frac{\sin\alpha}{2}\big[(1+\cos\theta) - \lambda(1+\cos\lambda\theta)\big]\mathrm{d}\phi \tag{4.28}$$

for (4.15) and

$$A_{\mathrm{S}} = \frac{\sin\alpha}{2}\big[(1-\cos\theta) - \lambda(1-\cos\lambda\theta)\big]\mathrm{d}\phi\,, \tag{4.29}$$

for (4.22). As before, the gauge field A_{N} vanishes at the south pole $\theta = \pi$, while the gauge field A_{S} vanishes at the north pole $\theta = 0$. Correspondingly, the bundle must be non-trivial since there is no nowhere vanishing gauge field. On the non-trivial overlap of the coordinate patches, a U(1) transformation between the gauge fields can be established as $U = e^{\mathrm{i}\sin(\alpha)\phi(1-\lambda)}$ in $A_{\mathrm{S}} = A_{\mathrm{N}} - \mathrm{i}U^\dagger \mathrm{d}U$. Note in particular that for $\lambda = 1$, this transformation U reduces to one, providing an early hint that in this case, the bundle is trivial as the coordinates in each patch are equal, i.e. related by a transformation equal to unity. We will shortly see this made manifest by calculating the geometric phase. Both the gauge

fields (4.28) and (4.29) lead to the same field strength, i.e. symplectic form

$$\Omega = \mathrm{d}A_{\mathrm{N}} = \mathrm{d}A_{\mathrm{S}} = \frac{\sin\alpha}{2}\big(\sin\theta - \lambda^2 \sin\lambda\theta\big)\mathrm{d}\theta \wedge \mathrm{d}\phi\,. \tag{4.30}$$

As a consistency check, note that the gauge fields as well as the field strength for $\lambda = 0$ reduce to the results (4.21), (4.23) and (4.24) obtained earlier. Also, the U(1) transformation between the gauge fields for $\lambda = 0$ reduces to the one discussed below (4.23). The same is true for the geometric phase obtained by integrating (4.30) over $\mathbb{S}^2$,

$$\Phi_{\mathrm{G}} = \int_{\mathbb{S}^2} \Omega = \pi \sin\alpha\big[2 - \lambda(1 - \cos\lambda\pi)\big]\,, \tag{4.31}$$

matching (4.25) for $\lambda = 0$. In fact, as mentioned earlier, for $\lambda = 1$ the geometric phase vanishes. For any other value $0 \leq \lambda < 1$ however, the geometric phase (4.31) is non-trivial.

We point out again that all states $U^{(\lambda)}|\psi\rangle$ obtained from the ground state $|\psi\rangle$ have the same entanglement properties, i.e. the entanglement entropy of any of these states is given by (4.5). However, the geometric phase (4.31) for any of these states is different. We have therefore found a one-parameter family of states $U^{(\lambda)}|\psi\rangle$ with parameter λ that all have the same entanglement properties but are nevertheless distinguished by their geometric phases. The geometric phases for different λ therefore provide a fine structure of entanglement. In the light of the results of [165] on wormholes in quantum mechanics indicated by a non-exact symplectic form in the path integral, for $\lambda \neq 1$ we interpret this one-parameter family of states carrying a fine structure of entanglement as wormhole microstates in the path integral. The presence of these microstates amounts to a non-factorisation of the partition function of the system. We view this as a microscopic manifestation of entanglement creating spacetime as reviewed in sec. 3.2.2. While in the current setting, we discuss a simple quantum system of two interacting qubits, where the wormholes are actually replica wormholes, in sec. 4.2.3 we will show that the fine structure of entanglement is also present for actual gravitational wormholes.

Finally, we point out that the fine structure of entanglement can in principle be observed in actual experiments. Geometric phases are observable by performing interference experiments. In our case, the interference between any two states of the one-parameter family of states $U^{(\lambda)}|\psi\rangle$ with different λ_1 and λ_2 enables to quantify the relative geometric phase, i.e. the difference between (4.31) evaluated for λ_1 and λ_2. Moreover, entanglement can be measured using interference experiments, see e.g. [467]. To obtain sound results in such measurements, it is important that the necessary states can be prepared with high precision. In particular, the states to be measured have to be prepared in large numbers to generate an adequate number of different measurements forming the basis for

a solid statistical analysis. One platform for such measurements is provided by liquid-state nuclear magnetic resonance, which provides experimental access to multiple qubits [468]. Moreover, superconducting quantum circuits as well as quantum dots coupled to an optical cavity [469] can be used to analyse controlled qubit pairs using quantum tomography [470–472]. Using e.g. quantum tomography, all coefficients of the state can be measured. From these measurement results, the geometric phase (4.31) can be recovered.

4.2. An Application with a Holographic Dual: the Thermofield Double State

We have discussed in detail in the previous sec. 4.1 how entanglement and in particular non-factorisation are understood and characterised by the geometric phase. In this section, we aim to apply the same reasoning to a setup with a known gravitational dual, namely the TFD state (3.52). This state is holographically dual to the eternal black hole [112], as reviewed in sec. 3.2.1. We start this analysis by first drawing analogies to the two-qubit system of the previous section in deriving the TFD state for this system in sec. 4.2.1. Next, we briefly analyse the general TFD state in light of the SZK construction in sec. 4.2.2. In the same section, we define a topological phase for the TFD state that probes the topology of the parameter space, as opposed to the geometry of state space measured by the geometric phase defined within the SZK construction. For this topological phase, we discuss an analogous fine structure as discussed for the two-qubit system. To conclude, we show how the topological phase defined for the TFD state can be obtained by a calculation in gravity for a specific setting in JT gravity in sec. 4.2.3.

4.2.1. Thermalising Entanglement

In sec. 2.1.2 we have discussed how the entanglement structure of the vacuum state in QFT provides a notion of temperature for a local observer associated to a subregion. In particular, the Rindler observer with constant acceleration a associated to either of the Rindler wedges $\mathrm{Rin}_{>/<}$ experiences thermal physics at temperature $T = \frac{a}{2\pi}$. While this temperature arises by calculating the reduced density operator and is therefore due to the entanglement structure, it should be stressed that as far as the Rindler observer is concerned, this is an actual physical temperature. This is closely akin to the Hawking temperature [223, 228]. In the following, we show that entanglement induces a temperature not only in QFT, where vast amounts of entanglement are available, but even the entanglement between two qubits as in (4.5) is sufficient. We also discuss the geometric

origin of this temperature in terms of the geometric phase.

The entanglement temperature is derived by using (2.21) written slightly differently to resemble the thermal density operator. Namely, while in (2.21) the reduced density operator is implicitly normalised, in the following it is more convenient to make the normalisation explicit and write

$$\rho^{(1)} = \frac{e^{-K^{(1)}}}{\operatorname{tr} e^{-K^{(1)}}}\,, \tag{4.32}$$

where $\rho^{(1)}$ is given by (4.4) and $K^{(1)}$ is the modular Hamiltonian. Note that making the normalisation $\operatorname{tr} e^{-K^{(1)}}$ explicit is useful since it is closer to the usual way of denoting the thermal density operator, with the (modular) partition function given as $Z_{\text{mod}}(K^{(1)}) = \operatorname{tr} e^{-K^{(1)}}$. Moreover, we point out that the analogous computational steps can be performed using $\rho^{(2)}$, i.e. the reduced density operator of the second spin. Up to different signs in intermediate steps of the following calculation, all results are the same, including in particular the resulting entanglement temperature.

To derive the entanglement temperature we make an ansatz for the modular Hamiltonian $K^{(1)}$. Since the reduced density operator $\rho^{(1)}$ is diagonal, the ansatz for the modular Hamiltonian should be diagonal as well. Therefore, it has to be a linear combination of the identity $\mathbb{1}$ and the third Pauli matrix σ_z. However, including a term $\propto \mathbb{1}$ into the ansatz for $K^{(1)}$ and inserting into (4.32), this term will always drop out since $[\mathbb{1}, \sigma_z] = 0$. We may therefore use the ansatz

$$K^{(1)} = \frac{h}{2}\sigma_z\,, \tag{4.33}$$

where h is an open coefficient. We point out that since the diagonal form for (4.4) can always be established since the Schmidt decomposition always exists, we did not restrict generality with this ansatz. Inserting this ansatz into (4.32) and equating with the reduced density operator (4.4) results in two equations,

$$\kappa_\uparrow^2 = \frac{e^{-h}}{1+e^{-h}} \quad \text{and} \quad \kappa_\downarrow^2 = \frac{1}{1+e^{-h}}\,, \tag{4.34}$$

where $\kappa_\uparrow, \kappa_\downarrow$ are the Schmidt coefficients (4.3). Due to the normalisation of $\rho^{(1)}$, both equations (4.34) yield the same solution for h. Due to exponential functions in (4.32), the straightforward solution to (4.34) includes a term $\propto \mathrm{i}\pi k$ where $k \in \mathbb{Z}$. Demanding that the temperature is real imposes $k = 0$, which chooses the principal branch of the

straightforward solution. We then find that the coefficient h is given by

$$h = \ln \frac{\kappa_{\downarrow}^2}{\kappa_{\uparrow}^2} = \ln \frac{1+\sin\alpha}{1-\sin\alpha}\,. \tag{4.35}$$

To obtain the entanglement temperature, we note that the modular Hamiltonian (4.33) can be interpreted as describing the (z-component of the) single qubit $S_{1,z}$ interacting with the environment. The interaction strength is given by h, which has the interpretation as the interaction energy expressed in units of the temperature. To be precise, h is given by the energy E measured in terms of the 'thermal' energy T_{ent},[5]

$$h = \frac{E}{T_{\text{ent}}} \tag{4.36}$$

Note that this ratio of energies is consistent with the requirement that h is dimensionless. The temperature arises due to the necessity of introducing a scale in which the magnetic energy is measured. Equating the ratio (4.36) with the expression for h given in (4.35) we obtain the entanglement temperature,

$$\beta_{\text{ent}} = \frac{1}{T_{\text{ent}}} = \frac{1}{E} \ln \frac{1+\sin\alpha}{1-\sin\alpha}\,. \tag{4.37}$$

Using the result for the geometric phase of the two-qubit system (4.25), the entanglement temperature can be expressed only by Φ_{G} as

$$\beta_{\text{ent}} = \frac{1}{T_{\text{ent}}} = \frac{1}{E} \ln \frac{2\pi+\Phi_{\text{G}}}{2\pi-\Phi_{\text{G}}}\,. \tag{4.38}$$

This manifests that the entanglement temperature in quantum theory has a geometric origin. By tuning the geometric phase to appropriate values, the full temperature range is covered. For vanishing entanglement, $\Phi_{\text{G}} = 2\pi$ and the denominator inside the logarithm in (4.38) goes to zero. Since in this case the logarithm diverges, the temperature goes to zero, $T_{\text{ent}} \to 0$. Note that since $0 \leq \Phi_{\text{G}} \leq 2\pi$, the denominator approaches zero from above and the argument of the logarithm is always positive, ensuring that the temperature is always real. Vanishing entanglement is therefore interpreted as the single qubit experiencing no temperature. On the other hand, maximal entanglement corresponds to $\Phi_{\text{G}} = 0$. In this case, the argument of the logarithm is equal to one and the logarithm vanishes. Therefore, the temperature diverges, $T_{\text{ent}} \to \infty$. In this case, the single qubit experiences thermal physics at infinite temperature. Note that in these considerations, the value for E is arbitrary but fixed.

[5] Note that we work in natural units $k_{\text{B}} = 1$.

We point out that in deriving the entanglement temperature (4.38) we also have derived the TFD state (3.52) for the two-qubit system. In particular, using the above result (4.37) the Schmidt decomposed version of the ground state (4.2) is rewritten as

$$|\psi\rangle = \frac{1}{\sqrt{Z(\beta_{\text{ent}})}}\left(|\downarrow_1\downarrow_2\rangle + e^{-\beta_{\text{ent}}\frac{E}{2}}|\uparrow_1\uparrow_2\rangle\right), \tag{4.39}$$

where $Z(\beta_{\text{ent}}) = 1 + e^{-\beta_{\text{ent}}E}$. This is the TFD state (3.52) with two energies $E_1 = 0$ and $E_2 = E$. In the previous paragraph, we discussed how the entanglement properties are encoded in the entanglement temperature. The analogous behaviour is found for the general TFD state (3.52). The limits $T \to 0$ and $T \to \infty$ reduce the TFD state to a product state and a maximally entangled state, respectively. We discuss this in more detail shortly in sec. 4.2.2. We emphasise that the above form (4.39) of the state (4.2) can be obtained for any arbitrary state $|\psi'\rangle$ of a two-qubit system, which can be seen as follows. The derivation of the entanglement temperature expresses β_{ent} using the Schmidt coefficients, cf. (4.35). The Schmidt coefficients are defined for any arbitrary state and therefore also for any arbitrary state $|\psi'\rangle$ of a two-qubit system. Moreover, also the relation between the geometric phase and the entanglement temperature (4.38) holds for any arbitrary two-qubit system. This is since, as we showed in sec. 4.1.2, the Schmidt coefficients of a two-qubit system depend on one parameter only. This parameter is always related to the geometric phase Φ_{G} defined using the SZK construction. In particular, any two-qubit state $|\psi'\rangle$ can be written as

$$|\psi'\rangle = \sqrt{\frac{2\pi - \Phi'_{\text{G}}}{4\pi}}\,|\uparrow_1\uparrow_2\rangle + \sqrt{\frac{2\pi + \Phi'_{\text{G}}}{4\pi}}\,|\downarrow_1\downarrow_2\rangle\,, \tag{4.40}$$

where Φ'_{G} is the geometric phase of $|\psi'\rangle$ as defined in sec. 4.1.2. Of course, the explicit expression for Φ'_{G} is specific to the system under consideration, i.e. the interactions contained in the corresponding Hamiltonian. Inserting the relation between the geometric phase and the entanglement temperature (4.38) into (4.40), the TFD state (4.39) for this system follows directly.

Using the result for the TFD state of the two-qubit system, the reduced density operator $\rho^{(1)}$ assumes the form of the thermal density operator $\rho^{(1)}_{\text{th}}$ at temperature β_{ent}. Correspondingly, the entanglement entropy (4.5) is rewritten as the thermal entropy $S = \beta_{\text{ent}}\langle E\rangle + \ln Z(\beta_{\text{ent}})$, where $\langle E\rangle = \frac{1}{Z(\beta_{\text{ent}})}\sum_{n=1}^{2} E_n e^{-\beta_{\text{ent}}E_n} = \frac{1}{Z(\beta_{\text{ent}})} E e^{-\beta_{\text{ent}}E}$. Therefore, we arrive at the conclusion that the entanglement structure between two qubits gives rise to a thermodynamic description of the physics experienced by the single qubit. This is closely analogous to the temperature experienced by the Rindler observer. In the simple two-qubit

system, the Rindler observer associated to either of the subregions $\text{Rin}_{>/<}$ is replaced by either of the single qubits. In particular, expectation values of observables $\mathfrak{O}^{(1)}$ associated to the single qubit are written as thermal expectation values,

$$\langle \mathfrak{O}^{(1)} \rangle = \text{tr}\left(\rho^{(1)}\mathfrak{O}^{(1)}\right) = \frac{1}{Z(\beta_{\text{ent}})}\,\text{tr}\left(e^{-\beta_{\text{ent}}\tilde{K}^{(1)}}\mathfrak{O}^{(1)}\right), \tag{4.41}$$

where we defined $\tilde{K}^{(1)} = T_{\text{ent}}K^{(1)}$ which is interpreted as the physical Hamiltonian of the thermal system at temperature β_{ent}. The above result (4.41) implies that using only local observables, the single qubit is not able to distinguish whether the measurement results are due to the entanglement between the single qubit and its environment or due to a non-trivial *physical* temperature equal to β_{ent}. By our above analysis, this emergence of temperature is directly related to the non-trivial geometry of the projective Hilbert space indicated by the geometric phase Φ_{G}.

4.2.2. Geometric Phase(s) of the Thermofield Double State

We have established in the previous section that even in quantum systems as simple as two interacting qubits, a non-vanishing entanglement entropy allows for defining a notion of temperature by interpreting the entanglement entropy as a thermal entropy. Using the geometric phases defined by the SZK construction, it is manifest that both entanglement as well as temperature have a geometric explanation. Moreover, this allowed for determining the factorisation properties of the projective Hilbert space. In the following, we apply the above results to the TFD state. This is particularly interesting as the TFD state is considered the dual description of the eternal black hole in Anti-de Sitter spacetime, as reviewed in sec. 3.2.1.

To start, we repeat the general form of the TFD state (3.52) in a system with N energy levels,

$$|\text{TFD}\rangle = \frac{1}{\sqrt{Z(\beta)}}\sum_{n=1}^{N} e^{-\beta\frac{E_n}{2}}|n_L, n_R^*\rangle\,. \tag{4.42}$$

This state provides a pure state description of thermal physics at temperature β. The reduced density operator is simply the thermal density operator, and vice versa, the TFD state is the purification of the thermal density operator with $\dim\mathscr{H}^L = \dim\mathscr{H}^R = N$. The state (4.42) has the advantage that the measurement result of an observable in either of the subsystems $\mathfrak{O}^{L/R}$ can be written as an expectation value in the TFD state without

explicitly using the reduced density operator,

$$\langle \mathfrak{O}^{L/R} \rangle = \langle \text{TFD} | \mathfrak{O}^{L/R} | \text{TFD} \rangle \tag{4.43}$$

where $\mathfrak{O}^{L/R}$ are operators that act non-trivially only on $|n_{L/R}\rangle$ but trivially on $|n_{R/L}\rangle$, respectively. This is the generalisation of our result in (4.41). To discuss the TFD state in light of the SZK construction [166], we note that the TFD state as given in (4.42) is already written in Schmidt decomposed form. The Schmidt coefficients κ_n are given by the square roots of the Boltzmann weights,

$$\kappa_n = \frac{e^{-\beta \frac{E_n}{2}}}{\sqrt{Z(\beta)}} \,. \tag{4.44}$$

Clearly, all of the Schmidt coefficients are non-vanishing for generic values of E_n and β. Therefore, the multiplicity of vanishing Schmidt coefficients appearing in the generic orbit (2.93) is zero, $m_0 = 0$. Moreover, assuming that the energy levels are non-degenerate, i.e. $E_n \neq E_m$ for all $n \neq m$, all of the Schmidt coefficients are different as well. Therefore, all other multiplicities appearing in (2.93) are equal to one, $m_{n\neq 0} = 1$. This determines the entanglement orbit of the TFD state to be given by (2.94),

$$\mathscr{O}_{|\text{TFD}\rangle} = \frac{\text{U}(N)}{\text{U}(1)^N} \times \frac{\text{SU}(N)}{\mathbb{Z}_N} \,. \tag{4.45}$$

Dropping the assumption of non-degeneracy, the first factor in this orbit changes accordingly. As an example, suppose that one of the energies E_{n^*} appears twice, so $m_{n^*} = 2$. This yields $\frac{\text{U}(N)}{\text{U}(2)\times\text{U}(1)^{N-2}}$ for the first factor. Since the Schmidt coefficients (4.44) are generically non-zero, the second factor does not change when energy levels are degenerate.

The entanglement orbit (4.45) and its variations in the presence of degeneracy make explicit that the projective Hilbert space is not factorised, $\mathscr{P}(\mathscr{H}) = \mathbb{C}\text{P}^{N^2-1} \neq \mathbb{C}\text{P}^{N-1} \times \mathbb{C}\text{P}^{N-1}$. The factorised case $\mathscr{P}(\mathscr{H}) = \mathbb{C}\text{P}^{N-1} \times \mathbb{C}\text{P}^{N-1}$ only appears in a special limit. As mentioned in the previous section, the entanglement temperature (4.38) vanishes in the limit of vanishing entanglement. For the TFD state (4.42), in the limit $T \to 0$, i.e. $\beta \to \infty$, all Schmidt coefficients (4.44) but one go to zero. This is seen as follows. Assuming $E_n > 0$, all exponentials in (4.44) tend to zero in the limit $\beta \to \infty$. However, the exponentials are divided by the square root of the partition function, which is given by the sum of all of these exponentials. In the limit $\beta \to \infty$, this sum is dominated by the exponential with the lowest energy as this tends to zero most slowly. In principle, we are free to choose which E_n has the smallest value, but an intuitive and canonical choice is

E_1. Therefore, in the limit $\beta \to \infty$ we can approximate the denominator in (4.44) as

$$\lim_{\beta\to\infty} Z(\beta) = \lim_{\beta\to\infty} \sum_{n=1}^{N} e^{-\beta E_n} \approx e^{-\beta E_1} \,. \tag{4.46}$$

Therefore the Schmidt coefficients (4.44) are approximated as $e^{-\beta\frac{E_n-E_1}{2}}$ with $E_n - E_1 > 0$ for $n \neq 1$. In the limit $\beta \to \infty$, we therefore have that

$$\lim_{\beta\to\infty} \kappa_n = \lim_{\beta\to\infty} e^{-\beta\frac{E_n-E_1}{2}} = \begin{cases} \lim_{\beta\to\infty} 1 = 1 & \text{for } n = 1 \\ 0 & \text{for } n \neq 1 \,. \end{cases} \tag{4.47}$$

With these limiting values for the Schmidt coefficients, the TFD state (4.42) reduces to a product state,

$$\lim_{\beta\to\infty} |\mathrm{TFD}\rangle \to |1_L 1_R\rangle \,. \tag{4.48}$$

The multiplicities important in the SZK construction are $m_0 = N - 1$ and $m_1 = 1$, determining the orbit (2.96) for vanishing entanglement,

$$\mathscr{O}_{\lim_{\beta\to\infty}|\mathrm{TFD}\rangle} = \mathbb{C}\mathrm{P}^{N-1} \times \mathbb{C}\mathrm{P}^{N-1} \,, \tag{4.49}$$

which is precisely the factorised submanifold of the projective Hilbert space.

In principle, the above analysis can also be stated in terms of the geometric phase for the TFD state (4.42). While an explicit calculation for arbitrary N is quite involved, the simple instance of $N = 2$ is sufficient to illuminate this. In this case, there are only two Schmidt coefficients κ_1 and κ_2, given as in (4.44) with energies E_1 and E_2. Following the calculations described in sec. 4.1.2, the geometric phase for the TFD state with $N = 2$ is found as

$$\Phi_{\mathrm{G}} = 2\pi \frac{e^{-\beta E_1} - e^{-\beta E_2}}{e^{-\beta E_1} + e^{-\beta E_2}} \,. \tag{4.50}$$

Redefining the energies E_n conveniently, we set $E_1 = 0$ and $E_2 = E$. Note that this is always possible, already on the level of the TFD state (4.42). The necessary shift of all energies $E_n \to E_n - E_1$ simply cancels due to the normalisation by the partition function $Z(\beta)$. Inverting (4.50) for the temperature, we find exactly the relation (4.38) for $\beta = \beta_{\mathrm{ent}}$. As a side remark, this is consistent with our earlier statement below (4.39) that the TFD state version for a generic two-qubit state can always be obtained. Coming back to the

discussion of (4.50), the geometric phase determines the entanglement orbit structure discussed previously. As before in sec. 4.1.2, the geometric phase is equal to 2π if and only if the projective Hilbert space is factorised.

The geometric phase for the TFD state given in (4.50) characterises the entanglement properties of the state. Moreover, it can be used to determine whether the projective Hilbert space is factorised, cf. (4.49). There exists however another notion of geometric phase for the TFD state which, following our discussion in sec. 2.2.1, should rather be regarded as a topological phase [183]. This phase is sensitive to the topology of the parameter space of the theory, rather than the curvature (i.e. the geometry) of the projective Hilbert space induced by the entanglement. Defining this phase is motivated by observations on black hole physics in AdS/CFT. As we have reviewed in sec. 3.2.1, time is not defined globally in the spacetime of an eternal black hole. Rather, time is defined in the left and right exterior wedges of the black hole, i.e. t_L and t_R. We briefly summarise the consequences of this observation, discussed in detail in sec. 3.2.1, in the following for the convenience of the reader. Since the time-like Killing vector switches sign at the black hole horizon when the time t_R in the right exterior is chosen to flow in one direction, the time t_L in the left exterior has to flow in the opposite direction, cf. fig. 3.5. As time is not defined globally, the relation between the two time coordinates is not fixed uniquely. Rather, there can be an offset δ between the two times, defined as $t_L = 2\delta - t_R$. The offset is usually introduced deep in the bulk at the horizon, while times are naturally identified, i.e. $t_L = t_R$, at the boundary [182]. This offset specifies how the boundary CFTs are glued to the black hole bulk geometry. For each value of δ, the dual state to this geometry can be computed using the Hartle–Hawking wave functional [447]. As we discussed in sec. 3.2.1, the resulting states $|\mathrm{TFD}\rangle_\alpha$ can be understood as time-shifted TFD states, obtained by time evolution with the sum of the boundary Hamiltonians $H_+ = H_L + H_R$ [182]. While evolving with H_+ leads to the phase factors $e^{i\alpha_n}$ within $|\mathrm{TFD}\rangle_\alpha$ denoted in (3.54), the evolution of the TFD state by the difference of the Hamiltonians $H_- = H_L - H_R$ is trivial since the individual contributions cancel out, cf. (3.53). In other words, the difference of the Hamiltonians annihilates the TFD state. On the bulk side, this represents an isometry of the spacetime.

The time-shifted TFD states $|\mathrm{TFD}\rangle_\alpha$ define a class of states dual to the eternal black hole for each set of phases $\{\alpha\}$. Each set of phases corresponds to a different choice for δ. Therefore, δ is part of the parameter space of the theory. As δ has the interpretation of time, the naturally dual variable is expected to have an interpretation of energy. Indeed, while H_- generates a symmetry of the TFD state, evolution by H_+ can be used to alter the set of phases. Therefore, H_+ generates motion in the parameter space and can be considered the second variable of the parameter space. Motivated by this observation, we

define a connection on parameter space by evolving the TFD state with H_+ and taking an exterior derivative w.r.t. the parameter δ, analogous to the usual definition of a connection as in (4.20),

$$A = \mathrm{i}\langle \mathrm{TFD}|U^\dagger \mathrm{d}U|\mathrm{TFD}\rangle\,, \tag{4.51}$$

where $U = e^{\mathrm{i}H_+\delta}$. We point out that this definition does not depend on choosing $|\mathrm{TFD}\rangle$, but equivalently any of the other states $|\mathrm{TFD}\rangle_\alpha$ could have been used. To obtain the topological phase, the connection defined in (4.51) has to be integrated along a closed path,

$$\Phi^{(\mathrm{TFD})} = \oint A\,. \tag{4.52}$$

Given the form of the time-shifted TFD states (3.54), we find that δ has the periodicity $\delta \sim \delta + \frac{\pi}{E_n}$ for each individual energy eigenvalue E_n. Integrating the connection A along this path yields the topological phase. While δ is a periodic variable, E_n is not compact. Therefore, also the parameter space is not a compact manifold. In particular, it is a two-dimensional manifold, where δ and E_n can be understood as angular and radial coordinates, respectively. However, at the origin the angular coordinate loses its meaning. In particular, the periodicity of δ is not defined at $E_n = 0$. This is analogous to our discussion in sec. 4.1.2, where at the north and south pole one of the angular coordinates were not defined. In the present case, that means that the parameter space has the topology of the punctured plane $\mathbb{R}^2\backslash\{0\}$. Paths around the puncture cannot be contracted to a single point, resulting in non-trivial topological phase factors. To be more precise, at every energy E_n (i.e. every radius), the corresponding angular path with periodicity $\delta \sim \delta + \frac{\pi}{E_n}$ leads to a non-trivial phase factor, i.e. a winding number. Combining all these angular paths at different radii, the punctured plane is formed. In sec. 4.2.3, we will find the same result on the topology of parameter space from the bulk perspective.

Before calculating this topological phase for the explicit example of the two-qubit system, we comment on the fine structure of entanglement for the topological phase of the TFD state, as well as the analogy of this phase with the geometric phase discussed in secs. 4.1.2 and 4.1.3. In the previous section, we have found that the geometric phase (4.31) following from the transformation $U^{(\lambda)}$ vanishes when the transformations on both qubits are equal, i.e. when $\lambda = 1$, and does not vanish otherwise. How is this realised in the present case for the TFD state? The transformations we consider are time translations. In particular, since time runs in opposite directions on each boundary (cf. fig. 3.5), the transformation $U = e^{\mathrm{i}H_-\delta}$ is interpreted as performing the same transformation on each boundary. Indeed, since

this transformation is a symmetry of the TFD state, the connection defined analogously to (4.51) for this transformation and the resulting topological phase vanishes. So also in the holographic context, we find that performing the same transformation on both subsystems does not amount to picking up a phase factor, corresponding to $\lambda = 1$ in sec. 4.1.3. On the other hand, the transformation using H_+ does generate a phase. In particular, using the symmetry of the TFD state, every transformation parametrised by δ acting on both subsystems can be brought to a transformation acting on only one of the subsystems,

$$e^{\mathrm{i}(\#_1 H_L + \#_2 H_R)\delta}|\mathrm{TFD}\rangle = e^{\mathrm{i}(\#_1 H_L + \#_2 H_R)\delta} e^{\mathrm{i}\#_2 (H_L - H_R)\delta}|\mathrm{TFD}\rangle = e^{\mathrm{i}(\#_1 + \#_2) H_L \delta}|\mathrm{TFD}\rangle\,, \tag{4.53}$$

where $\#_1, \#_2$ can be any numbers. While in this equation the resulting transformation acts only on the left boundary, the same can be reasoned for a transformation effectively acting only on the right boundary. Analogously to the two-qubit system, we find that for a transformation acting only on one of the subsystems, the state picks up a phase, corresponding to $\lambda = 0$ in sec. 4.1.3. In particular, as we noted in sec. 3.2.1, the additional phases do not affect the entanglement entropy contained in the TFD state. Correspondingly, the topological phase of the TFD state (4.52) can be regarded as a fine structure of entanglement.

To elucidate the previous general discussion, in the following we compute the topological phase of the TFD state in an explicit example, namely the TFD state of the two-qubit system derived in sec. 4.2.1. The TFD state is given in (4.39). The Hamiltonian necessary to define the evolution as in (4.51), as well as the periodicity of δ, is given by the modular Hamiltonian $K^{(1)}$ in (4.33) with h given (e.g.) by (4.36). To be precise, the evolution in (4.51) is defined using the physical instead of the modular Hamiltonian. However, the physical Hamiltonian $H^{(1)}$ in the present case can be obtained by simply rescaling the modular Hamiltonian with the temperature, $H^{(1)} = T_{\mathrm{ent}} K^{(1)}$. While this rescaling alters the explicit expressions for the connection as well as the periodicity of δ, the result for the topological phase is invariant under this rescaling. As a first step in the computation, we note that indeed evolving (4.39) by the difference of $H^{(1)}$ and its analogue $H^{(2)}$ is a symmetry of the state. On the other hand, evolution with the sum of these operators for a duration δ allows for defining the periodicity of this parameter,

$$e^{\mathrm{i}(H^{(1)} + H^{(2)})\delta}|\psi\rangle = \frac{1}{\sqrt{Z(\beta_{\mathrm{ent}})}}\left(e^{-2\mathrm{i}E\delta}|\downarrow_1\downarrow_2\rangle + e^{2\mathrm{i}E\delta} e^{-\beta_{\mathrm{ent}}\frac{E}{2}}|\uparrow_1\uparrow_2\rangle\right). \tag{4.54}$$

The periodicity δ_{P} for δ is defined such that the time-evolved state is precisely equal to the original state, i.e. evolution for δ results in the same state as evolution for $\delta + \delta_{\mathrm{P}}$. In

the above case, this determines the periodicity as

$$\delta_{\mathsf{P}} = \frac{\pi r}{E}\,, \tag{4.55}$$

where $r \in \mathbb{Z}$ is an integer. Evaluating the connection (4.51) for the present case is straightforward and results in

$$A = 2E\frac{1 - e^{-\beta_{\text{ent}}E}}{1 + e^{-\beta_{\text{ent}}E}}\,. \tag{4.56}$$

Integrating this connection over the periodicity (4.55), the topological phase follows as

$$\Phi^{(\mathsf{TFD})} = \int_0^{\delta_{\mathsf{P}}} A = 2\pi r\frac{1 - e^{-\beta_{\text{ent}}E}}{1 + e^{-\beta_{\text{ent}}E}} = \Phi_{\mathsf{G}} r\,, \tag{4.57}$$

where in the last equality we inserted the geometric phase (4.25) calculated as a measure of entanglement and factorisation in sec. 4.1.2.

We pointed out before that the phase $\Phi^{(\mathsf{TFD})}$ defined for the TFD state is of a topological nature and in particular has an interpretation as a winding number. These statements can be justified considering the result in (4.52). On the right-hand side appears the integer, which counts how often the evolution returns to the original state. Put more abstractly, it counts how often the path in the parameter space with topology $\mathbb{R}^2\backslash\{0\}$ wraps around the puncture at the origin. The other factor Φ_{G} can be understood as follows. Usually, when defining a winding number, the integral involved in the computation is normalised by 2π, which cancels the volume of the circle $\mathbb{S}^1$ along which the integral is performed. However in the present case, the angular coordinate is not periodic by 2π, but by (4.55). Correspondingly, the volume differs from 2π. Rather, the geometric phase Φ_{G} appears, which as discussed in sec. 4.1.2 is equal to the volume of the corresponding entanglement orbit, cf. the second paragraph below (4.25). This change in volume is induced by the non-vanishing entanglement between the two qubits. Moreover, we note that for maximal entanglement the topological phase (4.57) vanishes. This happens since for maximal entanglement, time evolution as in (4.54) leaves the state completely invariant, as occurs for evolution using the difference of the Hamiltonians already for arbitrary entanglement.

Finally, let us point out that this topological phase is also accessible to measurements in principle. Using quantum approximate optimisation algorithms for transverse field Ising models [473], TFD states can be prepared experimentally with high accuracy. Adjusting this algorithm in a proper way to prepare the time-shifted TFD state (3.54) instead of the usual TFD state (3.52) enables to experimentally probe the entanglement structure provided by the TFD state and also the topological phase defined above. Such experiments are an

important step towards probing wormhole(-like) features such as the topological phase in the lab. In the following section, we discuss how this topological phase arises from bulk considerations. In particular, we discuss in more detail how this topological phase is related to the wormhole interpretation as the dual bulk geometry to the TFD state.

4.2.3. Topological Phase in JT Gravity

We have now understood how a topological phase for the TFD state can be defined. This phase probes the topology of the parameter space of the theory and in principle even is accessible in actual experiments. In the following, we show how the same phase arises in the gravitational picture by analysing the phase space of the theory. This will in particular enable us to make precise which bulk features are probed by this topological phase by specifying a particular class of bulk diffeomorphisms responsible for generating this phase. We discuss this in detail for the case of JT gravity using insights gained in [466] (see also [139]).

Of particular importance to this analysis are the time-shifted TFD states $|\text{TFD}\rangle_\alpha$. We have briefly reviewed already in sec. 3.2.1 that these define a class of states dual to the eternal black hole that arise by time evolution for an amount δ of the TFD state $|\text{TFD}\rangle$ using H_+. To obtain the phase space of the gravitational theory, it is important to note that $|\text{TFD}\rangle_\alpha$ may also be defined directly in the path integral formalism using the Hartle–Hawking wave functional. Given the black hole geometry with Lorentzian signature, the TFD state is obtained by Wick rotating to Euclidean signature, fixing a time slice and performing the path integral on that slice as described in sec. 3.2.1. In particular, for the state $|\text{TFD}\rangle$, the slice $\delta = 0$ is chosen. Correspondingly, to obtain the states $|\text{TFD}\rangle_\alpha$, we simply choose to perform the path integral at the different slice $\delta \neq 0$. This is visualised on the left of fig. 4.3. The necessary steps of the calculation are mostly unchanged, except when introducing the anti-unitary operator Θ. Before, we used this operator to define $|n^*_>\rangle = \Theta^\dagger |n_<\rangle$. This definition is however equally valid when including an overall phase factor. As pointed out before, an anti-unitary operator is essentially always written as a product of the time-reversal operator $\mathscr{T}$ and any unitary operator V. Therefore, we are free to change $V \to V' = e^{i\alpha_n} V$. Clearly, V' is still unitary. This can equivalently be phrased as defining a new time-reversal operator $\mathscr{T}$ that reflects about $\delta \neq 0$ instead of $\delta = 0$, without changing V [455]. However, including the additional phases for $\delta \neq 0$ allows for properly incorporating the choice of time slice $\delta \neq 0$. Indeed, completing the calculational steps of sec. 3.2.1 with this choice of including the phase factors $e^{i\alpha_n}$ in the definition of Θ naturally leads to the time-shifted TFD states defined using the Hartle–Hawking wave functional.

To explain how the topological phase of the previous section arises in the gravitational picture, the concept of asymptotic symmetries is important. These symmetries are understood by analysing the fall-off behaviour of bulk diffeomorphisms close to the boundary. While in the bulk, diffeomorphisms are a symmetry, not all diffeomorphisms are well-defined symmetries of the boundary theory. In the context of AdS/CFT, the study [365] provides an early example, with two copies of the Virasoro group as the asymptotic symmetry of three-dimensional Anti-de Sitter spacetime. Moreover, the asymptotic symmetries for rotating black holes in four bulk dimensions are analysed in [474], which also provides an intuitive introduction to asymptotic symmetries. In general, the asymptotic symmetries arise from putting boundary conditions such that the variational principle is well-defined. Considering a D-dimensional manifold $\mathscr{M}$ with boundary, the variation of the Einstein–Hilbert action includes the term

$$\delta S \subset \int_{\partial\mathscr{M}} \mathrm{d}^{D-1}x\sqrt{\gamma}\, T_{ij}\delta\gamma^{ij}\,, \tag{4.58}$$

where γ is the induced metric on the boundary, with $\delta\gamma^{ij}$ its variation. The components T_{ij} arise by the variation and form the energy-momentum tensor on the boundary [433]. To set this boundary term to zero, usually one imposes Dirichlet boundary conditions on the induced metric, i.e. $\delta\gamma^{ij} = \mathscr{C}^{ij}$, where $\mathscr{C}^{ij}$ is a tensor with constant entries. Asymptotic symmetries then correspond to bulk diffeomorphisms that do not break these boundary conditions. In other words, these bulk diffeomorphisms have to approach constants close to the boundary. Among these diffeomorphisms, there exist two subclasses distinguished by whether the corresponding constant vanishes or not. If this constant vanishes, the corresponding diffeomorphism is referred to as trivial, and non-trivial for non-vanishing constant. The non-trivial diffeomorphisms are also referred to as large gauge transformations and change the dual state that the boundary theory is in. Trivial diffeomorphisms do not change this state. Using these transformations, the asymptotic symmetry group $\mathscr{G}_{\text{asy}}$ is defined as a quotient of all allowed diffeomorphisms by the trivial diffeomorphisms. Accordingly, an element of $\mathscr{G}_{\text{asy}}$ should be considered as a representative of an equivalence class of diffeomorphisms. This equivalence class contains all non-trivial diffeomorphisms related to each other by a trivial diffeomorphism. This is visualised for time translations, which are always part of $\mathscr{G}_{\text{asy}}$, in fig. 4.3.

Time translations are also the important transformations when applying these techniques to the time-shifted TFD states. We pointed out before that the time-shifted states $|\text{TFD}\rangle_\alpha$ arise by time evolution using the sum of the boundary Hamiltonians H_+. On the other hand, evolution by H_- is a symmetry of the TFD state and an isometry of the bulk spacetime. Therefore, evolution by H_+ corresponds to a non-trivial bulk diffeomorphism

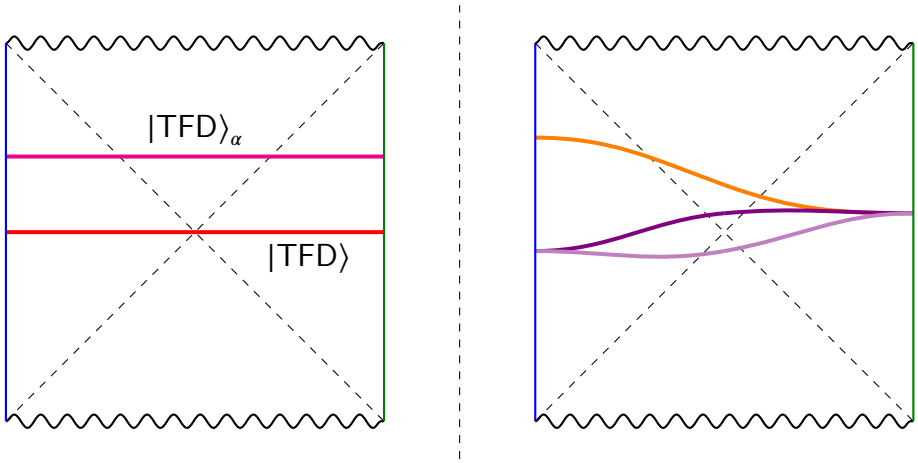

Figure 4.3: On the left, two time slices (red and magenta) of the eternal black hole geometry are shown. Performing the Euclidean path integral at the respective slices leads to the states $|\text{TFD}\rangle$ and $|\text{TFD}\rangle_\alpha$. On the right, the types of bulk diffeomorphisms are shown. The violet and light violet lines represent the bulk diffeomorphisms related by a trivial diffeomorphism, while the orange line is a bulk diffeomorphism related to the other two lines by a non-trivial diffeomorphism.

and evolution by H_- corresponds to a trivial diffeomorphism. An explicit form for the bulk diffeomorphism corresponding to evolution by H_+ was discussed in [454, 455]. All other bulk diffeomorphisms related to this particular one by the evolution of H_- form an equivalence class. Considering evolution by H_+, we might for example combine this with another evolution using H_- such that the combined transformation acts only on degrees of freedom of one boundary, which however results in the same boundary state. This associates a bulk interpretation to the discussion of the previous section around (4.53). As visualised in fig. 4.4, evolutions by H_+ and H_- correspond to fixing different time slices than the canonical one on which the Euclidean path integral is computed. While H_+ simply amounts to fixing a different time slice with $\delta \neq 0$, evolution by H_- corresponds to a time slice which looks quite complicated, yet still has $\delta = 0$ and indeed is completely equivalent to the canonical horizontal slice at $\delta = 0$.

Given this observation, it is clear also from the bulk perspective that evolution by H_+ changes the state, and thereby defines a non-trivial path in the phase space of the theory. The corresponding coordinates of the phase space are given by δ and H_+, but not H_-, since for the asymptotic symmetry group, we quotiented the allowed transformations by the trivial diffeomorphisms. The coordinates δ and H_+, carrying the notions of time and energy, respectively, are dual to each other. As expected, the phase space is even dimensional and can be given a symplectic structure. We will shortly discuss this in an explicit example for JT gravity. Before that however, we point out that apart from time translations, also other symmetries can be considered. Much like the Hamiltonians H_L and H_R in the present

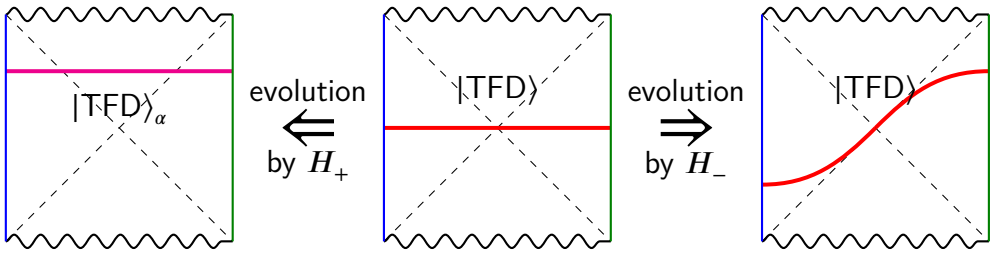

Figure 4.4: Visualisation of the effect of trivial and non-trivial diffeomorphisms on the TFD state. In the middle, the canonical time slice at $\delta = 0$ leading to the usual TFD state is visualised. On the left, the non-trivial diffeomorphism corresponding to H_+ leads to a different slice with $\delta \neq 0$ and the time-shifted TFD state. On the right, the trivial diffeomorphism corresponding to H_- changes the form of the time slice at $\delta = 0$, but does not change the physical properties, and in particular not the dual TFD state.

discussion, other symmetries will have generators Q_L and Q_R. Evolving the appropriately adjusted TFD state by the difference of these generators results in a symmetry of the adjusted TFD state, while evolution by the sum leads to additional phase factors which depend on a parameter corresponding to the considered symmetry. As an example, this could be a rotational symmetry, with the corresponding parameter analogous to δ specifying how the angles in the left and right boundary are oriented w.r.t. each other. For each of these parameters, a phase factor and corresponding connection can be defined as in (4.51). The parameter space formed by these parameters includes every classical solution, i.e. every bulk geometry satisfying the corresponding Einstein equations. In the current two-sided setup, this parameter space follows from the asymptotic symmetry group by taking an appropriate quotient. Each boundary has the asymptotic symmetry group $\mathscr{G}_{\text{asy}}^{(L/R)}$, so the full symmetry is given by $\mathscr{G}_{\text{asy}}^{(L)} \otimes \mathscr{G}_{\text{asy}}^{(R)}$. To account for the isometries of the spacetime, this has to be quotiented by the diagonal subgroup $\mathscr{G}_{\text{D}}$ of this product. This quotient provides the parameter space or moduli space $\mathscr{G}_{\text{M}}$ of the theory,

$$\mathscr{G}_{\text{M}} = \frac{\mathscr{G}_{\text{asy}}^{(L)} \otimes \mathscr{G}_{\text{asy}}^{(R)}}{\mathscr{G}_{\text{D}}} \,. \tag{4.59}$$

Quantisation of this parameter space provides the projective Hilbert space. For more details on this general construction see e.g. the first appendix of [135] (see also [475]). The topological phase factors introduced above probe the topology of this parameter space. For the scope of discussing non-factorisation, time translations are sufficient, which is why we focus on this case in the following discussion. In particular, time translations are present for any dimension of bulk and boundary, while e.g. the possible rotations depend on the specific setting.

Let us give an explicit example for the above in JT gravity based on the results of [466],

which we first briefly state in the following. On a manifold $\mathscr{M}$ that is asymptotically an Anti-de Sitter spacetime with metric g, JT gravity is a version of two-dimensional gravity coupled to the Dilaton field ϕ [426, 427]. The action of this theory is given by

$$S_{\mathrm{JT}} = 2\pi\phi_0\chi(\mathscr{M}) + \int_{\mathscr{M}} \mathrm{d}^2x\sqrt{-g}\,\phi(R[g]+2) + 2\int_{\partial\mathscr{M}} \mathrm{d}t\sqrt{\gamma}\,\phi(K-1)\,, \tag{4.60}$$

where ϕ_0 is the constant part of the dilaton field, $\chi(\mathscr{M})$ is the Euler character of the manifold and K is the extrinsic curvature of the boundary of $\mathscr{M}$. Note that the boundary is one-dimensional and only consists of time. Varying this action w.r.t. the metric and the dilaton, the equations of motion are found as [466]

$$R[g]+2=0 \quad \text{and} \quad (\nabla_\mu\nabla_\nu - g_{\mu\nu})\phi = 0\,, \tag{4.61}$$

where ∇_μ is the covariant derivative for the metric with components $g_{\mu\nu}$. A solution to these equations describing a black hole can be found and, expressed in Schwarzschild coordinates, is given by [466]

$$\mathrm{d}s^2 = -(r^2 - r_{\mathrm{S}}^2)\mathrm{d}t^2 + \frac{\mathrm{d}r^2}{r^2 - r_{\mathrm{S}}^2} \quad \text{and} \quad \phi = \phi_{\mathrm{b}} r\,, \tag{4.62}$$

where $r_{\mathrm{S}} = \frac{\phi_{\mathrm{h}}}{\phi_{\mathrm{b}}}$. Here ϕ_{h} and ϕ_{b} are the values of the dilaton at the horizon and the asymptotic boundary, respectively. In particular, a horizon is present as long as $\phi_{\mathrm{h}} > 0$. Correspondingly, fixing ϕ_{h} specifies the precise solution to the equations of motion and therefore, ϕ_{h} is part of the phase space of the theory. The other variable of the parameter space is given by δ, as discussed previously. To obtain the symplectic form on parameter space, the Hamilton equations of motion in the form (2.53) become useful. The symplectic form is determined by calculating derivatives of the Hamiltonian w.r.t. each of the parameters. The left and right Hamiltonians in the present setting are identified as the component T_{tt} of the boundary energy-momentum tensor, resulting in [466]

$$H_L = \frac{\phi_{\mathrm{h}}^2}{\phi_{\mathrm{b}}} = H_R\,. \tag{4.63}$$

As expected, the difference H_- of these Hamiltonians is a trivial operator and does not appear as a variable in parameter space, as opposed to their sum H_+. The two equations defining this system are simple, as the time δ obviously changes with time while ϕ_{h} is constant, so [466]

$$\partial_\delta\delta = 1 \quad \text{and} \quad \partial_\delta\phi_{\mathrm{h}} = 0\,. \tag{4.64}$$

Using (2.53) allows to derive the symplectic form. In parameter space coordinates $x = (\delta, \phi_h)$, this equation is written as

$$\partial_\delta x^a = \left(\Omega^{-1}\right)^{ab} \partial_b H \,, \tag{4.65}$$

where in our current setting $H = H_+$. Using the equations of motion (4.64) and the derivatives of the Hamiltonian $\partial_\delta H_+ = 0$ and $\partial_{\phi_h} H_+ = \frac{4\phi_h}{\phi_b}$ results in the symplectic form [466]

$$\Omega = \frac{4\phi_h}{\phi_b} \mathrm{d}\delta \wedge \mathrm{d}\phi_h = \mathrm{d}\delta \wedge \mathrm{d}H_+ \,. \tag{4.66}$$

The second equality makes manifest that δ is the canonically dual variable to H_+.

In the following, we use the above results to obtain the topological phase of the TFD state defined in sec. 4.2.2 by analysing the topology of the parameter space of JT gravity. The left and right Hamiltonians generate the time translations as part of the asymptotic symmetry groups. In particular, since the boundary for JT gravity only has the time dimension, time translations are the only transformations contained in $\mathscr{G}_{\text{asy}}^{(L/R)}$. Therefore, the asymptotic symmetry groups are simply $\mathrm{U}(1)$ transformations generated by the respective Hamiltonians. The symmetry of the TFD state generated by H_- as the isometry of the bulk solution provides another factor of $\mathrm{U}(1)$, which is precisely the diagonal subgroup of $\mathrm{U}(1) \otimes \mathrm{U}(1)$. Correspondingly, at fixed energy, the parameter space has the topology

$$\mathscr{G}_{\text{M}} = \frac{\mathrm{U}(1) \otimes \mathrm{U}(1)}{\mathrm{U}(1)} = \mathrm{U}(1) \simeq \mathbb{S}^1 \,. \tag{4.67}$$

The energy is specified by the value of ϕ_h. At each value for ϕ_h, the parameter space has the topology of a circle, which is not a simply connected manifold. In particular, to have a geometry with a horizon as in (4.62), ϕ_h has to be non-vanishing. Therefore, the symplectic form (4.66) on the parameter space is only defined for $\phi_h > 0$. In other words, it does not cover all of $\mathbb{R}^2$ in polar coordinates, but the origin is removed, i.e. the symplectic form is defined on the punctured plane $\mathbb{R}^2 \backslash \{0\}$, as obtained also on the quantum mechanical side below (4.52). Therefore, the same winding numbers as in sec. 4.2.2 can be defined as counting how often the path generated by H_+ winds around the puncture, analogously to what we obtained in the aforementioned section e.g. for the two-qubit example in (4.57).

The winding number arises due to the non-trivial topology of the parameter space, which in turn results from non-factorisation in the bulk. In particular, the path of integration to calculate the winding number is understood as entering the wormhole from one side, exiting on the other side and then closing in the exterior region. In particular, we can imagine

this path as stretching between the boundaries in the spirit of a Wilson line indicating the non-factorisation as discussed in sec. 3.2.2. In the upcoming sec. 5.1, we will make this more precise in the higher-dimensional setting of AdS_3/CFT_2.

Geometric Phases and Entanglement in AdS/CFT

5

The notion of geometric phases is not confined to quantum systems with finite dimensional Hilbert spaces, but can be straightforwardly generalised to the setting of QFT. This generalisation requires identifying the symmetry group of the system as well as a subgroup of said symmetry group that leaves state vectors invariant up to a phase. Quotienting out this subgroup provides the base space of a principal fibre bundle, where the fibre itself is given by the subgroup. This quotient space is also known as a coadjoint orbit. The holonomy of this fibre bundle is again a geometric phase. Two examples for this procedure important in holography, in particular AdS_3/CFT_2, are the *Virasoro Berry phase* [167] and the *modular Berry phase* [168–170]. For the former, the symmetry group in question is taken as the Virasoro group. The Virasoro Berry phase is understood as a probe of the geometry of the coadjoint orbit. As upon quantisation the coadjoint orbit provides the projective Hilbert space, this naturally generalises the analysis of the previous section, where we considered transformations of $U(n)$ acting on finite dimensional Hilbert spaces. Modular Berry phases on the other hand are holonomies picked up by parallel transport in the space of modular Hamiltonians of the CFT. Physically, this parallel transport is understood as a deformation of the CFT subregion measuring the entanglement. The modular Berry phase is therefore understood as a probe of the entanglement structure. In this section, we extend upon the results of sec. 4 to promote both the Virasoro and the modular Berry phase as diagnostic tools for non-factorisation in AdS_3/CFT_2. In particular, these phases are defined purely within the boundary theory such that non-factorisation of the boundary Hilbert space becomes manifest. These two phases are particularly good candidates in this task for the following reasons. First, the Virasoro Berry phase is defined in the same spirit as the geometric phase within the SZK construction of sec. 4.1.2. By our detailed analysis of this phase for two interacting qubits, we know that such phases can be used to diagnose non-factorisation. Moreover, the modular Berry phase probes the entanglement structure of the CFT. By the ER=EPR proposal the entanglement structure of the CFT encodes the connected bulk geometry. The non-factorisation induced by the connected bulk geometry therefore must also be encoded in the modular Berry phase.

A relation between wormhole physics and geometric phases has also been proposed in [165], based on a careful analysis of the partition function in generic quantum systems. We have already pointed to this work at the end of sec. 4.1.1. As this relation will be more

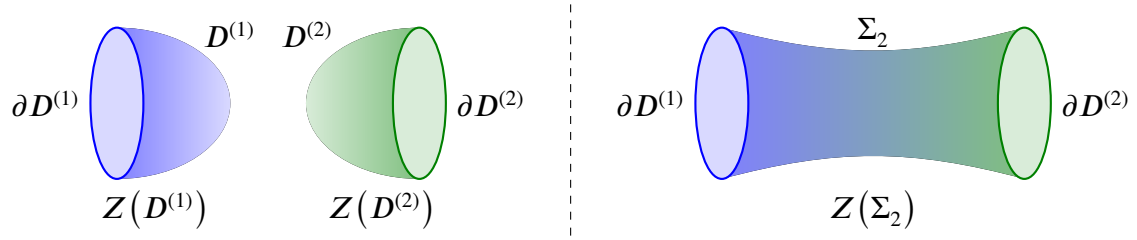

Figure 5.1: The two-point function of the thermal partition function is shown in two cases. On the left, the symplectic form of the thermal system is exact. In the partition function, the integral over $D^{(i)}$ reduces to a boundary integral and correspondingly, the full partition function factorises, $Z\left(D^{(1)} \times D^{(2)}\right) = Z\left(D^{(1)}\right) Z\left(D^{(2)}\right)$. On the right, the symplectic form is non-exact. The partition function is evaluated on the connected geometry Σ_2 and the integral over Σ_2 does not reduce to a boundary integral. Accordingly, the partition function does not factorise, $Z\left(\Sigma_2\right) \neq Z\left(D^{(1)}\right) Z\left(D^{(2)}\right)$.

important to the analysis in this section, let us briefly state the main idea. For a thermal system at inverse temperature β, the partition function is given by [476]

$$Z(\beta) = \int \left[\mathscr{D}X\right] \exp\left(\int_D \Omega - \oint_{\partial D} \mathrm{d}t\, H\right) = Z(D)\,, \tag{5.1}$$

where D is a disk with the thermal circle ∂D as a boundary, $\Omega = \Omega_{ab}\mathrm{d}X^a \wedge \mathrm{d}X^b$ is the symplectic form and X are the degrees of freedom of the system that the Hamiltonian H depends on. The second equality states that the thermal partition function is identified with the functional integral over the disk D bounded by the thermal circle [165]. If the symplectic form is exact the integral over D in the partition function reduces to an integral over ∂D. This happens e.g. for the canonical symplectic form $\Omega^{\mathrm{can}} = \mathrm{d}p \wedge \mathrm{d}q$, where $\int_D \Omega^{\mathrm{can}} = \oint_{\partial D} \mathrm{d}t\, p\partial_t q$ reduces to the familiar kinetic piece of the action. In this case, the disk D has no influence on the physics. This changes if Ω is non-exact since $\int_D \Omega$ does not reduce to an integral over ∂D. Since Ω is closed, $\mathrm{d}\Omega = 0$, the integral over D depends only on the boundary values of X and the geometrical features of D are not important. The topology of D however does matter for non-exact Ω. Wormholes can be introduced to the system by replacing the disk D with an arbitrary two-dimensional manifold Σ_n that has n thermal circles as boundaries. This allows to define the partition function for the wormhole with n mouths as $Z(\Sigma_n)$ interpreted as the n-point function of the single thermal partition function $\langle Z(\beta)^n \rangle$, as visualised in fig. 5.1 for $n = 2$. This partition function in particular does not factorise [165],

$$\langle Z(\beta)^n \rangle = Z(\Sigma_n) \neq Z(D)^n = \langle Z(\beta) \rangle^n\,. \tag{5.2}$$

The non-factorisation is a direct consequence of the non-exactness of Ω as in this case,

the boundary values of X on different boundaries are intrinsically linked by the non-trivial topology. From the perspective of the path integral, such links are understood as non-local terms in the symplectic form connecting different thermal circles.

By (2.83) geometric phases are defined as the integral of non-exact symplectic forms. Therefore, the above result of [165] provides a useful tool in studying non-factorisation due to wormhole physics using geometric phases. In this section we apply this method to analyse non-factorisation by computing Virasoro Berry phases in the CFT_2 dual to the black hole solution in AdS_3 known as the BTZ black hole [477, 478], and modular Berry phases in the CFT_2 dual to the BTZ black string. The black string is understood as a black hole solution with a non-compact horizon. In both cases, we identify non-local terms in the symplectic form which leads to the corresponding geometric phases. These non-local terms render the symplectic form non-exact and therefore signal non-factorisation by the arguments of [165]. This shows that both the Virasoro and modular Berry phases provide measures that signal the non-factorisation of the CFT Hilbert space.

We start our analysis in sec. 5.1 by briefly reviewing how Virasoro Berry phases are defined. We then show that Virasoro Berry phases for two entangled CFTs are coupled to each other, indicating non-factorisation. This manifests as an additional non-local term in the symplectic form spoiling the exactness. We demonstrate this for a toy model of $\text{U}(1)$ Chern–Simons theory as well as $\text{SL}(2,\mathbb{R})$ Chern–Simons theory, both considered on a spacetime with an annulus geometry. Next in sec. 5.2, we discuss modular Berry phases as another probe of spacetime wormholes, and in that non-factorisation. We start by briefly explaining the definition of modular Berry phases, followed by the explicit computation of the modular Berry curvature for the two-sided BTZ black string. We interpret the non-trivial modular Berry curvature as a probe for the spacetime wormhole. We finally discuss which aspects of the bulk spacetime are probed by the Virasoro and modular Berry phases as well as the topological phase defined for the TFD state in sec. 4.2.2 by specifying the kinds of bulk diffeomorphisms associated to these phase factors. The new results discussed in this section appeared in [185] and we mainly follow the presentation therein.

5.1. Virasoro Berry Phase

In the earlier sec. 4.1 we have discussed geometric phases in simple bipartite quantum systems, in particular for an interacting two-qubit system. The geometric phases defined in this context made use of the natural symmetry of bipartite $n \times n$-dimensional quantum systems, namely local unitary transformations of $\text{U}(n) \otimes \text{U}(n)$. This enabled us to explain the factorisation properties of the projective Hilbert space using the geometric phase. In this section, we generalise this approach to the setting of $\text{AdS}_3/\text{CFT}_2$. For CFT_2,

a straightforward generalisation of the geometric phase in quantum mechanical systems leads to defining the *Virasoro Berry phase* [167]. In the following sec. 5.1.1, we first briefly review how Virasoro Berry phases are defined as the holonomy of coadjoint orbits. For details on this derivation, we refer to [167]. This essentially reformulates the techniques used in the previous section in a way such that it is straightforwardly applicable to any symmetry group, in particular the Virasoro group relevant for CFT_2. With this machinery at hand, we show that the presence of an eternal black hole in the AdS_3 bulk spacetime is signalled from the boundary perspective by the Virasoro Berry phase. In particular, we derive the symplectic form and show that it is non-exact in the presence of the eternal black hole. To illustrate the essential features in this argument, we first discuss this for a $\mathrm{U}(1)$ Chern–Simons theory on an annulus topology as a toy model of the black hole in sec. 5.1.2. Generalising these insights to an $\mathrm{SL}(2,\mathbb{R})$ Chern–Simons theory on the annulus, which describes the actual spacetime black hole in AdS_3, we show again that the resulting symplectic form is non-exact in sec. 5.1.3. In both cases, we discuss the non-factorisation of the corresponding Hilbert spaces in terms of open Wilson lines, related to the respective geometric phases, stretching between the boundaries of the annuli.

5.1.1. Holonomy of Virasoro Coadjoint Orbits

The geometric phases computed in sec. 4.1 were sensitive to the geometric properties of the projective Hilbert space. This space was understood as the base space of a principal fibre bundle with fibre $\mathrm{U}(1)$. The fibre accounts for global phases of state vectors $|\psi\rangle$ that cannot be accessed by any local measurement. This construction naturally generalises as follows. Consider an arbitrary group G, with unitary representations $\mathfrak{u}(g)$ of group elements $g \in G$ acting on state vectors $|\psi\rangle$. Assuming that the group element may be parametrised by a parameter $s \in [0,1]$ such that $g_0 = \mathbb{1}$ and $g_1 = g$, the transformation g_s describes a path on the group manifold. To this path, the sequence of states $\mathfrak{u}(g_s)|\psi\rangle$ is associated. Assume further that there is a subgroup K of G such that transformations $k \in K \subset G$ leave the highest weight state vector $|\phi\rangle$ invariant up to an overall phase, $\mathfrak{u}(k)|\phi\rangle = e^{i\gamma}|\phi\rangle$. The subgroup K is called the stabiliser group. These transformations do not change between the rays (2.56). Therefore, the subgroup K naturally takes the place of $\mathrm{U}(1)$ used in our earlier discussions. In analogy to our discussion of the projective Hilbert space in sec. 2.2.1, transformations $k \in K$ only resulting in overall phases motivates defining the homogeneous space $\mathscr{G} = \frac{G}{K}$. This provides the base space $\mathscr{B}$ of a principal fibre bundle with fibre $\mathscr{F} = K$. The homogeneous space $\mathscr{G}$ is also known as a coadjoint orbit. Following the method of geometric quantisation, the coadjoint orbit provides the projective Hilbert space of the system under consideration in the presence of the symmetry

transformations described by K [263–265].

With the fibre bundle defined, the next step is to establish the notion of geometric phases testing whether the bundle is trivial. As reviewed in sec. 2.2.1, non-trivial geometric phases arise for non-trivial fibre bundles when state vectors acquire an overall phase when being transported along a closed path. In the present context, as pointed out above, transformations g_s are understood as implementing paths. Consider now a group element g_s that implements a closed path in the base space $\mathscr{G}$. Due to the stabiliser group K, i.e. the fibre, the sequence of states $\mathfrak{u}(g_s)|\phi\rangle$ does generally not return to exactly the initial highest weight state $|\phi\rangle$. Rather g_s may implement a path that is closed in the base manifold $\mathscr{G}$, but the endpoints of the path are at different positions in the fibre, cf. the left of fig. 2.13. In this case, the final state differs by an overall geometric phase, i.e. $\mathfrak{u}(g_1)|\phi\rangle = e^{\mathrm{i}\Phi_G}|\phi\rangle$. To quantify this phase factor, local gauge fields A on the fibre bundle are required. These are defined using the (left invariant) *Maurer–Cartan* form $A_{\mathrm{MC}} = \mathfrak{u}^\dagger(g_s)\mathrm{d}\mathfrak{u}(g_s)$ which is used to define parallel transport on the group manifold (for details see e.g. [269]). In this formulation, the derivative is w.r.t. s. Equivalently, one may also perform the derivative w.r.t. the parameters of the transformation $\mathfrak{u}(g_s)$, such as the Euler angles for compact groups G. These parameters are understood as local coordinates of the base space. In applications to physics, s is often understood as the physical time such that the path described by g_s is understood as an adiabatic variation of the parameters (i.e. the Euler angles). We will shortly provide a simple example to illustrate this in more detail. First however, the local gauge fields are defined by the Maurer–Cartan form as

$$A = \mathrm{i}\langle\phi|A_{\mathrm{MC}}|\phi\rangle\,. \tag{5.3}$$

The geometric phase is then defined as integrating A along the closed path implemented by g_s. Equivalently, more akin to what we have been discussing in previous sections, taking another derivative of the local gauge fields results in the symplectic form $\Omega = \mathrm{d}A$. Integrating the symplectic form over the two-dimensional surface bounded by the closed path defined by g_s yields the geometric phase, cf. (2.83).

Before applying the above mechanism to CFT_2, let us illustrate it for the simple example of $G = \mathrm{SU}(2)$. The highest weight state vector $|\phi\rangle$ is given by $|j\rangle$, where j denotes the total spin. This state vector is invariant, up to an overall phase, under transformations generated by σ_z, so the subgroup relevant for defining a coadjoint orbit is $K = \mathrm{U}(1)$. This is the stabiliser group for orbits of fixed j. The quotient of G by K results in the coadjoint orbit $\mathscr{G} = \frac{\mathrm{SU}(2)}{\mathrm{U}(1)} = \mathbb{C}\mathrm{P}^1$. This is the setup of a single qubit coupled to a magnetic field considered in the original paper introducing geometric phases in physics [163]. Unitary representations of $g \in G$ are unitary 2×2 matrices. In local coordinates, in this case the

Euler parametrisation, these are given by (4.15) and (4.22).[1] For these two unitaries, the local gauge fields follow using (5.3) for $|\phi\rangle = |j\rangle$. The corresponding symplectic form is proportional to the volume form of $\mathbb{C}\mathrm{P}^1 \simeq \mathbb{S}^2$,

$$\Omega = j \sin\theta \mathrm{d}\theta \wedge \mathrm{d}\phi \,. \tag{5.4}$$

Upon integrating this symplectic form over $\mathbb{S}^2$, the geometric phase follows as $\Phi_{\mathrm{G}} = 4\pi j$. This reproduces the well-known result that the Hopf fibration (2.84) is non-trivial [283]. Moreover, geometric quantisation of the coadjoint orbit enforces the half-integer quantisation of the spin, $2j \in \mathbb{Z}$, by the Weyl integrality condition (2.55).

Let us now discuss how this method is used to define the Virasoro Berry phase of [167]. As suggested by the name, these geometric phases start with the Virasoro group, i.e. $G = \mathrm{Vir}$. This is the group of conformal transformations in two spacetime dimensions at the quantum level, i.e. for a CFT_2.[2] The Virasoro group can be understood as centrally extending the group of diffeomorphisms $\mathrm{Diff}(\mathbb{S}^1)$ of the unit circle. Group elements of Vir are given by pairs (f, α), where $f \in \mathrm{Diff}(\mathbb{S}^1)$. The second entry $\alpha \in \mathbb{R}$ accounts for the non-trivial central charge c of the CFT_2. The highest weight state vectors are denoted as $|h\rangle$, with h the conformal weight. Here, two different stabiliser groups are possible, one of which is of particular importance for our purpose. If $h > 0$, the familiar case of $K = \mathrm{U}(1)$ arises, generated by the Virasoro algebra element l_0. However for $h = 0$, i.e. for the vacuum, the stabiliser group is bigger, $K = \mathrm{SL}(2,\mathbb{R})$. This is generated by the Virasoro algebra elements l_{-1}, l_0, l_1 which satisfy the algebra $\mathfrak{sl}(2,\mathbb{R})$, i.e. $[l_n, l_m] = (n-m)l_{n+m}$. Accordingly, there are the coadjoint orbits $\mathscr{G}_0 = \frac{\mathrm{Vir}}{\mathrm{SL}(2,\mathbb{R})}$ and $\mathscr{G}_h = \frac{\mathrm{Vir}}{\mathrm{U}(1)}$. By $\mathrm{AdS}_3/\mathrm{CFT}_2$, these orbits correspond to empty AdS_3 and, for certain values of h, to the case of our interest, namely the black hole in AdS_3. For details on these and other coadjoint orbits of the Virasoro group, we refer the interested reader to [481–484]. Quantisation of these coadjoint orbits produces the projective Hilbert spaces, which in this setting are more commonly referred to as the Verma modules.

The Virasoro coadjoint orbits provide the base space of principal fibre bundles, with fibres given by $\mathrm{U}(1)$ and $\mathrm{SL}(2,\mathbb{R})$ for $h > 0$ and $h = 0$. As for the simple case of $\mathrm{SU}(2)$ briefly discussed previously, local gauge fields can be defined for these fibre bundles. Following (5.3), this requires the Maurer–Cartan form (Θ, α_Θ) for the Virasoro group. As this form

[1] The path in the base space $\mathbb{C}\mathrm{P}^1 \simeq \mathbb{S}^2$ is parametrised by varying the two angular coordinates ϕ and θ. Equivalently, we may assume that these two coordinates are functions of a single parameter s that parametrises the path. For defining the symplectic form on parameter space, the first version has to be used, while the local gauge fields can be formulated in both versions.

[2] To be precise, the conformal group for CFT_2 is given by two copies of the Virasoro group, corresponding to left and right movers, see e.g. [479, 480]. Since these decouple and behave analogous to each other, we focus our discussion on only one of the copies in the following.

defines parallel transport on the group manifold, it must itself be an element of the group, i.e. it has a non-trivial central term α_Θ. An explicit expression has been computed in [482], which reads

$$(\Theta, \alpha_\Theta) = \left(\frac{\dot{f}}{f'}, \frac{1}{48\pi} \int \mathrm{d}\varphi \, \frac{\dot{f}}{f'} \left(\frac{f''}{f'} \right)' \right) . \tag{5.5}$$

Here, f implements the path on the group manifold and is written as a function of the spacetime coordinates t and φ of the CFT_2. Correspondingly, $\dot{f} = \partial_t f$ and $f' = \partial_\varphi f$. A unitary representation of (5.5) results in the Maurer–Cartan form A_{MC} used in (5.3)

$$A_{\mathrm{MC}} = \mathfrak{u}(\Theta) + c\,\mathfrak{u}(\alpha_\Theta) \,, \tag{5.6}$$

where c is the central charge of the CFT_2. Here $\mathfrak{u}(\Theta)$ and $\mathfrak{u}(\alpha_\Theta)$ are understood as unitary representations of the group elements $(\Theta, 0)$ and $(0, \alpha_\Theta)$, respectively. Evaluating the expression (5.3) for the local gauge field A results in [482] [3]

$$A = -\frac{1}{2\pi} \int \mathrm{d}\varphi \left[\left(h - \frac{c}{24} \right) \dot{f} f' - \frac{c}{24} \frac{\dot{f}}{f'} \left(\frac{f'''}{f'} - 2 \left(\frac{f''}{f'} \right)^2 \right) \right] . \tag{5.7}$$

The Virasoro Berry phase is then obtained by integration [167],

$$\Phi_{\mathrm{Vir}} = \int \mathrm{d}t \, A \,. \tag{5.8}$$

Associated to the path f are state vectors $\mathfrak{u}(f)|h\rangle$ that are contained within the same Verma module. Therefore, the phase factor (5.8) is interpreted as a probe for the geometry of the Verma module of the highest weight state vector $|h\rangle$.

We conclude this section with three remarks. First, let us point out that, while usually the circle and the corresponding transformations are parametrised by φ as in the above, an equivalent way is to use the light cone coordinate x^+ to parametrise the Virasoro group describing one half of CFT_2, and x^- for the other copy of the Virasoro group. This manifestly separates the left- and right-moving degrees of freedom of the CFT_2, each of which leads to a Virasoro Berry phase (5.8). Since these degrees of freedom are decoupled, the full Virasoro Berry phase of the CFT_2 is given by the sum of the individual ones, i.e. $\Phi_{\mathrm{Vir}}^{(\mathrm{CFT}_2)} = \Phi_{\mathrm{Vir}}^{(+)} + \Phi_{\mathrm{Vir}}^{(-)}$. Second, we note that the Virasoro Berry phase can also be termed the *geometric action* S_{geo} of the Virasoro group. Considering that Φ_{Vir} in (5.8) is written as an integral over the spacetime coordinates, the integrand can be

[3] Note that, compared to the referenced work, we use the inverse transformation. What we call f is their f^{-1}.

interpreted as encoding the dynamics of an action [482, 483]. In this interpretation, the dynamical field is the transformation f moving on a hollow cylinder [167].[4] This has a nice interpretation in the context of AdS_3/CFT_2 since three-dimensional Anti-de Sitter spacetime is topologically a cylinder, parametrised by the bulk coordinates t, r and φ, see e.g. [385]. Correspondingly the boundary, where the CFT_2 is defined, is the hollow cylinder parametrised by t and φ. The Virasoro Berry phase, i.e. the geometric action, therefore naturally attains the interpretation as describing the asymptotic dynamics of AdS_3. We shall see this explicitly in sec. 5.1.3. Third, we point out that the factor $h-\frac{c}{24}$ in parentheses in the first term in (5.7) can be expressed using the energy-momentum tensor T of the CFT_2. In particular, the expectation value of T in the highest weight state vector $|h\rangle$ results in $\langle h|T|h\rangle = h-\frac{c}{24}$. In the literature on coadjoint orbits of the Virasoro group, this expectation value is often used to specify the particular orbit considered. One defines an orbit label $b_0 = \frac{1}{2\pi}\langle h|T|h\rangle$ that designates the orbit. From this perspective, the stabiliser group K arises as all transformations that leave b_0 invariant.

5.1.2. An Illustrative Example: U(1) Chern–Simons Theory on the Annulus

As discussed in the introduction of sec. 5, non-factorisation can be understood by the non-exactness of the symplectic form of the considered system. Upon integration, non-exact symplectic forms yield geometric phases, cf. (2.83). Studying the Virasoro Berry phase therefore enables us to gain insights into the factorisation puzzle in the setting of AdS_3/CFT_2. In particular, Φ_{Vir} provides a quantity defined on the field theory side that signals non-factorisation. Making this precise for the eternal black hole in AdS_3 is the purpose of the upcoming sec. 5.1.3. To illustrate the necessary computational steps for the eternal black hole, in this section, we use the toy model of U(1) Chern–Simons theory. In particular, we show that a non-exact symplectic form arises in this setting when the theory is put on an annulus geometry. While the annulus resembles the topology of a wormhole, we point out that this toy model is not holographic by itself and only serves as an analogy.[5] U(1) Chern–Simons theory on an annulus was analysed in detail in [485]. In particular, the actions encapsulating the asymptotic dynamics were discussed. Deriving these actions enables us to compute the symplectic form Ω on phase space by first identifying the Hamiltonian of the theory and subsequently using (2.53) to calculate Ω, analogous to our calculation of the symplectic form in JT gravity (4.66) in sec. 4.2.3.

[4] To clarify, we use 'cylinder' for the three-dimensional filled object and 'hollow cylinder' for the surface of the cylinder.

[5] In particular, the equations of motion of the 'bulk' theory do not give rise to the Einstein equations, but rather to those of electrodynamics. Correspondingly, the 'bulk' is not a theory of gravity.

Chern–Simons theories are a special type of topological QFTs with gauge symmetry and can be defined on any three-dimensional manifold $\mathscr{M}$. As we pointed out in sec. 2.2.1 below (2.80), gauge theories can be understood as principal fibre bundles with fibre given by the gauge group G. The connection one-form for such a bundle induces local gauge fields A related by gauge transformations as in (2.80) and valued in the Lie algebra $\mathfrak{g}$ of G. The symplectic form follows as the curvature two-form of these gauge fields, $\Omega^{\text{CS}} = \mathrm{d}A$.[6] By this symplectic form, the Chern–Simons three-form $\mathscr{C}_3$ is defined by $\mathrm{d}\mathscr{C}_3 = \mathrm{tr}\left(\Omega^{\text{CS}} \wedge \Omega^{\text{CS}}\right)$, where the trace is over the indices of the gauge group G [486]. The action of Chern–Simons theory is then obtained as the integral of $\mathscr{C}_3$ over $\mathscr{M}$ [487]

$$S_{\text{CS}}[A] = \frac{k}{2\pi}\int_{\mathscr{M}} \mathscr{C}_3 = \frac{k}{4\pi}\int_{\mathscr{M}} \mathrm{tr}\left(A\wedge \mathrm{d}A + \frac{2}{3}A\wedge A\wedge A\right), \tag{5.9}$$

where k is referred to as the Chern–Simons level. For details on constructing this action, we refer the interested reader to [488].

In the following we are interested in analysing Chern–Simons theory for the case $G = \mathrm{U}(1)$ when considered on a manifold $\mathscr{M}$, representing the spacetime, with the topology of an annulus. Since $\mathrm{U}(1)$ is an abelian group, the Chern–Simons action (5.9) simplifies in that the second term $\propto A\wedge A\wedge A$ vanishes identically. Moreover, the manifold $\mathscr{M}$ is considered as $\mathbb{R}\times\Sigma$, where $\mathbb{R}$ represents the time direction. Correspondingly, Σ is the spatial manifold at any constant time slice, parametrised by a radial coordinate r and an angular coordinate φ. The annulus is specified by considering upper and lower bounds for the range of r, i.e. $r \in [r_{\text{i}}, r_{\text{o}}]$, corresponding to the inner (r_{i}) and outer (r_{o}) radii of the annulus. The annulus is topologically equivalent to a fixed time slice of a wormhole, as visualised in fig. 5.2. The inner and outer circles of the annulus are interpreted as the left and right asymptotic boundaries of the eternal black hole spacetime in AdS_3 at fixed time. Note however that at this stage, as pointed out before this is only an analogy as $\mathrm{U}(1)$ Chern–Simons theory is not a holographic theory. For this reason, we will refer to the wormhole in this section as 'topological', following the results of [165] on non-exact symplectic forms. The actual spacetime wormhole will be analysed in the following sec. 5.1.3.

We now compute the symplectic form for $\mathrm{U}(1)$ Chern–Simons theory on the annulus. The corresponding action was discussed in [485] and reads

$$S_{\text{CS}}[A] = \frac{k}{2\pi}\int_{\mathscr{M}} \mathrm{d}t\mathrm{d}r\mathrm{d}\varphi\left(A_\varphi \partial_t A_r + A_t \Omega^{\text{CS}}_{r\varphi}\right), \tag{5.10}$$

where $\Omega^{\text{CS}}_{r\varphi} = \partial_r A_\varphi - \partial_\varphi A_r$. The equation of motion obtained by varying this action w.r.t. A_t,

[6] Note that this is different from the symplectic form Ω on the phase space that we compute in this section, as indicated by the superscript.

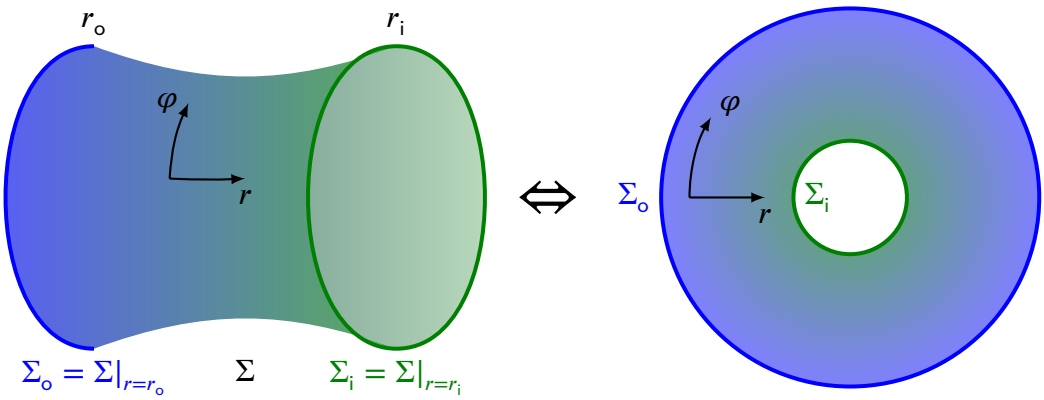

Figure 5.2: On the left, a constant time slice of the three-dimensional eternal black hole in an AdS spacetime is shown. Topologically, this is equivalent to an annulus as shown on the right. The inner and outer radii r_i and r_o of the annulus represent the asymptotic boundaries Σ_i and Σ_o, respectively.

i.e. $\Omega^{CS}_{r\varphi} = 0$, determines

$$A_r = \partial_r \mu(t, r, \varphi) \quad \text{and} \quad A_\varphi = \partial_\varphi \mu(t, r, \varphi) + k_0(t)\,. \tag{5.11}$$

Due to the annulus topology, circles in the φ-direction are not contractible and therefore $\oint \mathrm{d}\varphi\, A_\varphi$ is non-trivial, leading to a non-trivial holonomy. This is accounted for by $k_0(t)$ in the above solution (5.11), as

$$\oint \mathrm{d}\varphi\, A_\varphi = 2\pi k_0(t) \tag{5.12}$$

by using that μ is periodic $\mu(t, r, \varphi) = \mu(t, r, \varphi + 2\pi)$. Next, boundary conditions have to be put on A_t and A_φ both on the inner and the outer boundary. For the later analysis of the eternal black hole, the required conditions are $A_t = A_\varphi$ at r_o and $A_t = -A_\varphi$ at r_i [489]. In the gravitational context, this implies that time evolution on the two boundaries runs in the same direction. While U(1) Chern–Simons theory is only a toy model, the same boundary conditions are chosen. With these boundary conditions, a well-defined variational principle requires adding the term [485]

$$-\frac{k}{4\pi} \int \mathrm{d}t \left[\oint_{r=r_o} \mathrm{d}\varphi\, A_\varphi^2 + \oint_{r=r_i} \mathrm{d}\varphi\, A_\varphi^2 \right] \tag{5.13}$$

to the action. It is convenient to denote the values of μ at the inner and outer radii of the annulus as

$$\mu(t, r = r_i, \varphi) = \Psi(t, \varphi) \quad \text{and} \quad \mu(t, r = r_o, \varphi) = \Phi(t, \varphi)\,. \tag{5.14}$$

With this notation, adding (5.13) to the original action (5.10) and inserting (5.11) reduces the action to two boundary terms by performing the integral over r, resulting in [485]

$$S[\Phi,\Psi,k_0] = \frac{k}{4\pi}\int \mathrm{d}t\Bigg[\left(\oint \mathrm{d}\varphi\,\partial_t\Phi\partial_\varphi\Phi\right) - H_\Phi - \left(\oint \mathrm{d}\varphi\,\partial_t\Psi\partial_\varphi\Psi\right) - H_\Psi \\ + 2\left(\oint \mathrm{d}\varphi\,k_0\partial_t(\Phi-\Psi)\right) - 2H_0\Bigg]\,, \tag{5.15}$$

where the explicit dependence of the variables on t and φ is dropped to reduce clutter. Moreover, the three quantities H_Φ, H_Ψ and H_0 introduced in (5.15) constitute the Hamiltonian of the system [485],

$$H = \frac{k}{4\pi}\left(H_\Phi + H_\Psi + 2H_0\right) = \frac{k}{4\pi}\oint \mathrm{d}\varphi\left[(\partial_\varphi\Phi)^2 + (\partial_\varphi\Psi)^2 + 2k_0^2\right]. \tag{5.16}$$

The action (5.15) describes a theory of two chiral bosons. More precisely, at the inner boundary $\Sigma_\mathrm{i} = \Sigma|_{r=r_\mathrm{i}}$ the field Ψ is defined, while on the other boundary $\Sigma_\mathrm{o} = \Sigma|_{r=r_\mathrm{o}}$ the field is Φ. The individual dynamics are described by the two terms in the first line in (5.10). The second line describes the dynamics of the holonomy k_0. The holonomy serves as a coupling between the chiral bosons on the two boundaries. Moreover, the corresponding canonically conjugate momentum Π_0 is given in terms of the chiral bosons Φ and Ψ [485]

$$\Pi_0 = \frac{\partial L}{\partial(\partial_t k_0)} = -\frac{k}{2\pi}\oint \mathrm{d}\varphi\,(\Phi-\Psi)\,, \tag{5.17}$$

where L is the Lagrangian of the action (5.15) defined as $S = \int \mathrm{d}t\,L$. Using the form of A_r given in (5.11) together with the definition of Φ an Ψ in (5.14), the difference between Φ and Ψ can be expressed as a radial integration,

$$\Phi - \Psi = \mu(t, r=r_\mathrm{o},\varphi) - \mu(t, r=r_\mathrm{i},\varphi) = \int_{r_\mathrm{i}}^{r_\mathrm{o}} \mathrm{d}r\,A_r\,. \tag{5.18}$$

Therefore, the momentum Π_0 conjugate to the holonomy k_0 is understood as a Wilson line stretching between the two boundaries Σ_i and Σ_o. This Wilson line threads the topological wormhole of U(1) Chern–Simons theory on an annulus. Correspondingly, Π_0 indicates the non-factorisation from the boundary perspective. This is in line with the arguments of [462] on the importance of open Wilson lines when discussing Hilbert space factorisation, reviewed towards the end of sec. 3.2.2. In particular, the action (5.15) is invariant under $\Phi \to \Phi + \epsilon(t)$, $\Psi \to \Psi + \epsilon(t)$, posing a gauge symmetry. While the radial Wilson line corresponding to Π_0 itself is clearly invariant under this symmetry, cutting the Wilson line open into two pieces produces two operators that are no longer gauge-invariant. We stress

that this open Wilson line exists only for the non-trivial holonomy k_0, i.e. for the annulus representing the topological wormhole. If k_0 were trivial, the corresponding requirement $\oint \mathrm{d}\varphi\, A_\varphi = 0$ (cf. (5.12)) implements that Σ must have the disk topology since all circles in φ-direction are contractible.

Let us now derive the symplectic form for the above action (5.15). The variables spanning the phase space are the two chiral bosons Φ, Ψ, the holonomy k_0 and the conjugate momenta Π_Φ, Π_Ψ and Π_0. To derive the symplectic form we proceed as in sec. 4.2.3, making use of (2.53) or expressed in coordinates (4.65). To use this formula we first calculate Π_Φ and Π_Ψ,

$$\Pi_\Phi = \frac{\partial L}{\partial(\partial_t \Phi)} = \frac{k}{4\pi}\oint \mathrm{d}\varphi\, \partial_\varphi \Phi \quad \text{and} \quad \Pi_\Psi = -\frac{\partial L}{\partial(\partial_t \Psi)} = \frac{k}{4\pi}\oint \mathrm{d}\varphi\, \partial_\varphi \Psi\,. \tag{5.19}$$

Note that for the derivatives we replaced the difference $\Phi - \Pi$ in the second line of (5.15) by Π_0 using (5.17). With the above results for Π_Φ and Π_Ψ, we employ (4.65) to calculate

$$\begin{aligned}\partial_t \Phi &= \left(\Omega^{-1}\right)^{\Phi b}\partial_b H = \left(\Omega^{-1}\right)^{\Phi\Pi_\Phi}\partial_{\Pi_\Phi} H + \left(\Omega^{-1}\right)^{\Phi\Pi_\Psi}\partial_{\Pi_\Psi} H + \left(\Omega^{-1}\right)^{\Phi k_0}\partial_{k_0} H \\ &\overset{!}{=} \partial_{\Pi_\Phi} H\,, \end{aligned} \tag{5.20}$$

$$\begin{aligned}\partial_t \Psi &= \left(\Omega^{-1}\right)^{\Psi b}\partial_b H = \left(\Omega^{-1}\right)^{\Psi\Pi_\Phi}\partial_{\Pi_\Phi} H + \left(\Omega^{-1}\right)^{\Psi\Pi_\Psi}\partial_{\Pi_\Psi} H + \left(\Omega^{-1}\right)^{\Psi k_0}\partial_{k_0} H \\ &\overset{!}{=} \partial_{\Pi_\Psi} H\,. \end{aligned} \tag{5.21}$$

In evaluating the sum over b, we use that the Hamiltonian (5.16) depends only on Π_Φ, Π_Ψ and k_0. In going to the next lines, we demand that the sum equals the term expected by the Hamilton equations of motion. This fixes $(\Omega^{-1})^{\Phi\Pi_\Phi} = 1 = (\Omega^{-1})^{\Psi\Pi_\Psi}$ and all other components of Ω displayed above vanishing. To do the same calculation for the holonomy, we first need an expression for the time derivative of Π_0. Using (5.17) in combination with (5.18) this is obtained as

$$\partial_t \Pi_0 = -\frac{k}{2\pi}\oint \mathrm{d}\varphi \int_{r_\mathrm{i}}^{r_\mathrm{o}} \mathrm{d}r\, \partial_t A_r = -\frac{k}{2\pi}\oint \mathrm{d}\varphi \left(A_t|_{r=r_\mathrm{o}} - A_t|_{r=r_\mathrm{i}}\right), \tag{5.22}$$

employing $\Omega^{\mathrm{CS}}_{rt} = 0$ in the second equality to rewrite $\partial_t A_r = \partial_r A_t$. With the boundary conditions posed above $A_t|_{r=r_\mathrm{o}} = A_\varphi|_{r=r_\mathrm{o}}$ and $A_t|_{r=r_\mathrm{i}} = -A_\varphi|_{r=r_\mathrm{i}}$, the φ-integral in (5.22) can be evaluated using (5.12). The result is given by

$$\partial_t \Pi_0 = -2k_0\,. \tag{5.23}$$

This enables us to compute the remaining entries of the symplectic form,

$$\partial_t \Pi_0 = \left(\Omega^{-1}\right)^{\Pi_0\Pi_\Phi} \partial_{\Pi_\Phi} H + \left(\Omega^{-1}\right)^{\Pi_0\Pi_\Psi} \partial_{\Pi_\Psi} H + \left(\Omega^{-1}\right)^{\Pi_0 k_0} \partial_{k_0} H \overset{!}{=} \partial_{k_0} H \,. \tag{5.24}$$

Noting that $\partial_{k_0} H = -2k_0$ using the explicit form of H given in (5.16), this fixes $\left(\Omega^{-1}\right)^{\Pi_0 k_0} = 1$ and the other two components vanishing. With all components of the symplectic form determined, we obtain our result

$$\Omega = \mathrm{d}\Pi_\Phi \wedge \mathrm{d}\Phi + \mathrm{d}\Pi_\Psi \wedge \mathrm{d}\Psi + \mathrm{d}k_0 \wedge \mathrm{d}\Pi_0 \,. \tag{5.25}$$

The first two terms resemble the canonical symplectic form $\Omega^{\mathrm{can}} = \mathrm{d}p \wedge \mathrm{d}q$. As there is no explicit coupling between the two bosons of the form $\propto \Phi\Psi$ contained in the action (5.15), also in the symplectic form no such term appears. The particularly simple form of the first two terms results from using chiral bosons, which are a convenient parametrisation in that they provide Darboux coordinates on the phase space. The third term including k_0 and Π_0 shows the non-trivial coupling between the two boundaries by the holonomy k_0. In particular, the conjugate momentum Π_0 is expressed as an integral of both Φ and Ψ (cf. (5.17)) and therefore is a non-local variable. This non-locality is the hallmark of the annulus, i.e. the topological wormhole, and makes manifest the non-factorisation. In particular, this term does not appear if $k_0 = 0$ from the start. In this case, as we discussed above, circles are contractible and the annulus is reshaped to a disk. Considering two such discs, the asymptotic dynamics at the boundaries of the disks are again captured by chiral bosons Φ and Ψ, but there is no k_0. In this case, the symplectic form follows as

$$\Omega = \mathrm{d}\Pi_\Phi \wedge \mathrm{d}\Phi + \mathrm{d}\Pi_\Psi \wedge \mathrm{d}\Psi \,, \tag{5.26}$$

where no coupling between the discs is present and the phase space is factorised into the individual contributions of the two disks. Therefore, the non-locality induced by the presence of the holonomy k_0 shows the presence of the topological wormhole in the sense of [165], and in the sense of [462] by the open Wilson line threading the wormhole.

To conclude the analysis, we phrase the above results in terms of the coadjoint orbits introduced in sec. 5.1.1. This puts an important perspective on non-factorisation, closely analogous to what we have encountered in sec. 4.1.2 for the two-qubit model. The coadjoint orbit $\mathscr{G}$ for a symmetry group G was established by identifying the stabiliser group K and defining the coadjoint orbit as the quotient $\mathscr{G} = \frac{G}{K}$. In the present case of U(1) Chern–Simons theory, a single chiral boson theory with only one boundary present is described by a U(1) Kac–Moody algebra, generated by $\frac{k}{2\pi} A_\varphi$ [485]. These algebras are central extensions of loop algebras [490] and appear in conformal field theories with an additional

U(1) symmetry, see e.g. [480]. The corresponding Kac–Moody group is denoted by $\widehat{\mathrm{LG}}$. The stabiliser group arises by noting that the single chiral boson theory on the boundary possesses a U(1) gauge symmetry, realised as shifts $\Phi \to \Phi + \epsilon(t)$. Correspondingly, for a theory of only one chiral boson on a disk topology, the coadjoint orbit is given by

$$\mathscr{G} = \frac{\widehat{\mathrm{LG}}}{\mathrm{U}(1)} \,. \tag{5.27}$$

On this orbit, the symplectic form $\Omega = \mathrm{d}\Pi_\Phi \wedge \mathrm{d}\Phi$ is defined and upon quantisation, the projective Hilbert space $\mathscr{P}(\mathscr{H})$ is obtained. In the case of two discs with boundaries Σ_1 and Σ_2, we simply obtain this coadjoint orbit twice, i.e.

$$\mathscr{G} = \frac{\widehat{\mathrm{LG}}_1}{\mathrm{U}(1)_1} \times \frac{\widehat{\mathrm{LG}}_2}{\mathrm{U}(1)_2} \,, \tag{5.28}$$

with the symplectic form on this coadjoint orbit given by (5.26). Quantisation then produces the full projective Hilbert space as the product of the individual projective Hilbert spaces, i.e. a factorised projective Hilbert space $\mathscr{P}(\mathscr{H}) = \mathscr{P}(\mathscr{H})_1 \otimes \mathscr{P}(\mathscr{H})_2$. Here, it is important that each chiral boson theory has an individual U(1) gauge symmetry, indicated by the subscripts on U(1) in defining the coadjoint orbit. This in particular changes when putting the theory on an annulus. While each boundary still has a chiral boson described by the Kac–Moody algebra, the coupling of the chiral bosons by the holonomy k_0 reduces the stabiliser group to a single U(1). As we have pointed out before, the boundary action for U(1) Chern–Simons theory on the annulus is invariant only under the combined shift $\Phi \to \Phi + \epsilon(t)$, $\Psi \to \Psi + \epsilon(t)$ using the same $\epsilon(t)$. Correspondingly, the stabiliser group is given by a single U(1) which in particular is not confined to either boundary. The coadjoint orbit then follows as

$$\mathscr{G} = \frac{\widehat{\mathrm{LG}}_\mathrm{o} \otimes \widehat{\mathrm{LG}}_\mathrm{i}}{\mathrm{U}(1)} \,. \tag{5.29}$$

The symplectic form on this orbit is given by (5.25). Due to the common quotient by U(1) resulting from the holonomy k_0, the projective Hilbert space obtained by quantising this coadjoint orbit does not factorise. As a final remark, note that these results on non-factorisation are similar to our discussion of the two-qubit system. There, the factorised case $\mathbb{C}\mathrm{P}^1 \times \mathbb{C}\mathrm{P}^1$ corresponded to vanishing interaction between the qubits ($B \gg J$ in (4.1)), and correspondingly vanishing entanglement. For non-vanishing interaction, the submanifold of the projective Hilbert space was more complicated, $\mathbb{C}\mathrm{P}^1_\alpha \times \mathbb{C}\mathrm{P}^1$, and does not factorise symmetrically between the two qubits.

This finishes our discussion of the topological wormhole modelled by U(1) Chern–Simons theory on an annulus geometry. We have shown that the presence of the holonomy k_0 and the corresponding non-local conjugate momentum Π_0 allow us to diagnose non-factorisation of the projective Hilbert space from the boundary perspective, made manifest by additional terms in the symplectic form (5.25). As we show in the next section, applying the same reasoning to the eternal black hole will allow us to diagnose the non-factorisation of the boundary projective Hilbert space using the Virasoro Berry phases.

5.1.3. Generalising to SL(2,$\mathbb{R}$)

In this section, we generalise the analysis of the previous section from U(1) to SL(2, $\mathbb{R}$). The isometry group G of AdS_3 is given by SO(2, 2) (cf. (3.32)), which splits into two copies of SL(2, $\mathbb{R}$). As shown in [415, 491, 492], using the isometry group SL(2, $\mathbb{R}$) × SL(2, $\mathbb{R}$) as gauge group for Chern–Simons theory is an equivalent way of formulating gravity on three-dimensional Anti-de Sitter spacetime, at least at the classical level. In particular, the Einstein–Hilbert action using the metric g as a dynamical field can be written as the difference of two SL(2, $\mathbb{R}$) Chern–Simons actions,

$$S_{\mathrm{EH}}[g] = S_{\mathrm{CS}}[A] - S_{\mathrm{CS}}[\bar{A}]\,, \tag{5.30}$$

where A and $\bar{A}$ are the gauge fields charged under $\mathfrak{sl}(2,\mathbb{R})$ and the Chern–Simons level is identified as $k = \frac{L_{\mathrm{AdS}}}{4G_{\mathrm{N}}}$. The gauge fields A and $\bar{A}$ correspond to left and right movers, just as the dual CFT_2 has two copies of the Virasoro group describing left and right movers. As these two sectors decouple and behave analogously, we will only discuss the gauge field A explicitly. To examine the eternal black hole, this action is again considered on a manifold including an annulus, $\mathscr{M} = \mathbb{R} \times \Sigma$, as visualised in fig. 5.2.

As for the above case of U(1), the action of SL(2, $\mathbb{R}$) reduces to a boundary term by putting certain boundary conditions at the inner and outer radii r_{i} and r_{o} of the annulus. Due to the non-abelian nature of SL(2, $\mathbb{R}$) however, the derivation comes with more subtleties. In particular, the gauge field A is valued in $\mathfrak{sl}(2,\mathbb{R})$ and therefore represented as a 2×2 matrix. Beneficial to us, this reduction to boundary terms has been performed in [485]. In the following, we briefly point out important steps of this derivation and refer the interested reader to the aforementioned paper for details. The Chern–Simons action (5.9) for $G = \mathrm{SL}(2,\mathbb{R})$ reads

$$S_{\mathrm{CS}}[A] = \frac{k}{4\pi} \int_{\mathscr{M}} \mathrm{d}t\mathrm{d}r\mathrm{d}\varphi \; \mathrm{tr}\left(A_\varphi \partial_t A_r - A_r \partial_t A_\varphi + 2A_t \Omega^{(\mathrm{CS})}_{r\varphi} \right), \tag{5.31}$$

where $\Omega^{(\mathrm{CS})}_{r\varphi} = \partial_r A_\varphi - \partial_\varphi A_r + [A_r, A_\varphi]$. The A_t equation of motion enforces $\Omega^{(\mathrm{CS})}_{r\varphi} = 0$,

which is solved by

$$A_r = G^{-1}\partial_r G \quad \text{and} \quad A_\varphi = G^{-1}(\partial_\varphi + K_0)G\,. \tag{5.32}$$

This is the non-abelian generalisation of (5.11), where $G(t,r,\varphi) \in \mathrm{SL}(2,\mathbb{R})$ is periodic in φ and $K_0(t)$ accounts for the non-trivial holonomy due to the annulus topology.[7] To implement time evolution to run in the same direction on both boundaries the same boundary conditions as before are chosen, namely $A_t = A_\varphi$ at the outer radius r_o and $A_t = -A_\varphi$ at the inner radius r_i. Note that in this truly holographic setting, the inner and outer radii defining the annulus have the interpretation as the left and right asymptotic boundaries of the Anti-de Sitter bulk spacetime, as visualised in fig. 5.2. These boundary conditions require adding two boundary terms, one at each boundary, to make the variational principle well-defined. These terms are given by [485]

$$-\frac{k}{4\pi}\int \mathrm{d}t\left[\oint_{r=r_\mathrm{o}} \mathrm{d}\varphi\ \mathrm{tr}\left(A_\varphi^2\right) + \oint_{r=r_\mathrm{i}} \mathrm{d}\varphi\ \mathrm{tr}\left(A_\varphi^2\right)\right], \tag{5.33}$$

analogous to the U(1) case, cf. (5.13), except that the trace is included. Adding these terms to the action (5.31) and inserting (5.32), the action reduces to a total r-derivative. The integral over r can then be trivially performed to yield an action defined only on the two boundaries of the annulus [485]. In the same spirit as in (5.14), the boundary values of G at r_i and r_o are identified as dynamical fields on the boundary, $G(t, r = r_\mathrm{i}, \varphi) = l(t,\varphi)$ and $G(t, r = r_\mathrm{o}, \varphi) = h(t,\varphi)$. These fields l and h appear in the boundary action. However, since $G \in \mathrm{SL}(2,\mathbb{R})$, the same is true for l and h, i.e. these fields are not the same as the chiral bosons defined in (5.14) in the U(1) case. To obtain a chiral boson formulation also in the present case, the fields l and h are written in Gauss decomposition. This associates three dynamical scalar fields to each of h and l [485],

$$l = e^{Vl_1}e^{\Psi l_0}e^{Ul_{-1}} \quad \text{and} \quad h = e^{Yl_{-1}}e^{\Phi l_0}e^{Xl_1}\,, \tag{5.34}$$

where l_{-1}, l_0 and l_1 are the generators of $\mathfrak{sl}(2,\mathbb{R})$ and the six new fields all depend on both t and φ. This parametrisation is convenient for the following analysis since it is useful in the study of hyperbolic holonomies. Such holonomies are parametrised as $K_0(t) = k_0(t)l_0$ with $k_0(t) \in \mathbb{R}\backslash\{0\}$ and the eternal black hole in AdS_3 falls into that class [485]. Finally, to ensure an asymptotic Anti-de Sitter spacetime, boundary conditions have to be put on

[7] Note that for $G = e^{\mu} \in \mathrm{U}(1)$ and $K_0 \to k_0$, (5.32) reduces to (5.11). Note further that compared to [485], we have put a subscript on the holonomy K_0 to distinguish it from the stabiliser group K.

the components of A, namely

$$A_r|_{r=r_o} = 0\,, \quad A_\varphi|_{r=r_o} = l_{-1} + \mathscr{L}(t,\varphi)l_1\,, \tag{5.35}$$

where $\mathscr{L}(t,\varphi)$ is a dynamical field that specifies the bulk solution. For the fields that appeared in the definition of h in (5.34), these boundary conditions imply

$$e^{\Phi}\big(\partial_\varphi Y - k_0 Y\big) = 1, \quad \partial_\varphi \Phi + k_0 = 2X \quad \text{and} \quad \partial_\varphi X + X^2 = \mathscr{L}\,. \tag{5.36}$$

The inner boundary $r = r_i$ works analogously upon replacing $(\Phi, k_0) \to -(\Psi, k_0)$ and $(Y, X, \mathscr{L}) \to (V, U, \mathscr{M})$. These conditions enable to express Y, X and $\mathscr{L}$ in terms of Φ and k_0, and analogously for the fields on the other boundary. Inserting these expressions into the action, the boundary action for $\mathrm{SL}(2,\mathbb{R})$ Chern–Simons theory on the annulus is found [485],

$$S[\Phi,\Psi,k_0] = \frac{k}{4\pi}\int \mathrm{d}t \oint \mathrm{d}\varphi \left[\frac{1}{2}\partial_-\Phi\partial_\varphi\Phi - \frac{1}{2}\partial_+\Psi\partial_\varphi\Psi + k_0\big(\partial_-\Phi - \partial_+\Psi\big) - k_0^2\right], \tag{5.37}$$

where $\partial_\pm = \partial_t \pm \partial_\varphi$. As in the above case for $\mathrm{U}(1)$ this action describes two chiral bosons, defined on the two boundaries of the annulus. While Φ and Ψ do not share any explicit interaction, they are coupled by the holonomy k_0. The particular case of the eternal black hole in AdS_3 is obtained by setting $\mathscr{L} = \frac{M}{4} = \mathscr{M}$, where M is the mass of the black hole [485]. By the boundary conditions (5.36), this yields $k_0 = \sqrt{M}$. Returning to the general case, the holonomy k_0 has a conjugate momentum given by

$$\Pi_0 = -\frac{k}{4\pi}\oint \mathrm{d}\varphi\,(\Phi - \Psi)\,. \tag{5.38}$$

Due to the non-abelian nature of $\mathrm{SL}(2,\mathbb{R})$ this is not directly related to the radial Wilson line, as it was in the $\mathrm{U}(1)$ case (see [485] for details). It should however be noted that radial Wilson lines stretching between the boundaries do exist for $\mathrm{SL}(2,\mathbb{R})$ Chern–Simons theory, except that these are not given by Π_0. Moreover, Π_0 is again a non-local variable, as it depends on the variables Φ and Ψ defined on different boundaries. While Π_0 is invariant under the gauge symmetry $\Phi \to \Phi + \epsilon(t)$, $\Psi \to \Psi + \epsilon(t)$, the individual terms of (5.38) on each boundary $\propto \oint \mathrm{d}\varphi\,\Phi$ and $\propto \oint \mathrm{d}\varphi\,\Psi$ are not invariant on their own. This again realises the arguments of [462].

We are now in a position to compute the symplectic form on the phase space spanned by the chiral bosons Φ, Ψ, the holonomy k_0 and their corresponding conjugate momenta Π_Φ, Π_Ψ and Π_0. Following the steps performed in sec. 5.1.2 for the $\mathrm{U}(1)$ case, the Hamiltonian

in the present setting is given by

$$H = \frac{k}{8\pi} \oint \mathrm{d}\varphi \left[(\partial_\varphi \Phi)^2 + (\partial_\varphi \Psi)^2 + 2k_0^2 \right] . \tag{5.39}$$

Computing the symplectic form using (4.65) as in the previous section, we find

$$\Omega = \mathrm{d}\Pi_\Phi \wedge \mathrm{d}\Phi + \mathrm{d}\Pi_\Psi \wedge \mathrm{d}\Psi + \mathrm{d}k_0 \wedge \mathrm{d}\Pi_0 \,, \tag{5.40}$$

analogous to the U(1) case. Again we find the first two terms resembling the canonical symplectic form $\Omega^{\text{can}} = \mathrm{d}p \wedge \mathrm{d}q$ on each boundary. The third term manifests the non-trivial coupling between the two boundaries in terms of the holonomy k_0 and its non-local conjugate momentum Π_0. In particular, as pointed out before, the non-local variable Π_0 connects to the arguments of [462] on gauge-invariant two-sided operators that are no longer gauge-invariant when cut open. Note however that, while Π_0 is non-local, it is manifestly an operator of the boundary theory, as it is expressed using the boundary fields Φ and Ψ, analogous to the U(1) case. Demanding that only gauge-invariant operators can be present in the boundary theory consisting of the two chiral boson actions, this shows that the projective Hilbert space of the boundary theory must not be factorised in an inner-outer (i.e. left-right) fashion in order to properly include Π_0. It is worth stressing that all of this discussion is true as long as $k_0 \neq 0$. If this was the case, the geometry is no longer that of an annulus but that of a disk. Correspondingly, there are no non-contractible circles in φ-direction and the non-local operator Π_0 does not appear.

Let us finally discuss the above results in terms of coadjoint orbits. For $\mathrm{SL}(2,\mathbb{R})$ Chern–Simons theory as (one half of) a theory of gravity on three-dimensional Anti-de Sitter spacetime, it is known that the boundary CFT_2 is described by the Virasoro group [365]. Indeed, in the current setting of two boundaries, the Fourier modes of $\mathscr{L}$ and $\mathscr{M}$ fixing the gauge field component A_φ at the boundaries each form a set of the Virasoro algebra [485]. In our analysis, these two sets describe the right movers of the CFT_2 on the outer radius r_{o} and the left movers on the inner radius r_{i}.[8] Therefore, the group G is given by $\mathrm{Vir}_{\mathrm{o}} \times \mathrm{Vir}_{\mathrm{i}}$ defining Virasoro coadjoint orbits upon quotienting by the stabiliser group K. To obtain K, it is useful to first note that the boundary action in (5.37) can be rewritten into the difference of two geometric actions S_{geo} of the Virasoro group. This is obtained by parametrising the chiral bosons Φ and Ψ in terms of group elements f and g of the Virasoro groups $\mathrm{Vir}_{\mathrm{o}}$ and $\mathrm{Vir}_{\mathrm{i}}$, respectively [485],

$$\Phi = k_0(f - \varphi) - \ln\left(-k_0 \partial_\varphi f\right) \quad \text{and} \quad \Psi = k_0(\varphi - g) - \ln\left(k_0 \partial_\varphi g\right) . \tag{5.41}$$

[8] The other Chern–Simons action $S_{\mathrm{CS}}[\bar{A}]$ in (5.30) gives rise to the left movers on the outer radius r_{o} and the right movers on the inner radius r_{i}.

Inserting this into (5.37) the action is given by the difference of two geometric actions, or equivalently, by the difference of two Virasoro Berry phases,

$$S[\Phi, \Psi, k_0] = S_{\text{geo}}[f, b_0] - S_{\text{geo}}[g, b_0] = \Phi_{\text{Vir}_\text{o}} - \Phi_{\text{Vir}_\text{i}} \,. \tag{5.42}$$

By this rewriting, the coadjoint orbit label b_0 is related to the holonomy k_0 as [485]

$$b_0 = \frac{k}{8\pi} k_0^2 \,. \tag{5.43}$$

It is important to note that the geometric actions in (5.42) depend on different group elements f and g, but on the same orbit label b_0. For the example of the black hole, where $b_0 \propto k_0^2 = M$, this represents the physical requirement that the mass of the black hole has to be the same when measured from either boundary. The stabiliser group K is then obtained by identifying all transformations that leave b_0 invariant. By the above relation, this translates to finding transformations that leave the holonomy K_0 invariant. Noting that $K_0 = k_0 l_0$, the only transformations U that satisfy $U K_0 U^{-1} = K_0$ are generated by l_0. Therefore, the stabiliser group consists of a single generator and correspondingly, $K = \mathrm{U}(1)$. Note that this is a single factor of $\mathrm{U}(1)$, not one for each copy of the Virasoro group. This can also be understood by the fact that Π_0 is invariant only under the simultaneous transformation $\Phi \to \Phi + \epsilon(t)$, $\Psi \to \Psi + \epsilon(t)$, but not under the individual ones. Correspondingly, we obtain the coadjoint orbit for the boundary description of the eternal black hole in AdS_3 as

$$\mathscr{G} = \frac{\text{Vir}_\text{o} \otimes \text{Vir}_\text{i}}{\mathrm{U}(1)} \,. \tag{5.44}$$

The symplectic form on this orbit is given by (5.40). Quantising this coadjoint orbit, we obtain a projective Hilbert space $\mathscr{P}(\mathscr{H})$ which is not factorised since the coadjoint orbit itself is also not factorised. This non-factorisation arises due to the holonomy k_0. We point out that this diagnosis of non-factorisation uses the Virasoro Berry phase defined as the holonomy of the coadjoint orbit. Therefore, Virasoro Berry phases provide a useful tool in observing non-factorisation from the boundary, i.e. the CFT point of view.

5.2. Modular Berry Phase

Both the phase factors defined for the TFD state in sec. 4.2 and the Virasoro Berry phase of the previous sec. 5.1 are defined by analysing the allowed transformations on the system, forming the group G, and quotienting by transformations that pose a symmetry of the state

vector forming the group K. The phase factors are understood as probing the geometry of the coadjoint orbit $\mathscr{G} = \frac{G}{K}$ as the base space of a principal fibre bundle with fibre K. In this section, we analyse a third type of geometric phase factor known as the *modular Berry phase* [168–170]. This phase is defined as the holonomy obtained by parallel transport in the space of modular Hamiltonians. Physically, this is interpreted as transformations that deform the subregion A in the CFT.[9] Since the size of the subregion is important when it comes to the entanglement between the subregion and its complement, the modular Berry phase is considered a probe of the entanglement structure. In this section, we show that modular Berry phases provide a further probe of the bulk wormhole in AdS_3. To do so, in sec. 5.2.1 we first briefly review how modular Berry phases are defined, following the original works [168–170]. Subsequently in sec. 5.2.2 we turn to the setting of the black string in AdS_3. This object is understood as a black hole where the horizon is not compact [493]. For illustrative purposes, we first discuss how the modular Berry curvature arises for a single-sided black string. With this result at hand, we compute the modular Berry curvature for a two-sided black string. We discuss how our result signals the wormhole from a boundary perspective by properly incorporating the time-shift mode δ.

5.2.1. Modular Parallel Transport

Defining parallel transport in the space of modular Hamiltonians first requires a few details on modular Hamiltonians themselves. As we have reviewed in sec. 2.1.2 for the case of empty Minkowski spacetime, the modular Hamiltonian of a subregion arises when computing the reduced density operator for subregions in QFT. Moreover, in the context of AQFT and von Neumann algebras, the modular Hamiltonian $K_{(A)}$ of the subregion A in combination with the modular Hamiltonian of the complement $K_{(\bar{A})}$ generates an automorphism of the algebra $\mathscr{A}$ localised in the subregion A (cf. (2.113)),

$$e^{is\hat{K}}\mathscr{A}e^{-is\hat{K}} = \mathscr{A}\,, \quad \text{where} \quad \hat{K} = K_{(A)} - K_{(\bar{A})}\,. \tag{5.45}$$

In general, the modular Hamiltonian of an arbitrary subregion is a highly complicated and non-local operator. However, in certain cases explicit expressions can be obtained. This includes the modular Hamiltonian for the half spaces $K_>$ discussed in sec. 2.1.2, given by [222, 223]

$$K_> = \int_{x>0} \mathrm{d}x\, x\hat{T}_{00}\,. \tag{5.46}$$

[9] For clarity, note that A refers again to subregions, as opposed to the previous sec. 5.1 where the Chern–Simons gauge field was denoted by A.

The integrand is given by the generator of Lorentz boosts $\tilde{K}_>$, as reviewed around (2.34) and (2.36). In the context of an interval $A = [-R, R]$ in a two-dimensional CFT a similar result has been found by mapping this case to the above one of half spaces, i.e. Rindler wedges. Essentially, the weight factor x in the above integral is replaced by a more complicated function accounting for the restriction to the finite interval, resulting in [229]

$$K_{(A)} = \int_{x\in A} \mathrm{d}x \, \frac{R^2 - x^2}{R^2} \hat{T}_{00} \,. \tag{5.47}$$

More generally, any subregion of a CFT for which a map to the half space appearing in the Rindler case can be constructed can be expressed in the above way. The weighting factor in front of $\hat{T}_{00}$ is replaced by a specific function $f(x)$ accounting for the specific shape of the considered subregion [230]. Such functions are known for CFTs on a cylinder, which includes the case where the CFT is dual to the black string in AdS_3. For the Euclidean black hole in AdS_3, the dual CFT is defined on a torus. In this case, the modular Hamiltonian is not known, which is why we focus our discussion of modular Berry phases on the black string. While the modular Hamiltonian generally is non-local,[10] in holographic CFTs the situation is better. As the expectation value of the modular Hamiltonian computes the entanglement entropy, cf. (2.22), by the RT formula (3.37) to leading order in G_N the modular Hamiltonian must have a local piece [497, 498],

$$K_{(A)} = \frac{\widehat{\mathrm{Area}}(\partial \hat{A})}{4G_\mathrm{N}} + \mathcal{O}\left[\left(G_\mathrm{N}\right)^0\right] . \tag{5.48}$$

Here, $\widehat{\mathrm{Area}}$ is the area operator whose expectation value results in the area of the RT surface. By definition, this operator is localised in the subregion.

Modular Berry phases arise whenever the modular Hamiltonian has *modular zero modes*. These are given by self-adjoint operators $Q^{(i)}$ that commute with the modular Hamiltonian [168],

$$[Q^{(i)}, K_{(A)}] = 0 \,. \tag{5.49}$$

An obvious example of a zero mode is the modular Hamiltonian itself, but there can be more general operators. Just as the modular Hamiltonian, the modular zero modes generate an automorphism of the algebra $\mathscr{A}$ upon replacing $e^{\mathrm{i}s\hat{K}}$ by $U_Q = e^{\mathrm{i}s_{(i)}Q^{(i)}}$ in (5.45). Since all correlation functions of operators are invariant under this automorphism, the zero modes give rise to a gauge ambiguity in defining the operators of the algebra $\mathscr{A}$ in subregion

[10] See e.g. [494, 495] and [496] for modular Hamiltonians with non-local features for fermions on a torus and non-critical quantum chains, respectively.

A. The analogous arguments apply for operators of the commuting algebra $\mathscr{A}'$ of the complementary subregion $\bar{A}$. In particular, observers in A and $\bar{A}$ may choose their zero mode frames independently. This gauge ambiguity defines a fibre bundle, where the base space consists of all physically different modular Hamiltonians, i.e. modular Hamiltonians corresponding to different subregions A. The fibre includes all transformations by modular zero modes since those transformations are understood as a change of basis for the modular Hamiltonian. This can be seen by diagonalising $\hat{K}$ in a unitary basis U as $\hat{K} = U^\dagger \Delta U$, where Δ is the spectrum of $\hat{K}$. The spectrum includes information on the entanglement structure defined by the modular Hamiltonian. Since U_Q is a unitary transformation, the basis $U' = UU_Q$ is an equally valid choice. The spectrum Δ is not affected by this transformation, so the transformed modular Hamiltonian $\hat{K}' = U_Q^\dagger \hat{K} U_Q = U'^\dagger \Delta U'$ is physically equivalent to $\hat{K}$.

Writing $\hat{K}$ in a unitary basis is also convenient for defining a local gauge field on the fibre bundle. The gauge fields define parallel transport between physically different modular Hamiltonians, i.e. with different spectra. Denoting the eigenvalues of Δ as λ, consider small deformations $\lambda \to \lambda + \delta\lambda$. Physically, this means considering an interval of the CFT $\lambda = [u, v]$ on a fixed time slice and infinitesimally deforming this interval as $[u, v] \to [u + \mathrm{d}u, v + \mathrm{d}v]$.[11] Under such deformations, the basis and the spectrum change as [170]

$$\partial_\lambda \hat{K} \delta\lambda = \left[\hat{K}, U^\dagger \partial_\lambda U\right] \delta\lambda + U^\dagger \left(\partial_\lambda \Delta \delta\lambda\right) U \,. \tag{5.50}$$

As $\left[U^\dagger \left(\partial_\lambda \Delta \delta\lambda\right) U, \hat{K}\right] = 0$, the second term encoding the change in the spectrum is itself a zero mode. Since the interest lies not in the change of the spectrum but in the change of the basis, it is convenient to define a projector $\mathscr{P}_0$ onto the zero mode sector. For a zero mode $Q^{(i)}$, $\mathscr{P}_0\left(Q^{(i)}\right) = Q^{(i)}$, while for an operator $\mathfrak{a}$ that is not a zero mode, $\mathscr{P}_0(\mathfrak{a}) = 0$. Using this projector, the change of the basis U under the deformation of λ is written as [170]

$$\left[\hat{K}, U^\dagger \partial_\lambda U\right] \delta\lambda = \partial_\lambda \hat{K} \delta\lambda - \mathscr{P}_0\left(\partial_\lambda \hat{K} \delta\lambda\right) . \tag{5.51}$$

Noting that this fixes $U^\dagger \partial_\lambda U$ only up to additional zero modes motivates defining the local gauge field [170]

$$A = \mathscr{P}_0\left(U^\dagger \partial_\lambda U\right) . \tag{5.52}$$

[11] In the literature on modular Berry phases, it is common to denote the interval by λ, while in this thesis, subregions are usually denoted by A. In this section, we will use this interchangeably and specify whenever necessary.

It is straightforward to check that under a transformation by a modular zero mode U_Q, (5.52) indeed transforms as a gauge field (cf. (2.80))

$$A' = U_Q^\dagger A U_Q - U_Q^\dagger \delta U_Q \,, \tag{5.53}$$

where we denote by $\delta(\cdot) = \partial_\lambda(\cdot)\delta\lambda$ the exterior derivative on the space spanned by λ, analogous to d in (2.80). Parallel transport is then defined by the covariant derivative $\nabla_\lambda = \partial_\lambda + A$. As an operator, this can be formulated as [170]

$$V_{\delta\lambda} = U'^\dagger \partial_\lambda U' = U^\dagger \partial_\lambda U + A \,, \tag{5.54}$$

where as before $U' = U U_Q$. Therefore, $V_{\delta\lambda}$ correctly implements parallel transport under a change in the zero mode frame. This operator can be used to abstractly define modular parallel transport by [168]

$$\partial_\lambda \hat{K} - \mathscr{P}_0\big(\partial_\lambda \hat{K}\big) = \big[V_{\delta\lambda}, \hat{K}\big] \quad \text{and} \quad \mathscr{P}_0\big(V_{\delta\lambda}\big) = 0 \,. \tag{5.55}$$

The second equation implements that the parallel transport operator itself does not have any zero modes. The corresponding modular Berry curvature $\widehat{\Omega}$ is computed most conveniently as the commutator of two different $V_{\delta\lambda}$,

$$\widehat{\Omega}_{ij} = \big[V_{\delta\lambda_i}, V_{\delta\lambda_j}\big] \,. \tag{5.56}$$

As an aside, the same is obtained by the formula $\widehat{\Omega} = \delta A$ more familiar to us, but the above version will be more convenient in the explicit computation. Note also that in this formalism the modular Berry curvature $\widehat{\Omega}$ is an operator, as we will see explicitly shortly.

An explicit computation of (5.56) starts with finding an appropriate expression for $V_{\delta\lambda}$. A convenient way to do so is given by finding the eigenoperators E_κ of $\hat{K}$ satisfying [170]

$$\big[E_\kappa, \hat{K}\big] = \kappa E_\kappa \,. \tag{5.57}$$

Apart from the trivial solution $\kappa = 0$ with E_0 a zero mode,[12] this determines

$$E_\kappa = \partial_\lambda \hat{K} \,. \tag{5.58}$$

With $\kappa \neq 0$, the parallel transport operator $V_{\delta\lambda}$ satisfying (5.55) is given by [170]

$$V_{\delta\lambda} = \frac{1}{\kappa} \partial_\lambda \hat{K} \,. \tag{5.59}$$

[12] Note that zero modes are not allowed for $V_{\delta\lambda}$ by (5.55).

To see this, note that with $V_{\delta\lambda} \propto \partial_\lambda \hat{K}$ the second condition in (5.55) implies that $\mathscr{P}_0\big(\partial_\lambda \hat{K}\big) = 0$, which simplifies the first condition to $\partial_\lambda = \big[V_{\delta\lambda}, \hat{K}\big]$. Noting (5.57) with solution (5.58), this is clearly satisfied for (5.59). Inserting this operator into (5.56) yields the convenient result [499]

$$\widehat{\Omega}_{ij} = -\frac{2}{\kappa}\partial_{\lambda_i}\partial_{\lambda_j}\hat{K}\,\delta\lambda_i \wedge \delta\lambda_j\,, \tag{5.60}$$

so computing the modular Berry curvature reduces to computing derivatives of the modular Hamiltonian. As $\hat{K}$ is an operator, $\widehat{\Omega}$ is as well. The modular Berry phase is then given by integrating (5.60) over a two-dimensional surface that has a closed path as its boundary.

5.2.2. Modular Berry Curvature for the Two-Sided Black String

Let us now evaluate the modular Berry curvature in a few settings for the Euclidean black string in AdS_3, with the ultimate goal to compute it for the two-sided black string.[13] In all cases, the modular Hamiltonian $\hat{K}$ can be written as a linear combination of left-moving and right-moving parts,

$$\hat{K} = \hat{K}_+ + \hat{K}_-\,. \tag{5.61}$$

As usual, the discussion of these two parts is completely analogous, which is why we restrict ourselves to analysing only $\hat{K}_+$. Moreover, $\hat{K}_+$ is an element of the global conformal algebra $\mathfrak{sl}(2,\mathbb{R})$ and can therefore be expressed as a linear combination of the corresponding generators l_n,

$$\hat{K}_+ = s_1 l_1 + s_0 l_0 + s_{-1} l_{-1}\,. \tag{5.62}$$

The coefficients s_n are such that transformations by $\hat{K}_+$ do not change the interval endpoints in left-moving coordinates $\lambda_+ = [u_+, v_+]$.[14] Moreover, the transformation $e^{2\pi s \hat{K}_+}$ of the points w within the interval has to respect the periodicity of the Euclidean time, which imposes $w(s) = w(s + \mathrm{i})$, with $w(s)$ the solution to $\partial_s w = 2\pi \hat{K}_+ w$ [500].

To start our discussion, let us consider the scenario where the subregion A is the full constant time slice of the CFT. Since we have access to the full system, we expect that the modular Berry curvature vanishes. In this case, the modular Hamiltonian is given by the physical Hamiltonian rescaled by the temperature. For the general expression (5.62),

[13] As pointed out before, we perform these calculations for the black string since in this case, the modular Hamiltonian is known.

[14] Analogously, $\hat{K}_-$ preserves the interval endpoints in right-moving coordinates $\lambda_- = [u_-, v_-]$.

this implies [501]

$$\hat{K}_+ = \beta l_0 \,. \tag{5.63}$$

Constructing the eigenoperators E_κ by solving (5.57), the only possible solution is $E_\kappa \propto l_0$. This however is a zero mode since $E_\kappa \propto l_0$ solves (5.57) with $\kappa = 0$. Correspondingly, there is no parallel transport operator $V_{\delta\lambda}$ and the modular Berry curvature $\widehat{\Omega}$ vanishes as expected. This is reasonable since we have access to the full system and the zero mode frame can be fixed globally.

In the next step, we consider an actual subregion A of the CFT, in particular a finite interval $\lambda = [u, v]$. This is one of the cases where the modular Hamiltonian can be obtained by a map from the Rindler half space. This map was established in [501] and results in

$$\hat{K} = \frac{\beta}{\pi} \int_u^v \mathrm{d}x \, \frac{\sinh \frac{\pi x}{\beta} \sinh \frac{\pi(v-u-x)}{\beta}}{\sinh \frac{\pi(v-u)}{\beta}} T_{00} \,. \tag{5.64}$$

To obtain the expansion of $\hat{K}_+$ in terms of the generators of $\mathfrak{sl}(2,\mathbb{R})$, we first express the generators l_n for the thermal CFT on the cylinder in differential form as

$$l_1 = -\frac{\beta}{2\pi} e^{\frac{2\pi}{\beta} w} \partial_w \,, \quad l_0 = -\frac{\beta}{2\pi} \partial_w \quad \text{and} \quad l_{-1} = -\frac{\beta}{2\pi} e^{-\frac{2\pi}{\beta} w} \partial_w \,, \tag{5.65}$$

where w is the coordinate in the interval λ. Invariance of the endpoints u and v then provides constraints $\hat{K}_+ w|_{w=u,v} = 0$ that can be solved for s_1 and s_{-1},

$$s_1 = -\frac{s_0}{e^{\frac{2\pi}{\beta} u} + e^{\frac{2\pi}{\beta} v}} \quad \text{and} \quad s_{-1} = -\frac{s_0 e^{\frac{2\pi}{\beta}(u+v)}}{e^{\frac{2\pi}{\beta} u} + e^{\frac{2\pi}{\beta} v}} \,. \tag{5.66}$$

Inserting these coefficients into $\hat{K}_+$, the differential equation $\partial_s w = 2\pi \hat{K}_+ w$ can be solved for $w(s)$. Enforcing the periodicity condition $w(s) = w(s + \mathrm{i})$ enables to fix the remaining open coefficient s_0. Specifically, this leads to the condition

$$\frac{e^{\frac{2\pi}{\beta} v} - e^{\frac{2\pi}{\beta} u}}{e^{\frac{2\pi}{\beta} v} + e^{\frac{2\pi}{\beta} u}} s_0 = 1 \quad \text{which solves to} \quad s_0 = \coth \frac{\pi(v-u)}{\beta} \,. \tag{5.67}$$

With the modular Hamiltonian $\hat{K}_+$ determined, we now compute the (left-moving part of the) parallel transport operator $V_{\delta\lambda}$. To do so, we employ the result (5.59) to find

$$V_{\delta u} = \partial_u \hat{K}_+ \quad \text{and} \quad V_{\delta v} = -\partial_v \hat{K}_+ \,, \tag{5.68}$$

with κ determined as $\kappa = \pm 1$. Using these results to evaluate (5.56), or equivalently directly computing the derivatives of $\hat{K}_+$ w.r.t. u and v as in (5.60), the modular Berry curvature is found as

$$\widehat{\Omega} = \frac{4\pi^2}{\beta^2} \operatorname{csch} \frac{\pi(v-u)}{\beta} \hat{K}_+ \, \mathrm{d}v \wedge \mathrm{d}u \,. \tag{5.69}$$

As we are now considering a subregion of the CFT, the zero mode frame can be chosen independently within the subregion and its complement. Therefore, we find a non-vanishing modular Berry curvature and upon integrating, a non-trivial modular Berry phase. The entanglement between the subregions is non-trivial and governed by the RT-formula (3.37). The modular Berry phase probes this entanglement structure. Indeed, in the limit $|v-u| \gg \beta$ the modular Berry curvature (5.69) vanishes. Physically, this is understood as enlarging the interval $\lambda = [u, v]$ such that in the limit, the interval covers the full CFT. This is consistent with our earlier discussion around (5.63).

We are now ready to compute the modular Berry curvature for the two-sided black string, i.e. we consider two disjoint intervals in the CFT. To account for the two-sided nature of this setting, we denote the intervals as $\lambda_L = [u_L, v_L]$ and $\lambda_R = [u_R, v_R]$. The entanglement properties of this setting were analysed in [502], showing that there is a transition in the entanglement entropy. This transition corresponds to the two possible choices of connecting the endpoints of these two intervals. On the one hand, we may connect points located on the same boundary. On the other hand, we may connect points on opposite boundaries, where the corresponding RT surfaces stretch through the entire bulk and thereby pierce the two-sided black string. These two configurations are visualised in fig. 5.3. The transition between these two configurations can be phrased in terms of a single parameter ζ [503],

$$\zeta = \frac{\sinh \frac{\pi(u_L - v_R)}{\beta} \sinh \frac{\pi(u_R - v_L)}{\beta}}{\operatorname{csch} \frac{\pi(u_L - u_R)}{\beta} \operatorname{csch} \frac{\pi(v_L - v_R)}{\beta}} \,. \tag{5.70}$$

For $\zeta < 1$, the RT surfaces connect points on the same boundary, while for $\zeta > 1$, the surfaces stretch through the wormhole. The corresponding modular Hamiltonians were derived in [503]. For $\zeta < 1$, the modular Hamiltonian $\hat{K}_+$ is simply twice the result obtained in the case of a single interval,

$$\hat{K}_+ = \hat{K}_{+,L} + \hat{K}_{+,R} \,, \tag{5.71}$$

where $\hat{K}_{+,L}$ and $\hat{K}_{+,R}$ are given by (5.69) for $u = u_L, v = v_L$ and $u = u_R, v = v_R$, respec-

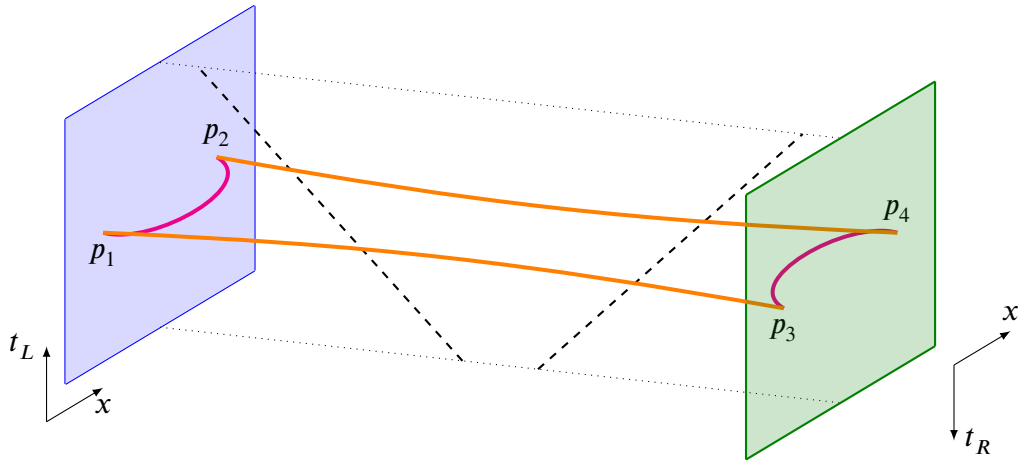

Figure 5.3: Visualisation of the two possible configurations of RT geodesics connecting the endpoints of two intervals in the CFT. The endpoints are indicated by p_i. Between the coloured rectangles representing the boundaries, the dashed lines indicate the horizons of the two-sided black string geometry. For $\zeta < 1$, ζ given in (5.70), the shortest geodesics connect points located in the same boundary, visualised by the magenta lines. For $\zeta > 1$, the shortest geodesics connect points on different boundaries, thereby stretching through the wormhole as represented by the orange lines.

tively. Accordingly, the same is true for the modular Berry curvature in this configuration,

$$\begin{aligned}\hat{\Omega}_+ = &\frac{4\pi^2}{\beta^2}\operatorname{csch}^2\frac{\pi(v_L-u_L)}{\beta}\,\hat{K}_{+,L}\,\mathrm{d}v_L\wedge\mathrm{d}u_L\\ &+\frac{4\pi^2}{\beta^2}\operatorname{csch}^2\frac{\pi(v_R-u_R)}{\beta}\,\hat{K}_{+,R}\,\mathrm{d}v_R\wedge\mathrm{d}u_R\,.\end{aligned}\tag{5.72}$$

This result is as expected for this configuration. As the RT surfaces do not stretch through the bulk but stay close to their corresponding boundaries, the wormhole is not probed. Correspondingly, the modular Berry phase is given by twice the result expected of a single-sided geometry. In the other case of $\zeta > 1$, the modular Hamiltonian for the interval $\lambda_u = [u_R, u_L]$ is given by [503]

$$\hat{K}_{+,\lambda_u} = \frac{\coth\frac{\pi(u_L-u_R)}{\beta}}{e^{\frac{2\pi}{\beta}u_L}+e^{\frac{2\pi}{\beta}u_R}}\,l_1 - \coth\frac{\pi(u_L-u_R)}{\beta}\,l_0 + \frac{\coth\frac{\pi(u_L-u_R)}{\beta}}{e^{-\frac{2\pi}{\beta}u_L}+e^{-\frac{2\pi}{\beta}u_R}}\,.\tag{5.73}$$

An analogous expression holds for the other interval $\lambda_v = [v_L, v_R]$. Calculating the derivatives w.r.t. the four endpoints to make use of (5.56) results in

$$\begin{aligned}\hat{\Omega}_+ = &\frac{4\pi^2}{\beta^2}\operatorname{csch}^2\frac{\pi(u_R-u_L)}{\beta}\,\hat{K}_{+,\lambda_u}\,\mathrm{d}u_R\wedge\mathrm{d}u_L\\ &+\frac{4\pi^2}{\beta^2}\operatorname{csch}^2\frac{\pi(v_R-v_L)}{\beta}\,\hat{K}_{+,\lambda_v}\,\mathrm{d}v_R\wedge\mathrm{d}v_L\,.\end{aligned}\tag{5.74}$$

Since the RT surfaces stretch through the bulk the modular Berry curvature consists of pieces that connect both boundaries. The corresponding modular Berry phase obtained by integrating (5.74) therefore is sensitive to the wormhole in the bulk and therefore can be considered as a probe of non-factorisation.

To make this more precise, we choose specific endpoints for the intervals. Following [502], we choose $p_1 = \left(-\frac{x}{2}, t_L = -t\right)$, $p_2 = \left(\frac{x}{2}, t_L = -t\right)$ on the left boundary and $p_3 = \left(-\frac{x}{2}, t_R = t\right)$, $p_4 = \left(\frac{x}{2}, t_R = t\right)$ on the right boundary. Here, we have identified the left and right boundary times. For this choice, in the phase $\zeta > 1$ the intervals λ_u and λ_v are given by the same range $\lambda = \left[-t + \mathrm{i}\frac{\beta}{2}, t\right]$ at fixed $\frac{x}{2}$ [502]. Evaluating the modular Berry curvature (5.74) for these endpoints of the interval results in

$$\widehat{\Omega}_+ \propto \mathrm{d}t \wedge \mathrm{d}t = 0\,. \tag{5.75}$$

This is consistent with the interpretation of the modular Berry phase as a probe of the choices of zero mode frames of each observer. When identifying the times in both boundaries, the zero mode frames in both boundaries are chosen exactly equal, so there is no modular Berry phase. However as we have reviewed in sec. 3.2.1, the presence of the horizon renders the time-like Killing vector to not be defined globally. This leads to the possibility of introducing the time-shift variable δ [182]. Including this time-shift as $t_L - \delta = t_R$ to the interval $\lambda = \left[-t - \delta + \mathrm{i}\frac{\beta}{2}, t\right]$ the modular Berry curvature is non-trivial,

$$\widehat{\Omega}_+ = \frac{4\pi^2}{\beta^2}\,\mathrm{sech}^2\,\frac{\pi(2t+\delta)}{\beta}\,\hat{K}_{+,\lambda}\,\mathrm{d}t \wedge \mathrm{d}\delta\,. \tag{5.76}$$

Similarly to the topological phase of the TFD state defined in (4.52), the time-shift variable δ has to be considered to diagnose non-factorisation. The non-trivial Berry curvature (5.76) arises only due to the presence of this time-shift variable. Since this variable is tied to the existence of the wormhole in the bulk, the modular Berry phase that follows from (5.76) by integration provides a tool to diagnose non-factorisation from the boundary perspective.

To conclude this section, let us compare the three phase factors detecting non-factorisation discussed in this thesis. First, the topological phase of the TFD state defined in (4.52) arises from transformations that are part of the asymptotic symmetry group, specifically time translations. In the bulk, asymptotic symmetries correspond to proper bulk diffeomorphisms. In the asymptotic region, such diffeomorphisms leave the bulk metric invariant, i.e. for a proper diffeomorphism ξ_{prop}, we have $\delta_{\xi_{\text{prop}}} g_{\mu\nu} = 0$ close to the boundary.[15] The

[15] Proper diffeomorphisms correspond both to asymptotic symmetries, where $\delta_{\xi_{\text{prop}}} g_{\mu\nu} = 0$ close to the boundary, and Killing symmetries, where $\delta_{\xi_{\text{prop}}} g_{\mu\nu} = 0$ everywhere. Due to the absence of the global time-like Killing vector, time translations cannot be Killing symmetries.

Virasoro Berry phase discussed in the first half of this section arises from improper diffeomorphisms ξ_{improp}, for which $\delta_{\xi_{\text{improp}}} g_{\mu\nu} \neq 0$. For details on both proper and improper diffeomorphisms in AdS/CFT, we refer the reader to [504]. For Virasoro Berry phases, while the stabiliser group corresponds to proper diffeomorphisms, the elements f generating the paths in the coadjoint orbit are elements of the Virasoro group. These transformations correspond to improper diffeomorphisms and induce so-called 'Virasoro hair' (see e.g. [505]). Since these diffeomorphisms lead to transformations of the boundary energy-momentum tensor, these diffeomorphisms are also referred to as state-changing [506]. Finally, modular Berry phases discussed in the second half of this section are referred to as shape-changing [506], as they arise from deforming the size of subregions within the CFT. Therefore, all three of these phase factors have slightly different origins and thereby probe slightly different features of the bulk spacetime. Nevertheless, as we have shown, all of them have in common that they can be used to diagnose non-factorisation from the boundary perspective.

Geometric Phases and Operator Algebras

6

The use of von Neumann algebras allows for rigorously discussing properties of physical systems. In particular, the type classification of von Neumann algebras enables statements about Hilbert space factorisation and entanglement in the given system. Therefore, using the language of operator algebras is well-suited to approach the factorisation puzzle of the eternal black hole in the context of the AdS/CFT correspondence. Given that the operator algebras on both the bulk and the boundary side can be identified correctly, a clear statement on Hilbert space factorisation can be made. Important progress has been made recently in [132, 133] and [134]. In the former two studies, it has been found that in the large N limit, the algebras describing the exterior of the eternal black hole as well as the dual boundary algebras are of type III_1. Moreover, these algebras share a non-trivial common centre, related to the mass of the black hole. In the latter paper, $\frac{1}{N}$-corrections to the type III_1 description were considered. These corrections enabled to refine the algebraic description by properly including the central element to the algebra. The resulting algebras are of type II_∞ and have a trivial centre. The Hilbert space of both type III and type II algebras never factorises, as we have reviewed in sec. 2.3.1. In the language of von Neumann algebras, the factorisation puzzle arises from using type I reasoning in the boundary. Therefore, this algebraic description shows that also the boundary Hilbert space is non-factorised.

We have shown in the previous sections in several instances that geometric phases are useful tools in diagnosing non-factorisation as well, especially from the boundary perspective. Therefore, the question naturally arises whether geometric phases can be used directly to characterise properties of von Neumann algebras. In this section, we show that the geometric phases calculated in sec. 4.1.2 can be used to distinguish between operator algebras of type II and type III. To this extent, we make use of the construction of hyperfinite type II and type III factors as limits of collections of entangled qubits [127, 325, 326]. In particular, we show that a tracial state on the algebra can be defined using a state vector with vanishing geometric phases. Such state vectors do not exist in the Hilbert space of type III algebras. The geometric phase defined in sec. 4.1.2 probes the geometry of the projective Hilbert space. Therefore, our result on the tracial state provides an explanation for the absence of the trace on type III algebras in terms of the geometry of the projective Hilbert space. Furthermore, we discuss how this result is realised in holography for the

eternal black hole. We furthermore discuss the factorisation of the operator algebras using the topological phase of the TFD state defined in sec. 4.2.2. We identify this topological phase as a probe for this algebraic factorisation in that this phase is non-trivial for the type III_1 case, where a non-trivial centre is present and vanishes for the type II_∞ case, where the centre is trivial. Generalising these insights, we discuss geometric phases in general as an indicator for missing information to a low-energy observer in a local description.

In sec. 6.1 we show that geometric phases allow us to distinguish between von Neumann algebras of type II and type III. In particular, state vectors with vanishing geometric phases define a tracial state and do not exist within the Hilbert space that a type III algebra acts on. We discuss how this is realised in holography for the eternal black hole and address how the topological phase of the TFD state (4.52) probes the factorisation properties of the operator algebras. Next in sec. 6.2, we propose geometric phases as an indicator for missing information to a local observer. We show that this is related to the presence of global symmetries and occurs for entangled as well as unentangled systems in several examples each. For entangled systems, we elaborate on how the geometric phase encodes information about the full Hilbert space of the theory, missing to the local low-energy observer. We comment on how this relates to the expected absence of global symmetries in a theory of quantum gravity. The new results discussed in this section appeared in [184] and we mainly follow the presentation therein.

6.1. Characterising Operator Algebras with Geometric Phases

In this section, we show that state vectors with vanishing geometric phases define traces and thereby distinguish algebras of type II and III. We elaborate on how this is realised in holography for the eternal black hole. We start our discussion of tracial states on von Neumann algebras with an illustrative example for two qubits in sec. 6.1.1. This simple instance, where the algebras are of type I and the existence of the trace is guaranteed, allows for a safe and rigorous analysis of the tracial state on these algebras. We show that only state vectors with vanishing geometric phases can be used to define tracial states as expectation values in said state vectors. We briefly discuss how this generalises for bipartite qunit systems, which are still described by operator algebras of type I, invoking insights on the SZK construction [166]. We then move on to generalise these results to algebras of type II and III in sec. 6.1.2. In particular, we show that the cyclic separating vector of a hyperfinite type III algebra is never a tracial state due to the presence of geometric phases. We further single out the cyclic separating vector of a hyperfinite type II algebra as

a state with vanishing geometric phases, thereby defining the trace on the algebra. Finally in sec. 6.1.3, we apply these results to the holographic scenario of the eternal black hole. We discuss the transition between type III and type II von Neumann algebras observed for the black hole in [134] in terms of the topological phase of the TFD state defined in sec. 4.2.2. Concluding the section, we elaborate on the relation between this topological phase and the non-trivial common centre of the type III_1 algebras found in [132, 133]. This allows us to interpret the topological phase as an indicator for the non-factorisation of the operator algebras.

6.1.1. A Trace for Two Qubits

To illustrate how the geometric phase, and thereby the geometry of state space, influence the possibility of defining a trace on the algebra of observables of the given system, we utilise again the system of two interacting qubits discussed in sec. 4.1. This sets the basis and the intuition behind our analysis to be discussed in sec. 6.1.2. For the two-qubit system, the individual single qubit Hilbert spaces $\mathscr{H}^{(i)}$ with $i = 1, 2$ are spanned by state vectors with 2 complex components. Correspondingly, the algebras of operators acting on these Hilbert spaces are of type $\mathrm{I}_2^{(i)}$. These consist of self-adjoint operators $\mathfrak{a}^{(i)}$ which, since the algebras act on Hilbert spaces of finite dimension, can be represented by Hermitian 2×2 matrices. The algebra acting on the full Hilbert space $\mathscr{H} = \mathscr{H}^{(1)} \otimes \mathscr{H}^{(2)}$ is given by the algebra formed by the tensor product of the individual algebras and is of type I_4.[1] Elements of $\mathrm{I}_4 = \mathrm{I}_2^{(1)} \otimes \mathrm{I}_2^{(2)}$ are given by tensor products of operators $\mathfrak{a}^{(1)} \otimes \mathfrak{a}^{(2)}$ and linear combinations thereof. In this tensor product sense, an operator acting only on one qubit is therefore understood as the tensor product with unity acting on the other qubit. The two algebras $\mathrm{I}_2^{(1)}$ and $\mathrm{I}_2^{(2)}$ commute with each other. Since everything in this setting is manifestly in a type I language, by definition the trace on both algebras $\mathrm{I}_2^{(i)}$ must exist. However, it will be illuminating to discuss how exactly the trace is defined in the algebraic language in this setting.

As discussed in the review on von Neumann algebras in sec. 2.3.1, a trace on the algebra follows from the existence of a tracial state ω_{tr}. As stated in def. 9, such a state is a positive linear functional that is cyclic in the argument. A generic state $\omega_{|\psi\rangle}$ on the algebra, not necessarily cyclic, can be defined as the expectation value in the state vector $|\psi\rangle$, cf. (2.101). To study the trace for the two-qubit system, we define a state on the algebra using the ground state (4.2). Expectation values of operators $\mathfrak{a}^{(i)} \in \mathrm{I}_2^{(i)}$ are then

[1] In general, $\mathrm{I}_{nm} = \mathrm{I}_n \otimes \mathrm{I}_m$. Moreover, the tensor product of operator algebras is understood to only include products of operators that are well-defined as an element of the product algebra, i.e. that respect the weak operator topology. This will however not influence the following discussion.

given by evaluating the state for these operators,

$$\langle \mathfrak{a}^{(i)} \rangle = \omega_{|\psi\rangle}(\mathfrak{a}^{(i)}) = \langle \psi | \mathfrak{a}^{(i)} | \psi \rangle \,. \tag{6.1}$$

To test whether this state is cyclic in the argument, we need to find a parametrisation for $\mathfrak{a}^{(i)}$ such that its action on the state vector $|\psi\rangle$ can be evaluated explicitly. As mentioned earlier, since the algebras are of type I_2, all operators can be represented by Hermitian 2×2 matrices. A convenient basis for such matrices is given by the Pauli matrices σ_i, spanning the Lie algebra $\mathfrak{su}(2)$, together with the 2×2 unity matrix $\mathbb{1}_2$. In the following, we always denote $\sigma_0 = \mathbb{1}_2$ for ease of notation. An arbitrary operator $\mathfrak{a}^{(i)}$ can then be written as

$$\mathfrak{a}^{(i)} = \mathsf{a}_n^{(i)} \sigma_n, \quad n \in \{0, x, y, z\}, \quad \mathsf{a}_n^{(i)} \in \mathbb{R} \,. \tag{6.2}$$

Note in particular that $\mathsf{a}_n^{(i)} \in \mathbb{R}$ is necessary for $\mathfrak{a}^{(i)}$ to be Hermitian. Considering two operators $\mathfrak{a}^{(i)}$ and $\mathfrak{b}^{(i)}$ parametrised in the above way, we test the cyclicity of the linear functional (6.1) by evaluating it on the commutator of the two operators. If the linear functional is cyclic, this has to vanish by definition. For the linear functional defined by the ground state (4.2), we however find

$$\omega_{|\psi\rangle}\big([\mathfrak{a}^{(i)}, \mathfrak{b}^{(i)}]\big) = 2\mathrm{i} \sin\alpha \left(\mathsf{a}_y^{(i)} \mathsf{b}_x^{(i)} - \mathsf{a}_x^{(i)} \mathsf{b}_y^{(i)}\right). \tag{6.3}$$

Since a state is only deemed tracial if it is cyclic in the argument for *any* operator, tuning the coefficients $\mathsf{a}_n^{(i)}$ and $\mathsf{b}_n^{(i)}$ is not sufficient. The only other option to make the r.h.s. of (6.3) vanishing is to set $\alpha = 0$. Harking back to the discussion in sec. 4.1.1, this means that the entanglement entropy is maximal, cf. (4.7). In particular, the ground state $|\psi\rangle$ given in (4.2) used to define the linear functional (6.1) reduces to one of the Bell states, as shown in (4.10).

We find that a maximally entangled state vector defines a tracial state on the algebras $\mathsf{I}_2^{(i)}$, i.e. $\omega_{|\mathrm{Bell}\rangle} = \omega_{\mathrm{tr}}$. This straightforwardly generalises to bipartite systems of two qunits.[2] The setting is the same as above, except that the algebras associated with the individual qunits are of type $\mathsf{I}_n^{(i)}$. An arbitrary state vector $|\psi\rangle$ of this system, written in Schmidt decomposition, is given by

$$|\psi\rangle = \sum_{l=1}^{n} \kappa_l |l_1, l_2\rangle \,. \tag{6.4}$$

An arbitrary Hermitian operator $\mathfrak{a}^{(i)}$ of the algebras $\mathsf{I}_n^{(i)}$ acting on the state vector (6.4) can

[2] Remember that these are more commonly referred to as qudits, however in this thesis we always use n instead of d for the dimension of quantum systems.

be parametrised analogously to (6.2), except that the 2×2 identity matrix and the Pauli matrices are replaced by the $n\times n$ identity matrix $\mathbb{1}_n$ and γ_l spanning the Lie algebra $\mathfrak{su}(n)$, respectively. This defines Hermitian $n\times n$ matrices as representations for the operators $\mathfrak{a}^{(i)}\in \mathsf{I}_n^{(i)}$ as

$$\mathfrak{a}^{(i)} = \sum_{l=0}^{n^2-1} \mathsf{a}_l^{(i)}\gamma_l\,, \tag{6.5}$$

where $\gamma_0=\mathbb{1}_n$. However, explicit matrix representations for γ_l are hard to obtain, especially for large n. Moreover, applying a particular γ_l on (6.4), the result is tedious to obtain. Luckily, an equivalent way of denoting $\mathfrak{a}^{(i)}$ utilises the basis introduced in (6.4) in writing general operators as

$$\mathfrak{a}^{(i)} = \sum_{l,m,k=1}^{n} \mathsf{a}_{km}^{(i)}|l_1,k_2\rangle\langle m_1,k_2|\,, \tag{6.6}$$

where $\mathsf{a}_{km}^{(i)}=\left(\mathsf{a}_{mk}^{(i)}\right)^*$ such that $\mathfrak{a}^{(i)}$ is Hermitian. The basis $|m_1k_2\rangle$ is of course the same as in the state vector (6.4). The coefficients $\mathsf{a}_{km}^{(i)}$ are linear combinations of the coefficients $\mathsf{a}_l^{(i)}$ in (6.5). The relation between these two ways of denoting $\mathfrak{a}^{(i)}$ can be understood as a basis transformation in the space of Hermitian $n\times n$ matrices from γ_l to $|l_1,k_2\rangle\langle m_1,k_2|$. The latter way of denoting the operators given in (6.6) is however much more convenient when evaluating the action on state vectors (6.4) explicitly, repeatedly using $\langle l_i|k_i\rangle=\delta_{lk}$, as we do in the following.

Using the state vector (6.4), we may again define a linear functional, i.e. a state $\omega_{|\psi\rangle}$. Parametrising two operators $\mathfrak{a}^{(i)}$ and $\mathfrak{b}^{(i)}$ as in (6.6), evaluating the state on the commutator of these operators enables to determine whether the state is tracial. Explicitly, we find

$$\begin{aligned}\omega_{|\psi\rangle}\left([\mathfrak{a}^{(i)},\mathfrak{b}^{(i)}]\right) &= \sum_{l,k,a,b,c,d,e,f=1}^{n} \kappa_l\kappa_k \mathsf{a}_{ab}^{(i)}\mathsf{b}_{de}^{(i)}\left(\delta_{la}\delta_{lc}\delta_{bd}\delta_{cf}\delta_{ek}\delta_{fk}-\delta_{ld}\delta_{lf}\delta_{ea}\delta_{fc}\delta_{bk}\delta_{ck}\right)\\ &= \sum_{l,k=1}^{n}\kappa_l^2\left(\mathsf{a}_{lk}^{(i)}\mathsf{b}_{kl}^{(i)}-\mathsf{a}_{kl}^{(i)}\mathsf{b}_{lk}^{(i)}\right)\\ &= \sum_{l,k=1}^{n}\mathsf{a}_{lk}^{(i)}\mathsf{b}_{kl}^{(i)}\left(\kappa_l^2-\kappa_k^2\right)\,.\end{aligned} \tag{6.7}$$

As before for two qubits, we find that the state defined by the state vector (6.4) is not generally cyclic in its argument. Moreover, a non-trivial cancellation between the individual summands in (6.7) depends on the specific operators in question and must therefore not be the solution for $\omega_{|\psi\rangle}$ to be a tracial state. However, each individual term vanishes precisely

when all Schmidt coefficients are equal, $\kappa_l = \kappa_k$ for all $l, k = 1, ..., n$. This generalises the above result for two qubits, as the general two qunit state vector in (6.4) with all Schmidt coefficients equal is maximally entangled. Conclusively, the tracial state ω_{tr} is defined by the maximally entangled state vector also for two qunits.

Before explaining the relation of this analysis to geometric phases, let us first briefly discuss how the tracial states are related to the usual notion of trace for matrix algebras. Evaluating the tracial state for a system of two qunits, defined by (6.4) with all Schmidt coefficients equal, on an arbitrary operator $\mathfrak{a}^{(i)}$, the result is given by

$$\omega_{\mathrm{tr}}(\mathfrak{a}^{(i)}) = \sum_{l=1}^{n} \kappa_l^2 \mathsf{a}_{ll}^{(i)} \,. \tag{6.8}$$

This is different from the familiar notion of the matrix trace, which equals the sum of the diagonal entries of the matrix,

$$\mathrm{tr}\, \mathfrak{a}^{(i)} = \sum_{l=1}^{n} \mathsf{a}_{ll}^{(i)} \,. \tag{6.9}$$

In particular, the tracial state evaluated on the identity matrix $\mathbb{1}_n$ equals one, while usually, the trace of the identity is equal to the dimension, in this case, n. There is however a simple solution to this mismatch. If all Schmidt coefficients are equal, the normalisation of the state vector (6.7) dictates that $\kappa_l = \sqrt{\frac{1}{n}}$ for all $l = 1, ..., n$. Therefore, the coefficients do not depend on the index l and can be pulled in front of the sum in (6.8), resulting in

$$\omega_{\mathrm{tr}}(\mathfrak{a}^{(i)}) = \frac{1}{n} \sum_{l=1}^{n} \mathsf{a}_{ll}^{(i)} \,. \tag{6.10}$$

Comparing with (6.9), we see that the tracial state is related to the usual matrix trace by a simple rescaling. As long as n is finite, we may write

$$\mathrm{tr}\, \mathfrak{a}^{(i)} = n\, \omega_{\mathrm{tr}}(\mathfrak{a}^{(i)}) \,. \tag{6.11}$$

This is precisely the rescaling mentioned below def. 9. For infinite-dimensional systems, which we will encounter in sec. 6.1.2, the notion of the matrix trace is ill-defined, as the r.h.s of (6.11) diverges for $n \to \infty$. As we reviewed in sec. 2.3.1 and will see explicitly shortly, the tracial state itself however is still meaningful.

We are now ready to relate the existence of the trace on the algebra to the value of the geometric phases of the state vectors. Tracial states are defined by maximally entangled state vectors. By the SZK construction reviewed in sec. 2.2.2, maximally entangled state

vectors form a Lagrangian submanifold of the projective Hilbert space. Therefore, such state vectors have a vanishing geometric phase, since the symplectic form on the entanglement orbit vanishes. Combining these observations, the tracial state for a two-qunit system is defined by a state vector with a vanishing geometric phase. Using the results for the two-qubit system (i.e. $n = 2$) discussed in sec. 4.1.2, we can put this statement into an equation. The linear functional defined by the ground state (4.2) of the two-qubit system when evaluated on the commutator of two arbitrary operators $\mathfrak{a}^{(i)}$ and $\mathfrak{b}^{(i)}$ is proportional to $\sin\alpha$, cf. (6.3). The same proportionality is found for the geometric phase Φ_{G} given in (4.25), which determines the entanglement properties of the state. Therefore, we may express (6.3) as

$$\omega_{|\psi\rangle}\big([\mathfrak{a}^{(i)},\mathfrak{b}^{(i)}]\big) \propto \Phi_{\mathrm{G}}\,. \tag{6.12}$$

As discussed in sec. 4.1.2, the geometric phase is a probe for the geometry (i.e. the non-trivial curvature) of the projective Hilbert space. Moreover, the geometric phase can be interpreted as the volume of the projective Hilbert space. The result (6.12) therefore associates a precise notion of geometry to the existence of a trace on the algebra of observables.

We point out that the above cyclicity test of the state $\omega_{|\psi\rangle}$ to discuss the notion of a tracial state can also be understood in terms of the modular operator Δ briefly introduced in sec. 2.3.2. For any state vector $|\psi\rangle$ a modular operator Δ_ψ is defined, satisfying $\Delta_\psi|\psi\rangle = |\psi\rangle$. By an anti-linear operator S_ψ which, for any $\mathfrak{a}^{(i)} \in \mathscr{A}^{(i)}$, is defined by $S_\psi\mathfrak{a}^{(i)}|\psi\rangle = \big(\mathfrak{a}^{(i)}\big)^\dagger|\psi\rangle$, the modular operator in turn is defined as $\Delta_\psi = S_\psi^\dagger S_\psi$. For more details on this see e.g. [192]. We might consider evaluating the state $\omega_{|\psi\rangle}$ for the combination of operators $\mathfrak{a}^{(i)}\Delta_\psi\mathfrak{b}^{(i)}$. Then, using the definition of Δ_ψ, we find

$$\begin{aligned}\omega_{|\psi\rangle}(\mathfrak{a}^{(i)}\Delta_\psi\mathfrak{b}^{(i)}) &= \langle\psi|\mathfrak{a}^{(i)}\Delta_\psi\mathfrak{b}^{(i)}|\psi\rangle = \langle\psi|\mathfrak{a}^{(i)}S_\psi^\dagger S_\psi\mathfrak{b}^{(i)}|\psi = \langle\big(\mathfrak{a}^{(i)}\big)^\dagger\psi|S_\psi^\dagger|S_\psi\mathfrak{b}^{(i)}\psi\rangle\\ &= \langle S_\psi\mathfrak{b}^{(i)}\psi|S_\psi|\big(\mathfrak{a}^{(i)}\big)^\dagger\psi\rangle = \langle\big(\mathfrak{b}^{(i)}\big)^\dagger\psi|\mathfrak{a}^{(i)}\psi\rangle = \langle\psi|\mathfrak{b}^{(i)}\mathfrak{a}^{(i)}|\psi\rangle\\ &= \omega_{|\psi\rangle}(\mathfrak{b}^{(i)}\mathfrak{a}^{(i)})\,,\end{aligned} \tag{6.13}$$

where we used the property $\langle\psi_1|\Upsilon^\dagger|\psi_2\rangle = \langle\psi_2|\Upsilon|\psi_1\rangle$, valid for arbitrary anti-linear operators Υ, in going to the second line. With this property of the modular operator Δ_ψ, we find that the state $\omega_{|\psi\rangle}$ is tracial when the corresponding modular operator is given by the identity, $\Delta_\psi = \mathbb{1}$, since then (6.13) determines $\omega_{|\psi\rangle}$ to be cyclic in its argument. This precisely corresponds to the state vector $|\psi\rangle$ being maximally entangled, consistent with our result (6.8). For the two-qubit case, this can be seen by noting that Δ_ψ is related to the exponential of the modular Hamiltonian $K^{(1)}$ given in (4.33) and its counterpart $K^{(2)}$

defined analogously. For maximal entanglement, both modular Hamiltonians vanish since the coefficient h vanishes, cf. (4.35). Equivalently, also including the case of two qunits, the modular operator can be calculated using the reduced density operators of the state vector $|\psi\rangle$ as $\Delta_\psi = \rho^{(1)} \otimes \left(\rho^{(2)}\right)^{-1}$. For maximal entanglement, $\rho^{(1)} = \frac{1}{n}\mathbb{1}_n = \rho^{(2)}$ and correspondingly we find $\Delta_\psi = \mathbb{1}_{n^2}$.

Furthermore, the relation between state vectors defining a tracial state on the algebra and such state vectors having vanishing geometric phase is consistent with the results of [507]. In this work, the notions of the Fubini–Study metric and the symplectic form for quantum systems established in [271] and reviewed in sec. 2.2.1 were generalised to a QFT setting by a path integral derivation. The action in the path integral is assumed to depend on a set of parameters s_k, such as the couplings in the action. Assuming small perturbations $s_k \to s_k + \delta s_k$ and expanding the Lagrangian to first order the authors of [507] define deformation operators $\mathscr{O}_k$. Using these deformation operators, the Fubini–Study metric and the symplectic form are computed by expectation values of the anti-commutator and the commutator of $\mathscr{O}_k$, respectively, generalising the expressions (2.65) and (2.67) obtained in [271] for quantum mechanical systems. In particular, the components of the symplectic form are (schematically) calculated as [507]

$$\Omega_{lk} \sim \langle 0|[\mathscr{O}_l, \mathscr{O}_k]|0\rangle\,, \tag{6.14}$$

where $|0\rangle$ is the ground state of the system. In [507], the ground state appears since the path integral was prepared such that at the infinite past, the system is in the ground state. However, this formalism can be generalised to arbitrarily excited state vectors $|\psi\rangle$, with the symplectic form given as in (6.14) by replacing $|0\rangle \to |\psi\rangle$ [508, 509]. Since the symplectic form is given by an expectation value of a commutator of operators, it looks similar in spirit to the expressions we used above to test whether a particular state vector defines a tracial state on the algebra, cf. (6.3) and (6.7). In particular, if the vacuum $|0\rangle$ or the excited state vector $|\psi\rangle$ are such that they define a tracial state, the symplectic form vanishes and the geometric phase vanishes since the tracial state is cyclic in the argument.

6.1.2. A Trace for Infinitely Many Qubits

Of course, the analysis of [507–509] is in a QFT setting and therefore, as discussed in sec. 2.3.2, generically refers to an algebra if type III (to be precise, type III_1) rather than type I as in the above cases of qubits and qunits. Rather, this comparison should be understood as an indicator that an analogous statement about the existence of the trace and the value of the geometric phase is also achievable in a QFT setting, i.e. for algebras of type III. This first indication is supplemented by another observation, which gives this

expectation a much stronger basis. In the previous section, we have shown that a linear functional $\omega_{|\psi\rangle}$ is cyclic in the argument if the geometric phase of the corresponding state vector $|\psi\rangle$ vanishes. For the two-qubit system, this is made mathematically precise in (6.12). Another useful form of this equation is found when expressing it using the entanglement temperature derived in sec. 4.2.1. Inverting (4.38) for the geometric phase Φ_G and inserting this into (6.12), we find that

$$\omega_{|\psi\rangle}\big([\mathfrak{a}^{(i)}, \mathfrak{b}^{(i)}]\big) \propto \left(1 - e^{-\beta_{\text{ent}} E}\right). \tag{6.15}$$

First of all, we note that this is consistent with the earlier result. The state $\omega_{|\psi\rangle}$ is cyclic in the argument in the limit $\beta_{\text{ent}} \to 0$, i.e. when $|\psi\rangle$ is maximally entangled. More important for the generalisation to algebras of type II and type III however is the observation that the r.h.s. of (6.15) scales with $1 - e^{-\beta_{\text{ent}} E}$. This is highly reminiscent of the behaviour of the linear functional $\omega_{|\text{TFD}\rangle}$ discussed below (2.111). The only difference is that for the two-qubit system, only one term $\propto \left(1 - e^{-\beta_{\text{ent}} E}\right)$ appears, while below (2.111) the number of such terms depends on the specific operators inserted into the linear functional. However, as reviewed in sec. 2.3.1, algebras of type II and type III can be constructed starting with finite collections of qubits and sending the number of qubits to infinity at the end [128, 325, 326]. The additional qubits then explain the presence of the additional terms. In the following, we make this precise by analysing the construction of algebras of type II and type III w.r.t. geometric phases in the spirit of the SZK construction. This will also allow us to explain the absence of a trace for algebras of type III by the non-trivial geometry of state space.

For the convenience of the reader, we start the analysis by restating a few ingredients reviewed in sec. 2.3.1. To construct an algebra of type III, a possible approach is to consider two collections of qubits which are pairwise entangled. Intuitively, the type III algebra is realised as an infinite tensor product of type I_2 algebras [192]. Each qubit pair, with one qubit from each collection, is therefore described by a state vector as in (2.110), which we denote in the following as

$$|\lambda_l\rangle = \sqrt{\frac{1}{1+\lambda_l}}\big(|\downarrow_1\downarrow_2\rangle_l + \sqrt{\lambda_l}\,|\uparrow_1\uparrow_2\rangle_l\big) \quad \text{with} \quad 0 < \lambda_l \leq 1\,. \tag{6.16}$$

The value of λ_l determines the entanglement between the two qubits, with $\lambda_l = 0$ and $\lambda_l = 1$ corresponding to vanishing and maximal entanglement, respectively. Note however that the case $\lambda_l = 0$ is excluded: every qubit pair has to have some non-vanishing amount of entanglement. As a physical example, we may consider the states (6.16) to represent

the ground state (4.2) of the two-qubit system discussed in sec. 4.1.1.[3] More specifically, every $|\lambda_l\rangle$ is represented by a ground state with in general different ratios of B and J. As an example, we might imagine that all of the qubits of the first collection, corresponding to $\vec{S}_1$ in (4.1), feel the same magnetic field B, but have different coupling strengths J_l to the qubits of the second collection, corresponding to $\vec{S}_2$. Then, the 'angle' α defined below (4.2) is different for every qubit pair, resembling the different λ_l. In particular, these parameters are related as

$$\lambda_l = \frac{1-\sin\alpha_l}{1+\sin\alpha_l} \quad \text{with} \quad \tan\alpha_l = 2\mu_B \frac{B}{J_l}\,. \tag{6.17}$$

Combining N such two-qubit state vectors (6.16) in a tensor product and sending N to infinity, the resulting state vector $|\Psi\rangle$ provides a cyclic and separating vector, with $|\Psi\rangle$ given by

$$|\Psi\rangle = \lim_{N\to\infty} \sqrt{\frac{1}{\prod_{l=1}^{N}(1+\lambda_l)}} \bigotimes_{l=1}^{N} \left(|\downarrow_1\downarrow_2\rangle_l + \sqrt{\lambda_l}\,|\uparrow_1\uparrow_2\rangle_l\right). \tag{6.18}$$

As stated below (2.111), the convergence properties of the sequence of λ_l determined which subclass of type III algebras is constructed starting with this state vector [326]. By the GNS construction [322, 323], a separable Hilbert space on which the type III algebras act reducibly is defined. In particular, there are two algebras of type III $\mathscr{A}^{(1)}$ and $\mathscr{A}^{(2)}$ which are each others commutant, $[\mathscr{A}^{(1)}, \mathscr{A}^{(2)}] = 0$.

As we have shown in sec. 4.2.1, any two-qubit state vector can be written in terms of its geometric phase characterising the entanglement as in (4.40). Therefore, also (6.16) can be put in this form. To obtain this explicitly, we note that (6.16) is already written in Schmidt decomposed form, with Schmidt coefficients given by

$$\kappa_\uparrow = \sqrt{\frac{\lambda_l}{1+\lambda_l}} \quad \text{and} \quad \kappa_\downarrow = \sqrt{\frac{1}{1+\lambda_l}}\,. \tag{6.19}$$

As shown in sec. 4.2.1, the Schmidt coefficients determine the entanglement temperature by (4.45). In the present case, we find

$$\beta_{\text{ent}} = \frac{1}{T_{\text{ent}}} = \frac{1}{E_l} \ln\frac{1}{\lambda_l}\,. \tag{6.20}$$

[3] The state vector (6.16) has qubits pointing in the same direction, while they point in the opposite direction in (4.2). This difference is fixed by rewriting (4.2) in Schmidt decomposition, as discussed above (4.3).

Note that here we choose E_l such that the entanglement temperature itself does not depend on l, i.e. it is the same for every qubit pair. While this is not strictly necessary from the point of view of the resulting algebra, it does provide a more intuitive physical picture. As far as the type of algebra is concerned, it only matters whether the product of E_l with β_{ent} varies with l, as is it this product which determines the convergence properties of the sequence of λ_l. However, physically speaking, it is more intuitive to have all qubit pairs experiencing the same temperature β_{ent} but different energy fluctuations E_l. In particular, with this choice the cyclic separating vector (6.18) expressed by β_{ent} and E_l is precisely the TFD state (2.111) discussed during the review of von Neumann algebras in sec. 2.3.1, with $\beta = \beta_{\text{ent}}$.

We now turn to discussing geometric phases in the above setting. Performing the steps of the calculation discussed in sec. 4.1.2 for the two-qubit state (6.16), i.e. changing the entries of the point in the entanglement orbit p given in (4.14) from (4.3) to (6.19), the geometric phase for each $|\lambda_l\rangle$ is found as

$$\Phi_{\text{G}}^{(l)} = 2\pi \frac{1-\lambda_l}{1+\lambda_l} = 2\pi \frac{1-e^{-\beta_{\text{ent}} E_l}}{1+e^{-\beta_{\text{ent}} E_l}} \,. \tag{6.21}$$

Consistent with the earlier results in sec. 4.1.2, this phase vanishes for maximal entanglement, where $\lambda_l = 1$ or equivalently $\beta_{\text{ent}} = 0$. Inverting (6.21) to express λ_l by $\Phi_{\text{G}}^{(l)}$, the state vectors (6.16) are written analogous to (4.40),

$$|\lambda_l\rangle = \sqrt{\frac{2\pi - \Phi_{\text{G}}^{(l)}}{4\pi}}\, |\uparrow_1\uparrow_2\rangle + \sqrt{\frac{2\pi + \Phi_{\text{G}}^{(l)}}{4\pi}}\, |\downarrow_1\downarrow_2\rangle \,. \tag{6.22}$$

In terms of the entanglement orbits of the SZK construction [166], each state vector $|\lambda_l\rangle$ is associated to a corresponding orbit $\mathbb{C}\text{P}^1_{\lambda_l} \times \mathbb{R}\text{P}^3$. With this way of denoting the state vector, the cyclic and separating vector (6.18) is written in a purely geometric fashion. This form will be more convenient when discussing the relation between the geometric phase and the existence of a trace on the algebra. As in sec. 6.1.1 for two qubits, we test this by studying the cyclicity properties of linear functionals, i.e. states on the algebra. In particular, we study the state $\omega_{|\Psi\rangle}$ defined by the cyclic and separating vector (6.18). To probe the cyclicity properties of this state, we again require a parametrisation of operators acting on the Hilbert space. Since each state vector $|\lambda_l\rangle$ contains two qubits, operators $\mathfrak{a}^{(i)}$ acting on it are again parametrised by the identity matrix and the Pauli matrices as in (6.2). Arbitrary operators $\mathfrak{a}_N^{(i)}$ acting on the N-fold tensor product of such state vectors

are then given by tensor products of operators acting on a single qubit pair,

$$\mathfrak{a}_N^{(i)} = \bigotimes_{l=1}^{N} \mathfrak{a}_l^{(i)}, \tag{6.23}$$

and arbitrary linear combinations of such tensor products. In the limit $N \to \infty$, arbitrary operators are again given by such tensor products. However, as discussed in sec. 2.3.1, to obtain a separable Hilbert space we do not consider all operators, but restrict to those we are interested in. The action of these operators on the cyclic and separating vector then generates the separable Hilbert space, i.e. a Hilbert space with countable dimension. In the current setting, that is we only consider operators that act on finitely many of the qubit pairs. So the relevant operators are given by the tensor product operators $\mathfrak{a}_K^{(i)}$ (and linear combinations thereof), with K finite. In a language more akin to QFT, this can be phrased as considering all finite polynomials in the Pauli matrices σ_n acting on K qubit pairs. For convenience, we can take these operators to act on the first K qubit pairs, with all other qubit pairs unaffected, i.e. those are acted on by the identity,

$$\mathfrak{a}_K^{(i)} = \left[\bigotimes_{l=1}^{K} \mathfrak{a}_l^{(i)}\right] \otimes \left[\bigotimes_{l=K+1}^{\infty} \mathbb{1}_2\right]. \tag{6.24}$$

On the level of state vectors, that means that by acting with such operators on $|\Psi\rangle$, only the coefficients of the first K qubit pairs can be changed, with all other entries unaffected. In particular, the first K qubit pairs in state vectors $\mathfrak{a}_K^{(i)}|\Psi\rangle$ can have different entanglement properties than those in $|\Psi\rangle$. In terms of the entanglement orbits, that means that such operators may change the orbit of finitely many $|\lambda_l\rangle$ from $\mathbb{C}\mathrm{P}^1_{\lambda_l} \times \mathbb{R}\mathrm{P}^3$ to some other $\mathbb{C}\mathrm{P}^1_{\lambda'_l} \times \mathbb{R}\mathrm{P}^3$ with $\lambda_l \neq \lambda'_l$, and even to the limiting cases $\mathbb{C}\mathrm{P}^1 \times \mathbb{C}\mathrm{P}^1$ and $\mathbb{1} \times \mathbb{R}\mathrm{P}^3$. All entanglement orbits corresponding to state vectors $|\lambda_l\rangle$ with $l > K$ are unaltered.

As a short technical intermezzo following [192], operators of the form (6.24) only approximate the operators that are actually contained in the algebra. That is, the above operators should be considered as elements of a 'pre-algebra' $\mathscr{A}_0^{(i)}$ that satisfies every requirement of a von Neumann algebra except that $\mathscr{A}_0^{(i)}$ is not closed under the weak operator topology, cf. def. 8.[4] The von Neumann algebra $\mathscr{A}^{(i)}$ is then obtained by adding certain limits to $\mathscr{A}_0^{(i)}$. To be more specific, interpreting $\mathfrak{a}_K^{(i)}$ as a sequence, an operator $\mathfrak{a}^{(i)} \in \mathscr{A}^{(i)}$ is defined in the limit $K \to \infty$ by $\mathfrak{a}^{(i)}|\Psi'\rangle = \lim_{K\to\infty} \mathfrak{a}_K^{(i)}|\Psi'\rangle$ if this limit exists for any state vector $|\Psi'\rangle \in \mathscr{H}$. We will make brief reverence to this subtlety after discussing the relation

[4] To be precise, in a similar fashion defining state vectors (6.18) gives rise to a countably infinite-dimensional vector space, also known as 'pre-Hilbert space' $\mathscr{H}_0$. Upon defining an inner product, e.g. by the natural pairing $\langle\cdot|\cdot\rangle$, on $\mathscr{H}_0$ with certain properties, cf. def. 1, $\mathscr{H}_0$ is completed to a separable Hilbert space $\mathscr{H}$. For more details see [192].

between the tracial state and the geometric phase in more detail, but it will not affect the overall discussion very much.

We are now in a position to analyse whether the cyclic ad separating vector (6.18) defines a state $\omega_{|\Psi\rangle}$ that is cyclic in the argument, i.e. a tracial state. We consider two operators $\mathfrak{a}_K^{(i)}$ and $\mathfrak{b}_K^{(i)}$ defined as in (6.24). To test the cyclicity, we have to evaluate $\omega_{|\Psi\rangle}\big([\mathfrak{a}_K^{(i)}, \mathfrak{b}_K^{(i)}]\big)$. This can be done by making use of the tensor product structure of the operators. In particular, the commutator of two tensor products can be rewritten as the sum of tensor products of commutators. More precisely, for arbitrary operators we have

$$\begin{aligned}[\mathfrak{a}\otimes\mathfrak{b}, \mathfrak{c}\otimes\mathfrak{d}] &= \mathfrak{ac}\otimes\mathfrak{bd} - \mathfrak{ca}\otimes\mathfrak{db} \\ &= \mathfrak{ac}\otimes\mathfrak{bd} - \mathfrak{ca}\otimes\big(\mathfrak{bd} - [\mathfrak{b},\mathfrak{d}]\big) \\ &= [\mathfrak{a},\mathfrak{c}]\otimes\mathfrak{bd} + \mathfrak{ca}\otimes[\mathfrak{b},\mathfrak{d}]\,. \end{aligned} \tag{6.25}$$

Used repeatedly, the commutator of operators composed as K-fold tensor products can be rewritten as a sum of K terms containing a single commutator of operators in one 'sector' of the tensor product, and simple products of operators in the other slots. As an example, writing $\mathfrak{b} = \mathfrak{e}\otimes\mathfrak{f}$ and $\mathfrak{d} = \mathfrak{g}\otimes\mathfrak{h}$ in (6.25), we find for the commutator of 3-fold tensor product operators

$$\begin{aligned}[\mathfrak{a}\otimes\mathfrak{e}\otimes\mathfrak{f}, \mathfrak{c}\otimes\mathfrak{g}\otimes\mathfrak{h}] &= [\mathfrak{a},\mathfrak{c}]\otimes\mathfrak{eg}\otimes\mathfrak{fh} + \mathfrak{ca}\otimes[\mathfrak{e}\otimes\mathfrak{f}, \mathfrak{g}\otimes\mathfrak{h}] \\ &= [\mathfrak{a},\mathfrak{c}]\otimes\mathfrak{eg}\otimes\mathfrak{fh} + \mathfrak{ca}\otimes[\mathfrak{e},\mathfrak{g}]\otimes\mathfrak{fh} + \mathfrak{ca}\otimes\mathfrak{ge}\otimes[\mathfrak{f},\mathfrak{h}]\,, \end{aligned} \tag{6.26}$$

where we used (6.25) to evaluate the commutator in the second term of the first line. Applying this method to the operators $\mathfrak{a}_K^{(i)}$ and $\mathfrak{b}_K^{(b)}$, it becomes manifest that only the first K qubit pairs play a role in evaluating $\omega_{|\Psi\rangle}\big([\mathfrak{a}_K^{(i)}, \mathfrak{b}_K^{(i)}]\big)$, as hinted at below (6.24). Since all qubit pairs $|\lambda_l\rangle$ with $l > K$ are acted on by the identity, due to the normalisation of $|\lambda_l\rangle$ these terms simplify to 1, multiplying the remaining K non-trivial terms, so

$$\begin{aligned}\omega_{|\Psi\rangle}\big([\mathfrak{a}_K^{(i)}, \mathfrak{b}_K^{(i)}]\big) &= \langle\Psi|[\mathfrak{a}_K^{(i)}, \mathfrak{b}_K^{(i)}]|\Psi\rangle \\ &= \Big[\bigotimes_{l=1}^{K}\langle\lambda_l|\Big]\Big[\bigotimes_{n=1}^{K}\mathfrak{a}_n^{(i)}, \bigotimes_{m=1}^{K}\mathfrak{b}_m^{(i)}\Big]\Big[\bigotimes_{p=1}^{K}|\lambda_p\rangle\Big]\,. \end{aligned} \tag{6.27}$$

This shows that the commutator of two operators $\mathfrak{a}_K^{(i)}$ and $\mathfrak{b}_K^{(i)}$ acting (non-trivially) on K qubit pairs is again an operator acting (non-trivially) on K qubit pairs, or in other words, the algebra generated by the operators $\mathfrak{a}_K^{(i)}$ is closed under forming commutators.

Evaluating (6.27), the second advantage in rewriting the commutator using (6.25) and (6.26) shows. Namely, due to the tensor product structure, the expectation value (6.27)

in the state vector of K qubit pairs boils down to a sum of products of single qubit pair expectation values. These single qubit expectation values only take one of the following forms,

$$\langle\lambda_l|[\mathfrak{a}_l^{(i)},\mathfrak{b}_l^{(i)}]|\lambda_l\rangle \quad \text{or} \quad \langle\lambda_l|\mathfrak{a}_l^{(i)}\mathfrak{b}_l^{(i)}|\lambda_l\rangle\,. \tag{6.28}$$

The first term involving the commutator is precisely what we computed in sec. 6.1.1 when we studied the trace for a two-qubit system. The result, given in (6.3), relates the expectation value of the commutator of two single-qubit pair operators directly to the geometric phase of the single qubit pair, cf. (6.12), multiplied by a function depending on the operators. In particular, this function is purely imaginary. For the second term in (6.28) we therefore expect that apart from an imaginary piece analogous to the result for the first term, there can only appear an additional real piece that cancels in the commutator,

$$\begin{aligned}\langle\lambda_l|[\mathfrak{a}_l^{(i)},\mathfrak{b}_l^{(i)}]|\lambda_l\rangle &= \langle\lambda_l|\mathfrak{a}_l^{(i)}\mathfrak{b}_l^{(i)}|\lambda_l\rangle - \langle\lambda_l|\mathfrak{b}_l^{(i)}\mathfrak{a}_l^{(i)}|\lambda_l\rangle \\ &= \langle\lambda_l|\mathfrak{a}_l^{(i)}\mathfrak{b}_l^{(i)}|\lambda_l\rangle - \langle\lambda_l|\mathfrak{a}_l^{(i)}\mathfrak{b}_l^{(i)}|\lambda_l\rangle^*\,.\end{aligned} \tag{6.29}$$

Indeed, using the parametrisation of single qubit pair operators (6.2) and the representation (6.22) for $|\lambda_l\rangle$ by straightforward calculation we find

$$\langle\lambda_l|\mathfrak{a}_l^{(i)}\mathfrak{b}_l^{(i)}|\lambda_l\rangle = \sum_{n=0,x,y,z} \mathrm{a}_{l,n}^{(i)}\mathrm{b}_{l,n}^{(i)} - \frac{\Phi_{\mathrm{G}}^{(l)}}{2\pi}\left(\mathrm{a}_{l,z}^{(i)}\mathrm{b}_{l,0}^{(i)} + \mathrm{a}_{l,0}^{(i)}\mathrm{b}_{l,z}^{(i)}\right) + \frac{\mathrm{i}\Phi_{\mathrm{G}}^{(l)}}{2\pi}\left(\mathrm{a}_{l,y}^{(i)}\mathrm{b}_{l,x}^{(i)} - \mathrm{a}_{l,x}^{(i)}\mathrm{b}_{l,y}^{(i)}\right). \tag{6.30}$$

Combining these results, we can find an expression for $\omega_{|\Psi\rangle}\big([\mathfrak{a}_K^{(i)},\mathfrak{b}_K^{(i)}]\big)$. The structure of this expression is intuitively clear. Using (6.25) to expand the commutator, (6.27) is rewritten as a sum over products of terms of the form in (6.28). In particular, each of these summands contains one expectation value of a commutator, with the remaining terms expectation values of a product of two operators. The former one is always proportional to the corresponding geometric phase $\Phi_{\mathrm{G}}^{(l)}$, while the latter ones have terms proportional to $\Phi_{\mathrm{G}}^{(l)}$ but also terms independent of the geometric phase. Therefore, starting with $\mathfrak{a}_K^{(i)}$, each summand contains polynomials in the geometric phases up to order K. In particular, no term is independent of any $\Phi_{\mathrm{G}}^{(l)}$, but due to the commutator scales at least linearly with a geometric phase. As an equation, this is summarised as

$$\begin{aligned}\omega_{|\Psi\rangle}\big([\mathfrak{a}_K^{(i)},\mathfrak{b}_K^{(i)}]\big) = &\sum_{l=1}^{K}\Phi_{\mathrm{G}}^{(l)}g_1^{(l)}(\mathfrak{a}_K^{(i)},\mathfrak{b}_K^{(i)}) \\ &+ \sum_{l_1,l_2=1}^{K}\Phi_{\mathrm{G}}^{(l_1)}\Phi_{\mathrm{G}}^{(l_2)}g_2^{(l_1,l_2)}(\mathfrak{a}_K^{(i)},\mathfrak{b}_K^{(i)}) + \mathcal{O}\Big[\big(\Phi_{\mathrm{G}}^{(l_n)}\big)^3\Big]\,,\end{aligned} \tag{6.31}$$

where g_i are functions capturing the dependence on the operators. The omitted terms are higher polynomials in the geometric phases and go up to a term $\propto \prod_{n=1}^{K} \Phi_{\mathrm{G}}^{(l_n)}$. As every term on the r.h.s. of (6.31) is proportional to at least one of the geometric phases, the state $\omega_{|\Psi\rangle}$ is a tracial state if and only if all geometric phases vanish. We point out that in the above calculation, we used operators acting on K qubit pairs, so it might seem as if it is sufficient for the trace to exist that the geometric phases of the first K qubit pair state vectors vanish, while the other can be non-vanishing. However, as we pointed out below (6.24), the operators of the actual von Neumann algebra $\mathscr{A}^{(i)}$ are obtained by adding the limits $\lim_{K\to\infty} \mathfrak{a}_K^{(i)}|\Psi'\rangle$ to the pre-algebra $\mathscr{A}_0^{(i)}$ consisting of $\mathfrak{a}_K^{(i)}$. Therefore, for a state to be cyclic in its argument for arbitrary operators of $\mathscr{A}^{(i)}$, the result in (6.31) shows that every geometric phase has to vanish.

Let us discuss the above result (6.31) in light of the different algebra subclasses of type III. By (6.21), the geometric phase $\Phi_{\mathrm{G}}^{(l)}$ of each qubit pair is determined by the value of λ_l. On the other hand, the values λ_l determine the type of the algebra. In the most generic case for type III_1, the λ_l are such that the sequence of λ_l does not converge, but there are at least two accumulation points $0 < \lambda_1^* \neq \lambda_2^* < 1$. Therefore, infinitely many of the λ_l take values different from 1, and correspondingly infinitely many geometric phases are different from zero. Correspondingly, the r.h.s. of (6.31) does not vanish for arbitrary operators, consistent with the fact that the algebra is of type III and does not allow for defining a trace. In a more fine-tuned case where the sequence converges to a single $0 < \lambda^* < 1$, the algebra is of type III_{λ^*}. Again infinitely many of the geometric phases do not vanish, so the trace is not defined. Finally, for type III_0, the sequence converges slowly to zero. Also in this case, infinitely many of the geometric phases (6.21) are non-vanishing and the trace is not defined. Note that we emphasised the fact that infinitely many of the λ_l are different from 1. This is important since by the action of the algebra, only finitely many of the qubit pair state vectors can be altered. Therefore, if the state defined by the state vector $|\Psi\rangle$ fails to be a tracial state, also every other state defined by a state vector $|\Psi'\rangle = \mathfrak{a}^{(i)}|\Psi\rangle$ cannot be tracial, since still infinitely many λ_l are different from 1 and the corresponding geometric phases do not vanish.

This changes significantly if we allow for infinitely many λ_l to be equal to 1. In particular, this implies that in the state vector $|\Psi\rangle$ given in (6.18), only finitely many qubit pairs have $\lambda_l \neq 1$. Still, this state vector does not define a trace since the r.h.s. of (6.31) does not vanish in general. However, by the action of the algebra, we are allowed to change finitely many of the qubit pair state vectors $|\lambda_l\rangle$. Therefore, there exists an operator $\tilde{\mathfrak{a}}^{(i)}$ such that the state vector $\tilde{\mathfrak{a}}^{(i)}|\Psi\rangle$ corresponds to (6.18) with $\lambda_l = 1$ for every l. Correspondingly by (6.21), every geometric phase of the qubit pairs within $\tilde{\mathfrak{a}}^{(i)}|\Psi\rangle$ vanishes and, invoking the result in (6.31), the state defined using this state vector is cyclic in its argument, i.e. is a

tracial state. With $\lambda_l = 1$ for all l, (6.18) contains only maximally entangled qubit pairs. Indeed, this is precisely the cyclic and separating vector discussed in sec. 2.3.1 used to define an algebra of type II_1, which has a trace. The trace on the other subclass of type II algebras is understood analogously. In particular, as discussed in sec. 2.3.1, algebras of type II_∞ are constructed by tensor products of type II_1 with type I_∞. Both these individual algebras have a trace, as we have just discussed for II_1 noting the vanishing of the geometric phases for the cyclic and separating vector of type II_1. Due to the tensor product structure, the trace on II_∞ is simply given by the product of the traces on the constituents,

$$\mathrm{tr}_{\mathrm{II}_\infty}(\mathfrak{a}) = \mathrm{tr}_{\mathrm{II}_\infty}(\mathfrak{a}_1) \cdot \mathrm{tr}_{\mathrm{I}_\infty}(\mathfrak{a}_2)\,, \tag{6.32}$$

where $\mathfrak{a} \in \mathscr{A}_{\mathrm{II}_\infty}$, $\mathfrak{a}_1 \in \mathscr{A}_{\mathrm{II}_1}$ and $\mathfrak{a}_2 \in \mathscr{A}_{\mathrm{I}_\infty}$. As discussed in sec. 2.3.2, the trace on II_∞ is not canonically normalised, which however does not directly affect the above decomposition of the trace. Therefore, the vanishing of the geometric phases for the state vector leading to the existence of the trace on II_1 implies that also the trace for II_∞ is defined. It follows that we find the analogous relation between the geometric phases and the trace for type II and type III algebras as in the simple two-qubit example. The trace is defined by a state where the corresponding state vector has vanishing geometric phases, which by the SZK construction is equivalent to the state being maximally entangled. This provides a geometric explanation for the non-existence of the trace on type III algebras, and the existence of the trace for type II algebras. In other words, calculating geometric phases for state vectors $|\Psi\rangle$ allows for a characterisation of the type of algebra at hand.

6.1.3. Realisation in Holography: the Eternal Black Hole

The discussion in the previous section made no reference to particular dynamics for the system under consideration. This allowed us to make statements about the general nature of von Neumann algebras using geometric phases. To illustrate the power of this approach, in the following let us discuss a particular realisation of our discussion in the holographic setting of the eternal black hole. This enables us to explain the transition between two types of operator algebras for the eternal black hole observed in [134] using the topological phase defined for the TFD state in sec. 4.2.2.

To provide sufficient context, let us first briefly summarise the results of [132, 133] and [134] on von Neumann algebras for the eternal black hole in Anti-de Sitter spacetime. The setting where the holographic duality is best under control is the weak form of the AdS/CFT correspondence. As reviewed in sec. 3.1.2, this in particular involves the limit of large N, with N the degree of the gauge group $\mathrm{SU}(N)$. While the field theory side in this limit becomes strongly coupled, the dual theory of gravity becomes classical, i.e. $G_\mathrm{N} \propto \frac{1}{N^2} \to 0$,

cf. (3.9). The bulk degrees of freedom therefore correspond to quantum fields propagating on a fixed classical background spacetime. Fixing this background to the eternal black hole, the bulk and boundary operator algebras were analysed in [132, 133]. The boundary operators considered are single-trace operators $\mathfrak{O}$. These gauge-invariant operators consist of polynomials of fields and derivatives of these fields. In particular, the operators $\mathfrak{O}$ have no explicit N dependence and are normalised such that k-fold correlation functions of these operators scale as N^{2-k}. To have a well-defined large N limit for such operators, the expectation values (i.e. $k = 1$) have to be subtracted, $\mathfrak{O}' = \mathfrak{O} - \langle\mathfrak{O}\rangle$, to cancel the linear divergence of the expectation value of $\mathfrak{O}$. This of course does not change the commutation relations between two such single-trace operators. In the large N limit, all correlation functions for $k > 2$ vanish, while the two-point functions scale as N^0. In the first step consider only the operators with non-trivial commutators with each other. Due to the large N behaviour of correlation functions, in the large N limit these non-trivial commutators result in c-numbers rather than other operators. Therefore, the operators $\mathfrak{O}'$ describe a generalised free field theory. The algebra formed by these subtracted single-trace operators $\mathfrak{O}'$ is a von Neumann algebra of type III_1. This can be argued using the duality between this boundary algebra and the bulk algebra defined on the classical background spacetime of the eternal black hole, which is of type III_1 like any algebra of a local region in a QFT (cf. the review in sec. 2.3.2). However, the classification as type III_1 can also be established without using holography by noting that the boundary algebra allows for half-sided modular inclusions (see also [510]), which only exist for algebras of type III_1 [511, 512]. The TFD state dual to the eternal black hole arises as the cyclic and separating vector of the boundary algebras.

With the two-sided setting of the eternal black hole, on both boundaries, the subtracted single-trace operators form algebras of type III_1, denoted as $\mathscr{A}_{L/R,0}$. These algebras are each other's commutants as they are spatially separated. Moreover, they are factors since they only contain operators with non-trivial commutation relations, so the centre must be trivial. The dual algebras $\mathscr{A}_{l/r,0}$ defined on the left and right exterior region of the eternal black hole describe the low-energy effective field theory on the classical background spacetime of the eternal black hole with fixed mass. To allow for varying mass, one has to consider an operator with the notion of energy, i.e. the Hamiltonians $H_{L/R}$. However, as opposed to the single-trace operators $\mathfrak{O}$, the Hamiltonians do not have a well-defined large N limit. In particular, in the presence of the eternal black hole, both the expectation value and two-point function of the Hamiltonian scale as N^2 [451, 513]. While the divergence of the expectation value can be removed as before by subtraction, $H'_{L/R} = H_{L/R} - \langle H_{L/R}\rangle$, the two-point functions of $H'_{L/R}$ still diverge as N^2. Therefore, the subtracted boundary Hamiltonians generating time translations are not part of the algebras $\mathscr{A}_{L/R,0}$. Defining

new operators $U_{L/R} = \frac{1}{N} H'_{L/R}$, these do not have divergent two-point functions and therefore may be included to the algebras, $\mathscr{A}_{L/R} = \mathscr{A}_{L/R,0} \otimes \mathscr{A}_{U_{L/R}}$. The algebras $\mathscr{A}_{U_{L/R}}$ are commutative and are formed by bounded functions of $U_{L/R}$. However in the large N limit, these operators are central elements since for any $\mathfrak{O}_{L/R} \in \mathscr{A}_{L/R,0}$ [132–134],

$$\left[U_{L/R}, \mathfrak{O}_{L,R}\right] = \frac{1}{N}\left[H'_{L/R}, \mathfrak{O}_{L/R}\right] = -\frac{\mathrm{i}}{N}\partial_t \mathfrak{O}_{L/R} \to 0\,. \tag{6.33}$$

The algebras $\mathscr{A}_{L/R}$ are therefore not factors as they contain elements that commute with all other elements of the algebras. Moreover, introducing two operators $U_{L/R}$ is not necessary, but one new operator U is sufficient. This is because the difference of the Hamiltonians $H_- = H_L - H_R = H'_L - H'_R$ is well-defined in the large N limit as the divergences cancel. Correspondingly in the language of von Neumann algebras, the symmetry of the TFD state by evolution using H_- is realised as the modular operator $\Delta^{-\beta H_-}$ acting on the TFD state as the identity [134],

$$\Delta^{-\beta H_-}|\mathrm{TFD}\rangle = |\mathrm{TFD}\rangle\,. \tag{6.34}$$

Since H_- is well-defined in the large N limit, the difference $U_L - U_R = \frac{1}{N} H'_-$ vanishes in the large N limit, thereby identifying U_L and U_R as operators. Correspondingly, there is only one operator U that is included as a central element in both the left and right algebra, so the centre is shared between both algebras. This is the algebraic version of the statement already encountered in sec. 5.1.3 that the mass of the black hole, corresponding to k_0 in (5.37), is a shared mode that is not confined to only one boundary.

Including $\frac{1}{N}$-corrections, the resulting algebras are quite different, as first shown in [134]. In particular, U is no longer a central operator, since allowing for $\frac{1}{N}$-corrections, the r.h.s. of (6.33) does not vanish. In this case, to properly include U to the algebras $\mathscr{A}_{L/R,0}$, it was observed that the previous definition of U receives corrections. This modifies the previously used algebra $\mathscr{A}_U$ to $\mathscr{A}_{\hat{H}_- + X}$, where $\hat{H}_-$ is the bulk dual to H_- and $X = \beta N U$. Moreover, to account for the non-trivial commutator between U and other operators $\mathfrak{O}_{L/R}$, instead of a tensor product one defines the full algebra as the crossed product between the single-trace algebras $\mathscr{A}_{L/R,0}$ and $\mathscr{A}_{\hat{H}_- + X}$, e.g. $\mathscr{A}_L = \mathscr{A}_{L,0} \rtimes \mathscr{A}_{\hat{H}_- + X}$.[5] As discussed in [134], the algebra $\mathscr{A}_{\hat{H}_- + X}$ is the modular automorphism group of the single-trace operator algebras, corresponding to the non-compact group of time translations. Moreover, this modular automorphism is outer since it is defined using $H_{L/R}$ which is not part of the single-trace operator algebras. It has been shown on general grounds that the crossed product of a

[5] Given this form of the left algebra, there are technical subtleties in defining the crossed product for the right algebra, discussed in detail in [134]. For our discussion, these subtleties are not important and we refer the interested reader to the aforementioned paper.

type III_1 von Neumann algebra by its modular automorphism group yields a type II_∞ factor when this automorphism group is non-compact [514, 515]. Since the algebra is now of type II, the entanglement entropy can be defined as traces and density operators now exist. As reviewed in sec. 2.3.2, this entropy is defined up to an arbitrary additive constant that stems from the presence of the outer automorphism group. As $\frac{1}{N}$-corrections correspond to finite G_N-corrections on the bulk side, the type II_∞ algebra provides a semiclassical description of gravity in the bulk.

Let us now discuss this transition in von Neumann algebras in light of our results derived in sec. 6.1.2 on geometric phases and the trace on the algebra. Combining this insight with our results of sec. 4.2.2 on geometric phases for the TFD state, the transition between type III and type II von Neumann algebras in the holographic setting of the eternal black hole can be understood. As we reviewed above, in the large N limit the eternal black hole admits a description in terms of two algebras $\mathscr{A}_{L/R} = \mathscr{A}_{L/R,0} \otimes \mathscr{A}_U$, both of type III_1 [132, 133]. Such algebras do not allow for defining a trace. As we have discussed in sec. 6.1.2, this can be understood as a consequence of the presence of geometric phases $\Phi_G^{(l)}$ (cf. (6.31)), or equivalently by the absence of a maximally entangled state vector. Indeed, the TFD state (3.52) is not maximally entangled, as we have discussed in sec. 4.2.2. In particular, the Schmidt coefficients (4.44) are all different and correspondingly, geometric phases as in (4.50) are defined. These phases probe the geometry of the entanglement orbits as defined by the SZK construction [166], as shown in sec. 4.1.2. Due to the presence of the geometric phases (4.50), the TFD state or any other state vector obtained by acting with an operator on the TFD state does not define a tracial state, made manifest by our result (6.31).

To explain the transition to the type II_∞ algebra of [134], the topological phase (4.52) has to be considered. Using the TFD state for the two-qubit system (4.39), we have demonstrated that the topological phase factor $\Phi^{(\mathrm{TFD})}$ is non-trivial only if the geometric phase Φ_G of the same state is non-trivial as well. Since the TFD state is understood as the dual description of an eternal black hole, our discussion of the qubit system naturally generalises to the algebraic description of black holes. As every state of a type III_1 algebra has geometric phases $\Phi_G^{(l)}$, the corresponding topological phases are non-vanishing. In the case where all of these geometric phases vanish, the corresponding state vector is maximally entangled. This provides a cyclic and separating vector of a type II algebra. As we show in (6.31), this particular vector defines a tracial state on the algebra. Although this construction uses qubit microstates, it is generally applicable to any set of microstates giving rise to the TFD state. The construction of sec. 6.1.2 therefore naturally encompasses the algebra of operators dual to a black hole spacetime. We have therefore found an explicit realisation of the relation between geometric phases and the trace on the algebra

for the eternal black hole in Anti-de Sitter spacetime. The phase factors $\Phi^{(\text{TFD})}$ defined in sec. 4.2.2 associated with time translations are defined for every state vector of a type III algebra, corresponding to the strict large N limit. However, there exists one particular state vector of a type II algebra where these phase factors vanish. This state vector defines the trace on the type II algebra, cf. (6.31), describing the eternal black hole when including $\frac{1}{N}$-corrections.

In this discussion, it is important to note that the phase factor (4.52) probes the topology of the parameter space as defined by the time translations, which are part of the asymptotic symmetry group. In the large N limit, where this phase factor is defined, the TFD state (3.52) and the time-shifted TFD states (3.54) are indistinguishable from any local low-energy observer [182, 454, 455], i.e. there are no observables that may probe differences between these states. As discussed in sec. 4.2.3, this gives rise to the non-trivial topology of the parameter space as $\mathscr{G}_M \simeq \mathbb{S}^1$, cf. (4.67). This treats left and right time translations by the compact group $\mathrm{U}(1)$. To connect to the crossed product of [134], it is however important to consider time translations as the non-compact group $\mathbb{R}$ instead of $\mathrm{U}(1)$. As mentioned before, the type II_∞ algebra arising by taking the crossed product requires that the modular automorphism group is non-compact. In light of the topological phase factor (4.52), the $\frac{1}{N}$-corrections considered in [134] allow for distinguishing between $|\text{TFD}\rangle$ and $|\text{TFD}\rangle_\alpha$. In particular, the periodicity of δ discussed below (4.52) is no longer defined, which essentially decompactifies $\mathrm{U}(1)$ into $\mathbb{R}$. With non-compact time translations, the topological phases vanish as now the parameter space $\mathscr{G}_M \simeq \mathbb{R}$ is topologically trivial. With the phase factors vanishing, the corresponding state vector defines the trace on the algebra.

To conclude this section, let us discuss the factorisation puzzle from the algebraic perspective. This puzzle arises due to type I reasoning. However, as we have explained above following [132, 133], the von Neumann algebras describing the eternal black hole in the large N limit are of type III_1. Such algebras act on a Hilbert space that does not admit a factorisation since these algebras do not have an irreducible representation, as we have reviewed in sec. 2.3.1. To be precise, the algebras $\mathscr{A}_{L/R}$, which are each other's commutants, act on a combined Hilbert space $\mathscr{H}$ that cannot be written as a factorised Hilbert space $\mathscr{H}_L \otimes \mathscr{H}_R$, at least not without introducing a cutoff. This makes the non-factorisation of the Hilbert space dual to the eternal black hole manifest. Apart from the Hilbert space non-factorisation, in the large N description even the algebras $\mathscr{A}_{L/R}$ are not factorised as they share the central operator U. This shared mode corresponds to the mass of the black hole, analogous to the holonomy k_0 of sec. 5.1.3. As we have shown in the aforementioned section, this shared mode appears as a coupling term in the chiral boson action (5.37) defined on an annulus geometry. Moreover, the topological phase $\Phi^{(\text{TFD})}$ defined for the

TFD state in (4.52) indicates the non-factorisation of the operator algebras. In particular, in the absence of the shared mode, the left and right time translations generated by H_L and H_R, respectively, correspond to different bulk isometries, each represented by U(1). The resulting parameter space $\mathscr{G}_M$ is then topologically trivial and there is no ambiguity in relating the left and right boundary times. With $\frac{1}{N}$-corrections, the algebras are deformed to type II factors [134]. For such algebras, irreducible representations do not exist either, and therefore they do not act on a factorised boundary Hilbert space as well. Truly factorised Hilbert spaces only arise for algebras of type I, which is the expected algebra type for a complete theory of quantum gravity (see e.g. [172] for a discussion in this direction). However, the algebras defined by the crossed product are factors, i.e. the centre is trivial. As we discussed above, in this case, the topological phase factor $\Phi^{(\mathrm{TFD})}$ vanishes, consistent with our interpretation of a non-trivial $\Phi^{(\mathrm{TFD})}$ indicating the non-factorisation of the operator algebras.

6.2. Geometric Phase and Missing Information

In the previous sec. 6.1 we have discussed in detail how geometric phases can be utilised to distinguish between types of von Neumann algebras, in particular between type II and III. In this section, we discuss the implications of non-vanishing geometric phases for the description of physical systems in a broader sense. We propose geometric phases as an indicator for missing information about the microscopic structure of the phase space. More precisely, whenever geometric phases are present, a local observer does not have access to the full Hilbert space. For systems without entanglement, this missing information is related to the presence of a global symmetry. This global symmetry enters in the quotient when defining the projective Hilbert space, cf. (2.57). The geometric phases resulting from this non-trivial fibre bundle allow us to distinguish between the projective Hilbert space and the full Hilbert space, where local observers only have access to local regions of the former, as we will make precise shortly. For systems with entanglement between two subregions, global symmetries generate phases in the overall state which cannot be measured by an observer restricted to one subregion. In particular, the phases do not influence any local measurement. As we elaborate on towards the end of this section, the theme of geometric phases indicating missing information also has an interesting relation to the expected absence of global symmetries in theories of quantum gravity. In the following sec. 6.2.1 we illustrate the relation between geometric phases and missing information for systems without entanglement in two examples, each time specifying which physics is behind the missing information. Next in sec. 6.2.2, we generalise this idea to systems with entanglement in three examples. Here we also relate our interpretation of the geometric

phase to the eternal black hole, in particular in light of the results on von Neumann algebras for the eternal black hole reviewed and discussed before.

6.2.1. Examples without Entanglement

We start the discussion with geometric phases in unentangled systems. In particular, we discuss a single qubit interacting with a magnetic field, which is the prototypical example of a system with geometric phases [163]. We show how the geometric phase enables us to determine the geometry and topology of the projective Hilbert space. We then continue to generalise this idea to the more advanced case of a single CFT,[6] where Virasoro Berry phases can be defined [167]. As we shall discuss, here the missing information is related to time translations and the origin of time in the CFT.

A Single Qubit

As a first demonstration of the relation between geometric phases and missing information, we consider the well-known setting of a single qubit interacting with a magnetic field, describing the Zeeman effect. The corresponding Hamiltonian was considered in the context of geometric phases by Berry in the seminal paper [163],

$$H = \mu_B \vec{B} \cdot \vec{S}\,, \tag{6.35}$$

where as in (4.1), μ_B is the Bohr magneton, $\vec{B}$ is the magnetic field and $\vec{S} = \frac{1}{2}\vec{\sigma}$ represents the qubit. The magnetic field is parametrised by the absolute value $B = |\vec{B}|$ and two angles ϕ and θ as $\vec{B} = B(\sin\theta\cos\phi, \sin\theta\sin\phi, \cos\theta)^T$, with the two angles specifying points on the Bloch sphere. As discussed in sec. 2.2.1, this system can be considered as a physical realisation of the Hopf fibration [283] with the Hilbert space $\mathscr{H} = \mathbb{S}^3$, the projective Hilbert space $\mathscr{P}(\mathscr{H}) = \mathbb{C}\mathrm{P}^1 \simeq \mathbb{S}^2$ and the gauge group $G = \mathrm{U}(1) \simeq \mathbb{S}^1$ providing the entire manifold $\mathscr{E}$, the base manifold $\mathscr{B}$ and the fibre $\mathscr{F}$ respectively. This is a non-trivial fibre bundle since $\mathbb{S}^3 \neq \mathbb{S}^2 \times \mathbb{S}^1$. Correspondingly, global coordinates cannot be defined but local coordinate patches have to be used. The gauge group $\mathrm{U}(1)$ describes coordinate transformations between these patches and leads to global phases of state vectors of the system described by (6.35). Such phases cannot be determined by working in only one coordinate patch. In other words, a local observer defined as an observer who has access only to one coordinate patch is missing the information about the geometric phase. In particular, from their local perspective, they cannot distinguish between the Hilbert space

[6] Of course, generically states in a CFT contain entanglement when imposing bipartition surfaces. In the sense discussed here, the absence of entanglement refers to the fact that the CFT itself is not entangled to any other system, as will be the case in later examples.

$\mathscr{H}$ and the projective Hilbert space $\mathscr{P}(\mathscr{H})$. The local observer has no way of determining the geometry and/or topology of the manifold they are defined on, as this requires access to both coordinate patches. We demonstrate this in the following explicitly.

The eigenstates of the Hamiltonian given in (6.35) are given by

$$|\xi_1\rangle = -e^{-i\phi}\sin\frac{\theta}{2}\,|\uparrow\rangle + \cos\frac{\theta}{2}\,|\downarrow\rangle\,, \tag{6.36}$$

$$|\xi_2\rangle = -\sin\frac{\theta}{2}\,|\uparrow\rangle + e^{i\phi}\cos\frac{\theta}{2}\,|\downarrow\rangle\,. \tag{6.37}$$

These two eigenstates are singular at the north pole $\theta = 0$ and the south pole $\theta = \pi$ respectively, since at these points the other angle ϕ is not defined. The two coordinate patches in combination of course cover all of the projective Hilbert space. The local gauge fields for the south and north pole coordinate patches are defined as in (2.63) using the state vectors (6.36) and (6.37) respectively,

$$A_S = i\langle\xi_1|d|\xi_1\rangle = \frac{1}{2}(1-\cos\theta)d\phi\,, \tag{6.38}$$

$$A_N = i\langle\xi_2|d|\xi_2\rangle = -\frac{1}{2}(1+\cos\theta)d\phi\,, \tag{6.39}$$

which are related by the U(1) transformation $U = e^{i\phi}$ following (2.80),

$$A_S = A_N - iU^\dagger dU\,. \tag{6.40}$$

Equivalently, also the state vectors (6.36) and (6.37) are related by this transformation, $|\xi_2\rangle = U|\xi_1\rangle$. Note that all of this is highly reminiscent of the discussion in sec. 4.1.2 regarding the geometric phase for the two-qubit system. However, compared to that system, in the present discussion, we do not have any entanglement. Comparing the local gauge fields (4.23) and (4.21) to (6.38) and (6.39), respectively, this manifests in the absence of the prefactor $\sin\alpha$. In particular, in sec. 4.1.1 it was shown that vanishing entanglement implies $\alpha = \frac{\pi}{2}$, where $\sin\alpha = 1$, consistent with the above results for the local gauge fields. Moreover, in the $\alpha = \frac{\pi}{2}$ implies that the ratio $\frac{B}{J}$ between the two parameters B and J in the two-qubit Hamiltonian diverges, so $B \gg J$ and the Hamiltonian in (4.1) reduces to the single-qubit Hamiltonian (6.35).

Calculating the field strength, i.e. the symplectic form Ω, associated to the local gauge fields,

$$\Omega = dA_N = dA_S = \frac{1}{2}\sin\theta d\theta\wedge d\phi\,, \tag{6.41}$$

the geometric phase of [163] follows by integration as in (2.83),

$$\Phi_{\mathrm{G}} = \int_{\mathbb{S}^2} \Omega = 2\pi \,. \tag{6.42}$$

Moreover by the Chern theorem [282] stated in (2.82), the Euler characteristic of the projective Hilbert space $\chi(\mathbb{C}\mathrm{P}^1)$ can be calculated. Using (6.41), the Euler characteristic follows as

$$\chi(\mathbb{C}\mathrm{P}^1) = \frac{1}{2\pi} \int_{\mathbb{C}\mathrm{P}^1} \sqrt{\det \Omega} = 2 \,. \tag{6.43}$$

Since $\chi = 2 - 2g$ where g is the number of holes of the manifold in question, this result shows that $\mathbb{C}\mathrm{P}^1$ does not have any holes. Since $\mathbb{C}\mathrm{P}^1$ is a real two-dimensional manifold, this makes manifest that $\mathbb{C}\mathrm{P}^1$ is homeomorphic to the sphere in two dimensions, $\mathbb{C}\mathrm{P}^1 \simeq \mathbb{S}^2$, as already stated earlier.[7] This simple example shows how the non-trivial fibre bundle defined above the projective Hilbert space and the corresponding geometric phase include information about the geometry and topology of this space inaccessible to a local observer. As alluded to earlier in sec. 2.2.1, such phases arise in condensed matter physics, most famously in the quantum Hall effect. The quantum Hall conductance is quantised in terms of Chern numbers [156, 157, 159], which has also been confirmed experimentally [158]. Such phases are therefore not only important in abstract mathematical discussions but define physically measurable quantities.

Virasoro Berry Phase in a Single CFT

We now turn to discussing missing information in the more complicated scenario of a single CFT. As discussed in sec. 5.1.1, here the Virasoro Berry phase Φ_{Vir} can be defined [167]. This phase is computed by integrating the local gauge field, cf. (5.8), for a given element of the Virasoro group, $(f, \alpha) \in \mathrm{Vir}$. Such group elements correspond to conformal transformations f that may act on highest weight states $|h\rangle$ in a suitable unitary representation $\mathfrak{u}(f)$. However, all states $|h\rangle$ with $h > 0$ have a global U(1) symmetry, representing the time translation invariance of the CFT generated by the Hamiltonian. For these particular transformations, the states $|h\rangle$ only pick up an overall phase, $|h\rangle \to e^{\mathrm{i}\Phi_{\mathrm{Vir}}}|h\rangle$. All such states lie in the same ray and are therefore indistinguishable by any local measurement, i.e. to any local observer. This enables to define the coadjoint orbit for states $|h\rangle$ as the

[7] In fact, any real two-dimensional compact manifold without holes is homeomorphic to $\mathbb{S}^2$, even seemingly more complicated ones such as the surface of a coffee mug without a handle.

quotient space

$$\mathscr{G} = \frac{\mathrm{Vir}}{\mathrm{U}(1)} \,. \tag{6.44}$$

Upon quantisation, this provides the projective Hilbert space for the CFT. As reviewed in sec. 2.2.1, this provides the base space of a fibre bundle, with fibre $\mathrm{U}(1)$. The holonomy of this fibre bundle is known as the Virasoro Berry phase [167].

To discuss missing information for the Virasoro Berry phase, we consider any highest weight state $|h\rangle$ with $h > 0$. Under an arbitrary conformal transformation f, this state transforms into $\mathfrak{u}(f)|h\rangle$. At each point along this path, there is a phase ambiguity of the state due to the $\mathrm{U}(1)$ symmetry. In other words, there is no local measurement distinguishing $\mathfrak{u}(f)|h\rangle$ and $e^{\mathrm{i}\Phi_{\mathrm{Vir}}}\mathfrak{u}(f)|h\rangle$. This phase ambiguity is interpreted as the freedom of the local observer to choose their origin of the time coordinate. Since no expectation value is sensitive to this choice for the origin, the phase factor $e^{\mathrm{i}\Phi_{\mathrm{Vir}}}$ represents missing information. In particular, much like the geometric phase within the SZK construction discussed in sec. 4.1.2 probes the geometry of the entanglement orbit, the Virasoro Berry phase is sensitive to the geometry of the Verma module defined for the highest weight state $|h\rangle$.

6.2.2. Examples with Entanglement

In the previous discussion, we have related non-trivial geometric phases to missing information in physical systems. In particular, we have discussed this for unentangled systems with global symmetries. In the following, we generalise this to systems with entanglement, which in particular enables us to discuss the setting of the eternal black hole in AdS/CFT in the context of missing information. We do so taking three different perspectives, following our earlier analyses of secs. 4.2 and 5. That is, we first discuss Virasoro Berry phases in entangled CFTs, building up on the results of sec. 5.1.3. We then move on to the topological phase of the TFD state defined in sec. 4.2.2 and finally turn to the modular Berry phases discussed in sec. 5.2.2.

Virasoro Berry Phase for Two Entangled CFTs

We have discussed the Virasoro Berry phase for two entangled CFTs dual to the eternal black hole in sec. 5.1.3. It arises due to independent choices of the time coordinate in each CFT, thereby indicating the missing information about the relation between the time coordinates. As we have reviewed in sec. 3.2.1, the eternal black hole is dual to two CFTs entangled in the TFD state. The black hole horizon causally separates these two CFTs.

Therefore, on each boundary, conformal transformations can be applied independently. For the current setting of two copies of a CFT_2, the asymptotic symmetry groups $\mathscr{G}_{\mathrm{asy}}^{(L/R)}$ are both given by the Virasoro group [365]. These of course also include time translations generated by the boundary Hamiltonians $H_{L/R}$. Local observers in each boundary may choose their origins of time independently. The misalignment between these choices for the origin of time results in the time-shift variable δ that appears in the time-shifted TFD states (3.54). The value of this time-shift is inaccessible to a local low-energy observer and therefore is interpreted as a piece of missing information, indicated by the corresponding phase factor acquired by the TFD state as shown in sec. 4.2.2. We discussed this in detail for the example of JT gravity in sec. 4.2.3. In the higher-dimensional setting of $\mathrm{AdS}_3/\mathrm{CFT}_2$ that we currently discuss, the same arguments apply. That is, while the asymptotic symmetry groups are now given by the Virasoro group instead of only $\mathrm{U}(1)$, the isometry of the spacetime is still described by a single $\mathrm{U}(1)$ generating the time-shift. This reflects that the mass of the black hole must be the same when measured from both boundaries. With these asymptotic symmetry groups, the parameter space of the theory follows using (4.59) or as

$$\mathscr{G}_{\mathrm{M}} = \frac{\mathrm{Vir} \otimes \mathrm{Vir}}{\mathrm{U}(1)}\,, \tag{6.45}$$

coinciding with the coadjoint orbit obtained in (5.44). This provides the base space of a fibre bundle with fibre $\mathrm{U}(1)$ and, upon quantisation, the projective Hilbert space. We have pointed out in the previous sec. 6.2.1 that the Virasoro Berry phase for a single CFT probes the geometry of the Verma module of the highest weight state $|h\rangle$, much like the geometric phase (4.25) discussed for the two-qubit system of sec. 4.1.2 probes the geometry of the entanglement orbit. For the present case of entangled CFTs, a further analogy can be made. The phase factor indicating missing information about the time-shift variable probes the topology of the parameter space (6.45) and is therefore understood as a generalisation of the topological phase factor of the TFD state (4.52) to the setting of $\mathrm{AdS}_3/\mathrm{CFT}_2$. In the context of the von Neumann algebras describing the eternal black hole in the large N limit [132, 133], this phase factor indicates the non-trivial common centre between the left and right algebras. This common centre corresponds to the constraint that the black hole mass must be the same when measured from both boundaries. In the parameter space (6.45), this is implemented by taking the common quotient of $\mathrm{Vir} \otimes \mathrm{Vir}$ by a single $\mathrm{U}(1)$. With the black hole mass being the conserved charge associated with the time shift mode, the Virasoro Berry phase in entangled CFTs results from the non-trivial centre.

The TFD Topological Phase

For the TFD state, the topological phase as defined in (4.52) arises precisely due to the time-shift δ between the left and right times. For the explicit example of JT gravity, we have shown in sec. 4.2.3 that this topological phase is in particular a winding number. This topological phase again describes missing information, which can be understood from the perspective of the algebra by invoking geometric quantisation. Within geometric quantisation, winding numbers appear in the spectrum of the 'prequantum' operator describing the canonically conjugate momentum (see e.g. [266]). In our example of JT gravity, this operator corresponds to the Hamiltonian. In a general setting, given that the topology of the parameter space is non-trivial as for the punctured plane $\mathbb{R}^2\backslash\{0\}$, the winding numbers appear in the spectrum of the prequantum momentum operator. This spectrum generally takes the form $\{r+\lambda\}$, where $r \in \mathbb{Z}$ is the winding number and $\lambda \in [0,1)$ is an ambiguity parameter that can be used to shift the local gauge field $A \to A+\lambda$ without changing the symplectic form $\Omega = \mathrm{d}A$, as $\mathrm{d}\lambda = 0$. Since λ appears in the spectrum, the prequantum operators defined for different choices for the value of λ are inequivalent. The operator algebra is therefore sensitive to the value of λ. On the contrary, for every fixed λ, the prequantum operators for different values of r define an equivalence class (for details see e.g. [266]). Therefore, the algebra of operators is not sensitive to the value of r, as these operators correspond to the same symplectic form and have an equivalent spectrum. In other words, a local observer has no way of measuring the value of r. We therefore term the information about r a missing information. In our particular example of the topological phase factor for the TFD state (4.52), this information about the winding number of the time-shift mode specifies the precise gluing of the bulk and boundary spacetimes and corresponds to the non-trivial centre of the von Neumann algebras, as discussed at the end of sec. 6.1.3.

Modular Berry Phase for a Bulk Wormhole

Finally, we turn to modular Berry phases as discussed in the context of the black hole in sec. 5.2.2. These are different to the previous two examples in that they are generated by the modular Hamiltonian rather than the physical Hamiltonian. Analogously however to the previous two examples, this phase arises due to a misalignment of the time coordinates of spatially separated local observers of the left and right boundary. In this case, time refers to the modular rather than the physical time. As a result of this misalignment of the modular time coordinates, the global state of the system contains additional phase factors. These are however inaccessible to the local low-energy observers. In particular, the reduced density operators of each observer are independent of these phases. Therefore, the modular

Berry phase as well indicates information missing to a local low-energy observer in terms of misaligned modular time frames.

To conclude this section, let us discuss the relation between geometric phases and missing information in the light of von Neumann algebras and quantum gravity. As alluded to in [516], any QFT that emerges as a low-energy limit of a full theory of quantum gravity is complete, in the sense that the operator algebra is a maximal set of all operators consistent with low-energy physics, as pointed out in earlier works based on insights of string theory [517, 518] and the AdS/CFT correspondence [519, 520]. This can be given another interpretation in terms of global symmetries. An incomplete theory, i.e. with missing operators, has a global symmetry. Therefore, a theory of quantum gravity is expected to not have global symmetries [519, 520]. In our above examples of geometric phases indicating missing information, we found that these geometric phases were defined using the global symmetries of the theory, in particular time translations. Therefore, in a full theory of quantum gravity, we expect that there are no geometric phases, as there are no global symmetries. Accordingly, studying geometric phases, in particular in holographic settings, is an important part of developing a complete theory of quantum gravity. As an example, we have shown in the sec. 6.1.3 that the absence of the geometric phase explains the transition from a type III_1 to a type II_∞ algebra for the eternal black hole. This absence is understood by including $\frac{1}{N}$-corrections, which makes the theory more complete, i.e. closer to the underlying theory of quantum gravity.

7 Geometric Quantum Discord

For pure states, the entanglement entropy is a sufficient measure of all possible quantum correlations. This however is no longer true when considering mixed states. There exist various generalisations for an entanglement measure for mixed states such as the entanglement of formation [242, 243], yet none of these generalisations are sensitive to all kinds of quantum correlations. For this purpose, as reviewed in sec. 2.1.3 quantum discord was defined [173–175], which captures quantum correlations beyond e.g. the entanglement of formation [174, 251] or entanglement negativity [252]. Unfortunately, considering generic states there is no efficient way to calculate quantum discord, as this calculation is an NP-complete problem [180]. Based on a necessary and sufficient condition for non-vanishing quantum discord, the authors of [181] proposed a measure known as *geometric quantum discord* (GQD) whose computation is less involved, as reviewed in sec. 2.2.2.

In the previous sections, in particular sec. 4, we have discussed entanglement properties and in particular non-factorisation using geometric phases and the SZK construction [166]. In this section, we show that computing GQD provides an alternative measure of non-factorisation. Since we are interested in applying this measure of non-factorisation to a holographic setting, in particular the TFD state as the dual description to the eternal black hole, we perform the analysis and computation of GQD for pure states only. Our result shows that GQD can be viewed as a quantity in quantum theory that diagnoses non-factorisation without necessarily referring to a bulk description. The GQD is defined in terms of the Hilbert–Schmidt norm, which induces a metric and therefore a notion of distance on state space [271], as we reviewed in sec. 2.2.1. W.r.t. this distance, the state χ minimising this norm is interpreted as the 'closest' state to the quantum state ρ under consideration. We also show that non-factorisation via GQD is consistent with the earlier discussion on geometric phases and entanglement orbits for the system of two interacting qubits discussed in secs. 4.1.1 and 4.1.2. When applied to the TFD state, we make explicit that GQD signals non-factorisation between the left and right CFTs in terms of the thermal partition function. In particular, the state minimising GQD for the TFD state is given by the so-called *thermomixed double state*, which provides a mixed state description of the eternal black hole with classical correlations across the ER bridge [182]. While this state was motivated in [182] by bulk considerations, our calculation shows that the TMD state can also be derived purely in the boundary. Noting that GQD is related to the second Rényi entropy, we propose how GQD can be calculated in the

dual gravitational description. We moreover show that GQD can be used to probe the microstates of the black hole. We discuss this by generalising the Hilbert–Schmidt norm of GQD to the Schatten norm. Calculating the Schatten norm of the difference between any of the time-shifted TFD states and the thermomixed double state results in overlaps probing $\frac{1}{N}$-corrections.

We start our analysis by computing GQD for arbitrary pure states in sec. 7.1 and discuss the properties of the resulting expression, in particular in light of non-factorisation. We then move on to utilise our result for the time-shifted TFD states in sec. 7.2 and show non-factorisation from the boundary perspective in terms of a non-vanishing GQD. We also discuss the state singled out in the minimisation process when computing GQD for the TFD state as this state has an interesting interpretation in the dual gravitational picture as well [182]. Finally in sec. 7.3, we study GQD, and a straightforward generalisation thereof, for the time-shifted TFD states (3.54) w.r.t. their interpretation as microstates of the eternal black hole. The new results discussed in this section appeared in [186] and we mainly follow the presentation therein.

7.1. For Arbitrary Pure States

We start our analysis of GQD by discussing in detail the result for GQD of arbitrary pure states $\rho = |\psi\rangle\langle\psi|$ in sec. 7.1.1. We briefly discuss the properties of the state minimising the Hilbert–Schmidt norm when computing GQD, which is always a c-c state in the sense of the classification discussed in sec. 2.1.3. Subsequently we show that this does not generalise to mixed states in an explicit example for the isotropic state, where the state minimising the norm is a q-c state. Finally, we discuss how GQD can be expressed by the second Rényi entropy, and moreover by the modular partition function, i.e. the partition function defined by the modular Hamiltonian. In sec. 7.1.2 we then show that non-factorisation as indicated by GQD is consistent with the notion of non-factorisation using geometric phases for the interacting two-qubit system discussed in secs. 4.1.1 and 4.1.2.

7.1.1. A Classical Approximation to Quantum Entanglement

The measure of quantum correlations GQD given in (2.98) can be evaluated exactly for arbitrary pure states $\rho = |\psi\rangle\langle\psi|$ of a bipartite Hilbert space $\mathscr{H} = \mathscr{H}^{(A)} \otimes \mathscr{H}^{(\bar{A})} = \mathbb{C}^n \otimes \mathbb{C}^n$. The GQD is determined by tuning the coefficients within a q-c state χ as given in (2.99) such that the Hilbert–Schmidt norm of $\rho - \chi$ is minimal. The (square of the) Hilbert–

Schmidt norm is given by

$$||\rho - \chi||^2 = \mathrm{tr}\left(\rho^2\right) - 2\,\mathrm{tr}(\rho\chi) + \mathrm{tr}\left(\chi^2\right). \tag{7.1}$$

Since ρ is a pure state, the first term is equal to 1. To evaluate the other two terms it is convenient to assume that the state vector $|\psi\rangle$ is written in Schmidt decomposition, which can be established for any pure state. The pure state ρ is then given by

$$\rho = \sum_{k,l=1}^{n} \kappa_k \kappa_l |k^{(A)}, k^{(\bar{A})}\rangle\langle l^{(A)}, l^{(\bar{A})}|\,. \tag{7.2}$$

Using χ as given in (2.99) upon renaming $|\phi_k^{(\bar{A})}\rangle \to |k^{(\bar{A})}\rangle$, the latter two terms in (7.1) evaluate to

$$\mathrm{tr}(\rho\chi) = \sum_{k=1}^{n} \kappa_k^2 q_k \langle k^{(A)}|\rho_k^{(A)}|k^{(A)}\rangle\,, \tag{7.3}$$

$$\mathrm{tr}\left(\chi^2\right) = \sum_{k=1}^{n} q_k^2\,\mathrm{tr}_{(A)}(\rho_k^{(A)}\rho_k^{(A)})\,, \tag{7.4}$$

where we made use of $\langle k^{(A)/(\bar{A})}|l^{(A)/(\bar{A})}\rangle = \delta_{lk}$. Inserting (7.3) and (7.4) into (7.1) we find the Hilbert–Schmidt norm to be

$$||\rho - \chi||^2 = 1 - 2\sum_{k=1}^{n} \kappa_k^2 q_k \langle k^{(A)}|\rho_k^{(A)}|k^{(A)}\rangle + \sum_{k=1}^{n} q_k^2\,\mathrm{tr}_{(A)}(\rho_k^{(A)}\rho_k^{(A)})\,. \tag{7.5}$$

In order to minimise (7.5) we have to find appropriate q_k as well as $\rho_k^{(A)}$. This is achieved by calculating derivatives w.r.t. q_k as well as the entries of $\rho_k^{(A)}$. Setting these derivatives to zero, we obtain conditions to determine all open parameters. As we have exactly as many equations as there are parameters, this provides a unique solution given by

$$q_k = \kappa_k^2, \quad \langle k^{(A)}|\rho_l^{(A)}|k^{(A)}\rangle = \delta_{kl}, \quad \mathrm{tr}_{(A)}\left(\rho_k^{(A)}\rho_k^{(A)}\right) = 1\,. \tag{7.6}$$

The third equation states that each $\rho_k^{(A)}$ is a pure state. Even more specifically, the second equation determines $\rho_k^{(A)}$ to

$$\rho_k^{(A)} = |k^{(A)}\rangle\langle k^{(A)}|\,. \tag{7.7}$$

These results are also obtained by computing q_k and $\rho_k^{(A)}$ from ρ using (2.49) and (2.50) with projectors $\Pi_k^{(B)} = \Pi_k^{(\bar{A})} = |k^{(\bar{A})}\rangle\langle k^{(\bar{A})}|$. This is necessary to be consistent with the fact that for pure states, $Q(A:\bar{A}) = S(\rho_{(A)})$. The quantum conditional entropy (2.48) has to

vanish in this case, which is precisely the case when every $\rho_k^{(A)}$ is a pure state.

Inserting (7.6) into (7.5) we obtain an expression for GQD valid for any pure state purely in terms of the Schmidt coefficients,

$$Q^{(2)} = (A : \bar{A}) = 1 - \sum_{k=1}^{n} \kappa_k^4 \,. \tag{7.8}$$

We have stated in sec. 2.2.2 that GQD provides a qualitative measure for quantum discord. For pure states, quantum discord reduces to the entanglement entropy. Therefore, (7.8) may vanish if and only if $S(\rho_{(A)}) = 0$. This is in fact realised by our result for GQD given in (7.8). The entanglement entropy vanishes if all Schmidt coefficients but one vanish, i.e. for $\kappa_{k^*} = 1$ and $\kappa_{k\neq k^*} = 0$ cf. (2.11). Since the Schmidt coefficients κ_k are real numbers constrained as $0 \leq \kappa_k^2 \leq 1$ and $\sum_{k=1}^n \kappa_k^2 = 1$, if any of the Schmidt coefficients is equal to one, all others have to vanish. In this case, (7.8) vanishes as well. The entanglement entropy is bigger than zero if at least two Schmidt coefficients are non-zero. If two Schmidt coefficients are non-zero, they have to be smaller than one, and correspondingly every positive power of these coefficients is smaller than one as well. For any $\lambda_k < 1$, a higher power yields a smaller value, in particular $\lambda_k^2 < \lambda_k^4$. Using again the normalisation we have $\left(\sum_{k=1}^n \kappa_k^2\right)^2 = \sum_{k=1}^n \kappa_k^4 + \Xi = 1$. Here Ξ represents all mixed products of Schmidt coefficients. In particular, due to the properties of the Schmidt coefficients $0 < \Xi < 1$ and correspondingly we find $\sum_{k=1}^n \kappa_k^4 < 1$. This also shows that GQD is positive semi-definite, consistent with its definition in terms of the Hilbert–Schmidt norm. So we find that (7.8) vanishes if and only if the pure state ρ does not contain entanglement.

We have determined the constituents of the q-c state minimising the Hilbert–Schmidt norm (7.5) as (7.6) and (7.7). This has an interesting consequence for the state χ as well. Inserting the results of the minimisation, χ is given by

$$\chi_{\text{min}} = \sum_{k=1}^{n} \kappa_k^2 |k^{(A)}, k^{(\bar{A})}\rangle\langle k^{(A)}, k^{(\bar{A})}| \,. \tag{7.9}$$

According to our discussion in sec. 2.1.3, this is not a q-c but a c-c state. The minimisation involved in computing GQD singles out a state with only classical correlations of the set of all states with vanishing discord, i.e. all q-c states. This observation has a nice connection to the 'geometric measure of quantum correlations' proposed in [521]. This alternative measure is defined analogously to GQD except that the minimisation is performed over states within $\mathscr{S}^{(c-c)}$. Our result for the state (7.9) minimising the Hilbert–Schmidt norm shows that, although $\mathscr{S}^{(c-c)} \subset \mathscr{S}^{(q-c)}$, for pure states ρ the measure of [521] and GQD are equivalent. For mixed states however, the measures are different as we demonstrate in

the following in an explicit example. This example will also be useful to illuminate how to calculate GQD explicitly.

To demonstrate computing GQD, a useful example is provided by the isotropic state [522] for two qubits,

$$\rho_{\text{iso}} = \frac{1-p}{4}\mathbb{1}_4 + \frac{p}{2}\big(|\uparrow_{(A)}\uparrow_{(\bar{A})}\rangle + |\downarrow_{(A)}\downarrow_{(\bar{A})}\rangle\big)\big(\langle\uparrow_{(A)}\uparrow_{(\bar{A})}| + \langle\downarrow_{(A)}\downarrow_{(\bar{A})}|\big)\,, \tag{7.10}$$

where $0 \leq p \leq 1$. This state is a superposition of the classical mixture described by the first term $\propto \mathbb{1}_4$ and the density operator of a maximally entangled pair of qubits in the second term. As pointed out before in sec. 2.1.3, quantum discord for the state (7.10) does not vanish except for $p = 0$, where ρ_{iso} is a purely classical state, while the state is separable below $p = \frac{1}{3}$ as indicated by the vanishing of the entanglement of formation below $p = \frac{1}{3}$ [174]. To compute GQD explicitly, we make an ansatz for χ, which in this case only consists of two terms,

$$\chi = q_\uparrow \rho_\uparrow^{(A)} \otimes |\uparrow_{(\bar{A})}\rangle\langle\uparrow_{(\bar{A})}| + (1-q_\uparrow)\rho_\downarrow^{(A)} \otimes |\downarrow_{(\bar{A})}\rangle\langle\downarrow_{(\bar{A})}|. \tag{7.11}$$

Note that we made use of $\sum_{k=\uparrow,\downarrow} q_k = 1$ to express $q_\downarrow$ in terms of $q_\uparrow$. Furthermore, we parametrise the reduced density operators $\rho_{\uparrow,\downarrow}^{(A)}$ in terms of three real parameters $\alpha_i, \beta_i, \gamma_i$ with $i = \uparrow, \downarrow$ as

$$\rho_i^{(A)} = \begin{bmatrix} \alpha_i & \beta_i + \mathrm{i}\gamma_i \\ \beta_i - \mathrm{i}\gamma_i & 1-\alpha_i \end{bmatrix}\,, \tag{7.12}$$

which ensures that χ as well as $\rho_i^{(A)}$ are properly normalised. With this ansatz, calculating the Hilbert–Schmidt norm (7.1) results in

$$\begin{aligned} ||\rho_{\text{iso}} - \chi||^2 = {} & \frac{3}{4}\big(1+p^2\big) - \frac{p}{2} + \big(p-2\big)\alpha_\downarrow + 2\big(\alpha_\downarrow^2 + \beta_\downarrow^2 + \gamma_\downarrow^2\big) \\ & + 2q_\uparrow^2\big[1 + \alpha_\uparrow\big(\alpha_\uparrow - 1\big) + \alpha_\downarrow\big(\alpha_\downarrow - 1\big) + \beta_\uparrow^2 + \beta_\downarrow^2 + \gamma_\uparrow^2 + \gamma_\downarrow^2\big] \\ & + q_\uparrow\big[p\big(1 - \alpha_\uparrow - \alpha_\downarrow\big) - 2\big(1 - 2\alpha_\downarrow + 2\alpha_\downarrow^2 + 2\beta_\downarrow^2 + 2\gamma_\downarrow^2\big)\big]\,. \end{aligned} \tag{7.13}$$

Computing GQD amounts to minimising this expression, which in turn requires tuning the open coefficients $q_\uparrow$ as well as $\alpha_i, \beta_i, \gamma_i$ such that the above expression is minimal. This is achieved by calculating the derivatives of the above expression w.r.t. each of these parameters and equating the results to zero and reinserting the result obtained for one

parameter into (7.13)before computing the next derivative, at the end we find

$$\begin{aligned} q_\uparrow = \frac{1}{2}, \quad \alpha_\uparrow = \frac{1+p}{2}, \quad \beta_\uparrow = 0 = \gamma_\uparrow \\ \alpha_\downarrow = \frac{1-p}{2}, \quad \beta_\downarrow = 0 = \gamma_\downarrow \,. \end{aligned} \tag{7.14}$$

Inserting these values into (7.13) we find the GQD for the isotropic state,

$$Q^{(2)}(A:\bar{A}) = \frac{p^2}{2} \,. \tag{7.15}$$

As expected, the GQD does not vanish except for $p = 0$ where also quantum discord vanishes [174]. In particular, it does not vanish for $p \leq \frac{1}{3}$, where the entanglement of formation is zero [253]. Using (7.14) the corresponding reduced density operators $\rho_i^{(A)}$ in the ansatz for χ are given by

$$\rho_\uparrow^{(A)} = \frac{1}{2}\begin{bmatrix} 1+p & 0 \\ 0 & 1-p \end{bmatrix}, \quad \rho_\downarrow^{(A)} = \frac{1}{2}\begin{bmatrix} 1-p & 0 \\ 0 & 1+p \end{bmatrix} . \tag{7.16}$$

Clearly, these reduced density operators are mixed states, as can be checked by calculating the purity (2.3) and noting that $\gamma(\rho_{\uparrow,\downarrow}^{(A)}) < 1$ for $p < 1$. Therefore, the state minimising the Hilbert–Schmidt norm is a q-c state, cf. (7.16), as opposed to the c-c state obtained in (7.9).

Since (7.9) is a purely classical state, by noting that GQD is defined in terms of a norm we arrive at an interesting result regarding the relation between ρ and χ_{min}. A norm induces a notion of distance between, in this case, states. Therefore, we find that χ_{min} is the *closest classical state* to the quantum state ρ. In other words, χ_{min} is the state with classical correlations that best approximates the quantum entangled state ρ. In particular, there is no q-c state that is able to approximate ρ better than the classical state χ_{min}. This is useful also in experimental physics. In a bipartite system, as far as local observables associated to only A or $\bar{A}$ are concerned, the expectation value of any observable is insensitive to whether it is calculated in the state ρ or χ_{min}. This is since the reduced density operators following from ρ and χ_{min} are equal. Therefore, an experimenter interested in observables of only the subsystem A or $\bar{A}$ does not need to prepare the full quantum state ρ, but the classical state χ_{min} is sufficient. See e.g. [523] for a discussion of the difficulty of preparing quantum states. While this is already an interesting observation for generic quantum systems, it will be a major point of our discussion in sec. 7.2.2 where we apply the current setting to states dual to black holes in light of the AdS/CFT correspondence.

The result for GQD in (7.8) has a close relation to the Rényi entropy discussed in

sec. 2.1.3. This measure of entanglement defined in (2.41) is determined by computing powers of the reduced density operator. To relate this to our current discussion, we first point out that (7.8) can be effectively written as

$$Q^{(2)}(A:\bar{A}) = 1 - \mathrm{tr}\left(\chi_{\mathrm{min}}^2\right). \tag{7.17}$$

Due to the simple structure of c-c states, the reduced density operator of χ_{min} for the subsystem A is obtained as[1]

$$\rho_{(A)} = \sum_{k=1}^{n} \kappa_k^2 |k^{(A)}\rangle\langle k^{(A)}|. \tag{7.18}$$

Notably, the entries are the same as in χ_{min}. Since calculating the reduced density operator simply removes vanishing entries in χ_{min}, we have

$$\mathrm{tr}\left(\chi_{\mathrm{min}}^2\right) = \mathrm{tr}\left(\rho_{(A)}^2\right). \tag{7.19}$$

Combining this with (7.17) and the definition (2.41), we find that GQD can be expressed by the second Rényi entropy of either χ_{min} or $\rho_{(A)}$,

$$Q^{(2)}(A:\bar{A}) = 1 - e^{-S^{(2)}(\chi_{\mathrm{min}})} = 1 - e^{-S^{(2)}(\rho_{(A)})}. \tag{7.20}$$

As we discussed in sec. 2.1.3, the calculation of the Rényi entropy is a well-known tool within QFT using the replica trick. Therefore, our result (7.20) shows that the quantity GQD is not restricted to quantum mechanics but is also accessible in QFT.

A non-trivial result for GQD, i.e. $Q^{(2)} > 0$, is understood as a statement of non-factorisation. In the following, we discuss that in terms of the partition function. In the upcoming sec. 7.1.2, we will demonstrate the non-factorisation also in terms of the projective Hilbert space in an explicit example. To reformulate (7.8) in terms of a partition function we introduce the modular Hamiltonian $K^{(A)} = -\ln \rho_{(A)}$ as defined in (2.21). Since the reduced density operator (7.18) is diagonal, so is $K^{(A)}$, with diagonal entries given by the negative logarithms of the entries of $\rho_{(A)}$. We may then define the *modular partition function* Z_{mod} in terms of the eigenvalues of the modular Hamiltonian as

$$Z_{\mathrm{mod}}(K^{(A)}) = \sum_{k=1}^{n} e^{-K_k^{(A)}}. \tag{7.21}$$

As mentioned below (2.24), this can formally be interpreted as the thermal partition func-

[1] The reduced density operator of $\bar{A}$ looks exactly the same with $A \to \bar{A}$.

tion with physical Hamiltonian $K^{(A)}$ at temperature $T = 1$. Using the modular partition function, the GQD for pure states can be expressed as

$$Q^{(2)}(A : \bar{A}) = 1 - \frac{Z_{\text{mod}}(2K^{(A)})}{Z_{\text{mod}}(K^{(A)})^2}\,. \tag{7.22}$$

Therefore, the GQD vanishes if $Z_{\text{mod}}(2K^{(A)}) = Z_{\text{mod}}(K^{(A)})^2$, that is if the (modular) partition function factorises.[2]

7.1.2. Factorisation of the Projective Hilbert Space 2.0

We will now discuss an explicit example of the above result for GQD using the two-qubit system whose entanglement properties we already analysed in sec. 4.1.1. This will enable us to show non-factorisation of the projective Hilbert space using GQD, providing a consistency and compatibility check with the earlier results on non-factorisation in sec. 4.1.2 involving the SZK construction [166]. We point out that the following discussion is not part of our original work [186], but has been performed for the purpose of writing this thesis as a cross check.

The two 'subregions' A and $\bar{A}$ used in the previous sec. 7.1.1 are each given by one of the two qubits, $A = \uparrow$ and $\bar{A} = \downarrow$. As discussed in the previously mentioned section, the Schmidt coefficients for the ground state of the two-qubit system are given by (4.3). We repeat them here for the convenience of the reader,

$$\kappa_\uparrow = \sqrt{\frac{1-\sin\alpha}{2}}, \quad \kappa_\downarrow = \sqrt{\frac{1+\sin\alpha}{2}}\,. \tag{7.23}$$

Accordingly, using our result (7.8), the GQD for the two-qubit system is given by

$$Q^{(2)}(\uparrow : \downarrow) = \frac{1}{2} - \frac{\sin^2\alpha}{2} = \frac{\cos^2\alpha}{2}\,. \tag{7.24}$$

Therefore, GQD vanishes for $\alpha = \frac{\pi}{2}$, which is the case of vanishing entanglement between the two spins as discussed in sec. 4.1.1. This provides an explicit realisation of the discussion in the previous sec. 7.1.1. To gain insights about the factorisation properties of the projective Hilbert space using the GQD, we use the geometric phase (4.25) derived for this system in sec. 4.1.2. Inverting this result, we express the parameter α in terms of the geometric phase Φ_{G} and insert it into the result for the GQD for the two-qubit system

[2] Note that by definition $Z_{\text{mod}}(K^{(A)}) = 1$ due to the normalisation of the state vector $|\psi\rangle$. We nevertheless include it to make the analogy with the upcoming formula (7.26) and the discussion in sec. 7.2.2 clearer.

(7.24), resulting in

$$Q^{(2)}(\uparrow:\downarrow) = \frac{1}{2}\left(1 - \frac{\Phi_G^2}{4\pi^2}\right). \tag{7.25}$$

This vanishes for $\Phi_G = 2\pi$. According to the SZK construction [166] reviewed in sec. 2.2.2 and discussed for this particular two-qubit system in secs. 4.1.1 and 4.1.2, the case $\Phi_G = 2\pi$ corresponds to the factorised submanifold $\mathbb{C}\mathrm{P}^1 \times \mathbb{C}\mathrm{P}^1$ of the full projective Hilbert space $\mathbb{C}\mathrm{P}^3$. To be specific, this particular submanifold is the product of the individual projective Hilbert spaces of each of the qubits. Therefore, while a vanishing GQD corresponds to the factorised submanifold, a non-zero GQD with $\Phi_G \neq 2\pi$ is associated to a non-factorised projective Hilbert space. This makes manifest how the non-factorisation of the projective Hilbert space is indicated by a non-vanishing GQD.

In sec. 4.2.1 we have derived the entanglement temperature β_{ent} for the two-qubit system, given in (4.38) in terms of the geometric phase. This temperature is defined such that the entanglement entropy assumes the form of the thermal entropy at temperature β_{ent}. Using this result, we may express the GQD for the two-qubit system (7.25) using the modular partition function as in (7.22). However, using the entanglement temperature, the modular partition function takes the form of the thermal partition function,

$$Q^{(2)}(\uparrow:\downarrow) = 1 - \frac{Z(2\beta_{\text{ent}})}{Z(\beta_{\text{ent}})^2}, \tag{7.26}$$

showing again non-factorisation in terms of the partition function.

The result (7.26) motivates that GQD is interesting for generic thermal systems and therefore in particular black holes with the TFD state as its holographic dual description. This is the topic of the next section.

7.2. For the Thermofield Double State

In the above, we have considered arbitrary pure states. In light of the AdS/CFT correspondence, these results are particularly interesting when applied to the TFD state. This state is the holographically dual description of the eternal black hole in Anti-de Sitter spacetime. As reviewed in sec. 3.2, this setting gives rise to the factorisation puzzle, as the two CFTs defined on the boundary do not share any interaction, however are connected by a semi-classical geometry in the bulk. Given the above results on non-factorisation indicated by the GQD of a generic pure state, when applied to the TFD state the GQD should be able to shed light on the factorisation puzzle, in particular on the factorisation properties of the

field theory. We study this in the following. We start in sec. 7.2.1 with a brief review of the decohered state ρ_{TMD} introduced in [182] providing a mixed state description of the eternal black hole. This state will be elementary to our discussion in sec. 7.2.2 where we discuss GQD for the TFD state. In particular, the TMD state will arise as the closest classical approximation χ_{min} in computing the GQD. Concluding this section, we discuss the implications of this result. To circumvent potential confusion, we point out that here we adopt a notation more common to holography in that we replace the arbitrary subregions A and $\bar{A}$ used before by the left and right CFTs, indicated by labels L and R, respectively.

7.2.1. Some Details on the TMD State

As reviewed in sec. 3.2.1, the eternal black hole in Anti-de Sitter spacetime is holographically dual to two CFTs entangled in the TFD state (3.52)

$$|\text{TFD}\rangle = \frac{1}{\sqrt{Z(\beta)}} \sum_n e^{-\beta \frac{E_n}{2}} |n_L, n_R^*\rangle \,, \tag{7.27}$$

which provides a state vector description of the black hole [112]. However, as argued in [182], in a more realistic scenario it is expected that due to interaction with the ambient spacetime of the black hole, the dual state decoheres and evolves into a mixed state, which does not have a state vector description. By decoherence, the quantum information contained in the TFD state is converted into classical correlation. The mixed state in question is constrained by the fact that for a local low-energy observer, the state looks thermal at the same temperature both before and after decoherence. To provide the necessary context for our analysis of GQD for the TFD state in sec. 7.2.2 we will briefly explain the consequences of these considerations along the lines of [182].

As we discussed earlier in sec. 3.2.2, the TFD state is not the unique pure state dual to the eternal black hole [454, 455]. Rather it is the dual state for a particular choice $\delta = 0$, where δ determines the relation between the left and right boundary times. For arbitrary δ, the dual state is given by the time-shifted TFD state (3.54),

$$|\text{TFD}\rangle_\alpha = \frac{1}{\sqrt{Z(\beta)}} \sum_n e^{i\alpha_n} e^{-\beta \frac{E_n}{2}} |n_L, n_R^*\rangle \,. \tag{7.28}$$

These phases can be understood as quantum information as they are not observable by a local low-energy observer [182]. An intuitive argument for that is that the local low-energy observer measures observables in the reduced density operator, which does not depend on δ. More intricate arguments involving correlation functions, both in the gravity and the field theory side, can be found in [455]. From the perspective of the local low-energy

observer, all of the time-shifted TFD states (7.28) therefore describe the same classical geometry for any set of phases $\{\alpha\}$, with elements $\alpha_n \in \{\alpha\}$ that are related to δ as well as the energies E_n as $\alpha_n = 2E_n\delta$. It is then natural from the perspective of the low-energy observer to describe the black hole by a superposition of all time-shifted TFD states instead of one particular instance. In particular, as the phases α_n are not measurable by a local low-energy observer, a natural description from their perspective is given by an incoherent sum of all states (7.28). This leads to defining the *thermomixed double state* (TMD state) as [182]

$$\rho_{\mathrm{TMD}} = \frac{1}{N}\sum_{\{\alpha\}} |\mathrm{TFD}\rangle_{\alpha\,\alpha}\langle\mathrm{TFD}| \,. \tag{7.29}$$

The sum includes all sets of phases $\{\alpha\}$. The normalisation $\frac{1}{N}$ implies that there are N different of such sets. Noting that the spectrum of CFTs is highly random, the sum can be performed using $\frac{1}{N}\sum_{\{\alpha\}} e^{\mathrm{i}(\alpha_n-\alpha_m)}$ [182],

$$\rho_{\mathrm{TMD}} = \frac{1}{Z(\beta)}\sum_n e^{-\beta E_n}|n_L, n_R^*\rangle\langle n_L, n_R^*| \,. \tag{7.30}$$

As previously mentioned, this state contains only classical correlations. In fact, $\rho_{\mathrm{TMD}} \in \mathscr{S}^{(c-c)}$ according to the classification discussed in sec. 2.1.3. A more precise understanding of the correlations within the TMD state can be obtained by considering the mutual information. As discussed in sec. 3.2.2, the mutual information for the TFD state (7.27), or its time-shifted generalisation (7.28), is equal to twice the entanglement entropy $S(\rho^{(L/R)})$, indicating the presence of quantum correlations. On the other hand, the factorised thermal state $\rho_{\mathrm{th}} = \rho^{(L)} \otimes \rho^{(R)}$ has vanishing mutual information, i.e. there is no correlation at all. For the TMD state, we find that $S(\rho_{\mathrm{TMD}}) = S(\rho^{(L/R)})$, and correspondingly also the mutual information is equal to $S(\rho^{(L/R)})$. In this sense, the TMD state can be understood as an intermediate state between the TFD state and the manifestly factorised state ρ_{th} without any kind of correlation, where $\rho^{(L/R)}$ are the reduced density operators of both the TFD and the TMD state [182]. With this background, we now calculate GQD for the TFD state and discuss the implications of the result in light of the factorisation puzzle.

7.2.2. A Classical Approximation to the TFD State

Given any pure state vector, upon calculating the Schmidt coefficients of this state vector the GQD is determined using (7.8). The time-shifted TFD state (7.28) is already written in Schmidt decomposition. The complex phases $e^{\mathrm{i}\alpha_n}$ drop out when calculating the Schmidt

coefficients explicitly,[3] resulting in

$$\kappa_n = \frac{e^{-\beta\frac{E_n}{2}}}{\sqrt{Z(\beta)}}\,. \tag{7.31}$$

Accordingly, using our result (7.8), the GQD is given by

$$Q^{(2)}(L:R) = 1 - \frac{\sum_n e^{-2\beta E_n}}{Z(\beta)^2} = 1 - \frac{Z(2\beta)}{Z(\beta)^2}\,, \tag{7.32}$$

realising (7.22) for the thermal modular Hamiltonian $K^{(L)} = \beta H_L$. Moreover, the state (7.9) minimising the Hilbert–Schmidt norm is given by

$$\chi_{\text{min}}^{(\text{TFD})} = \frac{1}{Z(\beta)} \sum_n e^{-\beta E_n} |n_L, n_R^*\rangle\langle n_L, n_R^*|\,. \tag{7.33}$$

Remarkably, this is precisely the TMD state (7.30). Therefore, the calculation allows for a novel interpretation of this state as the state that best approximates the (time-shifted) TFD state without including quantum correlations between the two CFTs. We emphasise that this above derivation does not require any considerations or assumptions about the dual gravitational theory such as the interactions between the black hole and its surrounding spacetime discussed in [182]. Rather, it is entirely quantum information theoretic with the TMD state arising by minimising a distance in state space.

First, we note that the GQD for the TFD state does not vanish. This is consistent with the fact that the entanglement $S(\rho^{(L/R)})$ contained within the TFD state is non-trivial since $\rho^{(L/R)}$ are thermal mixed states. Note also that the second Rényi entropy $S^{(2)}(\rho^{(L/R)})$ is proportional to the purity of $\rho^{(L/R)}$, so by (7.20), GQD vanishes if the reduced density operators describe pure states. Second, (7.32) again signals non-factorisation as it vanishes if and only if the partition function factorises, $Z(2\beta) = Z(\beta)^2$. Considering the form of the Schmidt coefficients (7.31) we expect that factorisation happens in the limit $\beta \to \infty$, as in this case the Schmidt coefficient with the lowest energy E_0 does not vanish but approaches one. All other Schmidt coefficients with $E_n > E_0$ are exponentially suppressed and vanish in the limit.[4] Accordingly, in this limit the TFD state reduces to a product state $\lim_{\beta\to\infty} |\text{TFD}\rangle_\alpha \to |0_L 0_R\rangle$ and there is no entanglement between the two CFTs. In the dual gravitational picture, this limit is understood as removing the black hole's interior. This is the region responsible for the wormhole interpretation of the two-sided black hole, cf. fig. 3.6. In this limit also the bulk yields a factorising picture since there are no

[3] Calculating GQD directly using the Hilbert–Schmidt norm and minimising the result, the phases will drop out due to the definition of the norm.

[4] We assume that the energies E_n are bounded from below.

quantum correlations supporting the ER bridge. Finally, we point out that the result (7.32) is reminiscent of a property of the TMD state discussed in [165, 182, 524]. In there it was shown that the kth power of ρ_{TMD} can be used to define the partition function of the k-fold wormhole,

$$\text{tr}\left(\rho_{\text{TMD}}^{k}\right) = \frac{Z(k\beta)}{Z(\beta)^{k}}\,. \tag{7.34}$$

For $k = 2$, this reproduces the second term in (7.32). We will discuss in sec. 7.3 how this relation motivates us to consider a generalisation of GQD in the context of black hole microstates.

We therefore find that the GQD is a useful quantity in diagnosing non-factorisation due to quantum correlations, both in generic quantum systems as well as in states with a holographic dual such as the time-shifted TFD states. In particular, in light of the results of [165, 182, 524], this gives GQD an interpretation in terms of wormhole physics. As discussed in sec. 2.2.2, GQD is a qualitative measure for quantum discord. Therefore, also a non-vanishing quantum discord implies non-factorisation due to quantum correlations. In the above discussion, we have shown this explicitly for pure states, where $Q(L:R) = S(\rho^{(L/R)})$. However, since quantum discord in general captures quantum correlations even beyond entanglement, we propose that *non-vanishing quantum discord implies non-factorisation* in the above sense for arbitrary states ρ. Whenever there are quantum correlations resulting in a non-factorisation of the (modular) partition function, the GQD and equivalently the quantum discord for that state will be non-zero. The GQD therefore provides an important probe of non-factorisation especially in the holographic context. Purely from the field theory perspective, typically there are no a priori arguments for non-factorisation since the two CFTs are spatially separated. The computation of GQD however is able to address this question in field theory language. In particular, at least for pure states, accessing GQD reduces to the computation of the second Rényi entropy, which is well-known in field theory.

In general, non-factorisation may also appear due to classical correlations. In particular, since the reduced density operators of the pure state ρ and the closest classical state χ_{min} are the same, the Rényi entropy appearing in GQD can be associated to the classical state χ_{min} as well. This suggests a close similarity with the description of the TMD state as a classical state describing the black hole after decoherence has set in [165, 182, 524]. However, the minimisation involved in computing GQD emulates quantum correlations as a classical state. Therefore, GQD highlights the role of quantum correlations for non-factorisation. While quantum correlations within a given state ρ are emulated as classical correlations within χ_{min}, any classical correlations within ρ do not influence GQD since

these can be cancelled by classical correlations within χ_{min}.

It is interesting also from the gravity perspective that GQD is determined by the second Rényi entropy. As for the entanglement entropy, described in sec. 3.1.3, also the Rényi entropies have a known gravitational dual, given by the areas of cosmic branes [525]. To compute the nth Rényi entropy $S^{(n)}$, a cosmic brane with non-trivial tension $T_n = \frac{n-1}{4nG_N}$ is inserted into the bulk spacetime. These branes react back on the geometry and create conical defects with deficit angle $\Delta\phi_n = 2\pi\frac{n-1}{n}$ [525]. While the entanglement entropy is obtained from $S^{(n)}$ in the limit $n \to 1$, cf. (2.40), in the dual bulk picture the cosmic brane becomes tensionless and the conical defect vanishes in this limit, reducing the cosmic brane to the usual RT surface [525]. Given the result for GQD in terms of the second Rényi entropy (7.20), this means that for pure states with a dual theory of gravity, the holographic dual to GQD is related to inserting a cosmic brane with tension $T_2 = \frac{1}{8G_N}$, creating a conical defect $\Delta\phi_2 = \pi$.

7.3. A Probe for Black Hole Microstates

As we pointed out before in sec. 7.2.1, the time-shifted TFD states (7.28) cannot be distinguished from the usual TFD state (7.27) by a local low-energy observer [455]. Moreover, since the TMD state has the same reduced density operator as the time-shifted TFD states, correlation functions within a time-shifted TFD state or the TMD state are the same for simple operators as considered in [351]. A high-energy observer however, who has access to measuring operators scaling as N or higher, is sensitive to the differences within these states.[5] Therefore, the quantum correlations within the time-shifted TFD states (7.28), as a distinguishing property to the TMD state containing only classical correlations, are understood as $\frac{1}{N}$-corrections. In the following sec. 7.3.1 we discuss these corrections and a generalisation of GQD in the light of black hole microstates. We conclude this section by discussing the relation between the microstates and non-factorisation in view of non-factorisation from the perspective of the path integral in sec. 7.3.2.

7.3.1. Microstate Overlaps and Geometric Quantum Discord

As discussed in sec. 3.2.1, the time-shifted TFD states are interpreted as microstates of the black hole [455]. Given a particular microstate, corresponding to a set of phases $\{\alpha\}$, the dual bulk description is completely fixed, in particular how the left and right time coordinates are related by δ and therefore how the bulk spacetime is glued to the boundaries.

[5] In principle, also a non-local observer is sensitive to these differences. However, non-local observers are not very physical, which is why we do not further study this direction.

To elucidate how these microstates relate to the GQD, we revisit the computation of the latter, focussing on different aspects than above.

Given the results of the previous sec. 7.2.2, we already know that the TMD state (7.30) minimises the Hilbert–Schmidt norm (7.1). In the following, when denoting GQD we therefore drop the minimisation and only denote the Hilbert–Schmidt norm with $\chi = \chi^{(\mathrm{TMD})}_{\mathrm{min}}$. As pointed out before in (7.17), effectively $Q^{(2)}(L:R) = 1 - \mathrm{tr}\left(\rho^2_{\mathrm{TMD}}\right)$. However, this relative sign appears only because of the overlap term,

$$Q^{(2)}(L:R) = 1 - 2\,\mathrm{tr}\left(\rho_{\mathrm{TFD}_\alpha}\rho_{\mathrm{TMD}}\right) + \mathrm{tr}\left(\rho^2_{\mathrm{TMD}}\right), \tag{7.35}$$

where $\rho_{\mathrm{TFD}_\alpha} = |\mathrm{TFD}\rangle_\alpha\,{}_\alpha\langle\mathrm{TFD}|$. Therefore, the GQD can be interpreted as comparing the microstate $|\mathrm{TFD}\rangle_\alpha$ to the average over the full ensemble of microstates ρ_{TMD}. The cancellation of the phases $e^{\mathrm{i}\alpha_n}$ in the overlap is understood as an implicit averaging, i.e. a self-averaging property of GQD. On the technical level, this property is due to the trace in (7.35). The importance of $\frac{1}{N}$-corrections in this calculation is seen as follows. We rewrite the overlap term in the above equation by expressing the TMD state in terms of microstates $|\mathrm{TFD}\rangle_\beta$ as in (7.29),

$$\begin{aligned}\mathrm{tr}\left(\rho_{\mathrm{TFD}_\alpha}\rho_{\mathrm{TMD}}\right) &= {}_\alpha\langle\mathrm{TFD}|\rho_{\mathrm{TMD}}|\mathrm{TFD}\rangle_\alpha \\ &= \frac{1}{N}\sum_{\{\beta\}} {}_\alpha\langle\mathrm{TFD}|\mathrm{TFD}\rangle_\beta\,{}_\beta\langle\mathrm{TFD}|\mathrm{TFD}\rangle_\alpha\,.\end{aligned} \tag{7.36}$$

To obtain the result for (7.35) we therefore need to know what the overlap of two microstates evaluates to. Up to $\frac{1}{N}$-corrections, all microstates $|\mathrm{TFD}\rangle_\alpha$ are orthogonal to each other [182],

$${}_\alpha\langle\mathrm{TFD}|\mathrm{TFD}\rangle_\beta = \delta_{\alpha\beta} + \mathcal{O}\left(\frac{1}{N}\right). \tag{7.37}$$

However, using this result directly in (7.36) does not lead to the result for GQD obtained above in (7.32) since

$$\mathrm{tr}\left(\rho_{\mathrm{TFD}_\alpha}\rho_{\mathrm{TMD}}\right) = \frac{1}{N}\sum_{\{\beta\}}\delta_{\alpha\beta}\delta_{\beta\alpha} = \frac{1}{N}\delta_{\alpha\alpha} = 1\,, \tag{7.38}$$

leading to $Q^{(2)}(L:R) = 2 + \mathrm{tr}\left(\rho^2_{\mathrm{TMD}}\right)$. This tells us that the $\frac{1}{N}$-corrections must not be neglected in this computation. In other words, evaluating the ensemble average, i.e. the sum $\sum_{\{\beta\}}$, of the square of the overlap ${}_\alpha\langle\mathrm{TFD}|\mathrm{TFD}\rangle_\beta$ does not commute with using the approximation (7.37), but we have to be more careful in this calculation. Without approximating as in (7.37), i.e. without neglecting $\frac{1}{N}$-corrections, the overlap of two microstates

is given by

$$ {}_{\alpha}\langle \text{TFD}|\text{TFD}\rangle_{\beta} = \sum_{n,m} e^{-i\alpha_n} \kappa_n e^{i\beta_m} \kappa_m \langle n_L, n_R^*|m_L, m_R^*\rangle = \sum_n \kappa_n^2 e^{i(\alpha_n - \beta_n)} . \tag{7.39} $$

Using (7.39) in (7.36) we find

$$ \begin{aligned} \text{tr}\left(\rho_{\text{TFD}_\alpha}\rho_{\text{TMD}}\right) &= \frac{1}{N}\sum_{\{\beta\}}\sum_{n,m} \kappa_n^2 e^{i(\alpha_n-\beta_n)} \kappa_m^2 e^{i(\beta_m-\alpha_m)} \\ &= \sum_{n,m} \kappa_n^2 \kappa_m^2 e^{i(\alpha_n-\alpha_m)}\delta_{nm} = \sum_n \kappa_n^4 = \frac{Z(2\beta)}{Z(\beta)^2} , \end{aligned} \tag{7.40} $$

where in the second equality we used again that $\frac{1}{N}\sum_{\{\beta\}} e^{i(\beta_m-\beta_n)} = \delta_{nm}$. This computation also shows explicitly the self-averaging property, i.e. the cancellation of the phases $e^{i\alpha_n}$. Although $\text{tr}\left(\rho_{\text{TFD}_\alpha}\rho_{\text{TMD}}\right)$ includes one sum $\sum_{\{\alpha\}}$ less than $\text{tr}\left(\rho_{\text{TMD}}^2\right)$, the results are of the same order. Using (7.40) in (7.36) leads to the result for GQD of the TFD state obtained earlier in (7.32).

We may also derive a result generalising (7.40) for the overlap (7.36) with ρ_{TMD} replaced by an arbitrary (integer) power of ρ_{TMD}. In this case,

$$ \begin{aligned} \text{tr}\left(\rho_{\text{TFD}_\alpha}\rho_{\text{TMD}}^{k-1}\right) &= \frac{1}{N^{k-1}} \sum_{\{\beta\}_1,\ldots,\{\beta\}_{k-1}} {}_{\alpha}\langle \text{TFD}|\text{TFD}\rangle_{\beta_1}\cdots{}_{\beta_{k-1}}\langle \text{TFD}|\text{TFD}\rangle_{\alpha} \\ &= \sum_n \kappa_n^{2k} = \frac{Z(k\beta)}{Z(\beta)^k}, \end{aligned} \tag{7.41} $$

where $k \in \mathbb{N}$. In this computation, we used (7.39) and $\frac{1}{N}\sum_{\{\beta\}_i} e^{i(\beta_m^{(i)}-\beta_n^{(i)})} = \delta_{nm}$ repeatedly. In light of (7.34), this overlap (7.41) is interpreted to include k-fold replica wormhole contributions. However, these replica wormholes arise due to an averaging over states [526–528] and not by the more familiar ensemble averaging. The ratio of partition functions (7.41) obtained as an overlap of TMD states and a microstate is closely analogous to the discussion of [529, 530]. In these works, an explanation for the black hole entropy in terms of counting microstates was studied. The microstates $|\psi_{m_n}\rangle$ were constructed as corresponding to collapsing shells of dust of mass m_n. Crucially, these shells are considered to be *within* the black hole. Moreover, the masses m_n are inertial masses, i.e. the limit $m_n \gg M$ considered in [529, 530], where M is the mass of the black hole, is not problematic since m_n do not contribute to the mass measured at infinity. The states associated to these dust shells have overlaps of the same form as in (7.41). In computing these overlaps beyond the lowest power $\langle\psi_{m_n}|\psi_{m_l}\rangle$, as in our analysis above resulting in (7.41) it is pivotal that higher power overlaps are not simply given by products of lower power overlaps.

The authors [529, 530] are interested mostly in astrophysical black holes formed by collapse. However, since the collapse of a gathering of mass to a black hole is a unitary process, also such black holes have a pure state description, at least immediately after the collapse before interaction with the ambient spacetime leads to decoherence. Since our result on GQD is valid for any pure state, and in particular a result such as (7.41) can be derived for arbitrary pure states with the TMD state replaced by the appropriate χ_{min},[6] our above analysis of GQD also holds for pure states as considered in [529, 530]. Vice versa, in sec. 7.2.2 we considered an eternal black hole as opposed to astrophysical black holes formed by collapse. Note also that in [529, 530] to construct the Hilbert space using the dust shell states time-reversal symmetry was assumed. For the eternal black hole, the notion of time-reversal symmetry is ambiguous [455] and the time-shifted TFD states can be interpreted as microstates of the black hole. Nevertheless, as time-reversal symmetry is important in [529, 530] only for constructing the states and not for the analysis of the states thereafter, the line of thought developed in [529, 530] applies to the time-shifted TFD states as well by replacing the dust shell masses m_n with sets of phases $\{\alpha\}_n$. Each set of phases corresponds to a particular microstate $|\text{TFD}\rangle_\alpha$. As pointed out below (7.29), the prefactor $\frac{1}{N}$ in the definition of the TMD state indicates that there are N different sets of phases $\{\alpha\}_n$. Therefore, counting microstates to obtain the thermodynamic entropy, it is sufficient to consider $N = e^{S_{\text{BH}}}$ sets of phases to account for the black hole entropy. The time-shifted TFD states corresponding to these phases are sufficient to span the Hilbert space.

Finally, we relate this discussion on black hole microstates to a generalised version of GQD. We have seen above in (7.40) that correctly including microstate contributions is essential to obtain the correct expression for GQD. The higher overlaps (7.41) will never show up in GQD as defined in (2.98). However, the Hilbert–Schmidt norm used to define GQD is a special case of the class of norms referred to as *Schatten norm*, defined as

$$||X||_{(n)} = \sqrt[n]{\text{tr}\left(\sqrt{X^\dagger X}^{\,n}\right)}, \tag{7.42}$$

where X is an arbitrary operator. We are interested in Hermitian operators $X^\dagger X = X^2$ which slightly simplifies the above expression for the Schatten norm. Note that the GQD is defined using the second power of the Schatten norm for $n = 2$. We therefore consider a quantity defined by the nth power of the nth Schatten norm for the black hole microstates

[6] For generic pure states, the thermal partition functions $Z(k\beta)$ have to be replaced by the modular partition functions $Z_{\text{mod}}(kK^{(A)})$.

$|\text{TFD}\rangle_\alpha$ and the closest classical state ρ_{TMD}, which by analogy with GQD we denote $Q^{(n)}$,

$$Q^{(n)}(L:R) = ||\rho_{\text{TFD}_\alpha} - \rho_{\text{TMD}}||^n_{(n)} \,. \tag{7.43}$$

Evaluating the right-hand side of this equation naturally gives rise to overlaps of the form $\text{tr}\left(\rho^n_{\text{TFD}_\alpha}\rho^m_{\text{TMD}}\right)$ which, since $\rho^n_{\text{TFD}_\alpha} = \rho_{\text{TFD}_\alpha}$, give rise to the overlaps computed in (7.41). Schematically, evaluating (7.43) therefore results in

$$Q^{(n)}(L:R) = 1 + \#_2 \frac{Z(2\beta)}{Z(\beta)^2} + ... + \#_n \frac{Z(n\beta)}{Z(\beta)^n} \,, \tag{7.44}$$

where $\#_k$ are numbers ensuring that $Q^{(n)}(L:R) = 0$ if all partition factorise and all of the ratios of partition functions in this expression are equal to 1. For $Q^{(n)}$, the ratio $\frac{Z(n\beta)}{Z(\beta)^n}$ is always the highest appearing contribution. However, we point out that in general, not every term is of precisely this form. Rather, e.g. for $n = 4$, also a term $\frac{Z(2\beta)^2}{Z(\beta)^4}$ appears. Alluding to the replica wormhole interpretation, these terms are interpreted as follows. While $Z(n\beta)$ corresponds to the wormhole with the highest number of mouths possible for $Q^{(n)}$, assuming n is even a contribution of the form $Z\left(\frac{n}{2}\beta\right)^2$ corresponds to two wormholes with $\frac{n}{2}$ mouths, each of which stretches between half of the available replicas of the theory. Moreover, using (7.34) each of the terms in (7.44) can be expressed by Rényi entropies up to $S^{(n)}$. As pointed out in sec. 7.2.2, all of these Rényi entropies can be calculated in the dual gravitational theory by inserting cosmic branes with the appropriate tension T_n [525].

7.3.2. Microstate Wormholes in the Path Integral

In the present sec. 7 we discuss non-factorisation as signalled by the GQD, while in previous secs. 4 and 5 we discussed non-factorisation in terms of geometric phases. We have already explained in sec. 7.1.2 how these two notions are related for the particular example of two entangled qubits. In the following, we extend this by discussing how non-factorisation can be found for any of the black hole microstates $|\text{TFD}\rangle_\alpha$ due to the non-exactness of the symplectic form of the system. We discuss this by combining the insights of [165] on non-exactness with the construction of [531]. The latter work provides a recipe to construct Hamiltonians with the TFD state as its ground state for arbitrary systems. We will first briefly review this construction, followed by our analysis of the symplectic form of the Hamiltonian with the TFD state as the ground state. Since the GQD is equal for all microstates, we will focus on the TFD state with $\delta = 0$. We finally compare GQD as an indicator for non-factorisation to the non-exactness of the symplectic form in terms of practicality.

The mechanism of [531] is based on the observation that operators of the form

$$d_k = e^{-\frac{\beta}{4}(H_L+H_R)}\left(\mathfrak{O}_{L,k} - \Theta\mathfrak{O}^\dagger_{R,k}\Theta^{-1}\right)e^{\frac{\beta}{4}(H_L+H_R)} \tag{7.45}$$

annihilate the TFD state [531]. Here, $H_{L/R}$ and $\mathfrak{O}_{L/R,k}$ are the Hamiltonians and any operators of the left and right theories, respectively. The anti-unitary operator Θ is the same as appearing in (3.49). Note in particular that for $\mathfrak{O}_{L/R} = H_{L/R}$, the exponentials and Θ cancel. As we have discussed in detail in sec. 3.2.1, the operator $H_L - H_R$ annihilates the TFD state. The operator (7.45) can therefore be understood as a generalisation of $H_L - H_R$ to arbitrary operators $\mathfrak{O}_{L/R,k}$. As d_k annihilates the TFD state a Hamiltonian with the TFD state as ground state can be constructed as $H = c_k d_k^\dagger d_k$ with positive constants c_k. While this in principle always works, the exponential of the Hamiltonian is complicated to calculate explicitly, especially when the systems in question are strongly coupled. A version more applicable to these cases is provided by considering

$$d_k = \mathfrak{O}_{L,k} - \Theta\mathfrak{O}^\dagger_{R,k}\Theta^{-1}\,, \tag{7.46}$$

used to define the Hamiltonian

$$H^{(\mathrm{TFD})} = H_L + H_R + c'_k d_k^\dagger d_k\,, \tag{7.47}$$

where c'_k are again positive constants. However, in this version they cannot be arbitrary but have to be chosen appropriately in order for the TFD state to be the ground state of (7.47). As shown in [531], this boils down to demanding that the eigenvalue thermalisation hypothesis (ETH) is valid for the system in question. However, the validity of ETH is a sufficient but not necessary condition. In particular, in the following we will make use of (7.47) for two harmonic oscillators. In this case, the two Hamiltonians resulting from (7.45) and (7.46) coincide for a particular choice of c'_k and ETH does not need to be studied.

For two harmonic oscillators, the only available operators are the position and momentum operators $x_{L/R}$ and $p_{L/R}$ satisfying the usual commutation relations. Of course, left operators commute with right operators. Invoking (7.46) of these two operators, the Hamiltonian (7.47) is given by [531]

$$H^{(\mathrm{TFD})} = \frac{1+c}{2}\left(p_L^2 + p_R^2\right) + \frac{(1+c)\omega^2}{2}\left(x_L^2 + x_R^2\right) + c\,p_L p_R - c\omega^2\,x_L x_R\,, \tag{7.48}$$

where the constants c'_k introduced in (7.47) are $c'_p = c$, $c'_x = c\omega^2$ with $c = \frac{1}{2}\operatorname{csch}^2\frac{\beta\omega}{4}$. By the reasoning of [165] explained in the introduction sec. 5, detecting non-factorisation for this system amounts to showing that the Hamiltonian $H^{(\mathrm{TFD})}$ is of the class of Hamiltonians

discussed in [165]. To do so, we diagonalise the Hamiltonian (7.48) in new position and momentum operators $x_\pm$ and $p_\pm$. Since the resulting diagonal Hamiltonian is the sum of two uncoupled harmonic oscillators in the new variables, we may introduce the corresponding creation and annihilation operators $a_\pm$ and $a_\pm^\dagger$ as

$$a_\pm = \sqrt{\frac{\omega}{2(1+c)}}\left(x_\pm + \mathrm{i}\frac{1+c}{\omega}p_\pm\right), \quad a_\pm^\dagger = \sqrt{\frac{\omega}{2(1+c)}}\left(x_\pm - \mathrm{i}\frac{1+c}{\omega}p_\pm\right), \tag{7.49}$$

resulting in the Hamiltonian

$$H^{(\mathrm{TFD})} = \epsilon_+ a_+^\dagger a_+ + \epsilon_- a_-^\dagger a_- \,, \tag{7.50}$$

where $\epsilon_+ = \frac{1}{\omega}\coth\frac{\beta\omega}{4}$ and $\epsilon_- = \frac{1}{\omega}\tanh\frac{\beta\omega}{4}$. Inspired by the coupled harmonic oscillators discussed in the appendix of [165], as a final step we combine the creation and annihilation operators into variables of SU(2) by writing $X_I = \frac{1}{2}a_k^\dagger \sigma_I^{kl} a_l$, with σ_I the Pauli matrices. These variables are chosen such that the quadratic Casimir operator of SU(2) is given by $J^2 = X_I X_I$. In particular, $J = a_+^\dagger a_+ + a_-^\dagger a_-$ and $X_3 = \frac{1}{2}(a_+^\dagger a_+ - a_-^\dagger a_-)$ can be used to write

$$H^{(\mathrm{TFD})} = \gamma J + \epsilon X_3 \,, \tag{7.51}$$

where $\gamma = \frac{1}{\omega}\coth\frac{\beta\omega}{2}$ and $\epsilon = \frac{1}{\omega}\operatorname{csch}\frac{\beta\omega}{2}$. This is precisely a Hamiltonian of the class discussed in [165], so the symplectic form of this system is non-exact when restricted to a quantisable orbit $J = j$, $2j \in \mathbb{N}$ in the sense of geometric quantisation [263–265]. Therefore, following [165], the partition function of this system does not factorise, consistent with our result for the GQD of the TFD state (7.32) as the microstates of the black hole.

Finally, to diagnose factorisation, we compare the non-exactness argument of [165] with the argument about GQD discussed in the previous sections. First of all, both sides diagnose non-factorisation in a consistent way, i.e. both sides predict the same behaviour. In terms of ease of computation, the measures are somewhat different. As mentioned earlier in (2.81), proving that a two-form Ω is non-exact, the integral $\int_\Sigma \Omega$ has to be calculated, where Σ is a closed two-dimensional surface. In specific examples this computation can be hard, especially if the dimension of the system and correspondingly of the phase space is large. In particular, as this integral has to vanish for any Σ, it is not sufficient to compute this only for one example. In such cases, evaluating GQD might be easier. To diagnose non-factorisation using GQD, it is sufficient to show that at least two Schmidt coefficients κ_k are non-zero since already then $\sum_{k=1}^n \kappa_k^4 < 1$ and the GQD is non-zero.

8 Conclusion and Outlook

The overarching question studied in this thesis concerns the factorisation of the projective Hilbert space. This was analysed both in quantum mechanical systems and also in light of the factorisation puzzle in more sophisticated holographic models. Let me now conclude by summarising the results obtained in this thesis and pointing out interesting directions of future research motivated by these results.

The dual description of the eternal black hole in Anti-de Sitter spacetime is given by the two CFTs entangled in the TFD state defined on the asymptotic boundaries [112]. In AdS/CFT, entanglement between subregions in the CFTs is computed holographically by the area of the RT surface [113, 114]. Combining these insights led to interpreting spacetime not as fundamental but rather as emerging from the underlying entanglement structure [115–117]. This set the stage for the ER=EPR proposal, stating that entanglement between quantum systems is equivalent to a wormhole geometrically connecting the quantum systems [118]. These considerations however also led to a puzzle within the AdS/CFT correspondence. In the bulk, the eternal black hole is a smooth and connected classical geometry, connecting the left and right asymptotic boundary. Therefore, the bulk Hilbert space is manifestly non-factorised. However from the boundary perspective, since the boundaries are spatially separated there is no classical interaction between the two CFTs. Accordingly, the boundary Hilbert space appears to be factorised. This mismatch in the Hilbert space structure has been coined the factorisation puzzle [120]. In light of this puzzle, in this thesis I studied factorisation in general quantum systems but particularly also in the holographic setting of the eternal black hole dual to the TFD state. The main result of my considerations is to identify geometric phases as a novel means to diagnose non-factorisation, in particular from a boundary perspective.

I started my analysis in sec. 4 by showing that entanglement in a model of two interacting qubits can be understood entirely using the geometric phase. Invoking the SZK construction [166], the value of the geometric phase served as a label for the entanglement orbits. These orbits arise in the SZK construction as submanifolds of the projective Hilbert space. The orbits have the structure of a principal fibre bundle, for which I developed a technique to calculate the symplectic form, resulting in the geometric phase upon integration. With this technique at hand, I established the geometric phase as a probe for the factorisation properties of the projective Hilbert space. Specifically, a factorised submanifold $\mathbb{C}\mathrm{P}^1 \times \mathbb{C}\mathrm{P}^1 \subset \mathbb{C}\mathrm{P}^3$ arises only for the particular value $\Phi_{\mathrm{G}} = 2\pi$ of the geo-

metric phase, corresponding to unentangled states. For entangled states, where $\Phi_G < 2\pi$, the submanifold does not factorise. In the next step, I defined a fine structure of the entanglement entropy. This manifests as a class of states with the same entanglement entropy but different geometric phases. Note that these geometric phases were defined slightly differently than those distinguishing the entanglement orbits. While those were defined using group elements acting only on a single qubit, the geometric phases obtained for states with the same entanglement use group elements that act on both qubits. This fine structure is accessible to experiments. Invoking the argument of [165] on non-exact symplectic forms, I briefly discussed how the presence of geometric phases enables to associate a wormhole-like interpretation to this simple two-qubit system. In the next step to make contact with AdS/CFT, I then applied the same techniques to the TFD state. This started by showing that the entanglement temperature follows from the geometry encoding the entanglement. In particular, I derived the TFD state for the two-qubit system and thereby showed that the entanglement temperature is given only in terms of the geometric phase. Considering the TFD state of a general system, I briefly discussed this state in light of the SZK construction, manifesting the non-factorisation of the projective Hilbert space that includes the TFD state. The factorised projective Hilbert space only appeared in the limit of vanishing temperature. Moreover, I defined a phase of topological nature for the TFD state, which is interpreted as a winding number. This was possible since in the dual description, the black hole metric does not allow for a globally defined time-like Killing vector. Therefore, relating the times in the left and right boundary of the black hole allows for introducing a relative shift variable δ. This shift variable appeared in the corresponding parameter space and is a physical bulk degree of freedom. The winding number arose due to the non-trivial topology of the parameter space, which was given by the punctured plane. Also this topological phase is accessible in experiments. Finally, I showed how the same winding number can be obtained on the gravity side in an explicit example in JT gravity. Analysing the asymptotic symmetries of the black hole metric for two-dimensional AdS spacetime, I found the same parameter space as before in the quantum mechanical analysis. The non-trivial topology and the corresponding winding number are a direct probe for the non-factorisation of the bulk spacetime. To sum up, in this section I established that geometric phases are an important tool in diagnosing the non-factorisation of the projective Hilbert space. This is present both in simple quantum mechanical models as well as in systems with a holographic dual. In particular, the topological phase of the TFD state was analysed both in gravity and on the quantum mechanical side, with matching results. This provides a direct probe of the non-trivial topology of the parameter space of the theory, resulting from the presence of a wormhole in the gravitational picture.

Sec. 5 concerned generalising the results of the previous section to the setting of

AdS_3/CFT_2. Specifically, I discussed the role of the Virasoro Berry phase as well as the modular Berry phase in detecting non-factorisation. Virasoro Berry phases arise by conformal transformations, while modular Berry phases result from deformations of subregions of the CFT. For the Virasoro Berry phase, I extended the results of [485]. Employing Chern–Simons theory on a spacetime with an annulus topology, I calculated the symplectic form for the theories on the boundaries of the annulus. This made use of the results of [485], where the actions of the theories on the boundaries were derived for Chern–Simons theory with gauge group $SL(2,\mathbb{R})$. This can be considered as the BTZ black hole, with the boundaries of the annulus corresponding to the left and right boundaries of the black hole. In particular, the non-trivial holonomy induced by the annulus topology corresponds to the mass of the black hole. In the symplectic form, the holonomy appeared with a non-local conjugate momentum. This non-locality provides a coupling between the actions on the boundaries of the annulus. These actions reduce to one copy of the geometric action of the Virasoro group each but coupled by the holonomy. Due to the coupling, I reasoned that the resulting projective Hilbert space understood as a coadjoint orbit of the Virasoro group is not factorised. For the modular Berry phase, I explicitly computed the modular Berry curvature in the setting of the two-sided BTZ black string. The modular Berry curvature received non-local contributions stretching between the left and right asymptotic boundaries, thereby piercing the wormhole. Therefore, the modular Berry phase is sensitive to the wormhole and is a probe of non-factorisation. In particular, these non-local contributions appeared when introducing the time-shift variable δ, as before for the topological phase of the TFD state. To sum up, I have shown that in the context of the wormhole in AdS/CFT, Virasoro Berry phases, modular Berry phases as well as the geometric and topological phases of the TFD state allow for diagnosing non-factorisation purely from a boundary point of view. This insight is an important step in resolving the factorisation puzzle.

In sec. 6 I used geometric phases to characterise types of von Neumann algebras. As a first step, I analysed the tracial state on the operator algebras associated to the two-qubit system of sec. 4. The outcome showed that the trace is defined by a state vector with a vanishing geometric phase, which by the SZK construction corresponds to maximally entangled state vectors. I then generalised this result to operator algebras of type II and type III, using the Araki–Woods construction of hyperfinite von Neumann algebra factors of said types. I showed that on an algebra of type III, there does not exist a tracial state due to the presence of geometric phases. This was found by an explicit calculation of a generic linear functional evaluated on the commutator of two arbitrary operators. For a tracial state, this has to vanish. For a generic state vector associated to an algebra of type III, this never vanishes but is proportional to the geometric phases contained in the chosen

state vector. This provides a geometric explanation for the absence of the trace on type III algebras. For type II algebras, there exists a state vector with maximal entanglement. By the SZK construction, this corresponds to vanishing geometric phases. By my earlier general result for the linear functional of the commutator, this shows that the trace on algebras of type II is defined by the state vector with vanishing geometric phases. Based on the recent studies on operator algebras for the eternal black hole in AdS/CFT [132–134], I have argued that the transition between the type III_1 algebra of [132, 133] and the type II_∞ algebra of [134] can be understood using the topological phase of the TFD state. In particular, as I explained in sec. 4, the topological phase probes the topology of the parameter space that arises by considering the asymptotic symmetries and the isometries of the bulk spacetime. In operator algebraic language, the non-trivial topology arises from the shared centre of the type III_1 algebras. This shared centre corresponds to the Hamiltonian, i.e. the mass of the black hole. The type II_∞ algebra arises when including $\frac{1}{N}$-corrections, which renders the centre trivial. This enabled me to explain the transition between the type III_1 and type II_∞ algebras using the topological phase of the TFD state. Notably, this phase vanishes exactly for the maximally entangled state vector defining the trace on the type II_∞ algebra. Operator algebras that share only a trivial centre are deemed factorised. I therefore interpret the topological phase of the TFD state as a diagnostic tool for the factorisation properties of the operator algebras. Generalising this insight, I proposed a new interpretation of geometric and topological phases in general as indicating missing information to a local observer. Such a local observer is not able to measure the global phases of state vectors. I elucidated on this novel interpretation with examples of varying complexity, ranging from a single qubit in a magnetic field to coupled Virasoro Berry phases and modular Berry phases as discussed in sec. 5. To sum up, in this section I have shown that geometric phases can be used to provide a geometric explanation for the absence of a tracial state for algebras of type III, and at the same time explain the existence of a tracial state for algebras of type II. Moreover, in an application to the eternal black hole in AdS/CFT, I discussed how the topological phase of the TFD state characterises factorisation on the level of operator algebras. This motivates to interpret geometric and topological phases more generally as an indicator for missing information to a local observer.

Finally, sec. 7 studies a measure of entanglement different from the entanglement entropy, namely geometric quantum discord (GQD). This measure is defined in terms of the Hilbert–Schmidt norm of the difference between the state of interest ρ and a state χ that is fixed by requiring the norm to be minimal. I show that this measure as well serves as a probe for non-factorisation. More specifically, I derive an explicit expression for GQD in terms of the Schmidt coefficients of any state vector $|\psi\rangle$. While $|\psi\rangle$ generically is

an entangled state, the state χ_{min} minimising the norm is found to only include classical correlations. Due to the definition of GQD in terms of a norm, this associates to χ_{min} the interpretation as the closest classical state to the entangled quantum state $\rho = |\psi\rangle\langle\psi|$. The result for GQD can be expressed both using the second Rényi entropy and the modular partition function. The latter is defined analogously to the thermal partition function upon replacing βH with the modular Hamiltonian $K^{(A)}$. I then show that GQD vanishes if and only if the modular partition function factorises. I check this explicitly for the interacting two-qubit system discussed in sec. 4. In particular, this calculation shows that the notion of non-factorisation of the projective Hilbert space using the geometric phase is consistent with the current notion using GQD. Applying these results to the TFD state allows me to interpret GQD as a diagnostic tool of non-factorisation from the boundary perspective. The state minimising GQD for the TFD state is given by the TMD state, proposed in [182] as the mixed state describing the black hole after interacting with its ambient spacetime. While this state was obtained in [182] by considerations of the bulk physics, using GQD I present an entirely quantum information theoretic derivation of the TMD state. This allows for the novel interpretation of the TMD state as the closest classical approximation to the TFD state. Based on the relation between GQD and the second Rényi entropy, I briefly discuss a possible bulk calculation of GQD. Finally, I generalise the Hilbert–Schmidt norm used to define GQD to the Schatten norm. This allows to use the generalised GQD as a probe of black hole microstates, which are given by the time-shifted TFD states. In particular, this shows that the generalised GQD as a measure of quantum correlations provides a tool to distinguish between the TFD state, the TMD state and the factorised thermal state, all of which are indistinguishable in local measurements. I finally relate the existence of these microstates to the argument on non-factorisation in terms of a non-exact symplectic form put forward in [165]. To sum up, in this section I have shown that non-factorisation can be diagnosed not only using geometric phases but also using GQD. In the holographic setting, GQD diagnoses non-factorisation from the boundary perspective. Moreover, the results on the TMD state and the black hole microstates suggest that in AdS/CFT, different information theoretic quantifiers of entanglement encode different aspects of the dual bulk picture. The combination of these quantifiers eventually allows to obtain a complete picture of the bulk in terms of entanglement properties, supporting the idea of 'entanglement creating spacetime'.

The above results further clarify the relationship between quantum information theory and theories of gravity, as suggested by the holographic principle and its most prominent realisation, the AdS/CFT correspondence. As I have shown in four distinct examples, quantities of quantum information theory, such as geometric phases as well as geometric

quantum discord, are well-suited to explain facets of gravitational theories. In particular, this includes the non-factorisation properties of the Hilbert space on the field theory side of the AdS/CFT correspondence in the presence of a black hole in the bulk. Moreover, I have discussed how geometric phases allow for characterising von Neumann algebras and indicate information missing to a local observer.

Outlook

Building on the results of this thesis, there are several interesting questions that can now be addressed. Let me elaborate on these possible future directions in the following.

A Flow of Entanglement In constructing the entanglement orbits by the SZK construction [166], local unitary transformations of the form $U = U_1 \otimes U_2 \in \mathrm{U}(n) \otimes \mathrm{U}(n)$ have been considered. Such transformations never alter the entanglement between $\mathscr{H}^{(1)}$ and $\mathscr{H}^{(2)}$ constituting the bipartite Hilbert space $\mathscr{H} = \mathscr{H}^{(1)} \otimes \mathscr{H}^{(2)}$ [188]. Linear combinations of such local unitary transformations $\widehat{U} = \sum_l c_l U_1^{(l)} \otimes U_2^{(l)}$ generally alter the entanglement. Such transformations may be understood as evolving the state vector $|\psi\rangle$ by an interaction Hamiltonian H_{int}. For simple two-qubit systems, an example is given by $H_{\mathrm{int}} = \gamma\left(\mathfrak{a}_1^\dagger \otimes \mathfrak{a}_2^\dagger + \mathfrak{a}_1 \otimes \mathfrak{a}_2\right)$, where $\mathfrak{a}_{1/2}^{(\dagger)} = \frac{1}{2}\left(\sigma_{x,1/2} \pm \mathrm{i}\sigma_{y,1/2}\right)$ act as raising and lowering operators, $\mathfrak{a}_{1/2}^\dagger|{\downarrow_{1/2}}\rangle = |{\uparrow_{1/2}}\rangle$ and $\mathfrak{a}_{1/2}|{\uparrow_{1/2}}\rangle = |{\downarrow_{1/2}}\rangle$. Starting at $t = 0$ with an unentangled state $|{\downarrow_1}, {\downarrow_2}\rangle$, evolution by $\widehat{U}(t) = e^{\mathrm{i}H_{\mathrm{int}}t}$ results in an entangled state, with maximal entanglement achieved for $t = t_{\mathrm{max}} = \frac{\pi}{4\gamma}$. This establishes a flow between entanglement orbits,

$$\mathbb{C}\mathrm{P}^1 \times \mathbb{C}\mathrm{P}^1 \xrightarrow{\widehat{U}(t)} \mathbb{C}\mathrm{P}^1 \times \mathbb{R}\mathrm{P}^3 \xrightarrow{\widehat{U}(t_{\mathrm{max}})} \mathbb{1} \times \mathbb{R}\mathrm{P}^3 \,. \tag{8.1}$$

Accordingly, the geometric phase computed for these orbits in sec. 4.1.2 changes under such transformations.

It will be interesting to generalise this to infinite-dimensional systems. For this purpose, a particularly promising setting is that of $\mathrm{AdS}_3/\mathrm{CFT}_2$, where $\hat{U}$ can be expressed using conformal transformations using the power of two-dimensional CFT. This unitary changes between coadjoint orbits of the Virasoro group. A CFT-transformation between the vacuum and a collapsing shell of matter, eventually resulting in the AdS_3-Vaidya geometry representing a black hole formed by collapse, has been considered in [532], based on earlier considerations in the bulk dual [533]. These transformations have recently gathered attention in the study of holographic complexity, where the entanglement orbits will be able to provide a complementary view of the same underlying physics [534]. The unitary

transformation considered in [532] implements an evolution by an interaction Hamiltonian, cf. eq. (A.3) in that paper, as we considered above for the qubit case. To establish the flow of entanglement for the eternal black hole in AdS_3/CFT_2, it will be important to find the unitary transformation that changes from two decoupled vacuum coadjoint orbits $\mathscr{G}_0 = \frac{\mathsf{Vir}}{\mathsf{SL}(2,\mathbb{R})}$ to the coadjoint orbit of the two-sided eternal black hole (5.44),

$$\mathscr{G}_0 \times \mathscr{G}_0 \xrightarrow{\hat{U}=?} \frac{\mathsf{Vir}\times\mathsf{Vir}}{\mathsf{U}(1)} \,. \tag{8.2}$$

Hawking–Page, Hagedorn and Geometric Phases The aforementioned flow between entanglement orbits is particularly interesting in light of the Hawking–Page phase transition between the eternal black hole and empty AdS [535]. Starting from the two-sided CFT vacuum $|\mathrm{vac}\rangle = |0_L, 0_R\rangle$, acting with an operator $\hat{U} \sim \exp\left(e^{-\beta\frac{E}{2}}\mathfrak{a}_L^\dagger \mathfrak{a}_R^\dagger\right)$ generates the TFD state dual to the eternal black hole [449]. Since this operator changes the entanglement properties of the state, it also changes the geometric phase in light of the SZK construction. Analysing this geometric phase and its alteration will be useful for providing an explanation of the Hawking–Page phase transition in terms of the geometry of the projective Hilbert space. In particular, this analysis provides a new perspective on the emergence of spacetime, specifically on the black hole interior region, by increasing the entanglement.

From the perspective of von Neumann algebras, the Hawking–Page transition is understood as the so-called Hagedorn transition. This latter transition arose in particle physics by studying the confined and deconfined phases of quark matter [536]. At a temperature referred to as the Hagedorn temperature T_{H}, the phase transition between confinement and deconfinement is understood as a transition between type I and type III algebras, respectively. More akin to holography, the Hagedorn transition has been observed in string theory [537] and $\mathscr{N} = 4$ supersymmetric Yang–Mills theory [451, 538]. This led to interpreting the Hawking–Page phase transition as a version of the Hagedorn phase transition with $T_{\mathsf{H}} = T_{\mathsf{HP}}$, where T_{HP} is the temperature where the Hawking–Page phase transition occurs. Indeed the transition between two type I_∞ algebras and two III_1 algebras has been found [132, 133]. It is also worth pointing out that a recent study of interacting Majorana fermions found a similar change between operator algebras [539]. Therefore, understanding the Hawking–Page phase transition in terms of entanglement orbits will also be useful for a geometric explanation of confinement/deconfinement described by the Hagedorn transition in terms of the geometry of the projective Hilbert space.

The Geometry of Parameter Space for $\mathscr{N} = 4$ SU(N) Yang–Mills Theory In a complementary approach to the above, it would be interesting to use the Lagrangian approach put forward in [507–509] to compute both the Fubini–Study metric and the sym-

plectic form in the setting of AdS/CFT. In this method, which we briefly mentioned at the end of sec. 6.1.1, parameters such as the couplings in the action are used to define deformation operators by assuming small variations in the parameters. Specifically the case of $\mathrm{AdS}_5/\mathrm{CFT}_4$ reviewed in sec. 3.1.2 might be interesting as the action of $\mathscr{N} = 4$ SU(N) Yang–Mills theory is known explicitly, cf. (3.20). Assuming small deformations in these parameters, the Fubini–Study metric as well as the symplectic form on the parameter space can be calculated as expectation values of the anti-commutator and commutator of the deformation operators. On the one hand, the symplectic form is interesting to compute geometric phases, i.e. to study whether it is non-exact. This would provide a further instance of probing non-factorisation from a boundary perspective in the archetypical setting of $\mathrm{AdS}_5/\mathrm{CFT}_4$, extending the results of this thesis. An interesting task in this context is to find out whether the 'black hole Berry phase' of [540], proposed as a probe of the number of black hole microstates, can be computed in this approach. On the other hand, it was observed in several examples that the geometry induced by the Fubini–Study metric is sensitive to phase transitions. In particular, its Ricci scalar shows a divergence at the transition, see e.g. [541–543] (see also [544] for a recent review). Therefore, it is a worthwhile purpose to examine the Fubini–Study metric on the parameter space of $\mathscr{N} = 4$ SU(N) Yang–Mills theory for signs of a phase transition, in particular the Hawking–Page phase transition.

Einstein Equations for Entanglement Orbits In our studies of entanglement orbits, complex projective spaces $\mathbb{C}\mathrm{P}^n$ naturally arose when quotienting the local unitary transformations $\mathrm{U}(n) \otimes \mathrm{U}(n)$ by the subgroup leaving a given state vector invariant up to an overall phase, cf. 2.93. On the other hand, complex projective space is a solution to the vacuum Einstein equations with positive 'cosmological' constant, cf. (2.73) [190]. It is an interesting question if also other solutions to the vacuum Einstein equations can be given an interpretation in terms of entanglement orbits, in particular Anti-de Sitter spacetime. It is worth noting that the metric of AdS_2 has been derived as the Fubini–Study metric on the parameter space of a class of Gaussian probability distributions [543, 545]. There is a grain of salt in that an infinite class of different distributions lead to the same metric. In the context of the emergence of spacetime from entanglement and quantum information, it remains to be determined whether this is a bug or a feature. It would moreover be interesting to find out whether the metric of the black hole in AdS_2 follows from less symmetric distributions. Moreover, assuming that Anti-de Sitter spacetime can indeed be given an interpretation as an entanglement orbit, a natural follow-up task is to study which entanglement orbits are associated to metrics with a horizon. Apart from black hole metrics, this also concerns metrics with a cosmological horizon, e.g. de Sitter spacetimes.

Geometric Phases in Quantum Gravity The geometric phases discussed in this thesis arose from the presence of global symmetries. This global symmetry manifested as leaving invariant state vectors up to a global phase. The fact that these global phase factors are inaccessible to a local observer although they do carry information about the physics of the system motivated our interpretation of geometric phases as indicating missing information in sec. 6.2. While global symmetries are present in most systems studied in physics, to the best of current knowledge a UV-complete theory of quantum gravity is believed to not have any global symmetry [516, 519, 520]. Correspondingly, there should not be any geometric phases in quantum gravity, which may be viewed as a guiding principle. Studying the geometric phases obtained in quantising the parameter space of gravitational theories following geometric quantisation will shed light on the possible Hilbert space structures of quantum gravity. To appreciate this statement, note that e.g. the Hilbert space structure of a single qubit obtained by geometric quantisation follows from the non-trivial geometric phase enforcing the half-integer quantisation of spin by the Weyl integrality condition. Moreover, while [132, 133] and [134] provide type III and type II von Neumann algebras describing gravity, respectively, quantum gravity is believed to allow for a type I operator algebra [172] (see also [546] for an approximate type I treatment of the type II algebra obtained in [134]). In this sense, analysing geometric phases might help in finding ways to eventually obtain a type I description of gravity.

Symmetry Resolved Tomita–Takesaki Theory From an operator algebraic point of view, global symmetries arise whenever there are non-trivial central operators. In this case, the Hilbert space can be written as a direct sum over Hilbert spaces associated to sectors with fixed charge q, i.e. $\mathscr{H} = \bigoplus_q \mathscr{H}_q$. Correspondingly, the operator algebra splits into a direct sum, $\mathscr{A} = \bigoplus_q \mathscr{A}_q$. The resulting block-diagonal structure motivates the concept of symmetry resolution [547, 548]. While originally studied in spin chains, this concept has been generalised to settings of AdS/CFT [549] and has also been analysed for particular elements of Tomita–Takesaki theory [550]. A complete symmetry resolution of Tomita–Takesaki theory and modular flow however has not yet been established. A particularly interesting question in this context is, given that the algebra $\mathscr{A}$ has a certain type, which type are the algebras $\mathscr{A}_q$ of each charge sector? An ideal starting point for this analysis is given by the construction of algebras of hyperfinite type II and type III algebras as limits of spin collections. Here, the magnetisation naturally arises as a global charge w.r.t. a symmetry resolution can be defined. As we have alluded to in our review of von Neumann algebras in sec. 2.3.1, these constructions have the advantages of being conceptually simple and explicit at the same time. In a project that I am part of, the first results suggest that in certain cases, the type of operator algebra may differ between $\mathscr{A}$ and $\mathscr{A}_q$ as type III

and type II, respectively [551]. This result would be significant since $\mathscr{A}$ does not allow for a trace, while the algebras $\mathscr{A}_q$ of each charge sector do. However, at the time of writing this thesis, more checks have to be run to prove this result.

A Holographic Dual for Quantum Discord Finally, computing quantum discord in holography would enable for a far more fine-grained probe of the entanglement structure than using the entanglement entropy. In particular, quantum discord captures quantum correlations that measures of entanglement cannot detect, i.e. quantum correlations beyond entanglement [174, 250–252]. A calculation of quantum discord on the gravity side of holography might therefore help greatly in developing a deeper understanding of how entanglement, or perhaps also other quantum correlations, are responsible for the emergence of spacetime. Unfortunately, generalising the definition of quantum discord from quantum mechanics to QFT is already a difficult task, let alone gravity. Note that strictly speaking, none of the terms in computing quantum discord is defined in QFT. All of the constituents require computing a trace, whereas QFT generically has a type III algebra which in turn does not have a trace. Therefore, the following should be understood in the presence of a cut-off, as the entanglement entropy in QFT. Whit this in mind, the main obstacle lies in the fact that quantum discord requires a minimisation over projective measurements. Progress on projective measurements in QFT has been made in [552, 553]. In the language of AQFT, projective measurements in QFTs with arbitrarily curved background spacetime have been formulated in [554, 555]. Also in the context of AdS/CFT, progress on projective measurements has been made [556, 557]. Combining these insights should enable to generalise quantum discord to QFT, although the explicit evaluation might still be complicated due to the minimisation over the projective measurements. As is often the case, probably the most promising starting point for these investigations is two-dimensional CFT. Here, the generators of the Virasoro group might serve as a canonical basis to express general measurement operators such that the minimisation can be performed.

Final Remarks

Notably, the concept of spacetime emerging from quantum entanglement, as elegantly encapsulated in the ER=EPR proposal, stands as a cornerstone in our quest to refine our comprehension of the AdS/CFT correspondence. Our analysis of geometric phases provides a novel quantum information-theoretic means of diagnosing non-factorisation induced by the wormhole in light of ER=EPR. This, in turn, paves the way for a more holistic and comprehensive understanding of quantum gravity, a pursuit that has long captured the imagination of physicists. Moreover, research in this domain has recently taken up the

application of operator algebraic methods. These methods not only provide a fresh perspective on the subject but also bring a newfound level of mathematical rigour to the field, ensuring that the explorations are firmly anchored in the realm of exact science. We have shown that geometric phases enable a classification of the type of operator algebra and account for a factorisation on the level of operator algebras. This represents a significant stride forward to analyse semiclassical aspects of gravity and the factorisation puzzle using quantities of quantum information theory.

As we look to the years ahead, the horizon of possibilities appears ever more enticing and promising. Indeed, the realm of quantum gravity and quantum information theory seems poised for further exciting breakthroughs. Yet, amidst the promise of future discoveries, it is essential to remain mindful of the vast expanse of unanswered questions that lie before us. These questions, some of which may yet elude our present understanding, serve as enigmatic challenges that demand our rigorous pursuit. The task of formulating the most pertinent and profound questions may well prove to be as arduous and momentous as the ultimate quest for definitive answers. In essence, the journey of exploration in this enigmatic realm continues to be an intellectual adventure of the highest order.

We are just an advanced breed of monkeys
on a minor planet of a very average star.
But we can understand the Universe.
That makes us something very special.

Stephen Hawking, in an interview with 'Der Spiegel', 1988

Publications

A

This thesis is based on the following papers, published in the displayed scientific journals:

[183] F. S. Nogueira, S. Banerjee, M. Dorband, R. Meyer, J. v. d. Brink and J. Erdmenger, *Geometric phases distinguish entangled states in wormhole quantum mechanics*, *Phys. Rev. D* **105** (2022) L081903, [2109.06190]

[185] S. Banerjee, M. Dorband, J. Erdmenger, R. Meyer and A.-L. Weigel, *Berry phases, wormholes and factorization in AdS/CFT*, *JHEP* **08** (2022) 162, [2202.11717]

[186] S. Banerjee, P. Basteiro, R. N. Das and M. Dorband, *Geometric Quantum Discord Signals Non-Factorization*, *JHEP* **08** (2023) 104, [2305.04952]

[184] S. Banerjee, M. Dorband, J. Erdmenger and A.-L. Weigel, *Geometric Phases Characterise Operator Algebras and Missing Information*, *JHEP* **10** (2023) 026, [2306.00055]

I also contributed to the following preprint published on arXiv that is not discussed in this thesis:

[558] M. Dorband, D. Grumiller, R. Meyer and S. Zhao, *Disorder in AdS_3/CFT_2*, 2204.00596

Bibliography

[1] E. Rutherford, *The scattering of alpha and beta particles by matter and the structure of the atom*, *Phil. Mag. Ser. 6* **21** (1911) 669–688.

[2] N. Bohr, *On the Constitution of Atoms and Molecules*, *Phil. Mag. Ser. 6* **26** (1913) 1–24.

[3] M. Planck, *On the Law of Distribution of Energy in the Normal Spectrum*, *Ann. Phys.* **4** (1901) 553.

[4] W. Pauli, *Über das Wasserstoffspektrum vom Standpunkt der neuen Quantenmechanik*, *Z. Phys.* **36** (1926) 336–363.

[5] E. Schrödinger, *Quantisierung als Eigenwertproblem*, *Ann. Phys.* **384** (1926) 361–376.

[6] A. Einstein and M. Born, *Born–Einstein Letters, 1916–1955*, Macmillan Science, Palgrave Macmillan New York, 1 ed., 2005.

[7] H. Everett, J. A. Wheeler, B. S. DeWitt, L. N. Cooper, D. V. Vechten and N. Graham, *The Many Worlds Interpretation of Quantum Mechanics*, Princeton University Press, 1973.

[8] W. Heisenberg, *Physics and Beyond: Encounters and Conversations*, Harper Torchbooks, Harper & Row, 1971.

[9] P. Ehrenfest, *Bemerkung über die angenäherte Gültigkeit der klassischen Mechanik innerhalb der Quantenmechanik*, *Z. Phys.* **45** (1927) 455–457.

[10] W. Pauli, *Über den Zusammenhang des Abschlusses der Elektronengruppen im Atom mit der Komplexstruktur der Spektren*, *Z. Phys.* **31** (1925) 765–783.

[11] W. Heisenberg, *Über den anschaulichen Inhalt der quantentheoretischen Kinematik und Mechanik*, *Z. Phys.* **43** (1927) 172–198.

[12] P. A. M. Dirac, *The Principles of Quantum Mechanics*, The International Series of Monographs on Physics 27, Oxford University Press, 4 ed., 1988.

[13] E. Schrödinger, *Discussion of Probability Relations between Separated Systems*, *Math. Proc. Cam. Phil. Soc.* **31** (1935) 555—563.

[14] E. Schrödinger, *Probability relations between separated systems*, *Math. Proc. Cam. Phil. Soc.* **32** (1936) 446–452.

[15] A. Einstein, B. Podolsky and N. Rosen, *Can quantum mechanical description of physical reality be considered complete?*, *Phys. Rev.* **47** (1935) 777–780.

[16] A. Einstein, *On the electrodynamics of moving bodies*, *Ann. Phys.* **17** (1905) 891–921.

[17] A. Einstein, *Ist die Trägheit eines Körpers von seinem Energieinhalt abhängig?*, *Ann. Phys.* **323** (1905) 639–641.

[18] A. Einstein, *The Field Equations of Gravitation*, *Sitzungsber. Preuss. Akad. Wiss. Berlin (Math. Phys.)* **1915** (1915) 844–847.

[19] A. Einstein, *Zur Allgemeinen Relativitätstheorie*, *Sitzungsber. Preuss. Akad. Wiss. Berlin (Math. Phys.)* **1915** (1915) 778–786.

[20] A. Einstein, *The foundation of the general theory of relativity.*, *Ann. Phys.* **49** (1916) 769–822.

[21] A. Einstein, *Explanation of the Perihelion Motion of Mercury from the General Theory of Relativity*, *Sitzungsber. Preuss. Akad. Wiss. Berlin (Math. Phys.)* **1915** (1915) 831–839.

[22] K. Schwarzschild, *On the gravitational field of a sphere of incompressible fluid according to Einstein's theory*, *Sitzungsber. Preuss. Akad. Wiss. Berlin (Math. Phys.)* **1916** (1916) 424–434, [physics/9912033].

[23] K. Schwarzschild, *On the gravitational field of a mass point according to Einstein's theory*, *Sitzungsber. Preuss. Akad. Wiss. Berlin (Math. Phys.)* **1916** (1916) 189–196, [physics/9905030].

[24] A. Friedman, *On the Curvature of space*, *Z. Phys.* **10** (1922) 377–386.

[25] E. Hubble, *A relation between distance and radial velocity among extra-galactic nebulae*, *Proc. Nat. Acad. Sci.* **15** (1929) 168–173.

[26] P. A. M. Dirac and N. H. D. Bohr, *The quantum theory of the emission and absorption of radiation*, *Proc. Roy. Soc. London Series A, Containing Papers of a Mathematical and Physical Character* **114** (1927) 243–265.

[27] P. A. M. Dirac and R. H. Fowler, *The quantum theory of the electron*, *Proc. Roy. Soc. London Series A, Containing Papers of a Mathematical and Physical Character* **117** (1928) 610–624.

[28] R. P. Feynman, *Space-time approach to nonrelativistic quantum mechanics*, *Rev. Mod. Phys.* **20** (1948) 367–387.

[29] P. Jordan and W. Pauli, *Zur Quantenelektrodynamik ladungsfreier Felder*, *Z. Phys.* **47** (1928) 151–173.

[30] F. J. Dyson, *The Radiation theories of Tomonaga, Schwinger, and Feynman*, *Phys. Rev.* **75** (1949) 486–502.

[31] S. L. Glashow, *The renormalizability of vector meson interactions*, *Nucl. Phys.* **10** (1959) 107–117.

[32] A. Salam and J. C. Ward, *Weak and electromagnetic interactions*, *Nuovo Cim.* **11** (1959) 568–577.

[33] S. L. Glashow, *Partial Symmetries of Weak Interactions*, *Nucl. Phys.* **22** (1961) 579–588.

[34] S. Weinberg, *A Model of Leptons*, *Phys. Rev. Lett.* **19** (1967) 1264–1266.

[35] H. Fritzsch, M. Gell-Mann and H. Leutwyler, *Advantages of the Color Octet Gluon Picture*, *Phys. Lett. B* **47** (1973) 365–368.

[36] D. J. Gross and F. Wilczek, *Ultraviolet Behavior of Nonabelian Gauge Theories*, *Phys. Rev. Lett.* **30** (1973) 1343–1346.

[37] H. D. Politzer, *Asymptotic Freedom: An Approach to Strong Interactions*, *Phys. Rept.* **14** (1974) 129–180.

[38] J. S. Schwinger, *On Quantum electrodynamics and the magnetic moment of the electron*, *Phys. Rev.* **73** (1948) 416–417.

[39] J. S. Schwinger, *Quantum electrodynamics. III: The electromagnetic properties of the electron: Radiative corrections to scattering*, *Phys. Rev.* **76** (1949) 790–817.

[40] X. Fan, T. G. Myers, B. A. D. Sukra and G. Gabrielse, *Measurement of the Electron Magnetic Moment*, *Phys. Rev. Lett.* **130** (2023) 071801, [2209.13084].

[41] S. Weinberg, *Infrared photons and gravitons*, *Phys. Rev.* **140** (1965) B516–B524.

[42] S. Weinberg, *The Quantum theory of fields. Vol. 1: Foundations*, Cambridge University Press, 6, 2005, 10.1017/CBO9781139644167.

[43] C. Kiefer, *Quantum gravity*, vol. 124, Clarendon, Oxford, 2004.

[44] S. W. Hawking, *Virtual black holes*, *Phys. Rev. D* **53** (1996) 3099–3107, [hep-th/9510029].

[45] F. Scardigli, *Generalized uncertainty principle in quantum gravity from micro - black hole Gedanken experiment*, *Phys. Lett. B* **452** (1999) 39–44, [hep-th/9904025].

[46] B. Mielnik, *Generalized quantum mechanics*, *Commun. Math. Phys.* **37** (1974) 221–256.

[47] T. W. B. Kibble, *Geometrization of quantum mechanics*, *Commun. Math. Phys.* **65** (1979) 189–201.

[48] A. Heslot, *Quantum mechanics as a classical theory*, *Phys. Rev. D* **31** (1985) 1341–1348.

[49] A. Ashtekar and T. A. Schilling, *Geometrical formulation of quantum mechanics*, pp. 23–65, Springer New York, New York, NY, 1999, 10.1007/978-1-4612-1422-9_3, [gr-qc/9706069].

[50] L. P. Hughston, *Geometry of stochastic state vector reduction*, *Proc. Roy. Soc. London* **452** (1996) 953–979.

[51] G. Veneziano, *Construction of a crossing - symmetric, Regge behaved amplitude for linearly rising trajectories*, *Nuovo Cim. A* **57** (1968) 190–197.

[52] Z. Koba and H. B. Nielsen, *Reaction amplitude for n mesons: A Generalization of the Veneziano-Bardakci-Ruegg-Virasora model*, *Nucl. Phys. B* **10** (1969) 633–655.

[53] M. A. Virasoro, *Alternative constructions of crossing-symmetric amplitudes with regge behavior*, *Phys. Rev.* **177** (1969) 2309–2311.

[54] J. A. Shapiro, *Electrostatic analog for the virasoro model*, *Phys. Lett. B* **33** (1970) 361–362.

[55] J. Scherk and J. H. Schwarz, *Dual Models for Nonhadrons*, *Nucl. Phys. B* **81** (1974) 118–144.

[56] T. Yoneya, *Connection of Dual Models to Electrodynamics and Gravidynamics*, *Prog. Theor. Phys.* **51** (1974) 1907–1920.

[57] A. Strominger and C. Vafa, *Microscopic origin of the Bekenstein-Hawking entropy*, *Phys. Lett. B* **379** (1996) 99–104, [hep-th/9601029].

[58] M. B. Green and J. H. Schwarz, *Anomaly Cancellation in Supersymmetric D=10 Gauge Theory and Superstring Theory*, *Phys. Lett. B* **149** (1984) 117–122.

[59] D. J. Gross, J. A. Harvey, E. J. Martinec and R. Rohm, *The Heterotic String*, *Phys. Rev. Lett.* **54** (1985) 502–505.

[60] P. Candelas, G. T. Horowitz, A. Strominger and E. Witten, *Vacuum configurations for superstrings*, *Nucl. Phys. B* **258** (1985) 46–74.

[61] E. Witten, *String theory dynamics in various dimensions*, *Nucl. Phys. B* **443** (1995) 85–126, [hep-th/9503124].

[62] J. H. Schwarz, *Physical States and Pomeron Poles in the Dual Pion Model*, *Nucl. Phys. B* **46** (1972) 61–74.

[63] E. Bergshoeff, E. Sezgin and P. K. Townsend, *Supermembranes and Eleven-Dimensional Supergravity*, *Phys. Lett. B* **189** (1987) 75–78.

[64] E. P. Verlinde, *Fusion Rules and Modular Transformations in 2D Conformal Field Theory*, *Nucl. Phys. B* **300** (1988) 360–376.

[65] E. Witten, *Two-dimensional gravity and intersection theory on moduli space*, *Surveys Diff. Geom.* **1** (1991) 243–310.

[66] A. Tsuchiya, K. Ueno and Y. Yamada, *Conformal Field Theory on Universal Family of Stable Curves with Gauge Symmetries*, *Adv. Stud. Pure Math.* **19** (1989) 459–566.

[67] G. Faltings, *A proof for the Verlinde formula*, *J. Algebraic Geom.* **3** (1994) 347–374.

[68] Y.-Z. Huang, *Vertex operator algebras, the Verlinde conjecture and modular tensor categories*, *Proc. Nat. Acad. Sci.* **102** (2005) 5352–5356, [math/0412261].

[69] M. Kontsevich, *Intersection theory on the moduli space of curves and the matrix Airy function*, *Commun. Math. Phys.* **147** (1992) 1–23.

[70] M. Mirzakhani, *Simple geodesics and Weil-Petersson volumes of moduli spaces of bordered Riemann surfaces*, *Invent. Math.* **167** (2006) 179–222.

[71] M. Mirzakhani, *Weil-Petersson volumes and intersection theory on the moduli space of curves*, *J. Am. Math. Soc.* **20** (2007) 1–24.

[72] B. Ovrut, *String Theory: Superstrings. A Theory of Everything?*, *Science* **242** (1988) 1584–1585.

[73] T. Banks, W. Fischler, S. H. Shenker and L. Susskind, *M theory as a matrix model: A Conjecture*, *Phys. Rev. D* **55** (1997) 5112–5128, [hep-th/9610043].

[74] J. M. Maldacena, *The Large N limit of superconformal field theories and supergravity*, *Adv. Theor. Math. Phys.* **2** (1998) 231–252, [hep-th/9711200].

[75] E. Witten, *Anti-de Sitter space and holography*, *Adv. Theor. Math. Phys.* **2** (1998) 253–291, [hep-th/9802150].

[76] S. S. Gubser, I. R. Klebanov and A. M. Polyakov, *Gauge theory correlators from noncritical string theory*, *Phys. Lett. B* **428** (1998) 105–114, [hep-th/9802109].

[77] J. K. Asbóth, L. Oroszlány and A. Pályi, *A Short Course on Topological Insulators*, Lecture Notes in Physics, Springer Cham, 1 ed., 2016, 10.1007/978-3-319-25607-8, [1509.02295].

[78] K.-H. Rehren, *Algebraic Holography*, *Annales Henri Poincaré* **1** (2000) 607–623, [hep-th/9905179].

[79] K.-H. Rehren, *QFT lectures on AdS-CFT*, in *3rd Summer School in Modern Mathematical Physics*, pp. 95–118, 2005, [hep-th/0411086].

[80] Planck collaboration, N. Aghanim et al., *Planck 2018 results. VI. Cosmological parameters*, *Astron. Astrophys.* **641** (2020) A6, [1807.06209].

[81] SPT-3G collaboration, L. Balkenhol et al., *Measurement of the CMB temperature power spectrum and constraints on cosmology from the SPT-3G 2018 TT, TE, and EE dataset*, *Phys. Rev. D* **108** (2023) 023510, [2212.05642].

[82] A. Strominger, *The dS / CFT correspondence*, *JHEP* **10** (2001) 034, [hep-th/0106113].

[83] M. Spradlin, A. Strominger and A. Volovich, *Les Houches lectures on de Sitter space*, in *Les Houches Summer School: Session 76: Euro Summer School on Unity of Fundamental Physics: Gravity, Gauge Theory and Strings*, pp. 423–453, 10, 2001, [hep-th/0110007].

[84] Y.-b. Kim, C. Y. Oh and N. Park, *Classical geometry of de Sitter space-time: An Introductory review*, *J. of the Kor. Phys. Soc.* **42** (2003) 573–592, [hep-th/0212326].

[85] D. Anninos, T. Hartman and A. Strominger, *Higher Spin Realization of the dS/CFT Correspondence*, *Class. Quant. Grav.* **34** (2017) 015009, [1108.5735].

[86] J. Cotler and A. Strominger, *Cosmic ER=EPR in dS/CFT*, 2302.00632.

[87] L. Susskind, *Holography in the flat space limit*, *AIP Conf. Proc.* **493** (1999) 98–112, [hep-th/9901079].

[88] J. de Boer and S. N. Solodukhin, *A Holographic reduction of Minkowski space-time*, *Nucl. Phys. B* **665** (2003) 545–593, [hep-th/0303006].

[89] D. Berenstein, *A Toy model for the AdS / CFT correspondence*, *JHEP* **07** (2004) 018, [hep-th/0403110].

[90] R. B. Mann, *Flat space holography*, *Can. J. Phys.* **86** (2008) 563–570.

[91] A. Bagchi and D. Grumiller, *Holograms of flat space*, *Int. J. Mod. Phys. D* **22** (2013) 1342003.

[92] A. Bagchi, R. Basu, A. Kakkar and A. Mehra, *Flat Holography: Aspects of the dual field theory*, *JHEP* **12** (2016) 147, [1609.06203].

[93] N. Arkani-Hamed, M. Pate, A.-M. Raclariu and A. Strominger, *Celestial amplitudes from UV to IR*, *JHEP* **08** (2021) 062, [2012.04208].

[94] A.-M. Raclariu, *Lectures on Celestial Holography*, 2107.02075.

[95] S. Pasterski, *Lectures on celestial amplitudes*, *Eur. Phys. J. C* **81** (2021) 1062, [2108.04801].

[96] G. Policastro, D. T. Son and A. O. Starinets, *The Shear viscosity of strongly coupled N=4 supersymmetric Yang-Mills plasma*, *Phys. Rev. Lett.* **87** (2001) 081601, [hep-th/0104066].

[97] A. Buchel and J. T. Liu, *Universality of the shear viscosity in supergravity*, *Phys. Rev. Lett.* **93** (2004) 090602, [hep-th/0311175].

[98] P. Kovtun, D. T. Son and A. O. Starinets, *Viscosity in strongly interacting quantum field theories from black hole physics*, *Phys. Rev. Lett.* **94** (2005) 111601, [hep-th/0405231].

[99] M. Luzum and P. Romatschke, *Conformal Relativistic Viscous Hydrodynamics: Applications to RHIC results at s(NN)**(1/2) = 200-GeV*, *Phys. Rev. C* **78** (2008) 034915, [0804.4015].

[100] S. A. Hartnoll, *Lectures on holographic methods for condensed matter physics*, *Class. Quant. Grav.* **26** (2009) 224002, [0903.3246].

[101] J. McGreevy, *Holographic duality with a view toward many-body physics*, *Adv. High Energy Phys.* **2010** (2010) 723105, [0909.0518].

[102] J. Zaanen, Y.-W. Sun, Y. Liu and K. Schalm, *Holographic Duality in Condensed Matter Physics*, Cambridge Univ. Press, 2015, 10.1017/CBO9781139942492.

[103] S. A. Hartnoll, A. Lucas and S. Sachdev, *Holographic Quantum Matter*, MIT Press, 2018, [1612.07324].

[104] O. Aharony, *The NonAdS / nonCFT correspondence, or three different paths to QCD*, in *NATO Advanced Study Institute and EC Summer School on Progress in String, Field and Particle Theory*, pp. 3–24, 12, 2002, [hep-th/0212193].

[105] J. Erdmenger, N. Evans, I. Kirsch and E. Threlfall, *Mesons in Gauge/Gravity Duals - A Review*, *Eur. Phys. J. A* **35** (2008) 81–133, [0711.4467].

[106] J. Erlich, *How Well Does AdS/QCD Describe QCD?*, *Int. J. Mod. Phys. A* **25** (2010) 411–421, [0908.0312].

[107] J. Casalderrey-Solana, H. Liu, D. Mateos, K. Rajagopal and U. A. Wiedemann, *Gauge/String Duality, Hot QCD and Heavy Ion Collisions*, Cambridge University Press, 2014, 10.1017/CBO9781139136747, [1101.0618].

[108] J. D. Bekenstein, *Universal upper bound on the entropy-to-energy ratio for bounded systems*, *Phys. Rev. D* **23** (1981) 287–298.

[109] S. W. Hawking, *Black hole explosions*, *Nature* **248** (1974) 30–31.

[110] S. W. Hawking, *Particle Creation by Black Holes*, *Commun. Math. Phys.* **43** (1975) 199–220.

[111] G. 't Hooft, *Dimensional reduction in quantum gravity*, *Conf. Proc. C* **930308** (1993) 284–296, [gr-qc/9310026].

[112] J. M. Maldacena, *Eternal black holes in anti-de Sitter*, *JHEP* **04** (2003) 021, [hep-th/0106112].

[113] S. Ryu and T. Takayanagi, *Holographic derivation of entanglement entropy from AdS/CFT*, *Phys. Rev. Lett.* **96** (2006) 181602, [hep-th/0603001].

[114] S. Ryu and T. Takayanagi, *Aspects of Holographic Entanglement Entropy*, *JHEP* **08** (2006) 045, [hep-th/0605073].

[115] M. Van Raamsdonk, *Comments on quantum gravity and entanglement*, 0907.2939.

[116] M. Van Raamsdonk, *Building up spacetime with quantum entanglement*, *Gen. Rel. Grav.* **42** (2010) 2323–2329, [1005.3035].

[117] B. Swingle, *Entanglement renormalization and holography*, *Phys. Rev. D* **86** (2012) 065007, [0905.1317].

[118] J. Maldacena and L. Susskind, *Cool horizons for entangled black holes*, *Fortsch. Phys.* **61** (2013) 781–811, [1306.0533].

[119] A. Einstein and N. Rosen, *The Particle Problem in the General Theory of Relativity*, *Phys. Rev.* **48** (1935) 73–77.

[120] J. M. Maldacena and L. Maoz, *Wormholes in AdS*, *JHEP* **02** (2004) 053, [hep-th/0401024].

[121] A. S. Wightman and L. Gårding, *Fields as Operator-Valued Distributions in Relativistic Quantum Theory*, *Arkiv f. Fysik, Kungl. Svenska Vetenskapsak* **28** (1964) 129–189.

[122] K. Osterwalder and R. Schrader, *Axioms For Euclidean Green's Functions*, *Commun. Math. Phys.* **31** (1973) 83–112.

[123] R. Haag and D. Kastler, *An Algebraic approach to quantum field theory*, *J. Math. Phys.* **5** (1964) 848–861.

[124] J. von Neumann, *Zur Algebra der Funktionaloperationen und Theorie der normalen Operatoren*, *Math. Ann.* **102** (1930) 370–427.

[125] F. J. Murray and J. von Neumann, *On Rings of Operators*, *Ann. Math.* **37** (1936) 116–229.

[126] F. J. Murray and J. von Neumann, *On Rings of Operators. II*, *Trans. Am. Math. Soc.* **41** (1937) 208–248.

[127] J. von Neumann, *On infinite direct products*, *Comp. Math.* **6** (1939) 1–77.

[128] J. von Neumann, *On Rings of Operators. III*, *Ann. Math.* **41** (1940) 94–161.

[129] J. von Neumann, *On Some Algebraical Properties of Operator Rings*, *Ann. Math.* **44** (1943) 709–715.

[130] F. J. Murray and J. von Neumann, *On Rings of Operators. IV*, *Ann. Math.* **44** (1943) 716–808.

[131] J. von Neumann, *On Rings of Operators. Reduction Theory*, *Ann. Math.* **50** (1949) 401–485.

[132] S. Leutheusser and H. Liu, *Causal connectability between quantum systems and the black hole interior in holographic duality*, *Phys. Rev. D* **108** (2023) 086019, [2110.05497].

[133] S. Leutheusser and H. Liu, *Emergent times in holographic duality*, *Phys. Rev. D* **108** (2023) 086020, [2112.12156].

[134] E. Witten, *Gravity and the crossed product*, *JHEP* **10** (2022) 008, [2112.12828].

[135] V. Chandrasekaran, G. Penington and E. Witten, *Large N algebras and generalized entropy*, *JHEP* **04** (9, 2023) 009, [2209.10454].

[136] E. Gesteau, *Large N von Neumann algebras and the renormalization of Newton's constant*, 2302.01938.

[137] K. Jensen, J. Sorce and A. Speranza, *Generalized entropy for general subregions in quantum gravity*, 2306.01837.

[138] J. Kudler-Flam, S. Leutheusser and G. Satishchandran, *Generalized Black Hole Entropy is von Neumann Entropy*, 2309.15897.

[139] G. Penington and E. Witten, *Algebras and States in JT Gravity*, 2301.07257.

[140] D. K. Kolchmeyer, *von Neumann algebras in JT gravity*, *JHEP* **06** (2023) 067, [2303.04701].

[141] L. Susskind, *Dear Qubitzers, GR=QM*, 1708.03040.

[142] T. Faulkner, M. Guica, T. Hartman, R. C. Myers and M. Van Raamsdonk, *Gravitation from Entanglement in Holographic CFTs*, *JHEP* **03** (2014) 051, [1312.7856].

[143] T. Jacobson, *Entanglement Equilibrium and the Einstein Equation*, *Phys. Rev. Lett.* **116** (2016) 201101, [1505.04753].

[144] N. Callebaut and H. Verlinde, *Entanglement Dynamics in 2D CFT with Boundary: Entropic origin of JT gravity and Schwarzian QM*, *JHEP* **05** (2019) 045, [1808.05583].

[145] C. Barcelo, S. Liberati and M. Visser, *Analogue gravity*, *Living Rev. Rel.* **8** (2005) 12, [gr-qc/0505065].

[146] A. R. Brown, H. Gharibyan, S. Leichenauer, H. W. Lin, S. Nezami, G. Salton et al., *Quantum Gravity in the Lab. I. Teleportation by Size and Traversable Wormholes*, *PRX Quantum* **4** (2023) 010320, [1911.06314].

[147] S. Nezami, H. W. Lin, A. R. Brown, H. Gharibyan, S. Leichenauer, G. Salton et al., *Quantum Gravity in the Lab. II. Teleportation by Size and Traversable Wormholes*, *PRX Quantum* **4** (2023) 010321, [2102.01064].

[148] J. Maldacena, *A simple quantum system that describes a black hole*, 2303.11534.

[149] A. Addazi et al., *Quantum gravity phenomenology at the dawn of the multi-messenger era—A review*, *Prog. Part. Nucl. Phys.* **125** (2022) 103948, [2111.05659].

[150] LIGO Scientific, Virgo collaboration, B. P. Abbott et al., *Observation of Gravitational Waves from a Binary Black Hole Merger*, *Phys. Rev. Lett.* **116** (2016) 061102, [1602.03837].

[151] M. H. Lynch, E. Cohen, Y. Hadad and I. Kaminer, *Experimental observation of acceleration-induced thermality*, *Phys. Rev. D* **104** (2021) 025015, [1903.00043].

[152] Event Horizon Telescope collaboration, K. Akiyama et al., *First M87 Event Horizon Telescope Results. I. The Shadow of the Supermassive Black Hole*, *Astrophys. J. Lett.* **875** (2019) L1, [1906.11238].

[153] Event Horizon Telescope collaboration, K. Akiyama et al., *First Sagittarius A* Event Horizon Telescope Results. I. The Shadow of the Supermassive Black Hole in the Center of the Milky Way*, *Astrophys. J. Lett.* **930** (2022) L12.

[154] NANOGrav collaboration, G. Agazie et al., *The NANOGrav 15 yr Data Set: Observations and Timing of 68 Millisecond Pulsars*, *Astrophys. J. Lett.* **951** (2023) L9, [2306.16217].

[155] C. Vafa, *Geometric physics*, in *International Congress of Mathematicians*, 8, 1998, [hep-th/9810149].

[156] T. Ando, Y. Matsumoto and Y. Uemura, *Theory of Hall Effect in a Two-Dimensional Electron System*, *J. Phys. Soc. Jap.* **39** (1975) 279–288.

[157] D. J. Thouless, M. Kohmoto, M. P. Nightingale and M. den Nijs, *Quantized Hall Conductance in a Two-Dimensional Periodic Potential*, *Phys. Rev. Lett.* **49** (1982) 405–408.

[158] K. v. Klitzing, G. Dorda and M. Pepper, *New Method for High-Accuracy Determination of the Fine-Structure Constant Based on Quantized Hall Resistance*, *Phys. Rev. Lett.* **45** (1980) 494–497.

[159] M. B. Hastings and S. Michalakis, *Quantization of Hall Conductance for Interacting Electrons on a Torus*, *Commun. Math. Phys.* **334** (2015) 433–471, [1306.1258].

[160] A. Kitaev, *Periodic table for topological insulators and superconductors*, *AIP Conf. Proc.* **1134** (2009) 22–30, [0901.2686].

[161] A. A. Belavin, A. M. Polyakov, A. S. Schwartz and Y. S. Tyupkin, *Pseudoparticle Solutions of the Yang-Mills Equations*, *Phys. Lett. B* **59** (1975) 85–87.

[162] T. Schäfer and E. V. Shuryak, *Instantons in QCD*, *Rev. Mod. Phys.* **70** (1998) 323–426, [hep-ph/9610451].

[163] M. V. Berry, *Quantal phase factors accompanying adiabatic changes*, *Proc. Roy. Soc. Lond. A* **392** (1984) 45–57.

[164] B. Simon, *Holonomy, the quantum adiabatic theorem, and Berry's phase*, *Phys. Rev. Lett.* **51** (1983) 2167–2170.

[165] H. Verlinde, *Wormholes in Quantum Mechanics*, 2105.02129.

[166] M. M. Sinolecka, K. Życzkowski and M. Kus, *Manifolds of equal entanglement for composite quantum systems*, *Acta Phys. Pol. B* **33** (2002) 2081, [quant-ph/0110082].

[167] B. Oblak, *Berry Phases on Virasoro Orbits*, *JHEP* **10** (2017) 114, [1703.06142].

[168] B. Czech, L. Lamprou, S. Mccandlish and J. Sully, *Modular Berry Connection for Entangled Subregions in AdS/CFT*, *Phys. Rev. Lett.* **120** (2018) 091601, [1712.07123].

[169] B. Czech, L. Lamprou and L. Susskind, *Entanglement Holonomies*, 1807.04276.

[170] B. Czech, J. De Boer, D. Ge and L. Lamprou, *A modular sewing kit for entanglement wedges*, *JHEP* **11** (2019) 094, [1903.04493].

[171] V. Chandrasekaran, R. Longo, G. Penington and E. Witten, *An algebra of observables for de Sitter space*, *JHEP* **02** (2023) 082, [2206.10780].

[172] E. Witten, *A Background Independent Algebra in Quantum Gravity*, 2308.03663.

[173] W. Zurek, *Einselection and decoherence from an information theory perspective*, *Ann. Phys.* **512** (2000) 855–864, [quant-ph/0011039].

[174] H. Ollivier and W. H. Zurek, *Quantum discord: A measure of the quantumness of correlations*, *Phys. Rev. Lett.* **88** (2001) 017901, [quant-ph/0105072].

[175] L. Henderson and V. Vedral, *Classical, quantum and total correlations*, *J. Phys. A: Mathematical and General* **34** (2001) 6899, [quant-ph/0105028].

[176] S. Kanno, J. P. Shock and J. Soda, *Quantum discord in de Sitter space*, *Phys. Rev. D* **94** (2016) 125014, [1608.02853].

[177] J. Martin and V. Vennin, *Real-space entanglement of quantum fields*, *Phys. Rev. D* **104** (2021) 085012, [2106.14575].

[178] J. Martin and V. Vennin, *Real-space entanglement in the Cosmic Microwave Background*, *JCAP* **10** (2021) 036, [2106.15100].

[179] T. Colas, J. Grain and V. Vennin, *Quantum recoherence in the early universe*, *Eur. Phys. Lett.* **142** (2023) 69002, [2212.09486].

[180] Y. Huang, *Computing quantum discord is NP-complete*, *New J. Phys.* **16** (2014) 033027, [1305.5941].

[181] B. Dakić, V. Vedral and Č. Brukner, *Necessary and Sufficient Condition for Nonzero Quantum Discord*, *Phys. Rev. Lett.* **105** (2010) 190502, [1004.0190].

[182] H. Verlinde, *ER = EPR revisited: On the Entropy of an Einstein-Rosen Bridge*, 2003.13117.

[183] F. S. Nogueira, S. Banerjee, M. Dorband, R. Meyer, J. v. d. Brink and J. Erdmenger, *Geometric phases distinguish entangled states in wormhole quantum mechanics*, *Phys. Rev. D* **105** (2022) L081903, [2109.06190].

[184] S. Banerjee, M. Dorband, J. Erdmenger and A.-L. Weigel, *Geometric Phases Characterise Operator Algebras and Missing Information*, *JHEP* **10** (2023) 026, [2306.00055].

[185] S. Banerjee, M. Dorband, J. Erdmenger, R. Meyer and A.-L. Weigel, *Berry phases, wormholes and factorization in AdS/CFT*, *JHEP* **08** (2022) 162, [2202.11717].

[186] S. Banerjee, P. Basteiro, R. N. Das and M. Dorband, *Geometric Quantum Discord Signals Non-Factorization*, *JHEP* **08** (2023) 104, [2305.04952].

[187] H. Reeh and S. Schlieder, *Bemerkungen zur Unitäräquivalenz von Lorentzinvarianten Feldern*, *Nuovo Cim.* **22** (1961) 1051–1068.

[188] M. A. Nielsen and I. L. Chuang, *Quantum Computation and Quantum Information: 10th Anniversary Edition*, Cambridge University Press, 2010, 10.1017/CBO9780511976667.

[189] J. von Neumann, *Mathematische Grundlagen der Quantenmechanik*, Springer, Berlin, Heidelberg, 2 ed., 1995, 10.1007/978-3-642-61409-5.

[190] I. Bengtsson and K. Życzkowski, *Geometry of quantum states: an introduction to quantum entanglement*, Cambridge university press, 2006, 10.1017/CBO9780511535048.

[191] T. Nishioka, *Entanglement entropy: holography and renormalization group*, *Rev. Mod. Phys.* **90** (2018) 035007, [1801.10352].

[192] E. Witten, *APS Medal for Exceptional Achievement in Research: Invited article on entanglement properties of quantum field theory*, *Rev. Mod. Phys.* **90** (2018) 045003, [1803.04993].

[193] L. Gurvits, *Classical Deterministic Complexity of Edmonds' Problem and Quantum Entanglement*, in *Proceedings of the thirty-fifth annual ACM symposium on Theory of computing*, STOC '03, (New York, NY, USA), p. 10–19, Association for Computing Machinery, 2003, 10.1145/780542.780545, [quant-ph/0303055].

[194] A. Peres, *Separability Criterion for Density Matrices*, *Phys. Rev. Lett.* **77** (1996) 1413–1415, [quant-ph/9604005].

[195] M. Horodecki, P. Horodecki and R. Horodecki, *Separability of mixed states: necessary and sufficient conditions*, *Phys. Lett. A* **223** (1996) 1–8, [quant-ph/9605038].

[196] H. Araki and E. H. Lieb, *Entropy inequalities*, *Commun. Math. Phys.* **18** (1970) 160–170.

[197] P. A. M. Dirac, *Note on Exchange Phenomena in the Thomas Atom*, *Math. Proc. Cam. Phil. Soc.* **26** (1930) 376–385.

[198] L. P. Hughston, R. Jozsa and W. K. Wootters, *A complete classification of quantum ensembles having a given density matrix*, *Phys. Lett. A* **183** (1993) 14–18.

[199] N. Gisin, *Stochastic quantum dynamics and relativity*, *Helv. Phys. Acta* **62** (1989) 363–371.

[200] N. Hadjisavvas, *Properties of mixtures of non-orthogonal states*, *Lett. Math. Phys.* **5** (1981) 327–332.

[201] E. T. Jaynes, *Information Theory and Statistical Mechanics. II*, *Phys. Rev.* **108** (1957) 171–190.

[202] N. D. Mermin, *What Do These Correlations Know about Reality? Nonlocality and the Absurd*, *Found. Phys.* **29** (1999) 571–587, [quant-ph/9807055].

[203] J. Watrous, *The Theory of Quantum Information*, Cambridge University Press, 2018, 10.1017/9781316848142.

[204] K. A. Kirkpatrick, *The Schrödinger-HJW Theorem*, *Found. of Phys. Lett.* **19** (2006) 95–102, [quant-ph/0305068].

[205] R. Clausius, *Ueber die bewegende Kraft der Wärme und die Gesetze, welche sich daraus für die Wärmelehre selbst ableiten lassen*, *Ann. Phys.* **155** (1850) 368–397, [https://onlinelibrary.wiley.com/doi/pdf/10.1002/andp.18501550306].

[206] W. Gibbs, *A Method if Geometrical Representation of the Thermodynamic Properties of Substances by Means of Surfaces*, *Trans. Conn. Acad.* **2** (1873) 382–404.

[207] L. Boltzmann, *Lectures on Gas Theory*, 1896&1898.

[208] J. v. Neumann, *Wahrscheinlichkeitstheoretischer Aufbau der Quantenmechanik*, *Nach. Ges. Wiss. Gött., Mathematisch-Physikalische Klasse* **1927** (1927) 245–272.

[209] L. Landau, *The damping problem in wave mechanics*, *Z. Phys* **45** (1927) 430–441.

[210] D. D. Blanco, H. Casini, L.-Y. Hung and R. C. Myers, *Relative Entropy and Holography*, *JHEP* **08** (2013) 060, [1305.3182].

[211] S. Popescu and D. Rohrlich, *Thermodynamics and the measure of entanglement*, *Phys. Rev. A* **56** (1997) R3319–R3321, [quant-ph/9610044].

[212] M. Horodecki, P. Horodecki and R. Horodecki, *Limits for Entanglement Measures*, *Phys. Rev. Lett.* **84** (2000) 2014–2017, [quant-ph/9908065].

[213] M. Horodecki, J. Oppenheim and R. Horodecki, *Are the Laws of Entanglement Theory Thermodynamical?*, *Phys. Rev. Lett.* **89** (2002) 240403, [quant-ph/0207177].

[214] V. Vedral and E. Kashefi, *Uniqueness of the Entanglement Measure for Bipartite Pure States and Thermodynamics*, *Phys. Rev. Lett.* **89** (2002) 037903, [quant-ph/0112137].

[215] C. H. Bennett, H. J. Bernstein, S. Popescu and B. Schumacher, *Concentrating partial entanglement by local operations*, *Phys. Rev. A* **53** (1996) 2046–2052, [quant-ph/9511030].

[216] K. Audenaert, M. B. Plenio and J. Eisert, *Entanglement Cost under Positive-Partial-Transpose-Preserving Operations*, *Phys. Rev. Lett.* **90** (2003) 027901, [quant-ph/0207146].

[217] F. G. S. L. Brandão and M. B. Plenio, *Entanglement theory and the second law of thermodynamics*, *Nature Phys.* **4** (2008) 873–877, [0810.2319].

[218] F. G. S. L. Brandão and M. B. Plenio, *A Reversible Theory of Entanglement and its Relation to the Second Law*, *Commun. Math. Phys.* **295** (2010) 829–851, [0710.5827].

[219] M. Berta, F. G. S. L. Brandão, G. Gour, L. Lami, M. B. Plenio, B. Regula et al., *On a gap in the proof of the generalised quantum Stein's lemma and its consequences for the reversibility of quantum resources*, *Quantum* **7** (2023) 1103, [2205.02813].

[220] L. Lami and B. Regula, *No second law of entanglement manipulation after all*, *Nature Phys.* **19** (2023) 184–189, [2111.02438].

[221] P. Calabrese and J. L. Cardy, *Entanglement entropy and quantum field theory*, *J. Stat. Mech.* **0406** (2004) P06002, [hep-th/0405152].

[222] J. J. Bisognano and E. H. Wichmann, *On the Duality Condition for Quantum Fields*, *J. Math. Phys.* **17** (1976) 303–321.

[223] W. G. Unruh, *Notes on black hole evaporation*, *Phys. Rev. D* **14** (1976) 870.

[224] W. Rindler, *Kruskal Space and the Uniformly Accelerated Frame*, *Am. J. Phys.* **34** (1966) 1174.

[225] D. Harlow, *Jerusalem Lectures on Black Holes and Quantum Information*, *Rev. Mod. Phys.* **88** (2016) 015002, [1409.1231].

[226] C. Callan and F. Wilczek, *On geometric entropy*, *Phys. Lett. B* **333** (1994) 55–61, [hep-th/9401072].

[227] M. Headrick, *Lectures on entanglement entropy in field theory and holography*, 1907.08126.

[228] G. L. Sewell, *Quantum fields on manifolds: PCT and gravitationally induced thermal states*, *Ann. Phys.* **141** (1982) 201–224.

[229] H. Casini, M. Huerta and R. C. Myers, *Towards a derivation of holographic entanglement entropy*, *JHEP* **05** (2011) 036, [1102.0440].

[230] J. Cardy and E. Tonni, *Entanglement hamiltonians in two-dimensional conformal field theory*, *J. Stat. Mech.* **1612** (2016) 123103, [1608.01283].

[231] L. Bombelli, R. K. Koul, J. Lee and R. D. Sorkin, *A Quantum Source of Entropy for Black Holes*, *Phys. Rev. D* **34** (1986) 373–383.

[232] M. Srednicki, *Entropy and area*, *Phys. Rev. Lett.* **71** (1993) 666–669, [hep-th/9303048].

[233] D. M. Capper and M. J. Duff, *Trace anomalies in dimensional regularization*, *Nuovo Cim. A* **23** (1974) 173–183.

[234] C. Holzhey, F. Larsen and F. Wilczek, *Geometric and renormalized entropy in conformal field theory*, *Nucl. Phys. B* **424** (1994) 443–467, [hep-th/9403108].

[235] A. Rényi, *On measures of information and entropy*, *Proceedings of the fourth Berkeley Symposium on Mathematics, Statistics and Probability 1960* **1** (1961) 547–561.

[236] M. Van Raamsdonk, *Lectures on Gravity and Entanglement*, in *Theoretical Advanced Study Institute in Elementary Particle Physics: New Frontiers in Fields and Strings*, pp. 297–351, 2017, 10.1142/9789813149441_0005, [1609.00026].

[237] S. F. Edwards and P. W. Anderson, *Theory of spin glasses*, *J. Phys. F: Metal Physics* **5** (1975) 965.

[238] M. Rangamani and T. Takayanagi, *Holographic Entanglement Entropy*, vol. 931, Springer, 2017, 10.1007/978-3-319-52573-0, [1609.01287].

[239] M. B. Plenio and S. Virmani, *An introduction to entanglement measures*, *Quantum Inf. Comput.* **7** (2007) 1–51, [quant-ph/0504163].

[240] L. Amico, R. Fazio, A. Osterloh and V. Vedral, *Entanglement in many-body systems*, *Rev. Mod. Phys.* **80** (2008) 517–576, [quant-ph/0703044].

[241] J. Eisert, M. Cramer and M. B. Plenio, *Colloquium: Area laws for the entanglement entropy*, *Rev. Mod. Phys.* **82** (2010) 277–306, [0808.3773].

[242] S. A. Hill and W. K. Wootters, *Entanglement of a Pair of Quantum Bits*, *Phys. Rev. Lett.* **78** (1997) 5022–5025, [quant-ph/9703041].

[243] W. K. Wootters, *Entanglement of Formation of an Arbitrary State of Two Qubits*, *Phys. Rev. Lett.* **80** (1998) 2245–2248, [quant-ph/9709029].

[244] C. H. Bennett, D. P. DiVincenzo, J. A. Smolin and W. K. Wootters, *Mixed-state entanglement and quantum error correction*, *Phys. Rev. A* **54** (1996) 3824–3851, [quant-ph/9604024].

[245] V. Vedral, M. B. Plenio, M. A. Rippin and P. L. Knight, *Quantifying Entanglement*, *Phys. Rev. Lett.* **78** (1997) 2275–2279, [quant-ph/9702027].

[246] V. Vedral, *The role of relative entropy in quantum information theory*, *Rev. Mod. Phys.* **74** (2002) 197–234, [quant-ph/0102094].

[247] G. Vidal and R. F. Werner, *Computable measure of entanglement*, *Phys. Rev. A* **65** (2002) 032314, [quant-ph/0102117].

[248] P. Calabrese, J. Cardy and E. Tonni, *Entanglement negativity in extended systems: A field theoretical approach*, *J. Stat. Mech.* **1302** (2013) P02008, [1210.5359].

[249] M. B. Plenio, *Logarithmic Negativity: A Full Entanglement Monotone That is not Convex*, *Phys. Rev. Lett.* **95** (2005) 090503, [quant-ph/0505071].

[250] P. Giorda and M. G. A. Paris, *Gaussian Quantum Discord*, *Phys. Rev. Lett.* **105** (2010) 020503, [1003.3207].

[251] M. Poxleitner and H. Hinrichsen, *Gaussian continuous-variable isotropic state*, *Phys. Rev. A* **104** (2021) 032423, [2105.03141].

[252] J. Dajka, M. Mierzejewski, J. Łuczka, R. Blattmann and P. Hänggi, *Negativity and quantum discord in Davies environments*, *J. Phys. A: Mathematical and Theoretical* **45** (2012) 485306, [1209.1536].

[253] R. F. Werner, *Quantum states with Einstein-Podolsky-Rosen correlations admitting a hidden-variable model*, *Phys. Rev. A* **40** (1989) 4277–4281.

[254] C. E. Shannon, *A mathematical theory of communication*, *Bell Syst. Tech. J.* **27** (1948) 379–423.

[255] N. J. Cerf and C. Adami, *Negative Entropy and Information in Quantum Mechanics*, *Phys. Rev. Lett.* **79** (1997) 5194–5197, [quant-ph/9512022].

[256] M. Horodecki, J. Oppenheim and A. Winter, *Partial quantum information*, *Nature* **436** (2005) 673–676, [quant-ph/0505062].

[257] M. Horodecki, J. Oppenheim and A. Winter, *Quantum State Merging and Negative Information*, *Commun. Math. Phys.* **269** (2007) 107–136, [quant-ph/0512247].

[258] N. Li, S. Luo and Z. Zhang, *Quantumness of bipartite states in terms of conditional entropies*, *J. Phys. A: Mathematical and Theoretical* **40** (2007) 11361.

[259] F. Liu, G.-J. Tian, G.-Y. Wen and F. Gao, *General bounds for quantum discord and discord distance*, *Quantum Inf. Proc.* **14** (2015) 1333–1341, [1411.3772].

[260] C. C. Rulli and M. S. Sarandy, *Global quantum discord in multipartite systems*, *Phys. Rev. A* **84** (2011) 042109, [1105.2548].

[261] A. Bera, T. Das, D. Sadhukhan, S. S. Roy, A. Sen(De) and U. Sen, *Quantum discord and its allies: a review of recent progress*, *Rep. Prog. Phys.* **81** (2017) 024001, [1703.10542].

[262] R. Abraham and J. E. Marsden, *Foundations of Mechanics*, AMS Chelsea Publishing, AMS Chelsea Pub./American Mathematical Society, 1967, 10.1090/chel/364.

[263] J.-M. Souriau, *Quantification géométrique*, *Commun. Math. Phys.* **1** (1966) 374–398.

[264] J.-M. Souriau, *Quantification géométrique. Applications*, *Annales de l'institut Henri Poincaré. Section A, Physique Théorique* **6** (1967) 311–341.

[265] B. Kostant, *Quantization and unitary representations*, in *Lectures in Modern Analysis and Applications III* (C. T. Taam, ed.), (Berlin, Heidelberg), pp. 87–280, Springer Berlin Heidelberg, 1970, 10.1007/BFb0079068.

[266] A. Carosso, *Geometric Quantization*, 1801.02307.

[267] H. Weyl, *The Theory of Groups and Quantum Mechanics*, Methuen and Company Limited, 1937.

[268] S. Kobayashi and K. Nomizu, *Foundations of Differential Geometry, Volume 2*, Foundations of Differential Geometry *by* Shoshichi Kobayashi and Katsumi Nomizu, Wiley, 1963.

[269] M. Nakahara, *Geometry, Topology and Physics, Second Edition*, Graduate student series in physics, Taylor & Francis, 2003.

[270] P. R. Chernoff and J. E. Marsden, *Properties of Infinite Dimensional Hamiltonian Systems*, Springer Berlin Heidelberg, Berlin, Heidelberg, 1974, 10.1007/BFb0073665.

[271] J. P. Provost and G. Vallee, *Riemannian Structure on Manifolds of Quantum States*, *Commun. Math. Phys.* **76** (1980) 289–301.

[272] B. G. Giraud and D. J. Rowe, *Curvature of the Slater determinant manifold*, *J. Phys. Lett.* **40** (1979) 177–180.

[273] G. Fubini, *Sulle metriche definite da una forme Hermitiana*, *Atti del Reale Istituto Veneto di Scienze, Lettere ed Arti* **63** (1904) 502–513.

[274] E. Study, *Kürzeste Wege im komplexen Gebiet*, *Math. Ann.* **60** (1905) 321–378.

[275] H. Heydari, *Geometric formulation of quantum mechanics*, 1503.00238.

[276] J. Anandan and Y. Aharonov, *Geometry of quantum evolution*, *Phys. Rev. Lett.* **65** (1990) 1697–1700.

[277] G. Gibbons, *Typical states and density matrices*, *J. Geom. Phys.* **8** (1992) 147–162.

[278] L. P. Hughston, *Geometric Aspects of Quantum Mechanics*, in *Twistor Theory* (S. A. Huggett, ed.), pp. 59–79, Marcel Dekker, 1995.

[279] R. Cirelli, A. Manià and L. Pizzocchero, *Quantum mechanics as an infinite-dimensional Hamiltonian system with uncertainty structure: Part I*, *J. Math. Phys.* **31** (1990) 2891–2897.

[280] R. Cirelli, A. Manià and L. Pizzocchero, *Quantum mechanics as an infinite-dimensional Hamiltonian system with uncertainty structure: Part II*, *J. Math. Phys.* **31** (1990) 2898–2903.

[281] S. Hassani, *Mathematical Physics: A Modern Introduction to Its Foundations, Second Edition*, Springer Science & Business Media, 2013, 10.1007/978-3-319-01195-0.

[282] S.-S. Chern, *On the Curvatura Integra in a Riemannian Manifold*, *Ann. Math.* **46** (1945) 674–684.

[283] H. Hopf, *Über die Abbildungen der dreidimensionalen Sphäre auf die Kugelfläche*, *Math. Ann.* **104** (1931) 637–665.

[284] H. Poincaré, *Sur les courbes définies par les équations différentielles (III)*, *Journal de Mathématiques Pures et Appliquées* **1** (1885) 167–244.

[285] L. E. J. Brouwer, *Über Abbildung von Mannigfaltigkeiten*, *Math. Ann.* **71** (1912) 97–115.

[286] R. W. Batterman, *Falling cats, parallel parking, and polarized light*, *Stud. Hist. Phil. Science Part B: Studies in History and Philosophy of Modern Physics* **34** (2003) 527–557.

[287] H. Lyre, *Berry phase and quantum structure*, *Stud. Hist. Phil. Science Part B: Studies in History and Philosophy of Modern Physics* **48** (2014) 45–51, [1408.6867].

[288] D. Jonathan and M. B. Plenio, *Entanglement-Assisted Local Manipulation of Pure Quantum States*, *Phys. Rev. Lett.* **83** (1999) 3566–3569, [quant-ph/9905071].

[289] M. Kuś and K. Życzkowski, *Geometry of entangled states*, *Phys. Rev. A* **63** (2001) 032307, [quant-ph/0006068].

[290] D. C. Brody and L. P. Hughston, *Geometric quantum mechanics*, *J. Geom. Phys.* **38** (2001) 19–53, [quant-ph/9906086].

[291] R. Mosseri and R. Dandoloff, *Geometry of entangled states, Bloch spheres and Hopf fibrations*, *J. Phys. A: Mathematical and General* **34** (2001) 10243, [quant-ph/0108137].

[292] I. Bengtsson, J. Brännlund and K. Życzkowski, *CPn, or, Entanglement Illustrated*, *Int. J. Mod. Phys. A* **17** (2002) 4675–4695, [quant-ph/0108064].

[293] K. Życzkowski and W. Słomczyński, *The Monge metric on the sphere and geometry of quantum states*, *J. Phys. A: Mathematical and General* **34** (2001) 6689, [quant-ph/0008016].

[294] M. Adelman, J. V. Corbett and C. A. Hurst, *The geometry of state space*, *Found. Phys.* **23** (1993) 211–223.

[295] I. Bengtsson, *A Curious Geometrical Fact about Entanglement*, *AIP Conference Proceedings* **962** (2007) 34–38, [0707.3512].

[296] V. P. Maslov, *Perturbation theory and asymptotic methods*, *Moscow State Univ* **34** (1965) .

[297] G. Darboux, *Sur le problème de Pfaff*, *Bulletin des Sciences Mathématiques et Astronomiques* **2e série, 6** (1882) 5–292.

[298] A. Miyake, *Classification of multipartite entangled states by multidimensional determinants*, *Phys. Rev. A* **67** (2003) 012108, [quant-ph/0206111].

[299] D. Girolami and G. Adesso, *Interplay between computable measures of entanglement and other quantum correlations*, *Phys. Rev. A* **84** (2011) 052110, [1111.3643].

[300] S. Luo and S. Fu, *Geometric measure of quantum discord*, *Phys. Rev. A* **82** (2010) 034302.

[301] M. F. Atiyah, *Topological quantum field theory*, *Publications Mathématiques de l'IHÉS* **68** (1988) 175–186.

[302] G. B. Segal, *The Definition of Conformal Field Theory*, pp. 165–171, Springer Netherlands, Dordrecht, 1988, 10.1007/978-94-015-7809-7_9.

[303] U. Schreiber, *AQFT from n-Functorial QFT*, *Commun. Math. Phys.* **291** (2009) 357–401, [0806.1079].

[304] T. Johnson-Freyd, *Heisenberg-Picture Quantum Field Theory*, pp. 371–409, Springer International Publishing, Cham, 2021, 10.1007/978-3-030-78148-4_13.

[305] S. Bunk, J. MacManus and A. Schenkel, *Lorentzian bordisms in algebraic quantum field theory*, 2308.01026.

[306] G. C. Wick, A. S. Wightman and E. P. Wigner, *The intrinsic parity of elementary particles*, *Phys. Rev.* **88** (1952) 101–105.

[307] G. Emch, *Algebraic Methods in Statistical Mechanics and Quantum Field Theory*, Interscience monographs and texts in physics and astronomy, Wiley-Interscience, 1972.

[308] M. H. Stone, *Linear Transformations in Hilbert Space*, *Proc. Nat. Acad. Sci.* **16** (1930) 172–175.

[309] J. von Neumann, *Die Eindeutigkeit der Schrödingerschen Operatoren*, *Math. Ann.* **104** (1931) 570–578.

[310] J. von Neumann, *Über Einen Satz Von Herrn M. H. Stone*, *Ann. Math.* **33** (1932) 567–573.

[311] M. H. Stone, *On One-Parameter Unitary Groups in Hilbert Space*, *Ann. Math.* **33** (1932) 643–648.

[312] L. Gårding and A. Wightman, *Representations of the Anticommutation Relations*, *Proc. Nat. Acad. Sci.* **40** (1954) 617–621.

[313] R. F. Streater and A. S. Wightman, *PCT, Spin and Statistics, and All That*, Princeton University Press, 1989.

[314] R. Haag, *Local Quantum Physics: Fields, Particles, Algebras*, Springer Science & Business Media, 1992, 10.1007/978-3-642-97306-2.

[315] H. Araki, *Mathematical Theory of Quantum Fields*, International series of monographs on physics, Oxford University Press, 1999.

[316] S. V. Strătilă and L. Zsidó, *Lectures on von Neumann Algebras*, Cambridge IISc Series, Cambridge University Press, Cambridge, 2 ed., 2019, 10.1017/9781108654975.

[317] S. V. Strătilă, *Modular Theory in Operator Algebras*, Cambridge IISc Series, Cambridge University Press, Cambridge, 2 ed., 2020, 10.1017/9781108489607.

[318] H. Halvorson and M. Muger, *Algebraic Quantum Field Theory*, pp. 731–864, North-Holland, Amsterdam, 2007, 10.1016/B978-044451560-5/50011-7, [math-ph/0602036].

[319] C. J. Fewster and K. Rejzner, *Algebraic Quantum Field Theory – an introduction*, ch. 1, pp. 11–61, Birkhäuser Cham, 2020, 10.1007/978-3-030-38941-3, [1904.04051].

[320] E. Witten, *Why Does Quantum Field Theory In Curved Spacetime Make Sense? And What Happens To The Algebra of Observables In The Thermodynamic Limit?*, pp. 241–284, Springer International Publishing, Cham, 2022, 10.1007/978-3-031-17523-7_11, [2112.11614].

[321] J. Sorce, *Notes on the type classification of von Neumann algebras*, 2302.01958.

[322] I. Gelfand and M. Naimark, *On the imbedding of normed rings into the ring of operators in Hilbert spaces*, *Recueil Mathématique [Mat. Sbornik] N.S.* **12(54)** (1943) 192–217.

[323] I. E. Segal, *Irreducible Representations of Operator Algebras*, *Bull. Am. Math. Soc.* **53** (1947) 73–88.

[324] R. Haag, N. M. Hugenholtz and M. Winnink, *On the Equilibrium states in quantum statistical mechanics*, *Commun. Math. Phys.* **5** (1967) 215–236.

[325] R. T. Powers, *Representations of Uniformly Hyperfinite Algebras and Their Associated von Neumann Rings*, *Ann. Math.* **86** (1967) 138–171.

[326] H. Araki and E. J. Woods, *A Classification of Factors*, *Publ. Res. Inst. Math. Sci., Kyoto University. Ser. A* **4** (1968) 51–130.

[327] I. E. Segal, *A Note on the Concept of Entropy*, *Indiana Univ. Math. J.* **9** (1960) 623–629.

[328] A. Connes and E. Størmer, *Entropy for Automorphisms of II_1 von Neumann Algebras*, *Acta Math.* **134** (1975) 289–306.

[329] H. Araki, *Inequalities in Von Neumann Algebras*, *Les rencontres physiciens-mathématiciens de Strasbourg - RCP25* **22** (1975) 1–25.

[330] H. Araki, *Relative Entropy of States of Von Neumann Algebras*, *Publ. Res. Inst. Math. Sci. Kyoto* **11** (1976) 809–833.

[331] H. Araki, *Type of von Neumann Algebra Associated with Free Field*, *Prog. Theor. Phys.* **32** (1964) 956–965.

[332] R. Longo, *Algebraic and modular structure of von Neumann algebras of Physics*, in *Operator algebras and applications, Part 2 (Kingston, Ont., 1980)*, vol. 38 of *Proc. Symp. Pure Math.*, pp. 551–566, Amer. Math. Soc., Providence, R.I., 1982, 10.1090/pspum/038.2/679537.

[333] M. Tomita, *On canonical forms of von Neumann algebras*, *Fifth Functional Analysis Sympos (Tôhoku Univ., Sendai, 1967), Math. Inst., Tohoku Univ., Sendai* (1967) 101–102.

[334] M. Takesaki, *Tomita's Theory of Modular Hilbert Algebras and its Applications*, Lecture Notes in Mathematics, Springer-Verlag, 1970, 10.1007/bfb0065832.

[335] A. Connes and C. Rovelli, *Von Neumann algebra automorphisms and time thermodynamics relation in general covariant quantum theories*, *Class. Quant. Grav.* **11** (1994) 2899–2918, [gr-qc/9406019].

[336] K. Fredenhagen, *On the Modular Structure of Local Algebras of Observables*, *Commun. Math. Phys.* **97** (1985) 79–89.

[337] U. Haagerup, *Conne's bicentralizer problem and uniqueness of the injective factor of type III1*, *Acta Math.* **158** (1987) 95–148.

[338] D. Buchholz, K. Fredenhagen and C. D'Antoni, *The Universal Structure of Local Algebras*, *Commun. Math. Phys.* **111** (1987) 123.

[339] R. Haag and B. Schroer, *Postulates of Quantum Field Theory*, *J. Math. Phys.* **3** (1962) 248–256.

[340] A. Strohmaier, R. Verch and M. Wollenberg, *Microlocal analysis of quantum fields on curved space-times: Analytic wavefront sets and Reeh-Schlieder theorems*, *J. Math. Phys.* **43** (2002) 5514–5530, [math-ph/0202003].

[341] R. Brunetti, K. Fredenhagen and R. Verch, *The Generally Covariant Locality Principle – A New Paradigm for Local Quantum Field Theory*, *Commun. Math. Phys.* **237** (2003) 31–68, [math-ph/0112041].

[342] R. M. Wald, *The History and Present Status of Quantum Field Theory in Curved Spacetime*, vol. 12, pp. 317–331, Birkhäuser Boston, 2012, 10.1007/978-0-8176-4940-1_16, [gr-qc/0608018].

[343] R. Brunetti and K. Fredenhagen, *Quantum Field Theory on Curved Backgrounds*, pp. 129–155, Springer Berlin Heidelberg, Berlin, Heidelberg, 2009, 10.1007/978-3-642-02780-2_5, [0901.2063].

[344] R. M. Wald, *The Formulation of Quantum Field Theory in Curved Spacetime*, vol. 14, pp. 439–449, Birkhäuser, New York, NY, 2018, 10.1007/978-1-4939-7708-6_15, [0907.0416].

[345] S. Hollands and R. M. Wald, *Axiomatic Quantum Field Theory in Curved Spacetime*, *Commun. Math. Phys.* **293** (2010) 85–125, [0803.2003].

[346] K. Fredenhagen and K. Rejzner, *Quantum field theory on curved spacetimes: Axiomatic framework and examples*, *J. Math. Phys.* **57** (2016) 031101, [1412.5125].

[347] C. J. Fewster and R. Verch, *Algebraic Quantum Field Theory in Curved Spacetimes*, pp. 125–189, Springer International Publishing, Cham, 2015, 10.1007/978-3-319-21353-8_4, [1504.00586].

[348] K. Sanders, *On the Reeh-Schlieder Property in Curved Spacetime*, *Commun. Math. Phys.* **288** (2009) 271–285, [0801.4676].

[349] C. Gérard and M. Wrochna, *Analytic Hadamard States, Calderón Projectors and Wick Rotation Near Analytic Cauchy Surfaces*, *Commun. Math. Phys.* **366** (2019) 29–65, [1706.08942].

[350] I. A. Morrison, *Boundary-to-bulk maps for AdS causal wedges and the Reeh-Schlieder property in holography*, *JHEP* **05** (2014) 53, [1403.3426].

[351] S. Banerjee, J.-W. Bryan, K. Papadodimas and S. Raju, *A toy model of black hole complementarity*, *JHEP* **05** (2016) 4, [1603.02812].

[352] C. Montonen and D. I. Olive, *Magnetic Monopoles as Gauge Particles?*, *Phys. Lett. B* **72** (1977) 117–120.

[353] N. Seiberg, *Electric - magnetic duality in supersymmetric nonAbelian gauge theories*, *Nucl. Phys. B* **435** (1995) 129–146, [hep-th/9411149].

[354] S. R. Coleman, *The Quantum Sine-Gordon Equation as the Massive Thirring Model*, *Phys. Rev. D* **11** (1975) 2088.

[355] E. Witten, *Nonabelian Bosonization in Two-Dimensions*, *Commun. Math. Phys.* **92** (1984) 455–472.

[356] J. H. Schwarz and A. Sen, *Duality symmetric actions*, *Nucl. Phys. B* **411** (1994) 35–63, [hep-th/9304154].

[357] J. H. Schwarz and A. Sen, *Duality symmetries of 4-D heterotic strings*, *Phys. Lett. B* **312** (1993) 105–114, [hep-th/9305185].

[358] A. Sen, *Dyon - monopole bound states, selfdual harmonic forms on the multi - monopole moduli space, and SL(2,Z) invariance in string theory*, *Phys. Lett. B* **329** (1994) 217–221, [hep-th/9402032].

[359] C. M. Hull and P. K. Townsend, *Unity of superstring dualities*, *Nucl. Phys. B* **438** (1995) 109–137, [hep-th/9410167].

[360] J. H. Schwarz, *An SL(2,Z) multiplet of type IIB superstrings*, *Phys. Lett. B* **360** (1995) 13–18, [hep-th/9508143].

[361] T. H. Buscher, *A Symmetry of the String Background Field Equations*, *Phys. Lett. B* **194** (1987) 59–62.

[362] T. H. Buscher, *Path Integral Derivation of Quantum Duality in Nonlinear Sigma Models*, *Phys. Lett. B* **201** (1988) 466–472.

[363] L. Susskind, *The World as a hologram*, *J. Math. Phys.* **36** (1995) 6377–6396, [hep-th/9409089].

[364] L. Susskind and E. Witten, *The Holographic Bound in Anti-de Sitter Space*, hep-th/9805114.

[365] J. D. Brown and M. Henneaux, *Central Charges in the Canonical Realization of Asymptotic Symmetries: An Example from Three-Dimensional Gravity*, *Commun. Math. Phys.* **104** (1986) 207–226.

[366] O. Aharony, S. S. Gubser, J. M. Maldacena, H. Ooguri and Y. Oz, *Large N field theories, string theory and gravity*, *Phys. Rept.* **323** (2000) 183–386, [hep-th/9905111].

[367] J. M. Maldacena, *TASI 2003 lectures on AdS / CFT*, in *Theoretical Advanced Study Institute in Elementary Particle Physics (TASI 2003): Recent Trends in String Theory*, pp. 155–203, 9, 2003, [hep-th/0309246].

[368] J. McGreevy, *TASI 2015 Lectures on Quantum Matter (with a View Toward Holographic Duality)*, in *Theoretical Advanced Study Institute in Elementary Particle Physics: New Frontiers in Fields and Strings*, pp. 215–296, 2017, 10.1142/9789813149441_0004, [1606.08953].

[369] M. Ammon and J. Erdmenger, *Gauge/gravity duality: Foundations and applications*, Cambridge University Press, Cambridge, 2015, 10.1017/CBO9780511846373.

[370] R. Bousso, *The holographic principle*, *Rev. Mod. Phys.* **74** (2002) 825–874, [hep-th/0203101].

[371] J. D. Bekenstein, *Black Holes and the Second Law*, *Lett. Nuovo Cim.* **4** (1972) 737–740.

[372] J. D. Bekenstein, *Black Holes and Entropy*, *Phys. Rev. D* **7** (1973) 2333–2346.

[373] J. D. Bekenstein, *Generalized second law of thermodynamics in black hole physics*, *Phys. Rev. D* **9** (1974) 3292–3300.

[374] S. W. Hawking, *Gravitational radiation from colliding black holes*, *Phys. Rev. Lett.* **26** (1971) 1344–1346.

[375] J. M. Bardeen, B. Carter and S. W. Hawking, *The Four Laws of Black Hole Mechanics*, *Commun. Math. Phys.* **31** (1973) 161–170.

[376] R. Bousso, *A Covariant entropy conjecture*, *JHEP* **07** (1999) 004, [hep-th/9905177].

[377] H. Casini, *Relative entropy and the Bekenstein bound*, *Class. Quant. Grav.* **25** (2008) 205021, [0804.2182].

[378] R. Bousso, Z. Fisher, S. Leichenauer and A. C. Wall, *Quantum focusing conjecture*, *Phys. Rev. D* **93** (2016) 064044, [1506.02669].

[379] C. B. Thorn, *Reformulating string theory with the 1/N expansion*, in *The First International A.D. Sakharov Conference on Physics*, The First International A.D. Sakharov Conference on Physics, 5, 1991, [hep-th/9405069].

[380] C. Rovelli, *Black hole entropy from loop quantum gravity*, *Phys. Rev. Lett.* **77** (1996) 3288–3291, [gr-qc/9603063].

[381] R. Gambini and J. Pullin, *Holography from loop quantum gravity*, *Int. J. Mod. Phys. D* **17** (2008) 545–549, [0708.0250].

[382] L. Smolin, *Holographic relations in loop quantum gravity*, 1608.02932.

[383] O. Sargin and M. Faizal, *Violation of the Holographic Principle in the Loop Quantum Gravity*, *Eur. Phys. Lett.* **113** (2016) 30007, [1509.00843].

[384] I. R. Klebanov and A. A. Tseytlin, *Entropy of near extremal black p-branes*, *Nucl. Phys. B* **475** (1996) 164–178, [hep-th/9604089].

[385] S. W. Hawking and G. F. R. Ellis, *The Large Scale Structure of Space-Time*, Cambridge Monographs on Mathematical Physics, Cambridge University Press, 2, 2023, 10.1017/9781009253161.

[386] J. Polchinski, *String theory. Vol. 1: An introduction to the bosonic string*, Cambridge Monographs on Mathematical Physics, Cambridge University Press, 12, 2007, 10.1017/CBO9780511816079.

[387] J. Polchinski, *String theory. Vol. 2: Superstring theory and beyond*, Cambridge Monographs on Mathematical Physics, Cambridge University Press, 12, 2007, 10.1017/CBO9780511618123.

[388] M. Kaku, *Introduction to superstrings and M theory*, Graduate Texts in Contemporary Physics, Springer, New York, 1999, 10.1007/978-1-4612-0543-2.

[389] B. Zwiebach, *A first course in string theory*, Cambridge University Press, 7, 2006, 10.1017/CBO9780511841682.

[390] K. Becker, M. Becker and J. H. Schwarz, *String theory and M-theory: A modern introduction*, Cambridge University Press, 12, 2006, 10.1017/CBO9780511816086.

[391] D. Tong, *String Theory*, 0908.0333.

[392] M. B. Green, J. H. Schwarz and E. Witten, *Superstring Theory Vol. 1: 25th Anniversary Edition*, Cambridge Monographs on Mathematical Physics, Cambridge University Press, 11, 2012, 10.1017/CBO9781139248563.

[393] M. B. Green, J. H. Schwarz and E. Witten, *Superstring Theory Vol. 2: 25th Anniversary Edition*, Cambridge Monographs on Mathematical Physics, Cambridge University Press, 11, 2012, 10.1017/CBO9781139248570.

[394] R. Blumenhagen, D. Lüst and S. Theisen, *Basic concepts of string theory*, Theoretical and Mathematical Physics, Springer, Heidelberg, Germany, 2013, 10.1007/978-3-642-29497-6.

[395] J. Dai, R. G. Leigh and J. Polchinski, *New Connections Between String Theories*, *Mod. Phys. Lett. A* **4** (1989) 2073–2083.

[396] V. Schomerus, *Strings for quantumchromodynamics*, *Int. J. Mod. Phys. A* **22** (2007) 5561–5571, [0706.1209].

[397] J. Polchinski, *Dirichlet Branes and Ramond-Ramond charges*, *Phys. Rev. Lett.* **75** (1995) 4724–4727, [hep-th/9510017].

[398] G. 't Hooft, *A Planar Diagram Theory for Strong Interactions*, *Nucl. Phys. B* **72** (1974) 461.

[399] P. Cvitanovic, *Group theory for Feynman diagrams in non-Abelian gauge theories*, *Phys. Rev. D* **14** (1976) 1536–1553.

[400] V. A. Novikov, M. A. Shifman, A. I. Vainshtein and V. I. Zakharov, *Exact Gell-Mann-Low Function of Supersymmetric Yang-Mills Theories from Instanton Calculus*, *Nucl. Phys. B* **229** (1983) 381–393.

[401] N. Seiberg, *Supersymmetry and Nonperturbative beta Functions*, *Phys. Lett. B* **206** (1988) 75–80.

[402] D. Z. Freedman, S. D. Mathur, A. Matusis and L. Rastelli, *Correlation functions in the CFT(d) / AdS(d+1) correspondence*, *Nucl. Phys. B* **546** (1999) 96–118, [hep-th/9804058].

[403] S. Lee, S. Minwalla, M. Rangamani and N. Seiberg, *Three point functions of chiral operators in D = 4, N=4 SYM at large N*, *Adv. Theor. Math. Phys.* **2** (1998) 697–718, [hep-th/9806074].

[404] M. Henningson and K. Skenderis, *The Holographic Weyl anomaly*, *JHEP* **07** (1998) 023, [hep-th/9806087].

[405] M. Henningson and K. Skenderis, *Holography and the Weyl anomaly*, *Fortsch. Phys.* **48** (2000) 125–128, [hep-th/9812032].

[406] J. E. Paton and H.-M. Chan, *Generalized veneziano model with isospin*, *Nucl. Phys. B* **10** (1969) 516–520.

[407] D. Garfinkle, G. T. Horowitz and A. Strominger, *Charged black holes in string theory*, *Phys. Rev. D* **43** (1991) 3140.

[408] G. T. Horowitz and A. Strominger, *Black strings and P-branes*, *Nucl. Phys. B* **360** (1991) 197–209.

[409] M. Gunaydin and N. Marcus, *The Spectrum of the s**5 Compactification of the Chiral N=2, D=10 Supergravity and the Unitary Supermultiplets of U(2, 2/4)*, *Class. Quant. Grav.* **2** (1985) L11.

[410] R. R. Metsaev and A. A. Tseytlin, *Type IIB superstring action in AdS(5) x S**5 background*, *Nucl. Phys. B* **533** (1998) 109–126, [hep-th/9805028].

[411] I. Bena, J. Polchinski and R. Roiban, *Hidden symmetries of the AdS(5) x S**5 superstring*, *Phys. Rev. D* **69** (2004) 046002, [hep-th/0305116].

[412] J. M. Drummond, J. Henn, G. P. Korchemsky and E. Sokatchev, *Dual superconformal symmetry of scattering amplitudes in N=4 super-Yang-Mills theory*, *Nucl. Phys. B* **828** (2010) 317–374, [0807.1095].

[413] J. M. Drummond, J. Henn, G. P. Korchemsky and E. Sokatchev, *Generalized unitarity for N=4 super-amplitudes*, *Nucl. Phys. B* **869** (2013) 452–492, [0808.0491].

[414] G. Arutyunov and S. Frolov, *Foundations of the $AdS_5 \times S^5$ Superstring. Part I*, *J. Phys. A* **42** (2009) 254003, [0901.4937].

[415] E. Witten, *(2+1)-Dimensional Gravity as an Exactly Soluble System*, *Nucl. Phys. B* **311** (1988) 46.

[416] A. Strominger, *Black hole entropy from near horizon microstates*, *JHEP* **02** (1998) 009, [hep-th/9712251].

[417] J. M. Maldacena and H. Ooguri, *Strings in AdS(3) and SL(2,R) WZW model 1.: The Spectrum*, *J. Math. Phys.* **42** (2001) 2929–2960, [hep-th/0001053].

[418] J. M. Maldacena, H. Ooguri and J. Son, *Strings in AdS(3) and the SL(2,R) WZW model. Part 2. Euclidean black hole*, *J. Math. Phys.* **42** (2001) 2961–2977, [hep-th/0005183].

[419] J. M. Maldacena and H. Ooguri, *Strings in AdS(3) and the SL(2,R) WZW model. Part 3. Correlation functions*, *Phys. Rev. D* **65** (2002) 106006, [hep-th/0111180].

[420] L. Eberhardt, M. R. Gaberdiel and R. Gopakumar, *Deriving the AdS_3/CFT_2 correspondence*, *JHEP* **02** (2020) 136, [1911.00378].

[421] P. Kraus, *Lectures on black holes and the AdS_3/ CFT_2 correspondence*, pp. 1–55, Springer Berlin Heidelberg, Berlin, Heidelberg, 2008, 10.1007/978-3-540-79523-0_4, [hep-th/0609074].

[422] R. Gopakumar and C. Vafa, *On the gauge theory / geometry correspondence*, *Adv. Theor. Math. Phys.* **3** (1999) 1415–1443, [hep-th/9811131].

[423] R. Gopakumar and C. Vafa, *Topological gravity as large N topological gauge theory*, *Adv. Theor. Math. Phys.* **2** (1998) 413–442, [hep-th/9802016].

[424] I. R. Klebanov and G. Torri, *M2-branes and AdS/CFT*, *Int. J. Mod. Phys. A* **25** (2010) 332–350, [0909.1580].

[425] E. Witten, *Five-brane effective action in M theory*, *J. Geom. Phys.* **22** (1997) 103–133, [hep-th/9610234].

[426] C. Teitelboim, *Gravitation and Hamiltonian Structure in Two Space-Time Dimensions*, *Phys. Lett. B* **126** (1983) 41–45.

[427] R. Jackiw, *Lower Dimensional Gravity*, *Nucl. Phys. B* **252** (1985) 343–356.

[428] S. Sachdev, *Holographic metals and the fractionalized Fermi liquid*, *Phys. Rev. Lett.* **105** (2010) 151602, [1006.3794].

[429] J. Maldacena and D. Stanford, *Remarks on the Sachdev-Ye-Kitaev model*, *Phys. Rev. D* **94** (2016) 106002, [1604.07818].

[430] V. Rosenhaus, *An introduction to the SYK model*, *J. Phys. A* **52** (2019) 323001, [1807.03334].

[431] C. Chamon, R. Jackiw, S.-Y. Pi and L. Santos, *Conformal quantum mechanics as the CFT_1 dual to AdS_2*, *Phys. Lett. B* **701** (2011) 503–507, [1106.0726].

[432] V. Balasubramanian and P. Kraus, *A Stress tensor for Anti-de Sitter gravity*, *Commun. Math. Phys.* **208** (1999) 413–428, [hep-th/9902121].

[433] S. de Haro, S. N. Solodukhin and K. Skenderis, *Holographic reconstruction of space-time and renormalization in the AdS / CFT correspondence*, *Commun. Math. Phys.* **217** (2001) 595–622, [hep-th/0002230].

[434] M. Bianchi, D. Z. Freedman and K. Skenderis, *Holographic renormalization*, *Nucl. Phys. B* **631** (2002) 159–194, [hep-th/0112119].

[435] I. Papadimitriou and K. Skenderis, *AdS / CFT correspondence and geometry*, *IRMA Lect. Math. Theor. Phys.* **8** (2005) 73–101, [hep-th/0404176].

[436] K. Skenderis, *Lecture notes on holographic renormalization*, *Class. Quant. Grav.* **19** (2002) 5849–5876, [hep-th/0209067].

[437] I. Papadimitriou, *Lectures on Holographic Renormalization*, *Springer Proc. Phys.* **176** (2016) 131–181.

[438] M. C. Escher, *Circle Limit IV: Heaven and Hell*, accessed and downloaded on 15th of June 2023 at https://www.reed.edu/math/wieting/essays/CapturingInfinity.pdf.

[439] T. Nishioka, S. Ryu and T. Takayanagi, *Holographic Entanglement Entropy: An Overview*, *J. Phys. A* **42** (2009) 504008, [0905.0932].

[440] V. E. Hubeny, M. Rangamani and T. Takayanagi, *A Covariant holographic entanglement entropy proposal*, *JHEP* **07** (2007) 062, [0705.0016].

[441] A. Lewkowycz and J. Maldacena, *Generalized gravitational entropy*, *JHEP* **08** (2013) 090, [1304.4926].

[442] X. Dong, A. Lewkowycz and M. Rangamani, *Deriving covariant holographic entanglement*, *JHEP* **11** (2016) 028, [1607.07506].

[443] T. Faulkner, A. Lewkowycz and J. Maldacena, *Quantum corrections to holographic entanglement entropy*, *JHEP* **11** (2013) 074, [1307.2892].

[444] S. N. Solodukhin, *Entanglement entropy of black holes and AdS/CFT correspondence*, *Phys. Rev. Lett.* **97** (2006) 201601, [hep-th/0606205].

[445] S. N. Solodukhin, *Entanglement entropy of black holes*, *Living Rev. Rel.* **14** (2011) 8, [1104.3712].

[446] E. Verlinde and H. Verlinde, *A Conversation on ER = EPR*, 2212.09389.

[447] J. B. Hartle and S. W. Hawking, *Path Integral Derivation of Black Hole Radiance*, *Phys. Rev. D* **13** (1976) 2188–2203.

[448] Y. Takahashi and H. Umezawa, *Thermo field dynamics*, *Collective Phenomena* **2** (1975) 55–80.

[449] W. Israel, *Thermo field dynamics of black holes*, *Phys. Lett. A* **57** (1976) 107–110.

[450] V. Balasubramanian, P. Hayden, A. Maloney, D. Marolf and S. F. Ross, *Multiboundary Wormholes and Holographic Entanglement*, *Class. Quant. Grav.* **31** (2014) 185015, [1406.2663].

[451] E. Witten, *Anti-de Sitter space, thermal phase transition, and confinement in gauge theories*, *Adv. Theor. Math. Phys.* **2** (1998) 505–532, [hep-th/9803131].

[452] J. Maldacena, D. Stanford and Z. Yang, *Diving into traversable wormholes*, *Fortsch. Phys.* **65** (2017) 1700034, [1704.05333].

[453] J. Maldacena and X.-L. Qi, *Eternal traversable wormhole*, 1804.00491.

[454] K. Papadodimas and S. Raju, *Local Operators in the Eternal Black Hole*, *Phys. Rev. Lett.* **115** (2015) 211601, [1502.06692].

[455] K. Papadodimas and S. Raju, *Remarks on the necessity and implications of state-dependence in the black hole interior*, *Phys. Rev. D* **93** (2016) 084049, [1503.08825].

[456] G. Festuccia and H. Liu, *The Arrow of time, black holes, and quantum mixing of large N Yang-Mills theories*, *JHEP* **12** (2007) 027, [hep-th/0611098].

[457] R. Bousso, X. Dong, N. Engelhardt, T. Faulkner, T. Hartman, S. H. Shenker et al., *Snowmass White Paper: Quantum Aspects of Black Holes and the Emergence of Spacetime*, 2201.03096.

[458] D. L. Jafferis and E. Schneider, *Stringy ER = EPR*, *JHEP* **10** (2022) 195, [2104.07233].

[459] D. Harlow et al., *TF1 Snowmass Report: Quantum gravity, string theory, and black holes*, 2210.01737.

[460] N. Engelhardt and Å. Folkestad, *Canonical purification of evaporating black holes*, *Phys. Rev. D* **105** (2022) 086010, [2201.08395].

[461] N. Engelhardt, *Algebraic ER=EPR*, Talk given at Strings 2023, 10.48660/23070038.

[462] D. Harlow, *Wormholes, Emergent Gauge Fields, and the Weak Gravity Conjecture*, *JHEP* **01** (2016) 122, [1510.07911].

[463] I. Heemskerk, *Construction of Bulk Fields with Gauge Redundancy*, *JHEP* **09** (2012) 106, [1201.3666].

[464] D. Kabat, G. Lifschytz, S. Roy and D. Sarkar, *Holographic representation of bulk fields with spin in AdS/CFT*, *Phys. Rev. D* **86** (2012) 026004, [1204.0126].

[465] D. Kabat and G. Lifschytz, *CFT representation of interacting bulk gauge fields in AdS*, *Phys. Rev. D* **87** (2013) 086004, [1212.3788].

[466] D. Harlow and D. Jafferis, *The Factorization Problem in Jackiw-Teitelboim Gravity*, *JHEP* **02** (2020) 177, [1804.01081].

[467] R. Islam, R. Ma, P. M. Preiss, M. Eric Tai, A. Lukin, M. Rispoli et al., *Measuring entanglement entropy in a quantum many-body system*, *Nature* **528** (2015) 77–83, [1509.01160].

[468] C. A. Ryan, M. Laforest and R. Laflamme, *Randomized benchmarking of single- and multi-qubit control in liquid-state NMR quantum information processing*, *New J. Phys.* **11** (2009) 013034, [0808.3973].

[469] A. Imamoğlu, D. D. Awschalom, G. Burkard, D. P. DiVincenzo, D. Loss, M. Sherwin et al., *Quantum Information Processing Using Quantum Dot Spins and Cavity QED*, *Phys. Rev. Lett.* **83** (1999) 4204–4207, [quant-ph/9904096].

[470] M. Steffen, M. Ansmann, R. C. Bialczak, N. Katz, E. Lucero, R. McDermott et al., *Measurement of the Entanglement of Two Superconducting Qubits via State Tomography*, *Science* **313** (2006) 1423–1425.

[471] M. H. Devoret and R. J. Schoelkopf, *Superconducting Circuits for Quantum Information: An Outlook*, *Science* **339** (2013) 1169–1174.

[472] C. Song, K. Xu, W. Liu, C.-p. Yang, S.-B. Zheng, H. Deng et al., *10-Qubit Entanglement and Parallel Logic Operations with a Superconducting Circuit*, *Phys. Rev. Lett.* **119** (2017) 180511, [1703.10302].

[473] D. Zhu, S. Johri, N. M. Linke, K. A. Landsman, N. H. Nguyen, C. H. Alderete et al., *Generation of thermofield double states and critical ground states with a quantum computer*, *Proc. Nat. Acad. Sci.* **117** (2020) 25402–25406, [1906.02699].

[474] M. Guica, T. Hartman, W. Song and A. Strominger, *The Kerr/CFT Correspondence*, *Phys. Rev. D* **80** (2009) 124008, [0809.4266].

[475] E. Witten, *A Note On The Canonical Formalism for Gravity*, 2212.08270.

[476] E. Witten, *A New Look At The Path Integral Of Quantum Mechanics*, *Surveys in Diff. Geome.* **15** (2010) 345–420, [1009.6032].

[477] M. Banados, C. Teitelboim and J. Zanelli, *The Black hole in three-dimensional space-time*, *Phys. Rev. Lett.* **69** (1992) 1849–1851, [hep-th/9204099].

[478] M. Banados, M. Henneaux, C. Teitelboim and J. Zanelli, *Geometry of the (2+1) black hole*, *Phys. Rev. D* **48** (1993) 1506–1525, [gr-qc/9302012].

[479] P. H. Ginsparg, *Applied Conformal Field Theory*, in *Les Houches Summer School in Theoretical Physics: Fields, Strings, Critical Phenomena*, 9, 1988, [hep-th/9108028].

[480] P. Di Francesco, P. Mathieu and D. Senechal, *Conformal Field Theory*, Graduate Texts in Contemporary Physics, Springer-Verlag, New York, 1997, 10.1007/978-1-4612-2256-9.

[481] E. Witten, *Coadjoint Orbits of the Virasoro Group*, *Commun. Math. Phys.* **114** (1988) 1.

[482] A. Alekseev and S. L. Shatashvili, *Path Integral Quantization of the Coadjoint Orbits of the Virasoro Group and 2D Gravity*, *Nucl. Phys. B* **323** (1989) 719–733.

[483] A. Alekseev and S. L. Shatashvili, *From geometric quantization to conformal field theory*, *Commun. Math. Phys.* **128** (1990) 197–212.

[484] B. Oblak, *BMS Particles in Three Dimensions*. PhD thesis, U. Brussels, Brussels U., 2016. 1610.08526. 10.1007/978-3-319-61878-4.

[485] M. Henneaux, W. Merbis and A. Ranjbar, *Asymptotic dynamics of AdS_3 gravity with two asymptotic regions*, *JHEP* **03** (2020) 064, [1912.09465].

[486] S.-S. Chern and J. Simons, *Characteristic forms and geometric invariants*, *Ann. Math.* **99** (1974) 48–69.

[487] E. Witten, *Quantum Field Theory and the Jones Polynomial*, *Commun. Math. Phys.* **121** (1989) 351–399.

[488] G. V. Dunne, *Aspects Of Chern-Simons Theory*, in *Topological aspects of low dimensional systems*, (Berlin, Heidelberg), pp. 177–263, Springer Berlin Heidelberg, 1999, 10.1007/3-540-46637-1_3.

[489] O. Coussaert, M. Henneaux and P. van Driel, *The Asymptotic dynamics of three-dimensional Einstein gravity with a negative cosmological constant*, *Class. Quant. Grav.* **12** (1995) 2961–2966, [gr-qc/9506019].

[490] A. Pressley and G. Segal, *Loop Groups*, Oxford mathematical monographs, Clarendon Press, 1988.

[491] A. Achucarro and P. K. Townsend, *A Chern-Simons Action for Three-Dimensional anti-De Sitter Supergravity Theories*, *Phys. Lett. B* **180** (1986) 89.

[492] E. Witten, *Quantization of Chern-Simons Gauge Theory With Complex Gauge Group*, *Commun. Math. Phys.* **137** (1991) 29–66.

[493] C. T. Asplund, N. Callebaut and C. Zukowski, *Equivalence of Emergent de Sitter Spaces from Conformal Field Theory*, *JHEP* **09** (2016) 154, [1604.02687].

[494] P. Fries and I. A. Reyes, *Entanglement and relative entropy of a chiral fermion on the torus*, *Phys. Rev. D* **100** (2019) 105015, [1906.02207].

[495] J. Erdmenger, P. Fries, I. A. Reyes and C. P. Simon, *Resolving modular flow: a toolkit for free fermions*, *JHEP* **12** (2020) 126, [2008.07532].

[496] V. Eisler, G. Di Giulio, E. Tonni and I. Peschel, *Entanglement Hamiltonians for non-critical quantum chains*, *J. Stat. Mech.* **2010** (2020) 103102, [2007.01804].

[497] D. L. Jafferis and S. J. Suh, *The Gravity Duals of Modular Hamiltonians*, *JHEP* **09** (2016) 068, [1412.8465].

[498] D. L. Jafferis, A. Lewkowycz, J. Maldacena and S. J. Suh, *Relative entropy equals bulk relative entropy*, *JHEP* **06** (2016) 004, [1512.06431].

[499] X. Huang and C.-T. Ma, *Berry Curvature and Riemann Curvature in Kinematic Space with Spherical Entangling Surface*, *Fortsch. Phys.* **69** (2021) 2000048, [2003.12252].

[500] L. Apolo, H. Jiang, W. Song and Y. Zhong, *Modular Hamiltonians in flat holography and (W)AdS/WCFT*, *JHEP* **09** (2020) 033, [2006.10741].

[501] T. Hartman and N. Afkhami-Jeddi, *Speed Limits for Entanglement*, 1512.02695.

[502] T. Hartman and J. Maldacena, *Time Evolution of Entanglement Entropy from Black Hole Interiors*, *JHEP* **05** (2013) 014, [1303.1080].

[503] Y. O. Nakagawa, G. Sárosi and T. Ugajin, *Chaos and relative entropy*, *JHEP* **07** (2018) 002, [1805.01051].

[504] G. Compère, P. Mao, A. Seraj and M. M. Sheikh-Jabbari, *Symplectic and Killing symmetries of AdS_3 gravity: holographic vs boundary gravitons*, *JHEP* **01** (2016) 080, [1511.06079].

[505] M. M. Sheikh-Jabbari and H. Yavartanoo, *On 3d bulk geometry of Virasoro coadjoint orbits: orbit invariant charges and Virasoro hair on locally AdS_3 geometries*, *Eur. Phys. J. C* **76** (2016) 493, [1603.05272].

[506] J. de Boer, R. Espíndola, B. Najian, D. Patramanis, J. van der Heijden and C. Zukowski, *Virasoro entanglement Berry phases*, *JHEP* **03** (2022) 179, [2111.05345].

[507] J. Alvarez-Jimenez, A. Dector and J. D. Vergara, *Quantum Information Metric and Berry Curvature from a Lagrangian Approach*, *JHEP* **03** (2017) 044, [1702.00058].

[508] B. Díaz, D. González, D. Gutiérrez-Ruiz and J. D. Vergara, *Classical analogs of the covariance matrix, purity, linear entropy, and von Neumann entropy*, *Phys. Rev. A* **105** (2022) 062412, [2112.10899].

[509] S. B. Juárez, D. Gonzalez, D. Gutiérrez-Ruiz and J. D. Vergara, *Generalized quantum geometric tensor for excited states using the path integral approach*, *Phys. Scripta* **98** (2023) 095106, [2305.11525].

[510] R. Jefferson, *Comments on black hole interiors and modular inclusions*, *SciPost Phys.* **6** (2019) 042, [1811.08900].

[511] H.-W. Wiesbrock, *Half-Sided modular inclusions of von-Neumann-Algebras*, *Commun. Math. Phys.* **157** (1993) 83–92.

[512] H. J. Borchers, *Half-Sided Translations and the Type of von Neumann Algebras*, *Lett. Math. Phys.* **44** (1998) 283–290.

[513] C. B. Thorn, *Infinite N_c QCD at Finite Temperature: is there an Ultimate Temperature?*, *Phys. Lett. B* **99** (1981) 458–462.

[514] M. Takesaki, *Duality for crossed products and the structure of von Neumann algebras of type III*, *Acta Math.* **131** (1973) 249–310.

[515] A. Connes, *Une classification des facteurs de type* III, *Annales scientifiques de l'École Normale Supérieure* **4e série, 6** (1973) 133–252.

[516] E. Witten, *Algebras, Regions, and Observers*, 2303.02837.

[517] J. Polchinski, *Monopoles, duality, and string theory*, *Int. J. Mod. Phys. A* **19S1** (2004) 145–156, [hep-th/0304042].

[518] T. Banks and N. Seiberg, *Symmetries and Strings in Field Theory and Gravity*, *Phys. Rev. D* **83** (2011) 084019, [1011.5120].

[519] D. Harlow and H. Ooguri, *Constraints on Symmetries from Holography*, *Phys. Rev. Lett.* **122** (2019) 191601, [1810.05337].

[520] D. Harlow and H. Ooguri, *Symmetries in quantum field theory and quantum gravity*, *Commun. Math. Phys.* **383** (2021) 1669–1804, [1810.05338].

[521] W.-z. Guo, *Correlations in geometric states*, *JHEP* **08** (2020) 125, [2003.03933].

[522] M. Horodecki and P. Horodecki, *Reduction criterion of separability and limits for a class of distillation protocols*, *Phys. Rev. A* **59** (1999) 4206–4216, [quant-ph/9708015].

[523] D. Girolami, *How Difficult is it to Prepare a Quantum State?*, *Phys. Rev. Lett.* **122** (2019) 010505, [1808.01649].

[524] H. Verlinde, *Deconstructing the Wormhole: Factorization, Entanglement and Decoherence*, 2105.02142.

[525] X. Dong, *The Gravity Dual of Renyi Entropy*, *Nature Commun.* **7** (2016) 12472, [1601.06788].

[526] J. Chakravarty, *Overcounting of interior excitations: A resolution to the bags of gold paradox in AdS*, *JHEP* **02** (2021) 027, [2010.03575].

[527] B. Freivogel, D. Nikolakopoulou and A. F. Rotundo, *Wormholes from Averaging over States*, *SciPost Phys.* **14** (2023) 026, [2105.12771].

[528] K. Goto, Y. Kusuki, K. Tamaoka and T. Ugajin, *Product of random states and spatial (half-)wormholes*, *JHEP* **10** (2021) 205, [2108.08308].

[529] V. Balasubramanian, A. Lawrence, J. M. Magan and M. Sasieta, *Microscopic origin of the entropy of black holes in general relativity*, 2212.02447.

[530] V. Balasubramanian, A. Lawrence, J. M. Magan and M. Sasieta, *Microscopic origin of the entropy of astrophysical black holes*, 2212.08623.

[531] W. Cottrell, B. Freivogel, D. M. Hofman and S. F. Lokhande, *How to Build the Thermofield Double State*, *JHEP* **02** (2019) 058, [1811.11528].

[532] T. Anous, T. Hartman, A. Rovai and J. Sonner, *Black Hole Collapse in the 1/c Expansion*, *JHEP* **07** (2016) 123, [1603.04856].

[533] S. Bhattacharyya and S. Minwalla, *Weak Field Black Hole Formation in Asymptotically AdS Spacetimes*, *JHEP* **09** (2009) 034, [0904.0464].

[534] J. Erdmenger, J. Kastikainen, T. Schuhmann and A.-L. Weigel, "work in progress." 2023.

[535] S. W. Hawking and D. N. Page, *Thermodynamics of Black Holes in anti-De Sitter Space*, *Commun. Math. Phys.* **87** (1983) 577.

[536] R. Hagedorn, *Statistical thermodynamics of strong interactions at high-energies*, *Nuovo Cim. Suppl.* **3** (1965) 147–186.

[537] J. J. Atick and E. Witten, *The Hagedorn Transition and the Number of Degrees of Freedom of String Theory*, *Nucl. Phys. B* **310** (1988) 291–334.

[538] B. Sundborg, *The Hagedorn transition, deconfinement and N=4 SYM theory*, *Nucl. Phys. B* **573** (2000) 349–363, [hep-th/9908001].

[539] P. Basteiro, G. Di Giulio, J. Erdmenger and Z.-Y. Xian, "in preparation." 2023.

[540] J. de Boer, K. Papadodimas and E. Verlinde, *Black Hole Berry Phase*, *Phys. Rev. Lett.* **103** (2009) 131301, [0809.5062].

[541] W. Janke, D. A. Johnston and R. Kenna, *Information geometry and phase transitions*, *Physica A* **336** (2004) 181, [cond-mat/0401092].

[542] P. Zanardi, L. Campos Venuti and P. Giorda, *Bures metric over thermal state manifolds and quantum criticality*, *Phys. Rev. A* **76** (2007) 062318, [0707.2772].

[543] J. Erdmenger, K. T. Grosvenor and R. Jefferson, *Information geometry in quantum field theory: lessons from simple examples*, *SciPost Phys.* **8** (2020) 073, [2001.02683].

[544] S. Mahmoudi, K. Jafarzade and S. H. Hendi, *A Comprehensive Review of Geometrical Thermodynamics: From Fluctuations to Black Holes*, 2307.00010.

[545] T. Clingman, J. Murugan and J. P. Shock, *Probability Density Functions from the Fisher Information Metric*, 1504.03184.

[546] R. M. Soni, *A Type I Approximation of the Crossed Product*, 2307.12481.

[547] M. Goldstein and E. Sela, *Symmetry-resolved entanglement in many-body systems*, *Phys. Rev. Lett.* **120** (2018) 200602, [1711.09418].

[548] J. C. Xavier, F. C. Alcaraz and G. Sierra, *Equipartition of the entanglement entropy*, *Phys. Rev. B* **98** (2018) 041106, [1804.06357].

[549] S. Zhao, C. Northe and R. Meyer, *Symmetry-resolved entanglement in AdS_3/CFT_2 coupled to U(1) Chern-Simons theory*, *JHEP* **07** (2021) 030, [2012.11274].

[550] G. Di Giulio and J. Erdmenger, *Symmetry-resolved modular correlation functions in free fermionic theories*, *JHEP* **07** (2023) 058, [2305.02343].

[551] G. Di Giulio, M. Dorband, J. Erdmenger and H. Scheppach, "work in progress." 2023.

[552] A. Ortega, E. McKay, A. M. Alhambra and E. Martín-Martínez, *Work distributions on quantum fields*, *Phys. Rev. Lett.* **122** (2019) 240604, [1902.03258].

[553] J. Polo-Gómez, L. J. Garay and E. Martín-Martínez, *A detector-based measurement theory for quantum field theory*, *Phys. Rev. D* **105** (2022) 065003, [2108.02793].

[554] C. J. Fewster and R. Verch, *Quantum fields and local measurements*, *Commun. Math. Phys.* **378** (2020) 851–889, [1810.06512].

[555] C. J. Fewster, *A generally covariant measurement scheme for quantum field theory in curved spacetimes*, in *Progress and Visions in Quantum Theory in View of Gravity: Bridging foundations of physics and mathematics*, 2019, [1904.06944].

[556] S. Antonini, B. Grado-White, S.-K. Jian and B. Swingle, *Holographic measurement and quantum teleportation in the SYK thermofield double*, *JHEP* **02** (2023) 095, [2211.07658].

[557] S. Antonini, B. Grado-White, S.-K. Jian and B. Swingle, *Holographic measurement in CFT thermofield doubles*, *JHEP* **07** (2023) 014, [2304.06743].

[558] M. Dorband, D. Grumiller, R. Meyer and S. Zhao, *Disorder in AdS_3/CFT_2*, 2204.00596.